

# **The Roles of MicroRNAs in Human Mesenchymal Stem Cell Adipogenesis**



A thesis submitted to the National University of Ireland as  
fulfilment of the requirement for the degree of

**Doctor of Philosophy**

By

**Annette Enright**

Regenerative Medicine Institute (REMEDI),  
College of Science,  
National University of Ireland, Galway

Thesis supervisors:  
Dr. Linda Howard  
Prof. Frank Barry

Date of Submission: March 2012

# Table of Contents

Introduction.....	1
1.1 Overview .....	2
1.2 Stem Cells .....	4
1.2.1 Mesenchymal Stem Cells.....	6
1.2.1.1 Isolation and In Vitro Characterization of Mesenchymal Stem Cell.....	7
1.2.1.2 Differentiation of Mesenchymal Stem cells in Vitro .....	8
1.3 Obesity and the Development of Adipose Tissue .....	9
1.3.1 White Adipose Tissue (WAT) .....	10
1.3.2 Brown Adipose Tissue (BAT) .....	10
1.3.3 Differences between WAT and BAT .....	11
1.3.4 Conversion of WAT to BAT.....	13
1.4 Study of Adipogenesis.....	14
1.5 MicroRNAs .....	21
1.5.1 History of miRNA Research.....	21
1.5.2 Genomic Location of miRNAs .....	22
1.5.3 Biogenesis of miRNAs.....	23
1.5.4 Mechanism of Translational Repression .....	26
1.5.5 Biological Roles of miRNAs .....	26
1.5.6 MiRNA Target Prediction.....	27
1.5.7 MiRNA target identification .....	29
1.5.7.1 Luciferase reporter assays .....	30
1.5.7.2 Immunoprecipitation of RISC components.....	30
1.5.7.3 HITS-CLIP .....	31
1.5.7.4 PAR-CLIP .....	32
1.5.7.5 RLM-RACE.....	32
1.5.7.6 Biotin tagged miRNA.....	32
1.5.8 MiRNAs in Stem Cells .....	33
1.5.8.1 MiRNAs in Embryonic Stem Cells (ESCs).....	33
1.5.8.1.1 Effects of Dicer Knockout on ES cell Behaviour.....	33
1.5.8.1.2 Effects of DGCR8 Knockout on ES cell Behaviour .....	34
1.5.8.1.3 MiRNA Profile of ES Cell .....	34
1.5.8.2 MiRNAs in Hematopoiesis .....	35
1.5.8.3 MiRNAs in Myogenesis and Cardiogenesis.....	36
1.5.9 MiRNAs in Adipogenesis.....	37
1.5.10 MiRNAs in Obesity .....	39
1.5.11 Therapeutic potential of miRNAs in the treatment of obesity.....	40
1.6 Aims And Objectives .....	42
2 Materials and Methods.....	44
2.1 Isolation, Expansion and Characterisation of human Mesenchymal Stem Cells (hMSCs).....	45
2.1.1 Isolation of MSCs.....	45
2.1.2 Characterisation of MSCs.....	46
2.1.2.1 Cell Surface Marker Analysis.....	46
2.1.2.2 Osteogenesis.....	47
2.1.2.2.1 Induction of osteogenic differentiation .....	47

2.1.2.2.2	Von Kossa Staining .....	48
2.1.2.2.3	Calcium Assay .....	48
2.1.2.4.2	Microscopic Analysis .....	53
2.1.2.4.3	Oil Red O Staining .....	54
2.1.2.4.4	Nile Red Staining.....	54
2.1.2.4.5	Ceiling Culture .....	55
2.2	Plasmid Preparation .....	56
2.2.1	Construction of miR-221/222 Overexpression Plasmid.....	56
2.2.2	Construction of p27 overexpression plasmid. ....	57
2.2.3	MiR-221, miR-222 and miR-126 Precursor Constructs .....	57
2.2.4	Sh-221, sh-222 and scramble shRNA Constructs.....	57
2.2.5	pMIR-REPORT miRNA Expression Reporter.....	57
2.2.6	GFP-expressing plasmid (pWPT-GFP) .....	58
2.3	Gene Delivery .....	59
2.3.1	Generation and Purification of Lentivirus .....	59
2.3.1.1	Titration of Lentivirus.....	60
2.3.1.1.1	Calculation of Titre Based on GFP Expression .....	60
2.3.1.1.2	Calculation of Titre Based on Gag integration into Genomic DNA61	
2.3.1.2	Lentiviral Transduction of Target Cells .....	63
2.3.1.2.1	Lentiviral Transduction of hMSCs with vectors of miRNA overexpression or shRNAs against miRNAs .....	63
2.3.1.2.2	Lentiviral Transduction of hMSCs with pWPT-p27 lentivirus.....	64
2.3.1.2.2.1	Effect on of pWPT-p27 transduction on hMSC number .....	64
2.3.1.2.2.2	Effect on of pWPT-p27 transduction on hMSC adipogenesis and p27 protein expression.....	64
2.3.2	Nucleofection .....	64
2.3.3	Jet pei Transfection.....	65
2.3.3.1	Luciferase vector transfection of 293T cells using Jet pei.....	65
2.3.3.1.1	Luciferase Reporter Assay .....	68
2.3.3.2	pWPT-p27 vector transfection of 293T cells .....	68
2.4	RNA Methods .....	70
2.4.1	Total RNA Isolation.....	70
2.4.2	Analysis of RNA Concentration and Integrity .....	70
2.4.3	Real-Time Polymerase Chain Rection (RT-PCR) .....	71
2.4.3.1	Real-Time Reverse Transcription (RT) PCR To Quantify Relative Transcript Levels .....	71
2.4.3.2	MiRNA Quantitation by Real-Time PCR.....	73
2.4.3.2.1	MiRNA Reverse Transcription.....	73
2.4.3.2.2	PCR of miRNA specific cDNA .....	73
2.4.4	MiRNA Microarray Techniques .....	76
2.4.4.1	Overview of MiChip Protocol .....	76
2.4.4.2	MiRNA Labelling for MiChip Hybridization .....	77
2.4.4.3	Sample Precipitation.....	78
2.4.4.4	Hybridisation of Labelled MiRNAs to MiChip.....	79
2.4.4.5	Post-hybridization Washing of MiChip .....	79
2.4.4.6	Scanning of MiChip Arrays and Image Analysis.....	80

2.4.4.7	Data Analysis .....	81
2.5	Protein Analysis Techniques .....	82
2.5.1	Protein Lysate Preparation and Western Blot Analysis .....	82
2.6	Statistical Analysis .....	83
3	Identification of MiRNAs Regulated During Mesenchymal Stem Cell	
	Adipogenesis .....	84
3.1	Introduction.....	85
3.1.1	Experimental Aims and Objectives .....	85
3.1.2	MiRNA Analysis Methods.....	86
3.1.2.1	MiChip System for MiRNA Analysis .....	87
3.2	Results .....	89
3.2.1	Isolation and Characterization of hMSCs .....	89
3.2.1.1	Surface Marker Analysis.....	90
3.2.1.2	Osteogenesis.....	91
3.2.1.3	Chondrogenesis .....	92
3.2.2	Adipogenesis .....	93
3.2.3	MiRNA Analysis at Day 5 of Adipogenesis.....	96
3.2.3.1	Differentiation of MSCs for Microarray Analysis .....	96
3.2.3.2	Verification of RNA quality for Microarray Analysis.....	98
3.2.3.3	Genespring Analysis Of Microarray Data.....	100
3.2.3.4	RT-PCR Confirmation of MiRNA Microarray Data .....	102
3.2.3.5	Analysis of MiRNA Expression at Day 5 of Adipogenesis .....	104
3.2.4	Isolating a Pure Population of MSC-Derived Adipocytes.....	105
3.2.5	Analysis of Changes in MiRNA Expression at Day 20 of Adipogenesis	106
3.2.5.1	GeneSpring Analysis of Day 20 Microarray Data .....	109
3.2.5.2	RT-PCR Confirmation of Day 20 Microarray Data.....	113
3.3	Discussion.....	118
3.3.1	Mesenchymal Stem Cells.....	118
3.3.2	Differentiation of hMSCs to adipocytes .....	118
3.3.3	Identification of Significantly Regulated MiRNAs at Day 5 of	
	Adipogenesis .....	120
3.3.4	Identification of Significantly Regulated MiRNAs at Day 20 of	
	Adipogenesis .....	121
3.3.5	MiRNAs Regulated during Adipogenesis .....	126
3.3.5.1	MiR-199 Cluster .....	127
3.3.5.2	MiR-125b .....	127
3.3.5.3	MiR-17-92 Cluster .....	127
3.3.5.4	MiR-371 .....	128
3.3.5.5	MiR-221 and MiR-222 .....	129
4	The Effects of Manipulation of Expression of MiR-221 and MiR-222 on	
	hMSC Adipogenesis .....	130
4.1	Introduction.....	131
4.1.1	Experimental Aims and Objectives.....	131
4.1.2	MiRNA and MSC.....	132
4.1.3	MiR-221 and MiR-222 .....	132

<b>4.2</b>	<b>Results .....</b>	<b>134</b>
4.2.1	MiR-221 and miR-222 are downregulated throughout hMSC adipogenesis.....	134
4.2.2	MiR-221 and miR-222 are downregulated in hMSC Osteogenesis and Chondrogenesis.....	136
4.2.3	Overexpression of miRNAs 221 and 222 in MSCs.....	138
4.2.4	Overexpression of miRNAs 221 and 222 in hMSCs reduces adipogenesis.....	144
4.2.5	Overexpression of miRNAs 221 and 222 in hMSCs does not affect hMSC osteogenesis.....	148
4.2.6	Overexpressing miR-221 and miR-222 reduces the upregulation of key transcripts during adipogenesis .....	149
4.2.7	Inhibition of activity of miRNAs 221 and 222 in MSCs .....	152
4.2.8	Potential targets of miR-221 and miR-222 in hMSC adipogenesis	157
4.2.8.1	Are miR-221 and miR-222 acting through p27 and/or p57 in adipogenesis? .....	158
4.2.8.2	P57 (Kip2, CDKN1C) .....	159
4.2.8.3	P27 (Kip1,CDKN1B).....	161
4.2.9	Co-expressing miR-221 and miR-222 causes a reduction in p27 protein but does not significantly reduce p27 transcript. ....	163
4.2.10	Luciferase Reporter Assay Confirms p27 as a direct target of miR-221 and miR-222 in HEK293T Cells .....	165
4.2.11	Inhibition of miR-221 and miR-222 activity causes an increase in p27 luciferase activity .....	169
4.2.12	Inhibition of miR-221 and miR-222 activity causes an increase in p27 transcript expression .....	171
4.2.13	Add back of p27 does not rescue miR-221 and miR-222 inhibition of adipogenesis.....	172
4.2.13.1	Construction of a p27 overexpression vector .....	172
4.2.13.2	Overexpression of p27 in MSCs overexpressing miR-221 and 222	175
4.2.13.3	Overexpression of p27 has no significant effect on hMSC adipogenesis.....	177
4.2.14	Identification of other targets for miR-221 and miR-222 in adipogenesis.....	179
4.2.14.1	PGC1 $\alpha$ as a potential target of miR-221 and miR-222 in hMSC adipogenesis.....	187
4.2.14.2	TLE3 as a potential target of miR-221 and miR-222 in hMSC adipogenesis.....	188
<b>4.3</b>	<b>Discussion.....</b>	<b>190</b>
4.3.1	Downregulation of miR-221 and miR-222 during hMSC differentiation.....	190
4.3.2	Overexpressing miR-221 and 222 significantly reduces hMSC adipogenesis.....	191
4.3.3	MiR-221 and miR-222 as safeguards of ‘stemness’ in hMSCs .	193

4.3.4	Cell number is significantly reduced in hMSCs with reduced activity of miR-221 and miR-222.....	194
4.3.5	What is the target(s) of miR-221 and miR-222 in hMSC adipogenesis? .....	195
4.3.6	P27 as a potential target for miR-221 and miR-222 in Adipogenesis .....	196
4.3.7	Luciferase reporter assays as a method of verifying an interaction between a miRNA and its target .....	197
4.3.8	Overexpression of p27 has no significant effect on levels of hMSC adipogenesis .....	199
4.3.9	Prediction of other miR-221 and miR-222 targets in adipogenesis	202
4.3.10	PGC1 $\alpha$ as a potential target for miR-221/222 in hMSC adipogenesis .....	203
4.3.11	TLE3 as a potential target for miR-221/222 in hMSC adipogenesis .....	204
4.3.12	Concluding remarks .....	206
5	Discussion.....	207
5.1	MiRNAs In The Regulation Of hMSC Adipogenesis .....	208
5.2	Identifying miRNAs regulated during hMSC Adipogenesis.....	208
5.2.1	MiRNA expression at day 5 of adipogenesis.....	208
5.2.2	MiRNA expression at Day 20 of Adipogenesis .....	210
5.3	MiR-221 and miR-222 .....	211
5.3.1	MiRNA-221 and miRNA-222 in hMSC Differentiation .....	211
5.3.2	Inhibiting the activity of miR-221 and 222 causes a reduction in hMSC number .....	213
5.3.3	MiR-221 and miR-222 target prediction.....	213
5.3.4	P27 as a target of miR-221 and miR-222 in hMSC Adipogenesis ....	214
5.3.5	Overexpression of p27 in hMSC Adipogenesis .....	217
5.3.6	Final Remarks .....	220
6	Bibliography .....	222

## List of Figures

Figure 1-1 Differentiation ability of Stem Cells.....	5
Figure 1-2 Relationship between white and brown adipogenesis.....	11
Figure 1-3 Transcriptional Cascade involved in Adipogenic Differentiation....	16
Figure 1-4 Genomic Locations of MiRNAs.....	22
Figure 1-5 Overview of the Biogenesis of MiRNAs.....	25
Figure 2-1 Schedule for Medium Changes during hMSC Adipogenesis.....	53
Figure 2-2 Overview of MicroRNA microarray (MiChip platform).....	76
Figure 3-1 Structure and definition of LNA.....	87
Figure 3-2 Characterisation of Cell Surface Proteins of HMSCs.....	90
Figure 3-3 Osteogenic Differentiation of hMSCs.....	91
Figure 3-4 Chondrogenic Differentiation of hMSCs.....	92
Figure 3-5 Adipogenic Differentiation of hMSCs.....	95
Figure 3-6 MSCs from 5 donors successfully differentiated to adipocytes.....	97
Figure 3-7 Quality of RNA verified by Bioanalyzer.....	99
Figure 3-8 GeneSpring analysis does not reveal significant changes in microRNA expression at day 5 of adipogenesis.....	101
Figure 3-9 RT-PCR confirms that there are no significant microRNA changes at day 5 of adipogenesis in MSCs isolated from 5 donors.....	103
Figure 3-10 Representative phase contrast micrographs of adipogenically differentiating MSCs before and after using the ‘Ceiling Culture’ method....	105
Figure 3-11 MSCs (4 donors) 20 days after adipogenic induction before and after Ceiling Culture.....	106
Figure 3-12 Quality of RNA verified by Bioanalyzer.....	108
Figure 3-13 GeneSpring analysis reveals a clear grouping of treated Vs control samples at day 20 of adipogenesis across 4 donors.....	110
Figure 3-14 Significantly regulated miRNAs (20) at day 20 of adipogenesis...111	111
Figure 3-15 Significantly regulated miRNAs (20) at day 20 of adipogenesis...112	112
Figure 3-16 - PCR confirms miR-221 and miR-222 are significantly downregulated across all donors at day 20 of adipogenesis.....	114
Figure 3-17 RT- PCR confirms miR-193a is upregulated at day 20 across all donors.....	115
Figure 3-18 RT-PCR analysis contradicts microarray results and shows miR-18a is upregulated at day 20 of adipogenesis.....	115
Figure 3-19 RT- PCR shows donor- donor variability in expression of miR-99a and miR-17-5p at day 20 of adipogenesis.....	116
Figure 3-20 Taken from ‘Current Methods of Adipogenic Differentiation of Mesenchymal Stem Cells’.....	123
Figure 4-1 Genomic localization of miR-221 and miR-222 on chromosome X.....	132
Figure 4-2 RT-PCR shows that miR-221 and miR-222 are downregulated during adipogenesis.....	135
Figure 4-3 RT-PCR shows that miR-221 and miR-222 are downregulated during osteogenesis and chondrogenesis.....	137
Figure 4-4 Nucleofection of hMSCs with miR-221/222 overexpression vector.....	140

Figure 4-5- RT-PCR shows that the expression of miR-126 does not change during adipogenesis.....	142
Figure 4-6 Lentiviral mediated overexpression of miR-221 and miR-222 72 hours post transduction.....	143
Figure 4-7 Overexpression of miR-221 or miR-222 reduces adipogenesis in hMSCs.....	146
Figure 4-8 Coexpression of miR-221 and miR-222 significantly reduces hMSC adipogenesis as measured by lipid accumulation.....	147
Figure 4-9 Overexpression of miR-221 and miR-222 has no significant effect on hMSCs undergoing osteogenesis.....	149
Figure 4-10 Coexpression of miR-221 and miR-222 in hMSCs reduces the upregulation of key transcripts during adipogenesis.....	151
Figure 4-11 Transduction of hMSCs with sh-221 and/or sh-222 significantly reduces expression of miR-221 and/or miR-222.....	153
Figure 4-12 The inhibition of miR-221 or miR-222 activity results in loss of hMSC.....	155
Figure 4-13 The inhibition of miR-221 or miR-222 activity causes significant loss of hMSCs 96 hours post transduction.....	156
Figure 4-14 P57 mRNA and protein expression 24hr, 48hr and 72 hour after induction of adipogenesis.....	160
Figure 4-15 P27 mRNA and protein expression 24hr, 48hr and 72 hour after induction of adipogenesis.....	162
Figure 4-16 Co-expressing miR-221 and miR-222 does not reduce p27 transcript during adipogenesis.....	163
Figure 4-17 Co-expressing miR-221 and miR-222 significantly reduces p27 protein 72 hours after the induction of adipogenesis.....	164
Figure 4-18 Luciferase reporter construct and Renilla vector construct used to identify relationship between miR-221/222 and p27.....	167
Figure 4-19 Luciferase Reporter assay identifies a direct relationship between miR-221/222 and p27.....	168
Figure 4-20 Luciferase activity of P27 luciferase reporter construct is significantly increased upon inhibition of miR-221 and/or miR-222.....	170
Figure 4-21 The inhibition of miR-221 or miR-222 activity causes a significant increase in the expression of p27 transcript.....	171
Figure 4-22 Transfection of 293Ts with pWPT-p27 vector significantly reduces cell number compared to control population.....	174
Figure 4-23 Transduction of MSCs with PWPT-p27 vector significantly reduces cell number compared to control population.....	174
Figure 4-24 Outline of p27 'add-back' to MSCs overexpressing miR-221 and 222 with appropriate controls.....	175
Figure 4-25 Transduction of hMSCs with PWPT-p27 vector causes an increase in p27 protein expression.....	176
Figure 4-26 Transduction of miR-221/222 overexpressing hMSCs with PWPT-p27 vector does not recover adipogenesis.....	178
Figure 4-27 Potential miR-221 and miR-222 targets: PGC1 $\alpha$ and TLE3 show increased expression 72 hours post induction of adipogenesis.....	182

**Figure 4-28 Potential miR-221 and miR-222 targets, MAP3K2, OSBPL3 and RFX7 show decreased expression 72 hours post induction of adipogenesis.....183**  
**Figure 4-29 Potential miR-221 and miR-222 targets, GPD and KLF2 show decreased expression 72 hours post induction of adipogenesis.....184**  
**Figure 4-30 Potential miR-221 and miR-222 targets, Mdm2 and FABP2 does not change in expression 72 hours post induction of adipogenesis.....185**  
**Figure 4-31 Expression of the potential miR-221/222 target PGC1 $\alpha$  protein cannot be detected in hMSCs undergoing adipogenesis.....187**  
**Figure 4-32 Expression of the potential miR-221/222 target TLE3 protein in the first 72 hours of hMSC adipogenesis.....189**

## List of Tables

Table 1-1 Differences in morphology, function and expression of genes involved in metabolism between a white fat cell and a brown fat cell.....	12
Table 1-2 Subset of Currently Available MiRNA Prediction Algorithms.....	28
Table 2-1 MSC donor information.....	45
Table 2-2 gag primer information.....	62
Table 2 -3 Jet Pei transfection of 293Ts with Luc-P27 or Luc-Empty in combination with miR-126/scramble shRNA, miR-221/sh-221, miR-222/sh-222 or a combination of miR-221 and miR-222 or sh-221 and sh-222.....	67
Table 2 -4 Jet Pei transfection of 293Ts with pWPT-GFP or pWPT-p27 vector.....	69
Table 2-5 Primers used for RT-PCR.....	72
Table 2-6 MicroRNA-specific reverse transcription mastermix.....	73
Table 2 -7 MicroRNA specific PCR mastermix.....	74
Table 2 -8 TaqMan MicroRNA specific probes used for RT-PCR.....	75
Table 2-9 MiChip labelling mastermix.....	77
Table 2-10 MiChip precipitation mix.....	78
Table 2-11 Post-hybridization washing protocol.....	79
Table 2-12 Primary Antibodies used in Western Blot Analysis.....	83
Table 3-1 Comparison of miRNA expression changes analysed by microarray and RT-PCR.....	117
Table 3-2 Published roles for identified miRNAs from microarray associated with MSC functions.....	126
Table 4-1 Potential miR-221 and miR-222 targets, their possible role in adipogenesis and the region of 3' UTR containing putative miR-221/222 binding sites.....	181
Table 4-2 Expression of potential miR-221/222 targets 72 hours post induction of adipogenesis.....	186
Table 5-1- P27 research in adipogenesis of 3T3L1 cells and hMSCs.....	216

## Abstract

The current epidemic of obesity has resulted in a renewed interest in the developmental origins of adipose tissue. Adipose tissue is formed from mesenchymal stem cells (MSCs) in a process known as adipogenesis. MicroRNAs (miRNAs) are small non-coding RNAs that inhibit translation by binding to the 3'UTR of their target genes. The aim of this study was to determine whether miRNAs play a role in the adipogenesis of bone marrow derived MSCs. Microarray analysis identified 20 miRNAs which were significantly regulated in adipogenically differentiating MSCs compared to undifferentiating MSCs, of which 11 were significantly downregulated and 9 were significantly upregulated. MiR-221 and miR-222 were significantly downregulated during hMSC differentiation to adipocytes. MiR-221 and miR-222 were overexpressed using lentiviral vectors to determine whether their reduction is necessary for adipogenic differentiation. MSCs overexpressing miR-221 and miR-222 displayed a significantly reduced ability to differentiate to adipocytes compared to control MSCs, as measured by lipid accumulation and expression of adipogenesis-related transcripts. MiRZip short hairpin RNAs (shRNAs) against miR-221 and miR-222 were lentivirally delivered to determine the effects of reduced miR-221 and miR-222 activity on hMSC adipogenesis. The reduction in activity of either miRNA caused a significant reduction in cell number. P27 is an experimentally confirmed target of miR-221 and miR-222 in cancer models. The overexpression of miR-221 and miR-222 reduced the levels of p27 protein but not mRNA 72 hours after the induction of adipogenesis. Direct interactions between the miRNAs and the 3'UTR of p27 were verified using luciferase reporters in HEK293T cells. To investigate whether preventing the reduction in p27 protein rescues the reduction in lipid accumulation, p27 was overexpressed in MSCs with reduced miR-221 and miR-222. This did not lead to a significant change in lipid accumulation in MSCs, suggesting that miR-221 and miR-222 do not act solely through an effect on this protein.

## Acknowledgements

From the bottom of my heart I would like to thank Dr. Linda Howard for everything she has done for me during my PhD; for all the encouragement, the excitement about results, for always having time for questions, for all the ‘nerdy science stuff’ and for the constant support and guidance. I’m so glad I was able to do my PhD with such an excellent supervisor.

To Prof. Frank Barry and everyone at REMEDI , both past and present; for their advice, support and of course for the craic and good times that we had! I couldn’t write these acknowledgements without mentioning the girls in the office- particularly Sinead and Janice. You two made it possible to have fun in the darkest of hours and truly are the silver lining of this final year!!

To the girls- To Siobhan, Aoife, Eleanor, Michelle, Gillian, Aisling, Gina, Lisa and Mary Quirke! I am grateful to each and every one of you for everything you have done during this time- for the cups of tea, the hugs, the phonecalls, the constant motivation, the ‘visits’ and most importantly; the listening ear. Thank you!

Thanks to John, Chris and Bronagh for being there through it all. Now finally that is the end of the ‘ student’ jokes!! Finally and ultimately to my parents- thanks for listening to me day in day out and for always believing in me. To Mom, my rock and my crutch who was there with me every step of the way. Your constant words of encouragement and support were what helped me to get through on the days when I thought I couldn’t. I would not have been able to do this without you- This is yours too!

## **Dedications**

**This thesis is dedicated to my parents, Tom and Breda.**

# Abbreviations

- **293T- Human Embryonic Kidney (HEK)293T cells**
- **3D – Three Dimensional**
- **AA2-P- Ascorbic acid 2-phosphate**
- **Ad -Adenovirus**
- **Adipo- Adipogenesis**
- **ADSC- Adipose-derived stem cell**
- **AIM- Adipogenic Induction Medium**
- **AMM- Adipogenic Maintenance Medium**
- **ANOVA - analysis of variance**
- **ASO- Antisense oligonucleotides**
- **BAT- Brown Adipose Tissue**
- **BM- Bone marrow**
- **BM-MSC -Bone marrow mesenchymal stem cells**
- **BMP- Bone morphogenic factor**
- **Bp – Base pair**
- **BSA-Bovine serum albumin**
- **C/EBP - CCAAT enhancer binding protein**
- **C-17- Nucleofector High Transfection program**
- **CCM- Complete Chondrogenic Medium**
- **CDK-Cyclin Dependent Kinase**
- **CDKN1A/B/C- Cyclin Dependent Kinase Inhibitor 1A/B/C**
- **cDNA – complementary DNA**
- **CKI- Cyclin dependent kinase inhibitor**
- **CKI- Cyclin Dependent Kinase Inhibitor**
- **CMV-Cytomegalovirus**
- **CO<sub>2</sub>-Carbon dioxide**
- **DAPI -4',6-diamidino-2-phenylindole**
- **DGCR8- Di-George Syndrome Critical Region 8**

- **DMEM – Dulbeccos Modified Essential Medium**
- **DMMB- Dimethylmethyline blue**
- **DMSO-Dimethyl sulfoxide**
- **DNA – Deoxyribonucleic Acid**
- **ECM -Extracellular matrix**
- ***E-Coli -Escherichia coli***
- **EDTA -Ethylenediamine tetraacetic acid**
- **ESC -Embryonic stem cell**
- **ESCC miRNAs- ES-cell-specific-cell cycle-regulating miRNAs**
- **FABP2- Fatty Acid Binding Protein 2**
- **FABP4- Fatty Acid Binding Protein 4**
- **FACS -Fluorescence activated cell sorting**
- **FBS-Fetal bovine serum**
- **FFA- Free Fatty Acid**
- **GAG -Glycosaminoglycan**
- **GAPDH- Glyceraldehyde 3-phosphate dehydrogenase**
- **gDNA- Genomic DNA**
- **GFP-Green fluorescent protein**
- **GPD2- Glycerol-3-phosphate dehydrogenase 2**
- **HCl-Hydrochloric acid**
- **HDAC4- Histone Deacetylase 4**
- **HITS-CLIP- High Throughput Sequencing of RNA isolated by Crosslinking Immunoprecipitation**
- **hMSC -Human mesenchymal stem cell**
- **HRP – Horse radish peroxidase**
- **hrs -Hours**
- **HSC- Hematopoietic stem cell**
- **HUVEC- Human Umbilical Vein Endothelial Cells**
- **IBMX/ MIX-3-methyl-isobutylxanthine**
- **ICM- Incomplete Chondrogenic Medium**

- **IPS- Induced Pluripotent Stem Cell**
- **IRES – Internal Ribosome Entry Site**
- **ISCT- International Society for Cellular Therapy**
- **ISCT- International Society for Cellular Therapy**
- **KLF3- Kruppel-Like Factor 3**
- **LB- Luria Bertani**
- **LNA- Locked Nucleic Acid**
- **Luc- P27- PMIR-Report vector containing 3'UTR p27**
- **Luc-Empty- PMIR-Report vector which does not contain a predicted 3' UTR**
- **MACS- Magnetic Activated Cell Sorting**
- **MAPK10- Mitogen-activated protein kinase 10**
- **MCE- Mitotic Clonal Expansion**
- **MDM2- Murine Double Minute 2**
- **Mins- Minutes**
- **MiRNA/ MiR- MicroRNA**
- **MOI -Multiplicity of infection**
- **mRNA- Messenger RNA**
- **MSC – Mesenchymal Stem Cell**
- **OSBPL3- Oxysterol binding protein-like 3**
- **PAR-CLIP- Photoactivable- Ribonucleoside-enhanced Crosslinking and Immunoprecipitation**
- **PBS-Phosphate buffered saline**
- **PCA- Principal Components Analysis**
- **PCR-Polymerase chain reaction**
- **PDGF – Platelet Derived Growth Factor**
- **PET/CT- Positron Emmission Tomography- Computed Tomography**
- **PGC1 $\alpha$ - PPAR $\gamma$  Co-activator- 1 $\alpha$**
- **PPAR $\gamma$  -Peroxisome proliferator activated receptor  $\gamma$**
- **PRDM16- PR Domain Containing 16**

- **pRL-Renilla Luciferase Vector Construct**
- **PVDF - Polyvinylidene Difluoride**
- **pWPT-GFP- GFP expressing vector**
- **pWPT-p27- p27 overexpression vector**
- **QC- Quality Control**
- **qRT-PCR – Quantitative Reverse Transcriptase PCR**
- **RCF-Relative centrifugal force**
- **RE – Restriction Enzyme**
- **RFX7- Regulatory factor X 7**
- **RISC- RNA Inteference Gene Silencing Complex**
- **RIN- RNA integrity number**
- **RLM-RACE- RNA Ligase Mediated-5' Rapid identification of cDNA Ends**
- **RNA Pol- RNA Polymerase**
- **RNA-Ribonucleic acid**
- **RPM-Revolutions per minute**
- **RT-PCR- Reverse transcription polymerase chain reaction**
- **RT-Reverse transcription**
- **SDS-PAGE-Dodium dodecyl sulphate polyacrylamide gel**
- **SDS-Sodium dodecyl sulphate**
- **SD-Standard deviation**
- **Sh-221/222- Short hairpin RNA against miR-221/222**
- **ShRNA- Short-hairpin RNA**
- **SiRNA- Small Interfering RNA**
- **TAE- Tris Acetate EDTA**
- **TBS-T- Tris Buffered Saline-Tween**
- **TGF-Transforming growth factor**
- **TLE3- Transducin-Like Enhancer protein 3**
- **TU/ml- Transducing Units per ml**
- **U-23- Nucleofector High Viability program**

- **UCP-1- Uncoupling Protein-1**
- **UTR- Untranslated Region**
- **WAT- White Adipose Tissue**

# 1 Introduction

## 1.1 Overview

Obesity is one of the biggest epidemics of the modern age. In 2008, the World Health Organization stated that there are 1.5 billion overweight adults in the world, of which 200 million men and 300 million women are obese. In 2010, 43 million children under the age of 5 were overweight. In Ireland, recent figures have shown that 61% of adults and 22% of children are overweight or obese (Oireachtas.ie 2011). Obesity is a multifactorial and complex condition (Kozak 2009) thought to develop either as a result of hypertrophy (increased adipocyte size) and hyperplasia (increased adipocyte number) or as a combination of both. This results in dysregulation of the normal functions of the adipose tissue. This is associated with conditions such as type II diabetes, hypertension and cardiovascular disease which are collectively known as metabolic syndrome (Spiegelman and Flier 1996; Kershaw and Flier 2004). This has propelled huge interest in the development and function of adipose tissue, of which adipocytes are the active cell. Adipose tissue is regarded to be of mesodermal origin and derived from mesenchymal stem cells (MSCs) in a process known as adipogenesis. In an attempt to further understand the origins of obesity, there is an increased focus on the factors involved in the pathway from MSC to adipocyte to adipose tissue formation.

In the past, research has been focused on transcription factors involved in the development of adipose tissue, with clear roles identified for the PPAR $\gamma$  and C/EBP families in regulating gene expression (Rosen, Walkey et al. 2000). Recently, non-coding RNAs, including microRNAs (miRNAs) have been identified as key regulators of eukaryotic gene expression with roles in nearly all developmental processes and proposed therapeutic implications in the areas of cancer and cardiovascular disease (Wahid, Shehzad et al. 2010).

Key roles are being elucidated for miRNAs in all aspects of adipose tissue development, including the development of white adipose tissue (WAT) (Esau, Kang et al. 2004; Kajimoto, Naraba et al. 2006), brown adipose tissue (BAT) (Sun, Xie et al. 2011) and in the development of obesity (Martinelli, Nardelli et al. 2010).

To maximise the development of therapeutic agents in the treatment of obesity, a comprehensive knowledge of all aspects of adipogenesis is required. This includes identifying the role of miRNAs in the pathway from undifferentiated MSC to adipocyte. It is hoped that the work in this thesis will help to address this by identifying the roles of miRNAs in adipogenesis of bone marrow derived human mesenchymal stem cells (hMSCs).

This introduction will be divided into three main sections, focusing first on MSCs, the development of adipose tissue and the use of MSCs as a model for the study of human adipogenesis. This will be followed by a section on miRNAs, their biogenesis, mechanism of action and current methods of target prediction and identification. The introduction will finish on the roles of miRNAs in adipogenesis and their future therapeutic potential in the treatment of obesity.

## 1.2 Stem Cells

A stem cell is defined as ‘a cell from the embryo, foetus or adult that has, under certain conditions the ability to reproduce itself for long periods or in the case of adult stem cells throughout the life of the organism. It can also give rise to specialized cells that make up the tissues and organs of the body.’(The National Institute of Health (NIH)’s report ‘Stem cells: Scientific Progress and Future Research Directions’). A stem cell is characterized by two properties; self-renewal and the ability to differentiate. Stem cells can be divided into a number of categories based on their differentiation ability as seen in Figure1-1.

Totipotent stem cells are derived from the fertilized egg, before blastocyst formation and can differentiate into the embryo, the extraembryonic membranes and all post embryonic tissues and organs.

Embryonic stem (ES) cells, derived from the inner cell mass of the blastocyst are pluripotent, meaning that they have the capacity to form cells from all three germ layers and presumably differentiate to any of the known 200 different cell types that make up the human body. These cells have great therapeutic potential but remain subject to ethical concerns regarding the destruction of human embryos required to obtain them.

In 2006, retroviral transduction of fibroblasts with 4 transcription factors (Oct3/4, Sox2, KLF4 and c-Myc) caused the cells to take on properties similar to those of an embryonic stem cell (Takahashi and Yamanaka 2006). These cells were named Induced Pluripotent Stem Cells (iPS) and potentially provide an alternative to ES cells for studying and treating human disease. IPS cells are potentially more useful than ES cells as they avoid the ethical issues while retaining the pluripotent differentiation capability. Epigenetic reprogramming is a critical event in the formation of iPS cells. As a somatic cell becomes an iPS cell, the transcriptional network begins to gradually switch from a somatic to a pluripotent state which is associated with large changes in epigenetic marks (Mattout, Biran et al. 2011). IPS cells display different epigenetic patterns of methylation to ES cells. These differences in methylation decrease with continuous passaging as the iPS cell loses the characteristics of the parent cell and resembles an ES cell more closely (Nishino,

Toyoda et al. 2011). Clearly, iPS research is still in its infancy with limited information available on the duration of nuclear reprogramming, the stability of the epigenetic changes, the presence of transgenes in the cell and teratoma formation (Yamanaka 2009; Hanna, Saha et al. 2010).

Many adult or ‘tissue’ stem cells are multipotent cells which have a more limited capacity than pluripotent cells and can differentiate into a number of cells from the within the same germ layer, while unipotent stem cells differentiate to form one type of differentiated cell (e.g. dermal stem cell.)

Adult stem cells (e.g. Mesenchymal Stem Cells) have a more restricted differentiation potential than ES cells but are not as ethically problematic. They can be easily isolated from a number of tissues and have reduced tumorigenicity concerns. The work described in this thesis is focused solely on mechanisms of differentiation of adult human Mesenchymal Stem Cells (hMSCs) isolated from the bone marrow (BM).

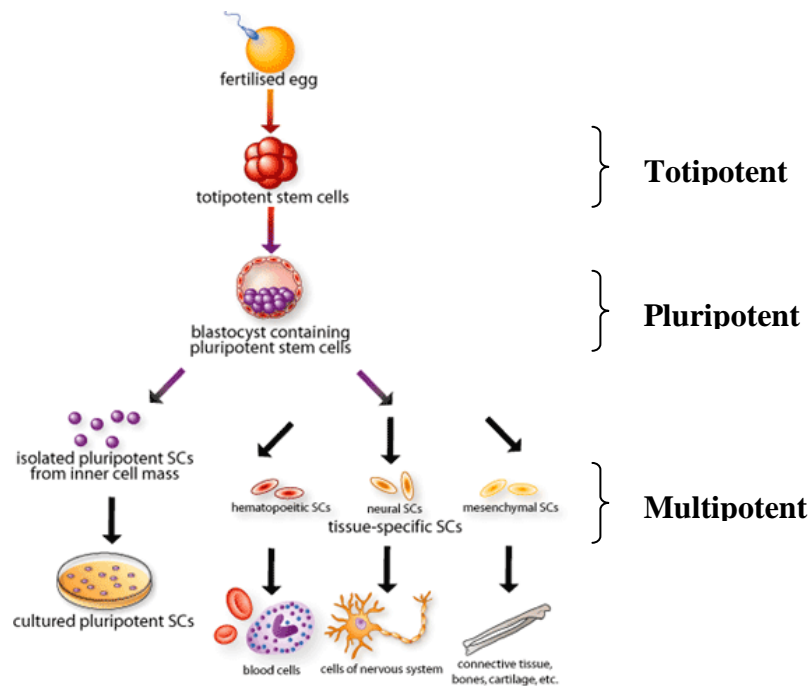


**Figure 1-1 Differentiation ability of Stem Cells**

Image adapted from <http://www.adult-stemcell-research.com/>

### 1.2.1 Mesenchymal Stem Cells

The bone marrow harbours two populations of stem cells; hematopoietic stem cells (HSC) and mesenchymal stem cells (MSC). HSCs are an extremely well characterized population of cells and their ability to generate and maintain the hematopoietic system has been exploited clinically (Giarratana, Kobari et al. 2005). In 1966, Friedenstein *et al* isolated the much rarer MSCs (0.01-0.001% of nucleated marrow cells) for the first time based on their ability to adhere to the tissue culture plastic (Friedenstein, Piatetzky et al. 1966). MSCs can differentiate to adipocytes, osteocytes and chondrocytes (Pittenger, Mackay et al. 1999), skeletal myoblasts (Bujan, Pascual et al. 2006) and cardiac myocytes (Xu, Zhang et al. 2004). Subsequently, MSCs have been isolated from nearly every tissue in the body including adipose tissue (Zuk, Zhu et al. 2001), dental pulp (Pierdomenico, Bonsi et al. 2005), skeletal muscle (Young, Mancini et al. 1995), umbilical cord blood (Bieback, Kern et al. 2004) and placenta (Castrechini, Murthi et al. 2010). The presence of MSCs in many tissues makes them an easily accessible source of cells from patients. This, combined with their limited immunogenicity (Uccelli, Moretta et al. 2006) and their ability to differentiate to numerous different cell types makes them a very attractive source of cells in the field of regenerative medicine and they are currently being evaluated in clinical trials. Despite this however, there is an incomplete understanding of the regulation of differentiation, commitment and plasticity of this cell population. An additional aim of this work is to increase the knowledge of this population by investigating the roles of miRNAs in hMSC adipogenesis.

### 1.2.1.1 Isolation and *In Vitro* Characterization of Mesenchymal Stem Cell

The MSCs used in the work described in this thesis are isolated from the superior iliac crest of the pelvis. MSCs can be isolated by direct plating of the bone marrow (BM) aspirate. The MSCs adhere to the tissue culture plastic whereas the HSCs and other cells present do not and can hence be removed through repeated media changes (Luria, Panasyuk et al. 1971). Alternatively, MSCs can be isolated based on the fractionation of the BM aspirate on a density gradient solution, which separates cell populations based on their density (Dazzi, Ramasamy et al. 2006). Recently, a number of groups are isolating MSCs by sorting the bone marrow based on expression of cell surface markers (CD271, CD56 and W5C4 antigen amongst others) (Deschaseaux, Gindraux et al. 2003; Rozemuller, Prins et al. 2010). Upon isolation, the hMSCs are cultured in a basal medium such as Dulbecco's modified essential medium (DMEM), in the presence of 10% fetal bovine serum (FBS) and an antibiotic solution. The medium is changed every 3-4 days which allows the cells to divide rapidly into single-cell derived colonies. As the cells reach high density, the colonies begin to coalesce and a larger, flatter morphology is evident (Pittenger, Mackay et al. 1999; Sekiya, Larson et al. 2002).

Differences in methods of isolation, culture methods and assessment of differentiation potential between labs have led to debate in the research community over the precise characteristics and definition of an MSC. In 2006, a report from the International Society for Cellular Therapy (ISCT) was published to clarify the definition of an MSC and its characterization, particularly in terms of cell surface markers. The ISCT stated that “multipotent mesenchymal stromal cell’ (MSC) is the currently recommended designation for the plastic-adherent cells isolated from BM and other tissues that have often been labelled mesenchymal stem cells.” They propose criteria with which to define MSCs. These include a requirement for the cells to adhere to plastic upon culturing and to differentiate to osteoblasts, adipocytes and chondrocytes upon standard *in vitro* differentiation conditions. MSCs must express the surface markers CD105, CD73 and CD90 ( 95% of the population) as measured by flow cytometry. They must lack expression of CD45,

CD34, CD14 or CD11b, CD79 $\alpha$  or CD19 and ~~H2A~~ class II (positive)(Dominici, Le Blanc et al. 2006).

### **1.2.1.2 Differentiation of Mesenchymal Stem cells *in Vitro***

MSCs are capable of multipotent differentiation, in that they can differentiate to cell types including osteoblasts, adipocytes and chondrocytes (Pittenger, Mackay et al. 1999). Although controversy exists, there is some evidence showing the differentiation of MSCs into neuronal cells (Jiang, Lv et al. 2010), cardiac myocytes (Xu, Zhang et al. 2004) and skeletal myoblasts (Saito, Dennis et al. 1995). Differentiation to adipogenic, osteogenic and chondrogenic lineages was used to characterize the cells used in this work. This will be discussed further in section 2.1.2.

### **1.3 Obesity and the Development of Adipose Tissue**

Adipose tissue was traditionally viewed as a reservoir merely for energy storage. However, it is now known that adipose tissue is a true endocrine organ capable of expressing and secreting endocrine hormones such as leptin and adiponectin. It is thus involved in neuroendocrine and immune functions as well as energy metabolism (Serrero and Lepak 1996; Kershaw and Flier 2004). The key role of adipose tissue as an endocrine organ is emphasised in times of excess adipose tissue which occurs either due to an increase in the size of the adipocytes (adipocyte hypertrophy) or an increase in the number of adipocytes (adipocyte hyperplasia). This is associated with metabolic diseases such as obesity, type II diabetes, hypertension and cardiovascular disease (Cristancho and Lazar 2011). The primary cell of adipose tissue is the adipocyte whose function is 'to store triacylglyceride during periods of calorific excess and to mobilize this reserve when expenditure exceeds intake' (Fruhbeck, Gomez-Ambrosi et al. 2001).

Adipose tissue is suspected to be of mesodermal origin however precise lineage tracing studies are yet to be performed. The adipocytes that make up the adipose tissue organ develop from MSCs in a process known as adipogenesis (Gesta, Tseng et al. 2007; Cristancho and Lazar 2011).

In mammals, the adipose tissue organ contains two distinct types of adipose tissue; white adipose tissue (WAT) and brown adipose tissue (BAT), which differs significantly from each other in development, morphology, function and gene expression.

### **1.3.1 White Adipose Tissue (WAT)**

WAT is the main form of adipose tissue in adult humans and is found in subcutaneous regions, such as the buttocks, thighs and abdomen and surrounding visceral organs, such as the omentum and intestines. It stores energy as triglycerides in lipid droplets which are used in times of fuel requirement such as fasting or starvation. Energy is supplied through the release of free fatty acids (FFAs) into the plasma by lipolysis where they are oxidized to provide energy (Arner 2003). Along with FFAs, WAT can release other factors such as tumour necrosis factor  $\alpha$  (TNF  $\alpha$ ), interleukin 6 and transforming growth factor  $\beta$ . This may account, at least in part for the development of insulin resistance which occurs during obesity (Arner 2003; Gesta, Tseng et al. 2007). WAT possesses a huge capacity for expansion and when the intake of energy exceeds energy expenditure, the excess energy is stored as excess adipose tissue. This increased adipose tissue mass initially leads to weight gain and can thus lead to obesity (Spiegelman and Flier 1996).

### **1.3.2 Brown Adipose Tissue (BAT)**

In direct contrast to the role of WAT, BAT is involved in the burning of fat and thus acts to expend energy rather than store it. This is achieved through a process known as adaptive thermogenesis. In this process, brown adipocytes release energy as heat by uncoupling respiration from ATP synthesis. This is mediated by the uncoupling-protein 1 (UCP-1), a protein highly expressed in BAT, but not in WAT (Billon and Dani 2011). The role of BAT in maintaining the energy balance and the prevention of obesity is well established in rodents and while there are suggestions that it plays the same role in adult humans, this remains to be confirmed. Until recently, it was believed that BAT was only present in small mammals and in newborn human infants where it functions to maintain body temperature. An insignificant and presumed non-functional amount of BAT was thought to be present in the adult human. However, recent morphological and PET/CT scanning techniques (Nedergaard, Bengtsson et al. 2007; Cypess, Lehman et al. 2009) have shown that although BAT does significantly decrease with aging (as the infant develops), there is a significant amount of metabolically active BAT present in the adult.

### 1.3.3 Differences between WAT and BAT

Recent studies have revealed that WAT and BAT differ in their developmental origins (Gesta, Tseng et al. 2007). There is evidence to suggest that although white and brown adipocytes develop from MSCs, there is a divergence between white pre-adipocytes and brown pre-adipocytes early in development (Figure 1-2) (Cristancho and Lazar 2011). In addition, lineage tracing experiments have shown that BAT and skeletal muscle are closer in developmental origins than WAT and BAT (Seale, Bjork et al. 2008). In fact, brown adipocytes and skeletal myocytes share a common progenitor until a transcription factor PRDM16 dictates their fate (Seale, Kajimura et al. 2007; Seale, Bjork et al. 2008).

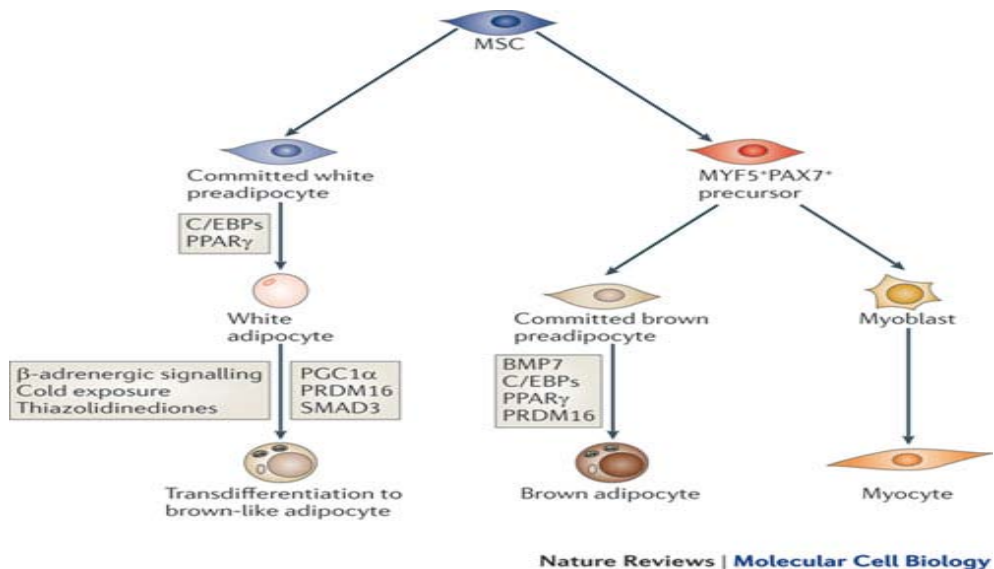


**Figure 1-2 Relationship between white and brown adipogenesis (Cristancho and Lazar 2011)**

As discussed above, both WAT and BAT are involved in energy balance but, while WAT acts mainly to store energy, BAT functions to dissipate energy in the form of heat during cold- and diet-induced thermogenesis (Rosen and Spiegelman 2000; Billon, Monteiro et al. 2008). In addition, BAT differs morphologically from WAT- BAT cells store lipid in multiple small fat droplets while lipid is stored in one large droplet which encompasses nearly the entire cell in cells from WAT. BAT possesses numerous mitochondria with many cristae and expresses uncoupling

protein-1 (UCP-1) at a high level in the cell compared to WAT (Ricquier and Bouillaud 2000). It also exhibits greater vascularisation than WAT. The differences in morphology, function and expression of genes involved in metabolism between a white fat cell and a brown fat cell are listed in Table 1-1.

<b>Characteristics</b>	<b>White fat cell</b>	<b>Brown fat cell</b>
<b>Morphology</b>	Unilocular appearance (single fat droplet)  Large cells (up to 200µm)	Multilocular appearance (numerous small lipid droplets)
<b>Function</b>	Storage of energy as triglycerides and mobilization as fatty acids  Secretion of adipocytokines (+++)*	Fat oxidation and thermogenesis  Secretion of adipocytokines (+)
<b>Expression of genes involved in metabolism</b>	Uncoupling protein 1 (0) Uncoupling protein 2 (+++) Uncoupling protein 3 (+/-) Subunit c of FO-ATPase (+) Respiratory chain genes (+) Fatty acid oxidation enzymes (+) Glycerol kinase (+/-)	Uncoupling protein 1 (+++) Uncoupling protein 2 (+) Uncoupling protein 3 (+) Subunit c of FO-ATPase (+/-) Respiratory chain genes (+++) Fatty acid oxidation enzymes (+++) Glycerol kinase (+++)

*\*no (0), very low or uncertain (+/-), moderate (++) and high (+++) expression.*

**Table 1-1- Differences in morphology, function and expression of genes involved in metabolism between a white fat cell and a brown fat cell**

Adapted from Langin et al (Tiraby and Langin 2003)

### 1.3.4 Conversion of WAT to BAT

The conversion of white fat (which normally specializes in the storage of energy) to brown-like fat cells (which actively release energy in the form of heat) is a very appealing and potentially therapeutically beneficial approach to tackling the problem of obesity. Manipulating the stores of WAT has not, in the past proved to be therapeutically advantageous- the disruption of normal differentiation instead leads to ectopic lipid storage and lipodystrophy in experiments performed (Seale, Bjork et al. 2008). However, experiments that increase BAT in animals display positive results, with the animals displaying a lean and healthy phenotype (Ghorbani, Claus et al. 1997). Furthermore, the loss of BAT function is associated with obesity (Lowell, V et al. 1993).

Elabd *et al* have shown that the treatment of human multipotent adipose-derived stem cells (hMADS) with the PPAR $\gamma$  agonist, rosiglitazone led to a switch from white adipose phenotype to a brown adipose phenotype (Elabd, Chiellini et al. 2009). A switch to the brown adipose phenotype was measured by the strong expression of UCP-1 mRNA and CIDEA (associated with UCP-1 expression in brown adipocytes) mRNA. An increase in the levels of mitochondrial carnitine palmitoyltransferase (CPT1B) was also observed, which is a sign of enhanced mitochondrial activity accompanied by an increase in oxygen consumption and uncoupling. The adenoviral transduction of human bone-marrow derived MSCs with PPAR $\gamma$  co-activator 1  $\alpha$  (PGC1- $\alpha$ ) significantly increased the expression of genes involved in mitochondrial activity and respiration (Huang, Chen et al. 2011). During adipogenic differentiation, these cells showed an increase in expression of brown fat markers and a decrease in the expression of markers of white adipogenesis. In addition, there were significant increases in the expression of thermogenic markers; cytochrome C and complex II. Interestingly, the overexpression of PGC1- $\alpha$  in MSCs inhibited the ability of the cell to differentiate to osteocytes (Huang, Chen et al. 2011). This evidence highlights PGC1- $\alpha$  as a potential therapeutic agent for the manipulation of MSCs towards a brown adipocyte phenotype. In a therapeutic setting, MSCs treated with an agent that elevates the levels of PGC1- $\alpha$ , such as BMP-2 could potentially be administered to obese

patients as a means of elevating the levels of brown fat present in the body (Huang, Chen et al. 2011).

## **1.4 Study of Adipogenesis**

Most of what is known of the process of adipogenesis has been gleaned from studies of the committed murine pre-adipocyte cell lines such as the 3T3-L1 and F442A lines established by Howard Green (Green and Meuth 1974). These fibroblast-like cells differentiate to fat cells when treated with the appropriate adipogenic stimulus. They are used as an appropriate model for studying the factors involved in differentiation from pre-adipocyte to mature adipocyte. As these cells possess a prior commitment to the adipogenic lineage, they are not ideal for studying the commitment step of adipogenic differentiation. The use of human pre-adipocytes as a model for adipogenesis is limited by their reduced proliferative ability, relative difficulty obtaining cells and variability between cells from different donors (Hauner and Entenmann 1991). Most importantly as with the 3T3-L1 cells, human pre-adipocytes are also committed to the adipogenic lineage (Entenmann and Hauner 1996).

### **1.4.1 Adipogenic Differentiation of Rodent 3T3L1 Cells**

Adipogenic differentiation of 3T3L1 cells is a very well characterized process which occurs in a number of key steps. The cells are grown to confluence where they undergo growth arrest. Adipogenic differentiation is induced using standard Dulbecco's modified Eagle's medium, 10% fetal bovine serum (FBS) and a combination of insulin, dexamethasone and IBMX (Scott, Nguyen et al. 2011). This causes the cells to re-enter the cell cycle and rapidly proliferate, known as 'mitotic clonal expansion' (MCE) (Tang, Otto et al. 2003). The prevention of this step is enough to inhibit adipogenic differentiation in this cell line (Reichert and Eick 1999). Next the cells enter a stage of post-mitotic, pre-differentiation growth arrest known as  $G_D$ . Then as differentiation begins, the cells enter a third and irreversible state of growth arrest concomitant with terminal differentiation (Morrison and Farmer 1999).

### **1.4.2 Adipogenic Differentiation of MSCs**

MSCs have emerged as an alternative system in which to study factors involved in human adipogenic differentiation, as well as a model to study the factors involved in commitment to the adipogenic lineage (Pittenger, Mackay et al. 1999; Janderova, McNeil et al. 2003). There is, however relatively limited information available regarding differentiation from MSC to mature adipocyte. It is often written that MSCs differentiate to preadipocytes and then to mature adipocytes where the conversion of the stem cell to pre-adipocyte is known as the determination or commitment step. The pre-adipocyte appears morphologically indistinguishable from the stem cell but has lost the potential to differentiate to other lineages (Rosen and MacDougald 2006; Gesta, Tseng et al. 2007). The next step, known as the terminal differentiation step occurs when the preadipocyte differentiates to a mature adipocyte. However, there is very little evidence to support this scenario and attempts to characterize an intermediary stage between the MSC and the mature adipocyte have proven unsuccessful (Rosen and Spiegelman 2000).

As mentioned, studies have shown that preventing the mitotic clonal expansion step in 3T3L1 cells prevents adipogenic differentiation (Reichert and Eick 1999). In contrast, there is no evidence of proliferation occurring in hMSCs or human preadipocytes after induction of adipogenesis (Qian, Li et al. 2010). MSCs and human preadipocytes treated with agents that block replication showed no difference in adipogenic differentiation compared to untreated cells (Janderova, McNeil et al. 2003) (Entenmann and Hauner 1996). Clearly, there are several important differences between human and rodent adipogenesis and further investigation is necessary to elucidate precisely what these differences are. Importantly, findings from studies of rodent adipogenesis are not necessarily transferable to human adipogenesis.

### 1.4.3 Transcriptional Regulation of Adipogenesis

Adipogenic differentiation depends on the coordinated regulation of a cascade of transcription factors for adipogenesis to successfully proceed as seen in figure 1-3, taken from (Rosen 2005). Most research has been focused on the roles of the transcription factor peroxisome proliferator-activated receptor gamma (PPAR $\gamma$ ) and members of the CCAAT-enhancer binding proteins (C/EBP) family.

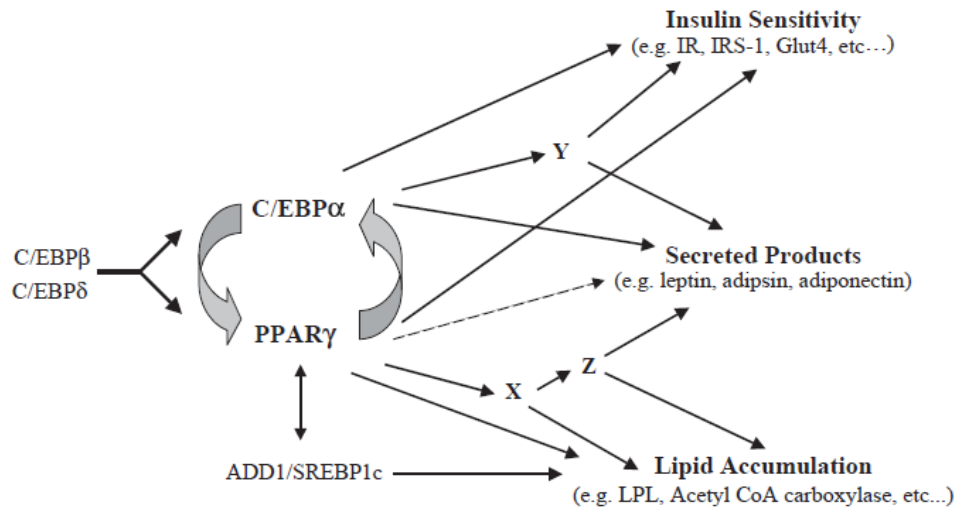


**Figure 1 -3 Transcriptional Cascade involved in Adipogenic Differentiation (Rosen 2005)**

#### **1.4.3.1 C/EBP Family**

The C/EBP family are members of the basic-leucine zipper class of transcription factors. C/EBP $\alpha$ ,  $\beta$ , and  $\delta$  play key roles in the progression of adipogenesis. Early after induction of adipogenesis in 3T3L1s both C/EBP $\beta$  and C/EBP $\delta$  mRNA and protein rises transiently (Yeh, Cao et al. 1995; Darlington, Ross et al. 1998). The forced expression of C/EBP $\beta$ , but not C/EBP $\delta$  is sufficient to induce differentiation in 3T3L1s without other adipogenic stimuli. Adipogenesis is accelerated in 3T3L1s with forced expression of C/EBP $\delta$  but the cells do not differentiate without additional hormonal stimulation (Wu, Xie et al. 1995; Yeh, Cao et al. 1995; Rosen and Spiegelman 2000). Approximately 85% of mice lacking the C/EBP $\beta$  and C/EBP $\delta$  genes (generated by gene targeting) died at an early neonatal stage. Of those remaining, the epididymal fat weight weighed significantly less in C/EBP $\beta$  (-/-)  $\delta$  (-/-) mice than wild-type mice. Primary embryonic fibroblasts isolated from C/EBP $\beta$  (-/-)  $\delta$  (-/-) mice showed a decreased ability to differentiate to adipocytes, demonstrating their necessity for adipogenesis (Tanaka, Yoshida et al. 1997).

C/EBP $\beta$  and C/EBP $\delta$  act to induce the expression of a third C/EBP member; C/EBP $\alpha$  and the transcription factor PPAR $\gamma$  (Wu, Bucher et al. 1996; Rosen 2005) *In vivo* studies have shown a very clear role for C/EBP $\alpha$  in the progression of adipogenesis. Mouse embryonic fibroblasts (MEFs) from C/EBP $\alpha$  null embryos showed little capacity to differentiate and interestingly showed very little expression PPAR $\gamma$  (will be discussed in further detail below) (Wu, Rosen et al. 1999)

#### **1.4.3.2 PPAR $\gamma$**

PPAR $\gamma$  is a member of the nuclear-receptor superfamily which has a critical role in the progression of adipogenesis. It is known as the ‘master regulator’ of adipogenesis because a factor has not been identified that can promote adipogenic differentiation in the absence of PPAR $\gamma$  (Rosen, Walkey et al. 2000). In addition, the forced expression of PPAR $\gamma$  in murine fibroblasts and myoblastic cell lines was sufficient to induce adipogenesis (Tontonoz, Hu et al. 1994; Hu, Tontonoz et al. 1995). Results show that PPAR $\gamma$  is necessary not only to induce adipogenesis but also to maintain the differentiated state. Expression of a dominant-negative PPAR $\gamma$

caused loss of lipid accumulation and decreased expression of adipogenic markers when delivered to differentiated 3T3L1 cells (Rosen and MacDougald 2006). The role of PPAR $\gamma$  in adipocyte development and function *in vivo* has been shown in a number of mouse models. PPAR $\gamma$   $-/-$  embryos died early in gestation (e10-e10.5) due to failure of normal placental development (Barak, Nelson et al. 1999). This model could not be used to study the role of PPAR $\gamma$  in adipose tissue development, therefore chimeric mice were generated using PPAR $\gamma^{+/+}$  and PPAR $\gamma^{-/-}$  embryonic stem cells (Rosen, Sarraf et al. 1999). This study highlighted the importance of PPAR $\gamma$  in adipose tissue development *in vivo* with the result that adipose tissue was preferentially derived from the wild type cells ( PPAR $\gamma^{+/+}$  ES cells). This group then performed *in vitro* differentiation of wild type and PPAR $\gamma^{-/-}$  ES cells and showed wild type cells to successfully achieve adipogenic differentiation while PPAR $\gamma^{-/-}$  cells failed to express markers of differentiation or accumulate lipid.

#### **1.4.3.3 A Cascade of transcription factors work together to promote adipogenesis**

A model of how adipogenic transcription factors work together to promote the differentiated adipogenic state is shown in figure 1-3. The model predicts that C/EBP $\beta$  and C/EBP $\delta$  are the first transcription factors induced after initiation of differentiation and these act to induce expression of PPAR $\gamma$  and C/EBP $\alpha$ . Current evidence suggests that expression of PPAR $\gamma$  is first induced by C/EBP $\beta$  and C/EBP $\delta$ , and PPAR $\gamma$  then induces expression of C/EBP $\alpha$  (Rosen and Spiegelman 2000). This is supported by a study showing PPAR $\gamma$  null ES cells fail to form adipocytes when exposed to differentiation medium *in vitro* and fail to express normal levels of C/EBP $\alpha$  even though expression of C/EBP $\beta$  and C/EBP $\delta$  is unaffected (Rosen, Sarraf et al. 1999). Importantly, a positive feedback loop occurs between C/EBP $\alpha$  and PPAR $\gamma$  where C/EBP $\alpha$  acts to maintain an elevated state of PPAR $\gamma$  throughout adipogenic differentiation (Wu, Rosen et al. 1999). C/EBP $\alpha$  null fibroblasts have reduced expression of PPAR $\gamma$  and show a reduced capacity to differentiate. The restoration of C/EBP $\alpha$  expression via a retrovirus encoding the transcription factor was sufficient to rescue PPAR $\gamma$  expression and also adipogenic

differentiation (Wu, Rosen et al. 1999). ADD1/SREBP1 is a highly expressed transcription factor with a potential role in adipogenesis. The overexpression of this factor increases differentiation, likely by inducing PPAR $\gamma$  expression (Kim, Wright et al. 1998; Fajas, Schoonjans et al. 1999)

#### **1.4.3.4 Role of Cell Cycle Proteins in the Progression of Adipogenesis**

As well as the transcription factors described above, the progression of adipogenesis also depends on the regulation of the cell cycle. Normal cell cycle control is dependent on a series of serine/threonine kinases called the cyclin-dependent kinases (CDKs), of which there are 7 in mammals (Lees 1995). The activity of each CDK is dependent upon the availability of a particular cyclin (the positive regulatory subunit of a CDK) and on the expression of a specific CDK inhibitor (CKI) (Dai and Grant 2003) (Nakayama and Nakayama 2006). A CKI is a protein that interacts with a cyclin-CDK complex to block kinase activity in response to signals from the environment or from damaged DNA. CKIs are divided into two major families based on evolutionary origins, structure and CDK specificities: the Ink4 (Inhibitor of CDK4) family and the Cip/Kip (Kinase Inhibitor Protein) family (Dai and Grant 2003). The Ink4 family includes p16<sup>Ink4a</sup>, p15<sup>Ink4b</sup>, p18<sup>Ink4c</sup> and p19<sup>Ink4d</sup> and specifically inhibits CDKs 4 and 6. The Cip/Kip family contains p21<sup>cip1</sup>, p27<sup>kip1</sup>, p57<sup>kip2</sup> which can bind to both cyclin and CDK subunits and can thus modulate the activities of cyclin D-, E-, A- and B-CDK complexes (Dai and Grant 2003; Besson, Dowdy et al. 2008).

There is very little evidence demonstrating the role of the cell cycle in MSC adipogenesis with most work performed on 3T3L1 pre-adipocytes. This work suggests that the regulation of cell cycle-related proteins, including cyclins, cyclin-dependent kinases (CDKs) and CDK inhibitors (CKIs) is essential in the progression of adipogenesis in 3T3L1 cells (Abella, Dubus et al. 2005; Fu, Rao et al. 2005; Sarruf, Iankova et al. 2005). As discussed, CKIs consist of two families of proteins, the Cip (Kip) family and the Ink4 family which play key roles in the exit of cells from the cell cycle (Nakayama and Nakayama 2006). Studies of the expression of

members of the Kip and Ink4 families of CKIs revealed expression patterns concomitant with distinct states of growth arrest during 3T3L1 adipogenesis (Morrison and Farmer 1999). The important role of these CKIs in 3T3L1 cells is evident when a knockdown of P21 resulted in reduced adipogenesis (Inoue, Yahagi et al. 2008). There is evidence also to suggest that CKIs are also implicated in the progression of hMSC adipogenesis, as the expression of both P27<sup>KIP1</sup> and P18<sup>INK4</sup> increases as adipogenic differentiation proceeds. In addition, the knockdown of each CKI prevented the progression of hMSC adipogenesis (Kang, Choi et al. 2008). The loss of P27<sup>kip1</sup> in mice leads to obesity due to an increase in preadipocytes suggesting that CKIs may be important in the regulation of adipocyte number (Naaz, Holsberger et al. 2004).

Taken together, these studies suggest an important coupling between growth arrest and adipocyte differentiation. While the expression of CKIs can accurately be attributed to the well characterized stages of 3T3L1 adipogenesis, much research is necessary to elucidate the role of the cell cycle and its associated proteins in adipogenic differentiation of hMSCs.

## 1.5 MicroRNAs

MicroRNAs (MiRNAs) are a family of small (21-25 nucleotides), non-coding RNAs that negatively regulate gene expression at the post-transcriptional level (Ambros 2003; Bartel 2004). Originally discovered in *C.elegans*, they have subsequently been identified in many multicellular organisms including *Drosophila*, mice and humans. MiRBase is the primary online database for miRNA information such as nomenclature, level of conservation, sequence information, target prediction and links to other resources for all published miRNAs (Griffiths-Jones 2006; Griffiths-Jones, Grocock et al. 2006; Griffiths-Jones, Saini et al. 2008). MiRBase (Release 18) currently lists 1527 miRNAs annotated in humans although the development of new detection methods (Glazov, Cottee et al. 2008) and prediction software (Huang, Fan et al. 2007) will likely cause this number to increase. Initially, it was predicted that miRNAs regulated 30% of human genes, however recent work has demonstrated that the majority of human genes are regulated by miRNAs (Friedman, Farh et al. 2009).

### 1.5.1 History of miRNA Research

The first miRNA, *lin-4* was discovered in 1993 by Ambros *et al* in *C. elegans* when performing a genetic screen for defects in the temporal control of post-embryonic development (Lee, Feinbaum et al. 1993; Wightman, Ha et al. 1993). They found that mutations in the *lin-4* gene disrupted the temporal regulation of *C. elegans* larval cell development. Previous work had shown that mutation of a gene encoding a nuclear protein *lin-14*, resulted in the opposite phenotype to a *lin-4* mutation (Ambros and Horvitz 1984). Further investigation revealed that *lin-4* encodes a 22-nucleotide non-coding RNA that has partial complementarity to the 3' UTR of the *lin-14* gene (Lee, Feinbaum et al. 1993) and acts to prevent translation of LIN-14 protein. A number of years later, a second miRNA was discovered, *let-7* which, similar to *lin-4*, binds to the 3' UTR of *lin-41* and *lin-57* and prevents their translation (Abrahante, Daul et al. 2003). Since then, the number of identified miRNAs has risen dramatically and miRBase (Release 18)

<http://www.mirbase.org/blog/2011/11/mirbase-18-released/>) now contains 18,226 entries which represents 21,643 mature miRNA products in 168 species

### 1.5.2 Genomic Location of miRNAs

MiRNAs are found in a number of different genomic settings as seen in figure 1-4. MiRNAs can be located intergenically in regions that are distinct from known transcription units. They can be located in the introns of coding or non-coding genes. The majority (40-70%) of all vertebrate miRNAs are intronic (Rodriguez, Griffiths-Jones et al. 2004). Figure 1-4B shows that introns can also encode another class of miRNA precursor- the 'mirtron'. The 'mirtron'- a term coined by the Bartel group (Ruby, Jan et al. 2007) is a miRNA precursor that is processed by a distinct, drosha-independent pathway. Two groups identified 14 short introns in *Drosophila*, and 4 in *C.Elegans* that mimic the structural features of pre-miRNAs, enter the miRNA-processing pathway after the microprocessor stage and give rise to ~22nt mature miRNAs (Okamura, Hagen et al. 2007; Ruby, Jan et al. 2007). Mammalian mirtrons have also been identified (Berezikov, Chung et al. 2007) but they have yet to be identified in plants. A small number of miRNAs are found overlapping the exons of non-coding transcripts and more rarely overlapping the exons of coding transcripts. In this case, the miRNA and the host gene are thought to be regulated by the host gene promoter (Rodriguez, Griffiths-Jones et al. 2004)

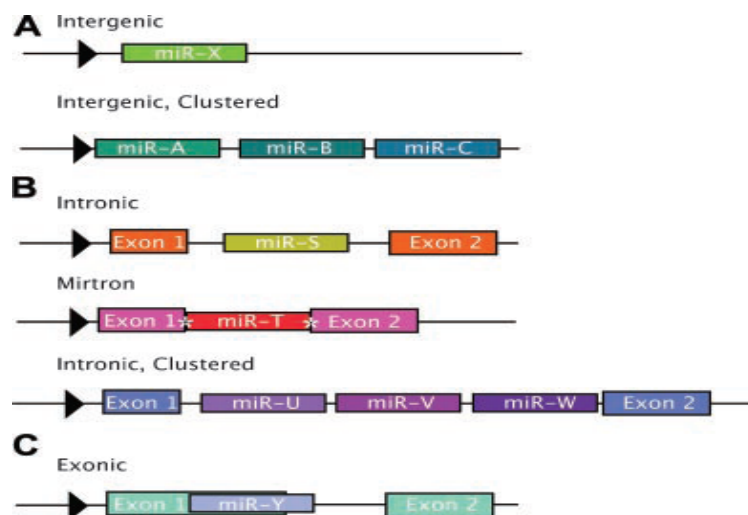


Figure 1-4 Genomic location of miRNAs (Olena and Patton 2009)

### 1.5.3 Biogenesis of miRNAs

The biogenesis of a mature and functional miRNA occurs via a number of key steps as seen in figure 1-5.

- 1- MiRNAs, transcribed in the nucleus by RNA polymerase II (Pol II), have a 7-methylguanosine cap and a 3' polyadenylated tail (poly (A)tail) (Cai, Hagedorn et al. 2004; Lee, Kim et al. 2004).
- 2- The cap and poly (A) tail are removed during subsequent processing. At this stage, the transcript has a stem-loop structure and is referred to as the pri-miRNA. Pri-miRNAs can be several kilobases in length and may contain one (monocistronic) or multiple (polycistronic) stem loop structures (Lee, Jeon et al. 2002).
- 3- In the nucleus, the long pri-miRNA is 'cropped' by the microprocessor complex to generate a precursor miRNA (pre-miRNA). The microprocessor complex (~650kDa) consists of the RNase III enzyme drosha and co-factors including the double-stranded RNA binding protein DGCR8 (Di-George critical region 8)(Lee, Jeon et al. 2002; Gregory, Yan et al. 2004), the DEAD box RNA helicases p68 and p72 as well as heterogenous nuclear riboproteins (Gregory, Yan et al. 2004).
- 4- Cleavage by the microprocessor complex releases the pre-miRNA (~60-70nt) hairpin structure complete with 3' 2 nucleotide overhangs ready for export to the cytoplasm. In the presence of Ran-GTP, Exportin-5 (Exp-5) shuttles the pre-miRNA structures to the cytoplasm for further processing (Bohnsack, Czaplinski et al. 2004).
- 5- In the cytoplasm, another RNase III enzyme, dicer recognizes the pre-miRNA hairpin structure and cuts it at the loop end resulting in a 22-nt duplex miRNA. As with the drosha processing, dicer processing takes place as part of a larger complex which includes the human immunodeficiency virus transactivating response RNA-binding protein (TRBP, known as loquacious in *Drosophila*) which contains three dsRNA-binding domains (Chendrimada, Gregory et al. 2005; Forstemann, Tomari et al. 2005). This complex is thought to stabilize the interaction of dicer with the pre-miRNA

structure. It is this instability that dictates which of the strands will be ultimately be the mature miRNA.

- 6- Next the RNA duplex is loaded onto the RNA induced gene silencing complex (RISC). The RISC complex is composed mainly of members of the Argonaute (AGO) family of proteins. The Argonautes are a well conserved family of proteins (Carmell, Xuan et al. 2002) which can be divided into three separate subgroups, one of which, the AGO family is associated with siRNAs and miRNAs (Yigit, Batista et al. 2006). There are 8 proteins in the AGO family, 4 of which (AGO1-4) are associated with human miRNA (Meister and Tuschl 2004). Studies in the mammalian system have identified AGO2 as the main miRNA cleaving enzyme and therefore been named the 'slicer argonaute' (Liu, Carmell et al. 2004; Meister, Landthaler et al. 2004). It is believed that the duplex is loaded onto the AGO2 protein while maintaining the association with members of the microprocessor complex. Due to imperfect base pairing and the presence of single nucleotide insertions the strands are not stable in the duplex. Once loaded, it is the strand that exhibits less stable base-pairing at its 5' end that remains associated with the complex (guide strand) while the other strand (passenger strand) is degraded (Mourelatos, Dostie et al. 2002; Kim, Han et al. 2009).

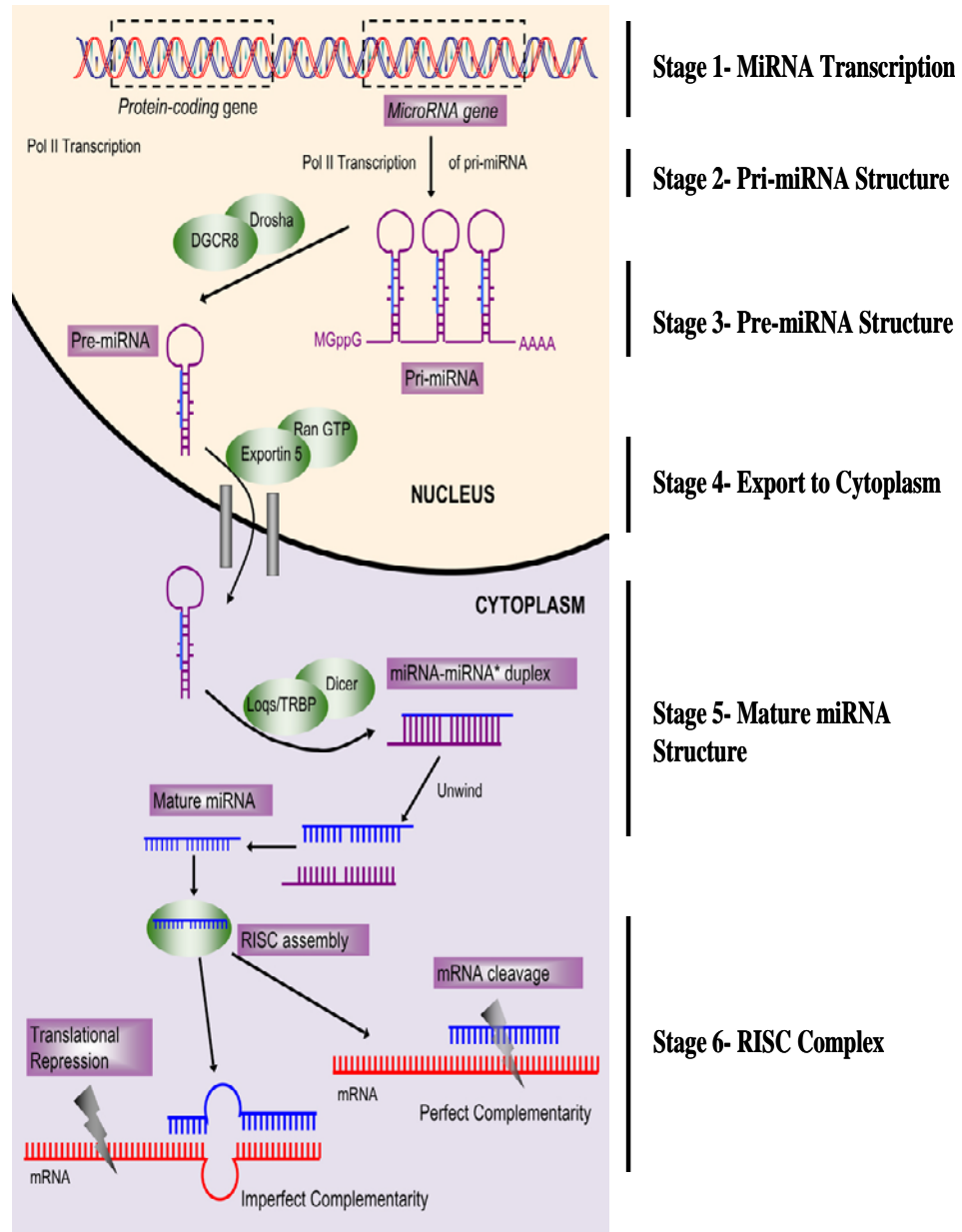


**Figure 1-5 Overview of the Biogenesis of MiRNAs (Kadri, Hinman et al. 2009)**

#### **1.5.4 Mechanism of Translational Repression**

It is known that translation is then repressed through pairing of the RISC complex via the ‘seed region’ of the miRNA. The ‘seed region’ refers to nucleotides 2-7 at the 5’ end of the miRNA, where extensive binding occurs between the miRNA and the 3’ UTR of the mRNA (Brennecke, Stark et al. 2005). There is evidence for repression at the initiation of translation step (Pillai, Artus et al. 2004; Ding and Grosshans 2009), while groups have also published evidence for repression at the post-initiation step (Seggerson, Tang et al. 2002; Petersen, Bordeleau et al. 2006). Recent work has shown that miRNAs could be repressing gene expression by sequestering the targeted mRNAs into mammalian processing bodies (P-bodies) (Liu, Rivas et al. 2005; Liu, Valencia-Sanchez et al. 2005). Another possibility is that the process of translation is not affected by the RISC complex but that the emerging polypeptides are degraded while another recent paper provided strong evidence that the destabilization of target mRNAs is the main reason for the observed protein reduction (Guo, Ingolia et al. 2010).

#### **1.5.5 Biological Roles of miRNAs**

The full extent of miRNA regulation on biological pathways is not known although roles have been ascribed to miRNAs in nearly all developmental processes. Target genes that are regulated by miRNAs are involved in many processes ranging from apoptosis (Cimmino, Calin et al. 2005; Zhou, Zhang et al. 2010; Zhang, Sun et al. 2012), homeobox regulation (Chen and Gorski 2008), viral infection (Ahluwalia, Khan et al. 2008; Li, Fu et al. 2009; Seo, Chen et al. 2009), cardiovascular disease (Cordes and Srivastava 2009; Kaneda and Fukuda 2009), spinal cord development (Sehm, Sachse et al. 2009), neuronal development (Makeyev, Zhang et al. 2007; Yu, Chung et al. 2008) to evolution (Zhang, Peng et al. 2007). Much work has been performed investigating the roles of miRNAs in cancer (Hossain, Kuo et al. 2006; Slaby, Svoboda et al. 2007; Chen, Alvero et al. 2008; Grady, Parkin et al. 2008; Coulouarn, Factor et al. 2009; Guttilla and White 2009; Takahashi, Forrest et al. 2009; Zhang, Guo et al. 2009; Lovat, Valeri et al. 2011), showing that disrupting the miRNA regulation of a single gene can lead to tumorigenesis (Mayr, Hemann et al.

2007). The picture that arises from this research is that miRNAs have the potential to regulate almost all aspects of cellular physiology.

### **1.5.6 MiRNA Target Prediction**

A key restriction in current miRNA research is the prediction and verification of the targets of specific miRNAs. Most prediction algorithms are based on the model where there is perfect complementarity between the ‘seed region’ of the miRNA and the mRNA (Lewis, Burge et al. 2005). Most predicted targets based on this sequence complementarity alone result in high number of false positives (Maziere and Enright 2007). Target prediction programs have evolved to incorporate other factors into their algorithms to produce more reliable results. These factors include the extent of base pairing between the miRNA and the mRNA, the level of thermodynamic stability between the miRNA and the mRNA, the level of conservation across species and the presence of multiple miRNA target sites (Min and Yoon 2010). Other features include the location and the accessibility of the miRNA target site (Saito and Saetrom 2010). It is hoped that an algorithm that can incorporate all of these features will significantly improve miRNA target prediction, however such an algorithm does not exist as of yet. Table 1-2 shows some of the prediction algorithms currently available and their method for target prediction. PicTar, miRanda and TargetScan are the algorithms used in these experiments for miRNA target prediction.

<i>Algorithm</i>	<i>Type of Method</i>	<i>Resource</i>
<b>miRanda</b>	Complementarity	<a href="http://www.microrna.org/microrna/home.do">http://www.microrna.org/microrna/home.do</a>
<b>miRanda MiRBase</b>	Complementarity	<a href="http://www.mirbase.org/">http://www.mirbase.org/</a>
<b>TargetScan</b>	Seed Complementarity	<a href="http://www.targetscan.org/">http://www.targetscan.org/</a>
<b>DIANA microT</b>	Thermodynamics	<a href="http://diana.cslab.ece.ntua.gr/microT/">http://diana.cslab.ece.ntua.gr/microT/</a>
<b>PicTar</b>	Thermodynamics	<a href="http://pictar.mdc-berlin.de/">http://pictar.mdc-berlin.de/</a>
<b>RNAHybrid</b>	Thermodynamics and statistical model	<a href="http://alk.ibms.sinica.edu.tw/cgi-bin/RNAhybrid/RNAhybrid.cgi">http://alk.ibms.sinica.edu.tw/cgi-bin/RNAhybrid/RNAhybrid.cgi</a>

**Table 1 -2 Subset of Currently Available MiRNA Prediction Algorithms  
( Adapted from (Maziere and Enright 2007))**

There are clearly a number of issues associated with the targets predicted by these programs. Experimental validation of the predicted targets shows a very low rate of true positives. In one study of the 45 predicted miRNAs which target cyclin D, only 7 could be experimentally validated (Jiang, Feng et al. 2009).

Importantly, these algorithms are all based on the same assumption that miRNAs only bind to the 3' UTR of target transcripts. Recently, a number of transcripts have been found to be targeted by a miRNA within the open reading frame (ORF) and the 5'UTR rather than the 3' UTR (Lytle, Yario et al. 2007; Forman, Legesse-Miller et al. 2008; Tay, Zhang et al. 2008). As a result, the common practice currently is to focus on those targets that are predicted by several algorithms. There remains much

to be learnt regarding miRNA target prediction. This is currently a limiting factor in deciphering the roles and functions of miRNAs.

### **1.5.7 MiRNA target identification**

As evident from the previous section, a miRNA can have several thousand predicted potential targets. This poses a challenge for the biological verification of these potential targets and so the next step in miRNA research is to develop a method or strategy with which to identify a given miRNA target with confidence.

A number of guidelines have been suggested by Elton *et al* to follow for definitively identifying a miRNA target (Kuhn, Martin et al. 2008), which include a predictable effect on target protein expression, altered biological function upon miRNA mediated regulation of target gene expression and the verification of an interaction between the miRNA and its predicted mRNA target. This group suggests that a miRNA target can only be identified when a number of these requirements have been met.

While identifying mRNAs or proteins which change in level may assist in suggesting predominant genes and pathways in which the miRNA could be involved, this does not necessarily point to a direct target. This is because it can be difficult to determine whether alterations in target levels occur because of direct interaction with miRNA or via a secondary, indirect effect. This is particularly evident when looking at the mRNA level of predicted targets. There can often be a modest change in expression level due to the fact that some miRNAs act by repressing translation without affecting expression at the mRNA level. It is appreciated however that this can be an efficient method of identifying miRNA targets confirmed by a recent report showing at least 84% of miRNA mediated repression was attributable to decreased mRNA abundance (Guo, Ingolia et al. 2010).

A number of methods are being developed as an attempt to more accurately identify an interaction between a miRNA and its predicted target. This will now be discussed in greater detail.

### **1.5.7.1 Luciferase reporter assays**

The standard method used to determine a direct interaction between a miRNA and its target are luciferase reporter assays. A luciferase reporter can be constructed by cloning the 3' UTR of the target gene downstream of the luciferase coding sequence. This reporter and the miRNA under investigation can then be delivered to a suitable cell where luciferase activity can be measured and analysed. Constructs with a mutated miRNA target site can be used in addition to demonstrate a direct miRNA effect where loss of regulation is observed. These assays can be used as a starting point to identify a miRNA:target interaction but it needs to be appreciated that these constructs do not demonstrate endogenous binding of the miRNA to the target, indeed it is recommended that these assays be performed in cells which have low levels of the endogenous miRNA. There are disadvantages of these assays that can lead to misleading results, for instance transfection of supra-physiological concentrations of a miRNA could result in two molecules with complementary surfaces engaging in non-physiological interactions (Bracken, Gregory et al. 2008; Thomson, Bracken et al. 2011). The reporter assay is a labour intensive method and is also very sensitive to variances in protocol such as method of transfection. They are dependent upon the region chosen for cloning and although miRNA targets regions are generally located in the 3'UTR of its target, this is not exclusive with evidence showing miRNA target regions present in the 5' UTR and protein coding regions (Lytle, Yario et al. 2007).

### **1.5.7.2 Immunoprecipitation of RISC components**

An alternative strategy involves isolating target mRNAs undergoing direct miRNA regulation by co-immunoprecipitation with a component of the RISC complex, Argonaute (Karginov, Conaco et al. 2007; Hendrickson, Hogan et al. 2008; Thomson, Bracken et al. 2011). These targets can then be identified by microarray or deep sequencing analysis. This method has been successfully applied to identify targets of miR-1 and miR-124a where exogenous epitope tagged Argonaute (AGO2 or AGO1) was expressed in HeLa or 293T cells with the miRNAs (Karginov, Conaco et al. 2007; Hendrickson, Hogan et al. 2008). The exogenous Argonaute was

immunoprecipitated using an antibody against the epitope tag. The precipitates were then analysed by microarray in comparison to a control sample. This method enriches active miRNA: mRNA target pairs allowing identification of mRNAs regulated at either the level of RNA degradation or translational repression.

There are also disadvantages to this method; this method could create an artificial interaction between RNA and proteins, which are normally segregated by cellular compartments. This methodology also depends on an interaction between the miRNA and its target that is stable enough to survive the immunoprecipitation process. If the interaction does not persist, key targets of the miRNA may not be identified (Thomson, Bracken et al. 2011). This analysis has been shown to be subject to variation through minor changes in protocol. Therefore, although this method has advantages over luciferase reporter assays, caution again needs to be taken when interpreting results and would need to be confirmed by additional results.

### **1.5.7.3 HITS-CLIP**

A method called HITS-CLIP (high throughput sequencing of RNA isolated by crosslinking immunoprecipitation) was recently adapted for use as a miRNA target identification strategy (Chi, Zang et al. 2009). HITS-CLIP uses UV- irradiation to crosslink RNA to associated RNA-binding proteins within cells which, thus allows them to be purified. This method can be used in association with Ago-immunoprecipitation procedure to ensure that the co-immunoprecipitation actually reflects cellular interactions. HITS-CLIP is performed on samples prior to immunoprecipitation, which are then subject to deep sequencing to identify the bound RNA. When this method is used in association with specific miRNA antisense inhibitors it becomes a very accurate method for miRNA:target identification (Thomson, Bracken et al. 2011). As with the other methods, there are drawbacks to this method also, including the low efficiency of crosslinking between the RNA and the proteins.

#### **1.5.7.4 PAR-CLIP**

Another variation on the Argonaute immunoprecipitation based methods is PAR-CLIP. PAR-CLIP is modified for isolating protein-associated RNAs, termed photoactivable- ribonucleoside-enhanced crosslinking and immunoprecipitation- it offers more efficient UV crosslinking by incubating cultured cells with a photoactivable nucleoside such as 4-thiouridine. It improves RNA recovery by 100 to 1000 fold compared to HITS-CLIP methodology and is capable of identifying the location of the crosslink and thus more precisely indicate the site of targeting. This is achieved because the 4-thiouridine that incorporates into RNA during co-incubation in cell culture results in thymidine to cytidine transitions more frequently in cross linked than non-cross linked sites, thereby marking sites of direct interaction.

#### **1.5.7.5 RLM-RACE**

If it is known that a miRNA prevents translation of its target by direct cleavage then the RNA ligase mediated-5' rapid identification of cDNA ends (5' RLM-RACE) may be used to confirm such targeting. In brief, this is a PCR based technique, where an RNA adapter is ligated to the free 5' phosphate of an uncapped mRNA produced from Argonaute2- directed mRNA cleavage (Thomson, Bracken et al. 2011). The ligation product can be reverse transcribed using a forward primer directed against the linker and a gene specific reverse primer which is subsequently PCR amplified, cloned and identified by sequencing (Thomson, Bracken et al.).

#### **1.5.7.6 Biotin tagged miRNA**

Another method involves isolating miRNA targets using biotinylated synthetic miRNAs (Orom and Lund 2007). Briefly, miRNA duplexes carrying a biotin group are transfected into cells of interest where the tagged miRNA strand locates to the RISC complex and associates with its endogenous target mRNA. Upon lysis of the cells, the miRNA:mRNA complexes can be captured on streptavidin beads and the mRNA target can be purified and identified (Orom and Lund 2007). This method has the advantage that it does not require overexpression of the miRNA or prior

knowledge of a potential target. It can thus, provide a more unbiased result than some of the other methods.

## **1.5.8 MiRNAs in Stem Cells**

### **1.5.8.1 MiRNAs in Embryonic Stem Cells (ESCs)**

Murine ES cells have been a significant model for studies investigating the roles of miRNAs in stem cell self-renewal and differentiation.

#### **1.5.8.1.1 Effects of Dicer Knockout on ES cell Behaviour**

To investigate the roles of miRNAs in murine ES cell function, knockouts of proteins crucial to the biogenesis of miRNAs, dicer and DGCR8 were generated. Bernstein *et al* showed that dicer is essential for early mouse development as its absence leads to lethality early (E7.5) in development. Analysis of the embryo revealed a complete depletion of stem cells (Bernstein, Kim et al. 2003). Using a conditional gene-targeting approach, Kanellopoulou *et al* created viable dicer-deficient ES cells which retained the ability to form colonies and retained expression of ES cell specific genes (Kanellopoulou, Muljo et al. 2005). Consistent with the results generated by Bernstein *et al*, the ES cells failed to differentiate in multiple assays. Although embryoid body-like structures were formed, they did not show any morphological evidence of differentiation and failed to express markers of differentiation such as *hnf4a*, *bmp4* and *gata1*. Dicer-deficient ES cells show significantly reduced proliferation compared to wild-type ES cells (Kanellopoulou, Muljo et al. 2005; Murchison, Partridge et al. 2005) with dicer-null ES cells having prolonged G1 and G0 phases of the cell cycle. Dicer-deficient germ stem cells (GSCs) in *Drosophila* showed a perturbed cell cycle with a delay in the G1/S transition, similar to the observation in murine embryonic stem cells (Hatfield, Shcherbata et al. 2005). From these studies, it is not clear if cell cycle regulation is necessary for stem cell division or whether the disturbed cell cycle is a consequence of other dicer dependent effects.

#### **1.5.8.1.2 Effects of DGCR8 Knockout on ES cell Behaviour**

Dicer is a key member of the RNA interference (RNAi) pathway which processes double stranded RNA (dsRNA) and other endogenous non-coding RNAs, including miRNAs. The results of a dicer knockout therefore cannot be attributed solely to miRNA-mediated effects (Hammond 2005). Di-George syndrome critical region 8 (DGCR8), a cofactor of drosha in the microprocessor complex is thought to be the only member of the processing pathway that is specific to miRNAs. A DGCR8 knockout is therefore of significant importance for the study of miRNA functions. Wang *et al* generated a DGCR8 knockout murine model and found that, like the dicer knockout, DGCR8-deficient ES cells were also defective in differentiation (Wang, Medvid et al. 2007). There are phenotypic differences between the dicer and the DGCR8 knockout, suggesting that dicer may play miRNA-independent roles in ES cell function. Where dicer knockout ES cells cease growing after 8 days in culture, DGCR8 knockout ES cells continue to grow after 16 days. In addition DGCR8 knockout ES cells display a stable reduction in proliferation while the proliferation defect seen in dicer knockout cells is transient and is overcome with time (Wang, Medvid et al. 2007).

#### **1.5.8.1.3 MiRNA Profile of ES Cell**

While these experiments point to a general role for miRNAs in ES cell behaviour, further analysis was required to ascertain the specific miRNAs involved in this process. Using conventional methods for cloning and sequencing small RNAs, Houbaviy *et al* identified that the miR-290-295 cluster (miR-290, miR-291, miR-292, miR-293, miR-294 and miR-295) was highly expressed in mouse ES cells. They also showed that this cluster was conserved in ES cells of placental mammals (Houbaviy, Dennis et al. 2005). Northern analysis showed that, while the miRNAs were highly expressed in ES cells, expression dropped during differentiation of the ES cells and expression of the miR-290-295 cluster was completely absent in adult mouse organs (Houbaviy, Murray et al. 2003). These results suggested that the miR-290-295 cluster played a role in maintaining pluripotency of ES cells. Other groups subsequently demonstrated that this cluster is specific to ES cells, showing in

fact that the cluster contains the most highly expressed miRNAs in mouse ES cells (Calabrese, Seila et al. 2007; Tang, Kaneda et al. 2007; Wang, Baskerville et al. 2008).

Wang *et al* showed that DGCR8 knockout ES cells had an altered cell cycle in which the cells accumulated in the G1 phase of the cycle. Upon further investigation, they found that all 5 members of the miR-290-295 family reduced the number of cells in the G1 phase and increased the number of cells in the S and G2-M phases. The cyclin E-CDK2 inhibitor CDKN1A was found to be a target of the cluster. Members of the miR-290-295 cluster were therefore seen as key regulators of the G1-S transition due to their ability to downregulate this key controller of the cell cycle. As a result the miR-290-295 cluster is also known as ES-cell-specific-cell cycle-regulating miRNAs (ESCC miRNAs) (Wang, Baskerville et al. 2008). Recently, Melton *et al* showed that the ESCC family and the let-7 family of miRNAs have opposing effects on ES cell self-renewal and differentiation (Melton, Judson et al. 2010). They show that ESCC miRNAs indirectly increases the expression of lin-28 which blocks the maturation of the let-7 family. As the ES cells differentiate they lose markers of pluripotency Oct4, Sox2 and Nanog which also results in a loss of ESCC miRNAs and lin-28. As a result, let-7 expression increases and differentiation proceeds (Melton, Judson et al. 2010).

#### **1.5.8.2 MiRNAs in Hematopoiesis**

MiRNAs also play important functional roles in other stem cell systems. A distinct miRNA profile has been identified for the best characterised adult stem cell; the hematopoietic stem cell. Specific roles have been assigned to a number of miRNAs with functions in this cell.

MiR-150 is highly expressed in lymph nodes, spleen and thymus. It decreases B-cell formation when overexpressed in hematopoietic stem cells (Zhou, Wang et al. 2007).

MiR-181 pushes mouse lymphoid progenitors towards B lymphoid development while miR-146 and miR-223 promote T lymphogenesis (Chen, Li et al. 2004).

Georgantas *et al* describe a complex model of miRNA-mediated regulation of hematopoietic stem cell differentiation (Georgantas, Hildreth et al. 2007). They report roles for miRNAs-16, -103 and -107 in blocking differentiation of later progenitor cells while miR-221, miR-222 and miR-223 appear to control the later stages of hematopoietic differentiation. In addition, roles for miR-17-5p, 20a and 106a have been described in monocytopoiesis (Fontana, Pelosi et al. 2007).

### **1.5.8.3 MiRNAs in Myogenesis and Cardiogenesis**

MiRNAs, particularly miR-1 and miR-133 also play key roles in skeletal muscle differentiation. Wang *et al* showed that although these miRNAs are clustered on the same chromosome and transcribed in a tissue-specific manner, they promote myogenesis in two distinct fashions. MiR-1 promotes myogenesis by targeting histone deacetylase 4 (HDAC4) while miR-133 enhances myoblast proliferation by targeting serum response factor (SRF), a transcription factor essential for muscle proliferation and differentiation (Chen, Mandel et al. 2006; Gangaraju and Lin 2009).

The two miRNAs also play regulatory roles in cardiogenesis. Similar to the opposing miRNA families involved in ES self-renewal, miR-1 and miR-133 play opposing roles in this process. MiR-1 promotes the formation of cardiac muscle progenitors whereas miR-133 represses the process (Ivey, Muth et al. 2008). MiR-206 downregulates connexin 43 and prevents the formation of gap junctions during cardiomyogenesis (Anderson, Catoe et al. 2006).

### 1.5.9 MiRNAs in Adipogenesis

The first report of miRNAs playing a role in adipogenesis was by Hay *et al* in 2003 who reported a role for miR-14 in the regulation of fat metabolism in *Drosophila* (Xu, Vernooy et al. 2003). MiR-14 emerged as a cell death repressor in a screen for new inhibitors of cell death in the fruit fly. The head of a miR-14 knockout fly had greatly enlarged adipocyte lipid droplets compared to wild type flies. Further investigation revealed that the knockout of this miRNA caused an increase in the levels of both triglycerides and diacylglycerides, while an increase in copy number of miR-14 had the opposite effect (Xu, Vernooy et al. 2003). Given the level of conservation previously described for miRNAs, it was therefore of interest to investigate if miRNAs were significant players in vertebrate adipogenesis.

A year later, Esau *et al* (Esau, Kang et al. 2004) were the first to identify a relationship between miRNAs and human adipogenesis, although many groups have since followed. They used two approaches to uncover miRNA(s) of significance during adipogenic differentiation. Using human white pre-adipocytes, they inhibited a panel of miRNAs and measured the effects on adipogenesis. They then measured changes in miRNA expression during adipogenesis by microarray and combined the results of the two experiments. MiR-143 was the only miRNA identified in both analyses. MiR-143 is upregulated in differentiated adipocytes compared to undifferentiated cells. Inhibition of the miRNA using anti-sense oligonucleotides (ASO) against miR-143 resulted in a dose-dependent inhibition of adipogenesis as measured by triglyceride accumulation. Bioinformatic analysis predicted ERK5 as a potential target of miR-143 although experimental validation of a direct relationship was not achieved (Esau, Kang et al. 2004). MiR-143 was the first adipogenesis specific miRNA to be reported in a human model and has since been verified by other groups working in both human and murine adipogenesis. Kajimoto *et al* also identified miR-143 as a miRNA whose expression changes significantly in a 3T3-L1 mouse model of adipogenesis (Kajimoto, Naraba et al. 2006). MiR-143 alone emerged as a key miRNA in both models of adipogenesis, suggesting that there may be distinct miRNAs involved in the adipogenic differentiation of murine 3T3-L1 and

human pre-adipocyte cells. Kajimoto *et al* did not find any dramatic changes in miRNA expression at early (days 1, 2 or 5) stages of adipogenesis. They suggested that miRNAs act to modulate adipocyte function in 3T3-L1 adipogenesis rather than initiate differentiation (Kajimoto, Naraba et al. 2006). They inhibited the expression of the miRNAs upregulated at day 9 of adipogenesis (miR-10b, 15, 26a, 34c, 98, 99a, 101, 101b, 143, 152, 183, 185, 224 and let-7b) but did not see any differences in the level of adipogenesis, even upon combined inhibition of several miRNAs. They claim that miRNAs do not appear to have a functional role in 3T3-L1 adipogenesis although other reports have since contradicted this claim.

Li's laboratory reported a role for members of the miR-17-92 cluster in 3T3-L1 adipogenesis (Wang, Li et al. 2008). They found that five members of the miR-17-92 cluster (miR-17-5p, miR-17-3p, miR-18, miR-19b and miR-20) were significantly upregulated after induction of adipogenesis and peaked at 4 hours and 24 hours after induction. In contrast to Kajimoto *et al* who used transient anti-sense oligonucleotides to inhibit miRNA expression, this group generated a stable 3T3-L1 cell line overexpressing the miR-17-92 cluster. This overexpression resulted in acceleration of adipogenesis of the 3T3-L1 compared to control cells as well as an increase in mRNA levels of adipogenic markers PPAR $\gamma$ , C/EBP $\alpha$ , and SREBP. Target analysis showed that several members of the miR-17-92 cluster target Rb2/p130. Both the mRNA and protein levels of this target were reduced in miR-17-92 overexpressing cells. Luciferase reporter assays confirmed a direct interaction between the cluster and Rb2/p130. Based on the peaks of expression of miR-17-92 at 4 hours (corresponding to reentering the cell cycle) and 24hours (corresponding to exiting the cell cycle) after hormonal induction, this group postulates that these miRNAs are linked to the clonal expansion stage of 3T3-L1 adipogenesis. Therefore, they showed for the first time that miRNAs are necessary for the progression of 3T3-L1 adipogenesis through modulating the re-entry and exit of cells into the cell cycle (Wang, Li et al. 2008).

These studies provide evidence for a role for miRNAs as important regulators of adipogenesis in a number of species. In the results described above however, it is important to note that manipulation of the miRNA alone is not sufficient to promote adipogenesis i.e. in the case of the miR-17-92 cluster and miR-143 and; overexpression in the absence of hormonal induction does not induce adipogenesis. In comparison to the studies on miRNAs in ES cells, there is very limited information available regarding the expression of miRNAs in MSCs and the roles that they play in the differentiation to the adipogenic lineage. Roles reported for miRNAs in hMSC differentiation since this work has commenced will be described in more detail in chapter 3.

#### **1.5.10 MiRNAs in Obesity**

MiRNA expression profiling was performed in adipocytes from normal mice compared to adipocytes from obese mice (Xie, Lim et al. 2009). MiRNAs which were upregulated in adipogenesis were downregulated in the obese state i.e. the expression of miR-103 and miR-143 is upregulated in adipogenesis but is downregulated in adipocytes from obese mice. TNF- $\alpha$  is a cytokine involved in chronic inflammation in obese adipose tissue. Treatment of 3T3-L1s with TNF- $\alpha$  showed an effect on miRNA expression similar to that seen in obesity i.e TNF- $\alpha$  decreased the expression of miR-103 and miR-143 in 3T3-L1 adipocytes. From these results, the authors attribute the obesity-associated changes seen in miRNA expression to the elevated levels of TNF- $\alpha$  in obese adipose tissue and likely due to other inflammatory cytokines in the environment (Xie, Lim et al. 2009).

MiRNA expression profiling has also been reported in human obese adipose tissue (Kloting, Berthold et al. 2009; Ortega, Moreno-Navarrete et al. 2010). MiRNA expression analysis was performed in different fat depots from overweight and obese patients. Paired samples of abdominal subcutaneous and intra-abdominal omental adipose tissue were isolated from 15 patients with either normal glucose tolerance (NGT) or type 2 diabetes (T2D). Changes in miRNA expression were seen between the NGT and the T2D patients with significant correlations associated with a number

of miRNAs (miR-17-5p, -132,-99a, -134, 181a, -145 and -197) and parameters of obesity (Kloting, Berthold et al. 2009).

In human subcutaneous adipose tissue, the overexpression of miR-519d was found to be associated with severe obesity (Martinelli, Nardelli et al. 2010). Another study revealed 71 miRNAs that significantly differed between pre- or mature adipocytes from lean and obese individuals (Ortega, Moreno-Navarrete et al. 2010). This revealed 22 miRNAs in human subcutaneous adipose tissue clearly associated with parameters of obesity. Taken together, these results suggest a very important interplay between miRNAs and cells differentiating to adipocytes, the dysregulation of which could have a role in the development of obesity.

#### **1.5.11 Therapeutic potential of miRNAs in the treatment of obesity**

MiRNAs are emerging as potential therapeutic agents in the treatment of diseases such as obesity for a number of reasons. Methods to reduce expression of miRNAs in a disease model have resulted in a real therapeutic benefit. Systemic administration of Locked Nucleic Acid (LNA) anti-miRs against miR-122 (a liver-specific miRNA with potential roles in fatty acid metabolism) resulted in a dose-dependent improvement of plasma cholesterol in a non-human primate model (Elmen, Lindow et al. 2008). Additionally, a drug aimed at reducing miR-122, SPC3649 is currently in phase II clinical trials for the treatment of Hepatitis C virus infection in humans (Wahid, Shehzad et al. 2010). To date, there are no known miRNA therapeutics available to reduce fat mass (McGregor and Choi 2011).

As described previously, the potential to convert WAT to BAT or to direct MSCs to the brown adipogenic lineage is a very appealing therapeutic prospect. A brown-fat enriched miRNA cluster, miR-193b-365 has been identified through comparing genome-wide miRNA expression patterns of mouse WAT, BAT and skeletal muscle. The forced expression of miR-193b and or miR-365 in C2C12 myoblasts induced markers of brown adipogenesis while myogenic markers were significantly decreased (Sun, Xie et al. 2011). The ability to induce brown adipose tissue-like

properties using agents to increase or decrease the expression of miRNAs highlights their potential therapeutic attraction for use in obesity and its related conditions.

In conclusion, further identification and characterization of miRNAs involved in adipogenesis both *in vitro* and *in vivo* may allow a better understanding of their mechanism of action. In turn, this could lead to the identification of novel therapeutic targets and strategies which could help in the development of new anti-obesity treatments.

## 1.6 Aims And Objectives

Obesity develops when energy intake exceeds energy expenditure and results in dysregulation of adipose tissue. Understanding the factors involved in adipogenic differentiation during fat cell development is necessary for the development of therapeutic targets to combat this disease. Most studies of adipogenic differentiation are performed on the rodent 3T3L1 cell line which differs to human adipogenic differentiation. To fully understand the process of human adipogenesis, it is therefore necessary to perform these studies on an appropriate human cell. Mesenchymal stem cells (MSCs) are an excellent model for the study of human adipogenesis due to their ease of isolation and their ability to expand *in vitro*. In addition, they do not possess a prior commitment to the adipogenic lineage.

MiRNAs (miRNAs) have been identified as key regulators of eukaryotic gene expression and are being pursued as potential therapeutic agents in the mitigation of a number of diseases. There is evidence to suggest a role for miRNAs in the treatment of obesity although no miRNA-based therapeutic currently exists to reduce fat mass. The identification and characterisation of miRNAs involved in hMSC adipogenic differentiation aims to enhance the information available on the development of adipose tissue. In turn, this could provide a new source of targets for potential therapeutic advances in the treatment of obesity.

At the time these experiments were performed a role had not been described for miRNAs in hMSC adipogenesis. It was the aim of this work to determine if miRNAs were involved in the process of hMSC adipogenesis. To achieve this, the miRNAs (if any) that are significantly regulated from undifferentiated MSC to adipogenic MSC would be identified. If miRNAs which change in expression level are identified, further experiments would be performed to investigate the effect of modulation of miRNA expression on hMSC adipogenesis. Should a demonstrable effect on the progression of adipogenesis be achieved, experiments to determine the interaction of the adipogenic-related miRNA with other factors involved in adipogenic differentiation would be attempted.

This body of work is separated into two sections and the objectives are summarized as follows:

**1. Identification of miRNAs Regulated during human MSC Adipogenesis**

This study aimed to identify miRNA(s) that were significantly regulated between undifferentiated and adipogenically differentiated in MSCs isolated from a number of donors. This was performed using MiChip; a microarray platform specifically designed for miRNA expression profiling based on the technology of Locked Nucleic Acids (LNA) probes.

**2. Analysis of the Effects of Manipulation of Expression of miRNAs on human MSC Adipogenesis.**

The aim of this study was to determine whether any of the miRNAs identified as being regulated in hMSC adipogenesis played a functional role in the regulation of differentiation. This was investigated through overexpression and knockdown of the miRNAs via lentiviral mediated vectors. The effects of manipulation of expression of miRNAs on hMSC adipogenesis were analyzed via lipid accumulation and expression of adipogenic associated transcripts. Experiments to identify the target(s) of the miRNAs were performed through analysis of mRNA and protein expression combined with luciferase reporter assays.

## **2 Materials and Methods**

*Note- All material was supplied by Sigma-Aldrich unless stated otherwise.*

## **2.1 Isolation, Expansion and Characterisation of human Mesenchymal Stem Cells (hMSCs)**

### **2.1.1 Isolation of MSCs**

Bone marrow aspirates were obtained from the iliac crest of healthy human donors through the donor program that is in place between REMEDI and the University College Hospital, Galway. All procedures were carried out with informed consent and approved by the Clinical Research Ethical Committee at the hospital. The criteria for isolation of MSCs requires that all donors are young (18-30) and healthy (negative for HIV, Hepatitis B and Hepatitis C). MSCs from donors 005-009 were used for the first miRNA microarray analysis. MSCs from donors 022, 023, 024 and 026 were used for the second miRNA microarray analysis. MSCs from donors 025,027, 028, 029, 047 and 051 were used for all other experiments. Information on all donors is listed in table 2-1.

<b>Donor Number</b>	<b>Gender</b>	<b>Age</b>
<b>005</b>	<b>Male</b>	<b>28</b>
<b>006</b>	<b>Male</b>	<b>25</b>
<b>007</b>	<b>Male</b>	<b>27</b>
<b>008</b>	<b>Male</b>	<b>25</b>
<b>009</b>	<b>Male</b>	<b>27</b>
<b>022</b>	<b>Female</b>	<b>18</b>
<b>023</b>	<b>Female</b>	<b>22</b>
<b>024</b>	<b>Male</b>	<b>18</b>
<b>025</b>	<b>Male</b>	<b>23</b>
<b>026</b>	<b>Male</b>	<b>25</b>
<b>027</b>	<b>Male</b>	<b>20</b>
<b>028</b>	<b>Female</b>	<b>18</b>
<b>029</b>	<b>Female</b>	<b>18</b>
<b>047</b>	<b>Male</b>	<b>28</b>
<b>051</b>	<b>Male</b>	<b>26</b>

**Table 2-1 MSC donor information**

Human MSCs were isolated according to previously published protocols (Prockop 1997; Conget and Minguell 1999). Briefly, aspirates were washed with low glucose DMEM with 1% Penicillin/Streptomycin and pelleted by centrifugation. The pelleted cells were suspended in MSC growth medium [Low glucose DMEM, 10% Fetal Bovine Serum (FBS) (Hyclone), 1% Penicillin/Streptomycin] and plated at a final density of approximately  $3 \times 10^5$  cells/cm<sup>2</sup>. They were placed in an incubator at 37°C, 5% CO<sub>2</sub>, 90% humidity and cultured for 5 days. The cells were washed with Phosphate Buffered Saline (PBS) to remove the unattached cells including red blood cells. Fresh medium was added and colonies of adherent cells were detected within 9 days. Cells were detached from the culture flask by incubation with 0.25% trypsin/EDTA in a 37°C, 5% CO<sub>2</sub> incubator. After 3-6 minutes, when the cells had detached the trypsin was inhibited by addition of an equal quantity of MSC growth medium. The cells were counted and seeded at a density of 5,000 cells/cm<sup>2</sup> in a T-175 flask in growth MSC medium. Medium was replaced every 3<sup>rd</sup> day and passaged when cells reach 70-80% confluency. This is every 4-6 days depending on the growth rate of the cells. The cells were expanded to passage 3 for experimental purposes.

## **2.1.2 Characterisation of MSCs**

### **2.1.2.1 Cell Surface Marker Analysis**

Cell surface marker analysis was performed to measure expression of CD73, CD90, CD105, CD34 and CD45 (Caroline Curtin, REMEDI). In brief, cells were trypsinised as before and resuspended in Magnetic Activated Cell Sorting (MACS) buffer (Miltenyl Biotec). Cells were pelleted at 300 x g for 5 mins and plated at 100,000 cells per well (in triplicate per sample) of a 96-well plate. Cells were incubated with the respective primary antibody at a dilution of 1µl in 10 µl MACS buffer for 30 mins on ice. Cells were centrifuged, supernatant was aspirated and cells were washed x 3 in MACS buffer. Cells were then diluted in 5% normal goat serum for 30 mins on ice. Medium was carefully aspirated and secondary antibody (Abcam) was added for 30 mins on ice. Controls included cells alone (no primary antibody) and cells incubated with a mouse IgG1-PE isotype control

antibody. Cells were then washed as before resuspended in PBS and analysed using the ExpressPlus software on the Guava Cytosoft machine (Guava Technologies).

### **2.1.2.2 Osteogenesis**

Osteogenesis can be induced in an hMSC monolayer culture by incubating the cells in the presence of  $\beta$ -glycerol-phosphate, ascorbic-acid-2-phosphate (AA2-P), dexamethasone and fetal bovine serum (Jaiswal, Haynesworth et al. 1997; Pittenger, Mackay et al. 1999; Muraglia, Corsi et al. 2003). The differentiated cells form aggregates or nodules and increase their alkaline phosphatase activity (Pittenger, Mackay et al. 1999). Maturation along the osteogenic lineage induces the expression of osteopontin, osteocalcin and collagen type I (Jaiswal, Haynesworth et al. 1997). Osteogenic differentiation is defined by the deposition of the mineral hydroxyapatite which is assessed after 2 weeks of culturing by staining with Alizarin Red. Successful differentiation can also be measured by calcium accumulation at the end of the assay (Pittenger, Mackay et al. 1999)

#### **2.1.2.2.1 Induction of osteogenic differentiation**

Human MSCs were plated at 30,000 cells per well of a 6-well plate and were left to adhere for 24 hours in a 37°C, 5% CO<sub>2</sub>, 90% humidity incubator. As undifferentiated controls, 3 wells were treated with hMSC growth medium [Low glucose DMEM, 10% Fetal Bovine Serum (FBS) (Hyclone), 1% Penicillin/Streptomycin]. For differentiation, 3 wells were treated with osteogenic medium [High glucose DMEM (Gibco); 100nM Dexamethasone, 50 $\mu$ M Ascorbic acid 2-Phosphate; 10mM  $\beta$  glycerophosphate; 10% FBS; 1% Penicillin/Streptomycin]. Both conditions were fed with their respective medium 3 times per week. Calcium deposition analysis was carried out between 14 and 17 days after inducing differentiation.

#### **2.1.2.2.2 Von Kossa Staining**

Von Kossa staining was used to analyse the extent of mineralization in osteogenically differentiated MSC culture. Wells were washed twice with PBS followed by fixation in 10% neutral buffered formalin for 30 minutes. The formalin was removed and the cells were rinsed 3 times with distilled water. Cells were incubated in 1% aqueous silver nitrate solution (1ml per well) in the dark for 10 minutes. Wells were washed three times with distilled water with last rinse left on. Lids were removed and the wells were exposed to bright light for 15 minutes on a white paper towel. The wells were rinsed three times with distilled water. The cells were dehydrated with 100% ethanol, the ethanol removed and the wells allowed to air-dry. Areas of mineralized calcium appear as black deposits upon microscopic analysis.

#### **2.1.2.2.3 Calcium Assay**

The accumulation of calcium in the extracellular space *in vitro* can be used to quantify osteogenic differentiation. Medium was removed from the plates and the cells were twice washed with PBS (Gibco). The cells and extracellular matrix were scraped from each well in 500µl of 0.5M HCL using a cell scraper. This was repeated with a further 500µl of 0.5M HCL and the two samples were pooled. The samples were shaken overnight at 4°C. Any debris remaining was pelleted at 3,000 x g for 5 minutes in a bench-top centrifuge. 10µl of supernatant used for the calcium assay added to the wells of a 96-well microtitre plate. Standards ranging from 0.05µg to 2.0µg calcium were prepared using the supplied calcium standard (STANBIO (Xresolphthalein complexone methodology (CPC)) liquicolour). To each standard, 10µl of 0.5N Hydrochloric acid (HCL) was added. A STANBIO (CPC) liquicolour working solution was prepared according to the manufacturer's instructions, 200µl of which was added to each sample and standard. These were left to incubate for at least 15 minutes in the dark at room temperature. Absorbance (550-650nm) was read using a plate reader and the amount of calcium in each undifferentiated and osteogenically differentiated sample determined against the standard curve of calcium.

### **2.1.2.3 Chondrogenesis**

The aim of the chondrogenic differentiation assay is to mimic the mesenchymal condensation seen during development. This is generally induced in hMSCs by forcing the aggregation of 300,000 to 500,000 cells to generate a pellet culture. The MSCs are then cultured in chondrogenic medium supplemented with transforming growth factor-  $\beta$ 3 (TGF-  $\beta$ 3.) This is a serum free medium containing dexamethasone, sodium pyruvate, proline ascorbic acid phosphate and ITS + supplement, which contains insulin, transferrin, selenous acid, linoleic acid and albumin (Sottile, Halleux et al. 2002). The cells are cultured for 3 weeks in this medium during which time there is an upregulation of the chondrogenic markers; collagen II, collagen XI, aggrecan, perlecan and syndecan (Bosnakovski, Mizuno et al. 2005). Assessment of chondrogenic differentiation is performed at the end of the assay by quantitation of glycosaminoglycans (GAG). For histological analysis, the pellets are stained with Safranin-O, Toluidine blue or Alcian blue to stain acid mucopolysaccharides, glycosaminoglycans and proteoglycans respectively (Pittenger, Mackay et al. 1999; Sottile, Halleux et al. 2002; Jackson, Jones et al. 2007).

#### **2.1.2.3.1 Induction of chondrogenic differentiation**

The human MSC chondrogenesis assay was carried out in a pellet format. Triplicate pellets (500,000 cells/pellet) were prepared for both control and chondrogenic treatments in 15ml polypropylene tubes (Sarsdedt, Wexford, Ireland). The cells were then pelleted at 300 x g for 5 minutes. As controls, cells were resuspended in 500 $\mu$ l incomplete chondrogenic medium (ICM) [High glucose DMEM; 1% ITS supplement (6.25 $\mu$ g/ml bovine insulin, 6.25 $\mu$ g/ml transferrin, 6.25 $\mu$ g/ml selenous acid, 5.33 $\mu$ g/ml linoleic acid, 1.25mg/ml BSA); 100nM Dexamethasone; 50 $\mu$ g/ml Ascorbic acid 2-Phosphate; 40 $\mu$ g/ml L-proline; 1mM sodium pyruvate; 1% Penicillin/Streptomycin] while cells for chondrogenic pellets were resuspended in 500 $\mu$ l complete chondrogenic medium (CCM) [ ICM and 10ng/ml Transforming Growth Factor  $\beta$ -3 (TGF $\beta$ -3)(R and D systems, Abingdon, England)]. All samples were again centrifuged at 800 x g. The tubes were placed in an incubator at 37°C,

5% CO<sub>2</sub>, 90% humidity with the tops loosened to allow gaseous exchange. The medium was changed on each of the samples 3 times per week. Analysis of chondrogenesis was performed 21 days after inducing chondrogenesis.

#### **2.1.2.3.2 Preparation of Pellets for Histology**

At day 21 pellets were washed twice in PBS and fixed in 10% neutral buffered formalin for 30 min. Pellets were stained slightly with Eosin and folded in pieces of Whatman filter paper (Whatman), pre-soaked in 10% neutral buffered formalin. Pellets were placed in individual tissue cassettes and processed in an automated tissue processor, Leica ASP300S, overnight. Pellets were removed from the cassettes and filter paper, and carefully placed in plastic tissue moulds which were then filled with paraffin wax from the Leica EG1150 H heated paraffin embedding system. Embedded pellets were left to cool on the Leica EG1150C cold plate. Pellets were cut at a thickness of 5 µm using the Leica RM2235 microtome, mounted on SuperSoft Plus microscopic slides (Gerhard-Menzel), and incubated at 60°C for 1 hour. Mounted sections were stored at room temperature until required for staining.

#### **2.1.2.3.3 Safranin O Staining**

The samples were deparaffinised and rehydrated using HistoClear (National Diagnostics) for 5 min (x2), 100% ethanol for 2 min (x2), 95% and 70% ethanol for 20 s, sequentially) followed by rinsing with dH<sub>2</sub>O for 1 min. The sections were then stained with Mayer's Haematoxylin for 6 min, which stains nuclei blue. The sections were then rinsed twice in fresh tap water for 2 min, then for 3 min. Sections were then transferred to 0.02% Fast Green FCF (in distilled water) for 4 min to stain the cytoplasm of the sections. This was followed by 3 s in 1% acetic acid and staining in 1% Safranin O solution for 6 min, to stain sulphated proteoglycans. The sections were then dehydrated through increasing ethanol concentrations (95% for 1 min, 100% for 2 min (x2)) followed by clearing in HistoClear for 2 min (x2). HistoMount (National Diagnostics) was applied to the slides and cover slips were placed on top.

The slides were then left overnight at room temperature to dry. Safranin O stains sulphated proteoglycans red/pink upon microscopic analysis.

#### **2.1.2.3.4 Calculating the Glycosaminoglycan (GAG) per unit DNA for Chondrogenesis Pellets**

The Glycosaminoglycan (GAG) content was analysed after 21 days of chondrogenesis using a dimethylmethylene blue (DMMB) assay (Petit, Masuda et al. 1996). Determination of GAG accumulation depends on the metachromatic change demonstrated by dimethylmethylene blue when complexed to GAG, and the consequent shift in the absorption spectrum of the dye. Pellets were digested with 200  $\mu$ l papain (1  $\mu$ g/ml in dilution buffer (50 mM sodium phosphate, pH 6.5, 2 mM N-acetyl cysteine, 2 mM Ethylenediamine tetracetic acid (EDTA))) overnight at 65°C. The samples were vortexed and 50 $\mu$ l of the solution was added to a well of a 96-well plate. Dilution buffer alone was used as a control. Each sample was assayed in triplicate. Standards ranging from 0.4 $\mu$ g to 2 $\mu$ g of chondroitin-6-sulphate were prepared (Sigma-Aldrich, Dublin, Ireland) and added to the wells of a 96 well plate. A stock solution of DMMB was prepared by dissolving 16mg DMMB in 5mls reagent grade 100% ethanol which was then combined with 3.04g glycine and 2.37g NaCl and 0.69ml of concentrated HCL (11.6M) in distilled water adjusted to pH 3 and volume adjusted to 1L. The solution was then kept in the dark. DMMB stock solution (200 $\mu$ l) was added to each well and incubated at room temperature for 5 minutes. The absorbance at 595nm was then read on a plate reader. A positive reaction results in a decrease in absorbance at 595 nm. The values obtained are compared against the chondroitin sulfate standard curve.

The DNA concentrations of the samples were measured using a PicoGreen assay (Invitrogen). Using the supplied DNA, stock standards ranging from 8ng to 800ng were prepared. PicoGreen solution (100 $\mu$ l) was added to each well and incubated at room temperature for 2-3 minutes. The plate was then read on a fluorescent plate reader using an excitation of 485nm and measuring emission at 538nm. DNA concentration was interpolated from the standard line. The total amount of DNA in

each sample was calculated. GAG accumulation as a measure of chondrogenic differentiation was expressed as  $\mu\text{g GAG}/\mu\text{g DNA}$ .

#### **2.1.2.4 Adipogenesis**

To induce adipogenesis in MSCs, the cells were cultured two days post confluence. The cells are exposed to three cycles of treatment which includes three days in adipogenic induction medium (AIM) followed by one day in adipogenic maintenance medium (AMM) (Okamoto, Aoyama et al. 2002; Janderova, McNeil et al. 2003). AIM is high glucose DMEM, serum and insulin with the addition of dexamethasone, indomethacin and 1-methyl-3 isobutylxanthine (Pittenger, Mackay et al. 1999). The adipogenic maintenance medium (AMM) is high glucose DMEM, serum and insulin. Successful differentiation is measured by the accumulation of lipid-filled droplets within cells. Adipogenic cells can then be visualised with Oil Red O which stains the lipid vacuoles red. This stain can be extracted and quantified as a means of determining the level of lipid accumulation within the population. Alternatively the adipocytes can be stained with the lipophilic fluorescent dye Nile Red (Greenspan, Mayer et al. 1985).

##### **2.1.2.4.1 Induction of adipogenic differentiation**

MSCs were plated at 300,000 cells/well ( $9.0\text{cm}^2$ ) of a 6-well plate and cultured until confluent in a  $37^\circ\text{C}$  5%  $\text{CO}_2$  90% humidity incubator. Dermal fibroblasts were set up in an identical fashion to serve as a control cell for adipogenic differentiation. Triplicate cultures were prepared for each condition. For comparison, undifferentiated samples treated with hMSC growth medium were set up in parallel. Adipogenesis was induced in the appropriate wells by replacing MSC growth medium with human MSC adipogenic induction medium (AIM) [High glucose DMEM; 10% FBS;  $1\mu\text{M}$  Dexamethasone;  $200\mu\text{M}$  Indomethacin; 1% Penicillin/Streptomycin;  $0.5\text{mM}$  isobutylmethylxanthine (MIX) solution;  $10\mu\text{g}/\text{ml}$  insulin] for 3 days. The medium was then replaced with human MSC adipogenic maintenance medium (AMM) [High glucose DMEM; 1% Penicillin/Streptomycin; 10% FBS;

10 $\mu$ g/ml insulin] for 1 day. This cycle was repeated twice more (Janderova, McNeil et al. 2003) (Figure 2-1).

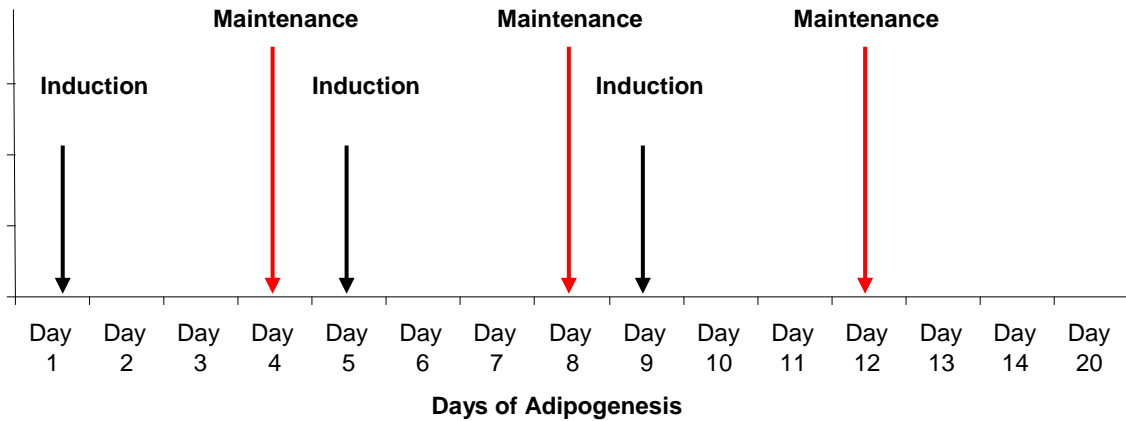


**Figure 2-1 Schedule for Medium Changes during hMSC Adipogenesis**

#### **2.1.2.4.2 Microscopic Analysis**

At day 14 the medium was removed and the cells washed with PBS. The cells were fixed in 10% neutral buffered formalin for 30 minutes. The formalin was removed and the cells were rinsed with distilled water. The cells were then stored in PBS until ready for analysis.

#### **2.1.2.4.3 Oil Red O Staining**

After 14 days of adipogenesis, the cells were stained with Oil Red O (Ramirez-Zacarias, Castro-Munozledo et al. 1992). Briefly, a 0.3% Oil Red O stock solution in 100% isopropanol was prepared. An Oil Red O working solution was made by mixing 6 parts of Oil Red O stock with 4 parts distilled water. After standing for 10 minutes the working solution was filtered using Whatman No.1 filter paper and used within 2 hours. PBS was removed from the cells and the Oil Red O stain was gently pipetted onto the cells until they are covered and left for 5 minutes. The stain was removed and 60% isopropanol was used to clear the excess stain. The cells were then rinsed with distilled water until the water ran clear. Haematoxylin was pipetted onto the plate and left to stain for 1 minute. The cells were rinsed 4 times with 2mls of distilled water and covered with water until microscopic analysis.

After microscopic analysis, the water was removed and the Oil Red O was extracted using 1ml of 100% isopropanol in 2 x 500µl aliquots. The isopropanol extracts were centrifuged at 3000 x g in a bench-top centrifuge to collect any debris at the bottom of the tube. 200µl of each supernatant was added to 3 wells of a 96-well plate. Oil Red O stain was quantified using a spectrophotometer at an absorbance at 490-520nm.

#### **2.1.2.4.4 Nile Red Staining**

After 14 days of adipogenesis, cells could also be stained with Nile Red stain. Nile Red (9-diethylamino-5H-benzo[alpha]phenoxazine-5-one) is a fluorescent stain that binds specifically to lipid droplets (Greenspan, Mayer et al. 1985). A stock 0.1% Nile Red in dimethyl sulfoxide (DMSO) was prepared, aliquotted and stored at -20°C. A working solution was prepared by diluting the stock solution 1:1000 with PBS. The solution was kept in the dark for up to 2 hours. To stain the cells 500µl of the Nile Red working solution was added to each well of cells for 90 minutes with the plate wrapped in tin foil to prevent photo-bleaching of the fluorescent stain. 4', 6-diamidino-2-phenylindole (DAPI) stain at a final concentration of 0.1µg/ml was then added to the cells for 5 minutes and also kept away from light. Nile Red

excited at 485nm and emits at 525nm. Each well was then washed 3 times with 1ml distilled water and the plates visualised using a fluorescent microscope.

#### **2.1.2.4.5 Ceiling Culture**

Ceiling Culture was used 20 days after inducing adipogenesis to separate the buoyant adipocytes from undifferentiated MSC at day 20 of adipogenesis. This technique exploits the buoyant property of lipid filled adipocytes by capturing them on the upper inner surface of a culture flask (Sugihara, Yonemitsu et al. 1987).

Briefly, 70mls of AMM was incubated in a loosely stoppered flask in a 37°C 5% CO<sub>2</sub> incubator for a minimum of 4-6hrs to allow gaseous exchange and permit CO<sub>2</sub> equilibration of the medium (Zhang, Kumar et al. 2000). Adipogenically differentiated MSCs were detached from the culture flask by incubation with 0.25% trypsin/EDTA in a 37°C, 5% CO<sub>2</sub> incubator. After 3-6 minutes the trypsin was neutralised by addition of an equal quantity of MSC growth medium. The cell suspension was pipetted into a sterile 50ml tube and centrifuged at 186 x g for 10 minutes to pellet the undifferentiated MSCs leaving the lipid filled adipocytes in the supernatant. The adipocyte- containing supernatant was gently pipetted into a T25 flask and filled entirely with the pre-equilibrated maintenance medium. The flask was closed with a solid (i.e. unfiltered) screw cap, inverted and incubated inverted in a 37°C, 5% CO<sub>2</sub> incubator overnight. Cells containing sufficient lipid float to the surface of the flask where they adhere. (Fernyhough, Vierck et al. 2004). The undifferentiated cells and those containing insufficient lipid to be buoyant will sink and adhere to the lower surface.

## 2.2 Plasmid Preparation

### 2.2.1 Construction of miR-221/222 Overexpression Plasmid

The full length sequence of the two miRNAs; miR-221 and miR-222 was amplified from human genomic DNA (A gift from Linda Howard, REMEDI) using Readymix Taq PCR reaction mix with MgCl<sub>2</sub> (Sigma-Aldrich). The primer sequences were as follows; Forward-5'-cgcagatcttttctccacagagcccctcc-3' Reverse gcggtcctttctctgcactct-3'. 25µl of Readymix Taq PCR reaction mix was added to an equal volume of template DNA (2µg), forward and reverse primers (each at a final concentration of 1µM) and water. Following amplification the PCR products were run on a 1% agarose gel and the 1Kb fragment excised from the gel. PcDNA™ 3.3-Topo® TA cloning vector (Invitrogen) is a Topo-adapted plasmid that allows rapid cloning downstream of the cytomegalovirus (CMV) promoter. The PCR product was generated as described above and 'ligated' as per the manufacturers instructions. The reaction mix was used to transform One Shot® Top10 Chemically Competent *E-Coli* (Invitrogen) as per manufacturers instructions (These *E-coli* cells are chemically treated to facilitate attachment of the plasmid DNA to the competent cell membrane). The transformation mix was then spread on Luria-Bertani (LB) agarose plates containing 1µg/ml ampicillin, which were incubated overnight at 37°C. The next day, aliquots of LB broth containing 1µg/ml ampicillin were inoculated with a single colony, then grown overnight at 37°C with vigorous shaking (~280rpm). Plasmid DNA was isolated using a Qiagen Plasmid Mini Prep (Qiagen) as per manufacturer's protocols. The concentration of the plasmid DNA was measured using the NanoDrop ND-1000 (NanoDrop). Restriction digests analysis of 1µg of plasmid DNA were carried out as per section 2.2.7. The inserts were verified by DNA sequencing (MWG Biotech – Genome Sequencing Services). It was noted that the insert was in correct orientation in 3 clones and in the reverse orientation in 2 clones. One of the correctly orientated clones was used for further experiments.

### **2.2.2 Construction of p27 overexpression plasmid.**

The protein coding sequence of p27 (without any 3' UTR) was amplified by RT-PCR from MSC total RNA using a proof reading polymerase (Phusion, Finnzymes) using forward gggagaaagattgtcaacg and reverse cgagctgtttacgtttgacgctc primers. The resulting amplicon was treated with Taq polymerase for 10 minutes at 70°C then transferred to the pCR8 Gateway Cloning vector (Invitrogen) by TOPO cloning; this was then used to transform *E.coli*. Plasmid DNA was then sequenced to ensure that no PCR-induced mutations had occurred and that the coding sequence was in the correct orientation. The p27 coding sequence was then transferred to a lentiviral vector backbone, pWPT which had been modified to incorporate a Gateway cloning cassette (a kind gift from Dr Andrew Hillmann) using recombinase (Invitrogen).

### **2.2.3 MiR-221, miR-222 and miR-126 Precursor Constructs**

Precursor clones for miRs-221,222 and 126 were purchased from System BioSciences and were received as *E-Coli* colonies on LB agar plates containing ampicillin.

### **2.2.4 Sh-221, sh-222 and scramble shRNA Constructs**

MiRZip constructs against miR-221 and miR-222 were purchased from System BioSciences. These are short hairpin RNAs (shRNAs) against miR-221 and miR-222 which were received as *E-Coli* colonies on LB agar plates containing ampicillin. A shRNA against a scramble sequence was also purchased to act as a shRNA transduction control.

### **2.2.5 pMIR-REPORT miRNA Expression Reporter**

pMIR- REPORT™ miRNA Expression Reporter (pMIR-REPORT) containing the 3'UTR of p27 (Luc-p27) and an 'empty' pMIR-REPORT without a cloned 3' UTR (Luc-Empty) were gifts from Gary Stein, Department of Cell Biology, University of Massachusetts Medical School, Worcester, Massachusetts. A Renilla luciferase control reporter vector (pRL-CMV) was received as a gift from Daniel O'Toole, Department of Anaesthesia, NUI Galway.

### **2.2.6 GFP-expressing plasmid (pWPT-GFP)**

A GFP-expressing plasmid (pWPT-GFP) was obtained from Lisa McGinley, REMEDI as a glycerol stock in *E-Coli* Stb13<sup>TM</sup> cells.

### **2.2.7 Lentivirus Packaging Plasmids and GFP-expressing plasmid**

Packaging plasmids for lentiviral production (pMD2.G; a VSVG encoding plasmid, psPax2; a packaging plasmid and pRSV-Rev; a Rev encoding plasmid) were obtained from Lisa McGinley, REMEDI as glycerol stocks in *E-Coli* Stb13<sup>TM</sup>. A loopful of glycerol stock was used to inoculate 2mls of sterile LB broth containing 1µg/ml ampicillin for 4-6 hours at 37°C.

For miR-221, miR-222, miR-126, sh-221, sh-222 and scramble shRNA; single colonies were picked and used to inoculate 2mls of sterile Luria-Bertani (LB) broth containing 1µg/ml ampicillin for 4-6 hours at 37°C.

All cultures were then treated as follows;

The cultures were then transferred to 200mls of sterile LB broth containing 1µg/ml ampicillin in a 1L culture flask and incubated overnight at 37°C with shaking. Bacteria were pelleted by centrifugation at 6000 x g for 15 minutes at 4°C. Plasmid DNA was isolated using a Qiagen Plasmid Maxi Prep (Qiagen) as per manufacturer's protocols. The concentration of the plasmid DNA was measured using the NanoDrop ND-1000 (NanoDrop). Restriction digests were carried out as recommended by the restriction enzyme supplier (New England Biolab-NEB). Briefly 1µg of plasmid were digested with 1µl of appropriate restriction endonuclease (20,000 units/ml) (*Bam*HI, *Sal*I, *Hind*III, *Mlu*I, *Xba*I) and 1µl of its corresponding optimised restriction endonuclease buffer (NEB) in a final volume of 10µl. Reactions were incubated at 37°C for 2-5hrs.

A 1% agarose gel was prepared using 1 X Tris Acetate EDTA (TAE) buffer (40mM Tris Acetate and 1mM EDTA). SYBR<sup>®</sup> Safe DNA gel stain (Invitrogen) was added to the agarose to allow visualization of DNA bands. Digested plasmid DNA was resolved on the gel and band sizes evaluated compared to 1Kb DNA ladder (New England Biolabs).

## 2.3 Gene Delivery

### 2.3.1 Generation and Purification of Lentivirus

HEK293T cells (293Ts) were transiently transfected with jet pei transfection reagent (Section 2.3.3) with transgene and packaging plasmids in order to produce lentiviral vector. 293Ts were plated at between 200,000 and 300,000 cells in 100mm diameter dishes. The cells were grown in 293T medium [Low glucose DMEM; 1% Penicillin/Streptomycin; 10% FBS]. Cells were grown until 70% confluent in a 37°C 5% CO<sub>2</sub> 90% humidity incubator. For each plate; 7µg transgene plasmid, 7µg of psPAX2.2, 3µg pMD2.G and 3µg of pRSV-Rev were diluted to a volume of 1.0ml using 150mM NaCl in a 15ml polypropylene tube (Sarstedt, Wexford, Ireland). The solution was vortexed, then centrifuged at 400 x g for 1 minute.

In a separate 15ml polypropylene tube 22µl of jet pei was diluted in 1.0ml of 150mM NaCl for each plate to be transfected. This was also vortexed and centrifuged at 400 x g for 1 minute to bring all the liquid to the bottom of the tube. The jetPEI solution was then added to the tube containing the plasmid solution. The jetPEI and plasmid solution was vortexed and again gently centrifuged. The solution was incubated at room temperature for 30 minutes, before adding it drop-wise to each plate directly to the culture medium. Each plate was swirled gently then placed in a 37°C, 5% CO<sub>2</sub>, 90% humidity incubator overnight. The medium was replaced with fresh 293T culture medium and the cells were incubated for a further 24 hours under the same conditions; during this time viral vector produced by the cells will accumulate in the medium. Viral vector was harvested by collecting the supernatants from the dishes, passing it through a 0.45µm filter then storing at 4°C overnight in a sealed polypropylene tube. Fresh medium was added to the transfected cells to collect the viral vector for another 24 hours. The second harvest of vector was filtered and combined with the first harvest and stored at 4°C until concentration (normally ≤ 24 hours). The vector was centrifuged in Sorvall ultracentrifuge tubes @27,000rpm (630 rotor), at 4°C for 2.5 hours. The supernatant was aspirated and each viral vector pellet was resuspended in sterile 1% PBS-

Albumin (50µl) and left at 4°C. The resuspended viral vector was pooled, aliquotted and stored at –80°C until required.

### **2.3.1.1 Titration of Lentivirus**

For determining the titer of lentiviral vectors, HeLa cells were plated at 100,000 cells/well of a 6-well plate and left in a 37°C 5% CO<sub>2</sub> 90% humidity incubator for 24 hours to adhere. Volumes of concentrated viral vector (from 0.1µl to 10µl) were added to wells of cells in approximately 700µl of HeLa medium [LG DMEM, 10% FBS (Hyclone), 1% Penicillin/Streptomycin]. Untransduced HeLa cells were used as controls. The plates were incubated at 37°C 5% CO<sub>2</sub> 90% humidity. After 24 hours the medium was replaced by 3mls fresh medium. The cells were ready to determine the viral vector titre 48 hours later.

#### **2.3.1.1.1 Calculation of Titre Based on GFP Expression**

The medium was removed from the well and the cells were washed with PBS, then detached using 0.25% trypsin/EDTA. The trypsin was inhibited by adding normal medium and 4% paraformaldehyde (PFA) (400µl) added to the cells. The cell suspension was left at room temperature for 10-20 minutes, then centrifuged at 500 x g for 5 minutes. The supernatant was removed from the pellet; the cells were washed twice with PBS, resuspended in 200µl PBS and stored at 4°C until ready for FACS analysis. The percentage of cells expressing GFP was calculated by flow cytometric analysis of the samples using the Guava Express Plus program on the Guava Easyocyte machine.

The titre measured in Transducing Units per ml (TU/ml) of the vector was calculated using the following formula:

**Titre (TU/ml)=  $1 \times 10^5$  (target HeLa cells) x (%GFP+ve cells/100) / volume of virus vector supernatant in ml**

This method of titering can only be employed when the lentiviral vector to be titered contains a fluorescence protein such as GFP or RFP. This is a technically simple method of estimating the titre but does have limitations. Firstly, it assumes that the level of expression of the integrated vector is above the detection threshold of the assay. In this way, cells expressing low levels of GFP may not be detected by FACS analysis. For this reason, the titre of the lentiviral vector can be dependent on the strength of the promoter driving GFP expression and can thus lead to an unreliable and inaccurate titre. In addition, this method may not distinguish cells with multiple copies of the vector (Sastry, Johnson et al. 2002; Kutner, Zhang et al. 2009). A more reliable method of calculating titre is an RT-PCR based method for calculating the number of integrations of the gene gag into the genome of a population of transduced cells.

#### **2.3.1.1.2 Calculation of Titre Based on Gag integration into Genomic DNA**

Gag is a gene that encodes the precursor of internal virion proteins found in the retroviral genome. This is still present on the viral vector and can be quantified to indicate the number of integrations into a population of cells. The number of Gag integrations was measured by quantitative PCR. Genomic DNA (gDNA) was isolated from transduced and control cells using the DNeasy Blood and Tissue kit (Qiagen). The concentration of the gDNA was measured by using the NanoDrop to determine the A260/280. Genomic DNA (200ng of each sample) was combined with 3µl of 100mM forward Gag primer and 3µl of 100mM reverse Gag primer (Table 2.2) and amplified using the QuantiFastSYBR Green PCR kit (Qiagen). The SYBR green PCR conditions recommended by the QuantiTect primer manufacturers were followed; 95°C for 15 min, 40 cycles of: 94°C for 15 sec, 55°C for 30 sec, and 72 ° C for 30 sec (data was collected at the end of this step). Actin expression was measured in each sample using identical PCR conditions and primers detailed in table 2-2 to validate that there was equal DNA loading in all samples. A dissociation (melt) curve was also performed to verify that there were no contaminating products present in the reaction.

A standard curve was generated using gag gDNA templates ranging from  $5 \times 10^2$  to  $5 \times 10^7$  copy numbers (provided by Lisa McGinley, REMEDI) and the same PCR reagents and included in each run. All samples were amplified and quantified on a StepOne Plus (Applied Biosystems) real-time PCR machine in 96-well PCR plates (Applied Biosystems), as above. The number of gag sequences detected in the genomic DNA for each sample was determined from the standard curve.

Gene of interest	Forward	Reverse
<b>GAG</b>	GGAGCTAGAACGATTCGCAGTTA	GGTTGTAGCTGTCCCAGTATTTGTC
<b>Actin</b>	TCCGTGTGGATCGGCGGCTCCA	CTGCTTGCTGATCCACATCTG

**Table 2-2 gag primer information**

The number of detected gag copies was used to determine the titre as follows. The titre of the viral vector was calculated using the following formula:

$$\begin{aligned} \text{Titre (Titering Units/ml)} &= \text{Number gag sequences detected (Transduced HeLa)} \\ &- \text{Number gag sequences detected (Untransduced HeLa)} = X \\ &= (X / \text{Number gag sequences in 200ng HeLa gDNA i.e.7000}) (\text{Number of HeLa} \\ &\text{cells transduced i.e. 100,000}) / \text{volume of virus vector supernatant in ml} \end{aligned}$$

### **2.3.1.2 Lentiviral Transduction of Target Cells**

The volume of viral vector required to achieve the desired multiplicity of infection (MOI) was calculated according to the following formula:

**Desired MOI X (cell number seeded)/ Titre in Titering Units/ml = volume in ml of virus to be added to that number of cells.**

For example- To transduce 1,000,000 cells with a lentivirus which has a titre of  $5.2 \times 10^7$  TU/ml at an MOI 50, the following calculation would be performed:

$$\text{MOI } 50 \times (1,000,000) / 5.2 \times 10^7 = 0.486\text{ml}$$

#### **2.3.1.2.1 Lentiviral Transduction of hMSCs with vectors of miRNA overexpression or shRNAs against miRNAs**

MSCs to be transduced were cultured to 70% confluence in a T175 flask in a 37°C, 5% CO<sub>2</sub>, 90% humidity incubator in MSC growth medium. MSCs transduced with miR-126 were used as controls for miR-221 and miR-222 overexpression. MSCs were transduced with a vector encoding a scramble shRNA as a control for the shRNA miR-221 and miR-222 knockdown experiments. Prior to transduction the medium was replaced with 15mls fresh MSC growth medium. The volume of viral vector required to achieve the desired MOI was calculated using the above formula, then the appropriate volume of viral vector was added directly to the medium. The flasks were left in a 37°C 5% CO<sub>2</sub> 90% humidity incubator for 24 hours after which the medium was replaced with 30mls fresh MSC growth medium. Cells were maintained for an additional 48 hours before further experimentation.

### **2.3.1.2.2 Lentiviral Transduction of hMSCs with pWPT-p27 lentivirus**

#### **2.3.1.2.2.1 Effect on of pWPT-p27 transduction on hMSC number**

hMSCs (30,000) were plated in a 6-well plate and cultured in a humidified 37°C/5% CO<sub>2</sub> incubator for 24 hours. The cells were lentivirally transduced with either pWPT-p27 vector or pWPT-GFP vector at an MOI 50. A third population of MSCs were left untransduced. Each transduction was performed in triplicate. hMSC growth medium was replaced after 24 hours. The plates were incubated for an additional 48 hours at 37°C, 5% CO<sub>2</sub>, 90% humidity when all cell populations were counted.

#### **2.3.1.2.2.2 Effect on of pWPT-p27 transduction on hMSC adipogenesis and p27 protein expression**

Untransduced hMSCs and hMSCs previously transduced with miR-221 and 222 or miR-126 were plated for an adipogenesis assay and cultured to confluence. All populations were transduced with either pWPT-p27 viral vector or a GFP lentiviral vector at a MOI 50 or remained without further transduction. hMSC growth medium was replaced after 24 hours. Cells were maintained for a further 48 hours at which point all populations were induced to undergo adipogenesis as per section 2.1.2.4.1 or protein was isolated for western blot analysis as per section 2.5.1.

### **2.3.2 Nucleofection**

Human MSCs at passage 3 were washed with PBS and harvested by trypsinisation as per section 2.1.1. Cells ( $5 \times 10^5$ ) were resuspended in 100 µl of pre-warmed Human MSC Nucleofection Solution (Lonza). DNA in Tris-EDTA (TE) buffer was added to the cell suspension. The sample was transferred into a Lonza cuvette and placed into the holder of the Nucleofector Device II (Lonza Biosystems) and subjected to the High Transfection (HT) efficiency program or the High Viability (HV). The cuvette was removed immediately and 500 µl of pre-warmed growth medium was added to the cell suspension and transferred to a T25 cell culture flask. The cells were incubated in a humidified 37°C/5% CO<sub>2</sub> incubator until ready for analysis.

### **2.3.2.1 Nucleofection with miR-221/222 overexpression vector**

MSCs were nucleofected with miR-221/222 overexpression vector (2µg) (construction of this vector is described in section 2.2.1) using the HT program. Untransfected MSCs and MSCs nucleofected with empty pcDNA 3.3 vector (2µg) were used as controls. RT-PCR analysis to determine the expression levels of miR-221 and miR-222 was performed 24hours, 48hours and 72hours post nucleofection in all samples, compared to MSCs nucleofected with empty pcDNA 3.3 vector. In addition, MSCs were nucleofected without plasmid DNA using both the HT and the HV nucleofection programs.

### **2.3.3 Jet pei Transfection**

Jet pei DNA transfection reagent is linear polyethylenimine derivative that provides an alternative method to lipid transfection of delivering DNA to cells. It delivers DNA efficiently to cell while maintaining a high level of cell survival. Jet pei acts by compacting DNA into positively charged particules which can interact with anionic proteoglycans at the cell surface and can thus enter the cell by endocytosis. It acts to buffer the endosomal Ph and protects DNA from degradation (Boussif, Lezoualc'h et al. 1995; Akinc, Thomas et al. 2005).

#### **2.3.3.1 Luciferase vector transfection of 293T cells using Jet pei**

HEK293Ts (293Ts) (120,000) were plated in a 24-well plate and cultured in a humidified 37°C/5% CO<sub>2</sub> incubator until 60-70% confluent. To determine luciferase vector activity in 293T cells transfected with Luc-p27, miR-221/sh-221 and miR-222/sh-222 using jet Pei transfection reagent, mastermixes were prepared as per Table 2-3.

The cells were transfected with either 100ng Luc-p27 or 100ng Luc-Empty in combination with 400ng miR-221/sh-221, 400ng miR-222/sh-222 or 400ng miR-221/sh-221 and miR-222/sh-222 (200ng miR-221/sh-221 and 200ng miR-222/sh-222) (Table 2-3). All 293T cell populations were transfected with a Renilla luciferease vector (5% of luciferase vector concentration) to act as a transfection control. Luc-p27 and Luc-Empty cells transfected with 400ng miR-126/scramble shRNA were used as miRNA/shRNA controls. Cells transfected with 100ng Luc-

p27 or 100ng Luc-Empty without the addition of miRNAs/shRNAs were used as controls for luciferase activity. Each transfection was set up in triplicate. In tube A, plasmid DNA was diluted to 100µl using 150mM NaCl. In tube B, 4µl of Jet pei was diluted using 100µl of 150mM NaCl. The Jet pei solution was added to the plasmid solution and vortexed then centrifuged at 400x g for 1 minute. The jet pei/DNA solution was incubated at room temperature for 30 minutes, before adding it drop-wise to each well of cells. The plates were incubated for 48hours at 37°C, 5% CO<sub>2</sub>, 90% humidity after which luciferase analysis was performed.

	Mastermix 1	Mastermix 2	Mastermix 3	Mastermix 4	Mastermix 5
<b>Tube A</b>	<b>Luc-p27 + 5% Renilla No miRNA/shRNA</b>	<b>Luc-p27 + 5% Renilla miR-221 /sh-221</b>	<b>Luc-p27+ 5% Renilla miR-222 /sh-222</b>	<b>Luc-p27+ 5% Renilla miR-221/sh-221 and miR-222/sh-222</b>	<b>Luc-p27 + 5% Renilla miR-126/ Scramble shRNA</b>
<b>Luc-p27</b>	100ng	100ng	100ng	100ng	100ng
<b>miR-221/ Sh-221</b>	----	400ng	-----	200ng	-----
<b>miR-222/ Sh-222</b>	----	-----	400ng	200ng	-----
<b>miR-126/ Scramble shRNA</b>	----	-----	-----	-----	400ng
<b>150nM NaCl</b>	100µl	100µl	100µl	100µl	100µl
<b>Tube B</b>					
<b>Jet pei</b>	4µl	4µl	4µl	4µl	4µl
<b>150mM NaCl</b>	96µl	96µl	96µl	96µl	96µl

	Mastermix 1	Mastermix 2	Mastermix 3	Mastermix 4	Mastermix 5
<b>Tube A</b>	<b>Luc-Empty + 5% Renilla No miRNA/shRNA</b>	<b>Luc-Empty + 5% Renilla miR-221/ sh-221</b>	<b>Luc-Empty+ 5% Renilla miR-222/ sh-222</b>	<b>Luc-Empty+ 5% Renilla miR-221/sh-221 and miR-222/sh-222</b>	<b>Luc-Empty + 5% Renilla miR-126/Scramble shRNA</b>
<b>Luc-Empty</b>	100ng	100ng	100ng	100ng	100ng
<b>miR-221/ Sh-221</b>	----	400ng	-----	200ng	-----
<b>miR-222/ Sh-222</b>	----	-----	400ng	200ng	-----
<b>miR-126/ Scramble shRNA</b>	----	-----	-----	-----	400ng
<b>150nM NaCl</b>	100µl	100µl	100µl	100µl	100µl
<b>Tube B</b>					
<b>Jet pei</b>	4µl	4µl	4µl	4µl	4µl
<b>150mM NaCl</b>	96µl	96µl	96µl	96µl	96µl

**Table 2 -3 Jet Pei transfection of 293Ts with Luc-p27 or Luc-Empty in combination with miR-126/scramble shRNA, miR-221/sh-221, miR-222/sh-222 or a combination of miR-221 and miR-222 or sh-221 and sh-222.**

### **2.3.3.1.1 Luciferase Reporter Assay**

Medium was removed from all 293T cells. Cells were treated with 1x Passive Lysis Buffer (Promega) and left at room temperature for 5 minutes to ensure sufficient lysis. The lysate was pipetted up and down to ensure sufficient mixing and transferred to an eppendorf tube. The samples were then centrifuged at 13,000 x g for 5 minutes to pellet the debris.

For analysis of luciferase protein activity, 25µl of the cell lysate was added to the well of a 96 well plate. An equal volume of Bright-Glo luciferase reagent (Promega) was added to the samples in the 96-well plate and luminescence (1s) measured in a Wallac 1420 VICTOR3™ multilabel plate reader.

For analysis of Renilla luciferase activity, 25ul of the cell lysate was added to wells of a 96 well plate. RenillaGlo luciferase assay reagent was prepared from RenillaGlo buffer and 100x RenillaGlo substrate (e.g. 250µl buffer and 2.5µl substrate.) An equal volume (25µl) of this Renilla Glo luciferase assay reagent was added to each sample in the 96-well plate. Luminescence (1s) was again measured using the Wallac 1420 VICTOR3™ multilabel plate reader.

Luciferase activity values were normalized to renilla luciferase activity to account for variation in transfection efficiency. All samples were assayed in triplicate.

### **2.3.3.2 pWPT-p27 vector transfection of 293T cells**

HEK293Ts (293Ts) (120,000) were plated in a 6-well plate and cultured in a humidified 37°C/5% CO<sub>2</sub> incubator for 24 hours. The cells were transfected with either 400ng of pWPT-p27 vector or 400ng of pWPT-GFP vector as per table 2-4. In tube A, plasmid DNA was diluted to 100µl using 150mM NaCl. In tube B, 4µl of Jet pei was diluted using 100µl of 150mM NaCl. The jet pei solution was added to the plasmid solution and vortexed then centrifuged at 400x g for 1 minute. The jet pei/DNA solution was incubated at room temperature for 30 minutes, before adding it drop-wise to each well of cells. Each transfection was performed in triplicate. The plates were incubated for an additional 48hours at 37°C, 5% CO<sub>2</sub>, 90% humidity when all cell populations were counted.

<b>Tube A</b>	<b>None</b>	<b>pWPT-GFP vector</b>	<b>pWPT-p27 vector</b>
<b>DNA</b>	-----	400ng	400ng
<b>150mM NaCl</b>	-----	100μl	100μl
<b>Tube B</b>			
<b>Jet pei</b>	-----	4μl	4μl
<b>150mM NaCl</b>	-----	100μl	100μl

**Table 2 -4 Jet pei transfection of 293Ts with pWPT-GFP or pWPT-p27 vector**

## **2.4 RNA Methods**

### **2.4.1 Total RNA Isolation**

RNA isolation from samples was performed using Trizol reagent (Invitrogen), as per manufacturer's instructions. Briefly, after removing the culture medium, 1ml of Trizol reagent was added to each well then pipette several times to ensure all cells were collected. Samples to be compared were frozen at -80°C until required and then processed in parallel. The cell lysate was separated into 2 phases after the addition of 200µl of chloroform. The upper RNA- containing aqueous phase was carefully removed without collecting the interphase material and the RNA was precipitated using 500µl of isopropanol, mixing and centrifuging (12,000 x g for 10 minutes). The supernatant was removed and the pellet washed with 75% ethanol. After centrifugation, the supernatant was removed and the pellet was air-dried for 5-10 minutes. The RNA was dissolved in 40µl of RNase-free water.

### **2.4.2 Analysis of RNA Concentration and Integrity**

The concentration and purity of the RNA was then determined using the Nanodrop ND-1000 (Nanodrop Technologies). Samples with a A260/A280 ratio of RNA <1.8 were discarded. The RNA was then diluted to 100ng/µl using RNase-free water and the integrity of the RNA measured using the Agilent 2100 Bioanalyzer (Agilent Technologies) according to the manufacturers' instructions. The RNA integrity number (RIN) is a scale to score RNA integrity and ranges from 1 to 10 with 10 being the highest level of integrity. It is desirable for the RNA to be used in the microarray experiment to have a RIN greater than 7. It has been shown that the quality of the microarray results diminish below this number (Castoldi, Schmidt et al. 2008; Ibberson, Benes et al. 2009).

### **2.4.3 Real-Time Polymerase Chain Reaction (RT-PCR)**

#### **2.4.3.1 Real-Time Reverse Transcription (RT) PCR To Quantify Relative Transcript Levels**

The relative levels of transcripts present in the samples were quantified by real-time RT PCR. RNA (50ng of each sample) was combined with specific primers (Table 2-5) used at a final concentration of 0.5 $\mu$ M and amplified using the Qiagen Quantitect<sup>®</sup> Sybr<sup>®</sup> Green RT- PCR kit (Qiagen). The level of RNA polymerase II transcript was used as a normaliser. The SYBR green PCR conditions recommended by the QuantiTect primer manufacturers were followed; 95°C for 15 min, 40 cycles of: 94°C for 15 sec, 55°C for 30 sec, and 72 ° C for 30 sec (data was collected at the end of this step). A dissociation (melt) curve was run to verify there were no contaminating products present in the reaction.

Relative gene expression was analysed using the  $2^{-\Delta\Delta ct}$  method (Pfaffl 2001) (Livak and Schmittgen 2001). The average Ct was calculated for the gene of interest and the normalizing gene (RNA polymerase). The  $\Delta Ct$  (ct, gene of interest – Ct, RNA Pol) was determined. From this the  $2^{-\Delta\Delta ct}$  could be determined and the levels of gene expression calculated compared to control cells.

<b>Gene of interest</b>	<b>Accession number</b>	<b>Forward</b>	<b>Reverse</b>
<b>PPAR<math>\gamma</math></b>	NM_138711	CAAGAACAGATCCAGTGGTTGC	TTGGAAGGCTCTTCATGAGGC
<b>C/EBP<math>\alpha</math></b>	NM_004364	ACCCTCAGCCTTGTTTGTACTG	TTGTCATAACTCCGGTCCCTC
<b>FABP4</b>	NM_001442	GCCAGGAATTTGACGAAGTCAC	TACCAGGACACCCCCATCTCTAAG
<b>p27</b>	NM_004064	TGACTTGCATGAAGAGAAGCA	GCTGTCTCTGAAAGGGACATTAC
<b>p57</b>	NM_000076	CTGGGACCGTTCATGTAGC	CAAACCGAACGCTGCTC
<b>PGC1<math>\alpha</math></b>	NM_008904	AATGATTTTGATCAGAAGACACACATA	TTCAGAAAGATCAAGTTCAGGAAG
<b>TLE3</b>	NM_020908	AACCCAAGGAACGACGCCC	TGCGCAGAGCCGAGGCCATTATA
<b>FABP2</b>	NM_000134	TGGCGTTTGACAGCACTTGGA	TGTCATGAGCTGCAAGCTTCCTTT
<b>MAP3K2</b>	NM_006609	AATGGACATCAGCCCACCCAGCC	GCCAAGCAGTTTGCCCAATCTCCA
<b>OSBPL3</b>	NM_015550	AGGAGGTGGCGCTCCAGAGC	TGGGCCAGAAAAAGGTTTCGGGA
<b>RFX7</b>	NM_022841	ATGAAGGCACGTCGTTTGGGCA	TCAAGGTTGGGCAGTGTGGCAT
<b>GPD2</b>	NM_000408	ACGTCTGTAGGCCTAGGGAAGC	ACCTCCTCCAACAAGAATCGTCCC
<b>KLF2</b>	NM_016270	AACCTGGGATCGAACCACAGAGG	AGGCTGCACGATGACCGAAGG
<b>Mdm2</b>	NM-002392	CGCGCCCCGTGAAGGAAACT	TGCTCCTCACCATCCGGGGT
<b>RNA pol</b>	NM_000937	GGTGGAGCTGGATCGGAAGCACAT	CGATGCAGCGCAGGAAGACAT

**Table 2-5 Primers used for RT-PCR**

### 2.4.3.2 MiRNA Quantitation by Real-Time PCR

#### 2.4.3.2.1 MiRNA Reverse Transcription

A reverse transcriptase mastermix was prepared using the TaqMan© MiRNA Reverse Transcription kit (Applied Biosystems) as follows.

<i>Component</i>	<i>Mastermix</i>
dNTP mix (100mM total)	0.15 µl
Multiscribe™ RT enzyme (50U/ µl)	1.00 µl
10 x RT Buffer	1.5 µl
RNase Inhibitor (20U/µl)	0.19 µl
Nuclease- Free water	4.16 µl

**Table 2 -6 MiRNA-specific reverse transcription mastermix**

RT-PCR-based validation of changes in miRNA levels was performed using the same RNA samples that were analysed by microarray. The RNA was diluted to 2ng/µl using RNase-free water. RNA solution (5µl) was added to 7µl of reverse transcriptase mastermix, see table 2-6. This solution was then mixed gently and centrifuged at 300 x g for 30 seconds to ensure all the liquid was at the bottom of the tube. MiRNA specific primer, listed in table 2-8 (3µl at a concentration of 1nM) was added to the solution and gently mixed. The solution was kept on ice until transferred to the thermal cycler. MiRNA specific cDNA was synthesized as follows: 16°C for 30 minutes, 42°C for 30 minutes and 85°C for 5 minutes. RNU24 was used as an endogenous control.

#### 2.4.3.2.2 PCR of miRNA specific cDNA

Following reverse-transcription, the samples were diluted 1:15 with RNase-free water. A PCR mastermix was prepared for each miRNA primer using TaqMan 2X Universal PCR Master Mix, No AmpErase UNG<sup>a</sup> (Applied Biosystems) (Table 2-7). RNU24 is a small nucleolar RNA, which shows abundant and stable expression across many tissues and cell lines. This is one of the endogenous controls

recommended by the manufacturers for use in miRNA expression analysis studies ([http://www3.appliedbiosystems.com/cms/groups/mcb\\_marketing/documents/generaldocuments/cms\\_044972.pdf](http://www3.appliedbiosystems.com/cms/groups/mcb_marketing/documents/generaldocuments/cms_044972.pdf)). Primers against RNU24 were used as the endogenous control:

<i>Component</i>	<i>Volume (μl)/20 μl reaction</i>
MiRNA-specific probe	2.00
Taqman 2x Universal PCR master mix	10.00
RNase-free water	6.67
Product from RT reaction	1.3

**Table 2 -7 MiRNA specific PCR mastermix**

The samples were mixed gently and centrifuged to ensure all the sample is collected at the bottom of the well. The PCR was performed using the Applied Biosystems Step One Plus Real-Time PCR machine using the default settings for Auto Increment, ramp rate and data collection (default is 60°C). MiRNA specific PCR was performed using the following conditions; 95°C for 10 minutes, 40 cycles of 95°C for 15 seconds and 60°C for 1 minute (data was collected at the end of this step). As per section 2.4.3.1, relative gene expression was analysed using the the  $2^{-\Delta\Delta Ct}$  method. In this case, the average Ct was calculated for the miRNA of interest and the normalizing endogenous control (RNU24). The  $\Delta Ct$  (ct, gene of interest – Ct, RNU24) was determined. From this the  $2^{-\Delta\Delta Ct}$  could be determined and the levels of miRNA expression calculated compared to control cells.

<b>MiRNA</b>	<b>MiRBase Accession</b>	<b>Mature miRNA sequence</b>	<b>Applied Biosystems Assay ID</b>
<b>Hsa-miR-143</b>	<b>MI0000459</b>	<b>UGAGAUGAAGCACUGUAGCUC</b>	<b>002249</b>
<b>Hsa-miR-452</b>	<b>MI0001733</b>	<b>AACUGUUUGCAGAGGAAACUGA</b>	<b>002329</b>
<b>Hsa-Let-7b</b>	<b>MI0000063</b>	<b>UGAGGUAGUAGGUUGUGUGGUU</b>	<b>002619</b>
<b>Hsa-Let-7e</b>	<b>MI0000060</b>	<b>UGAGGUAGGAGGUUGUAUAGUU</b>	<b>002406</b>
<b>Hsa-Let-7g</b>	<b>MI0000433</b>	<b>UGAGGUAGUAGUUUGUACAGUU</b>	<b>002282</b>
<b>Hsa-Let-7i</b>	<b>MI0000434</b>	<b>UGAGGUAGUAGUUUGUGCUGUU</b>	<b>002221</b>
<b>Hsa-miR-221</b>	<b>MI0000298</b>	<b>AGCUACAUGUCUGCGGGUUUC</b>	<b>000524</b>
<b>Hsa-miR-222</b>	<b>MI0000299</b>	<b>AGCUACAUCUGGCUACUGGGU</b>	<b>002276</b>
<b>Has-miR-193a</b>	<b>MI0000487</b>	<b>AACUGGCCUACAAAGUCCCAG</b>	<b>000492</b>
<b>Hsa-miR-99a</b>	<b>MI0000101</b>	<b>AACCCGUAGAUCCGAUCUUGUG</b>	<b>000435</b>
<b>Hsa-miR-17-5p</b>	<b>MI0000071</b>	<b>CAAAGUGCUUACAGUGCAGGUAGU</b>	<b>000393</b>
<b>Hsa-miR-18a</b>	<b>MI0000072</b>	<b>UAAGGUGCAUCUAGUGCAGAUAG</b>	<b>002422</b>
<b>Has-miR-126</b>	<b>MI0000471</b>	<b>CAUUAUUACUUUUGGUACGCG</b>	<b>002228</b>

**Table 2 -8 TaqMan MiRNA specific probes used for RT-PCR**

## 2.4.4 MiRNA Microarray Techniques

### 2.4.4.1 Overview of MiChip Protocol

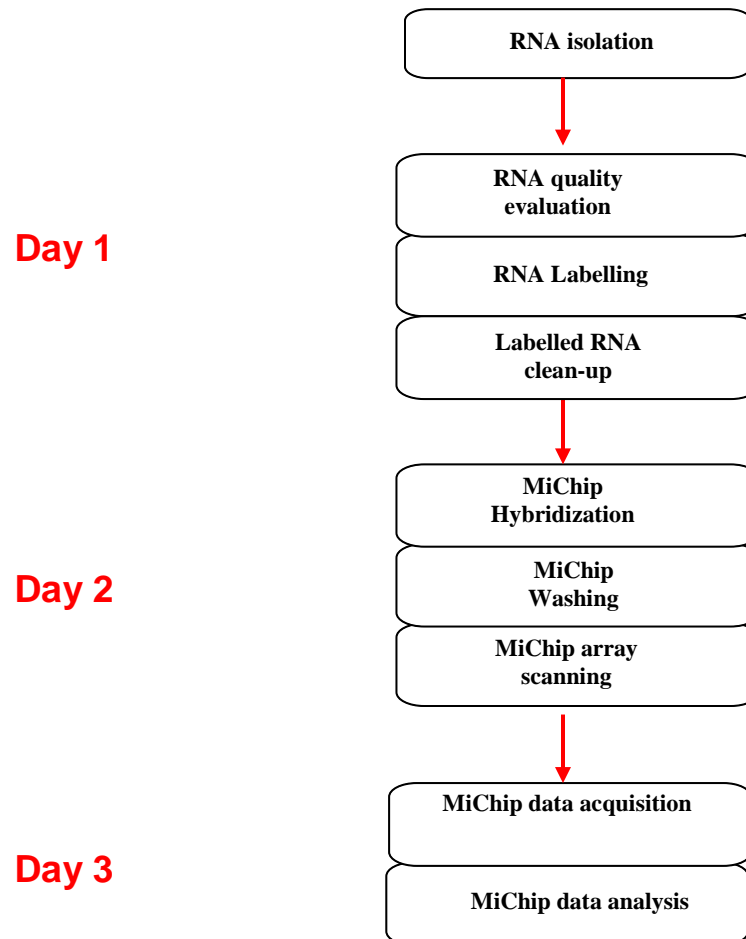


**Figure 2-2 Overview of MiRNA microarray (MiChip platform)**

The flow chart represents the stages in the microarray experiment (Castoldi, Schmidt et al. 2008).

#### 2.4.4.2 MiRNA Labelling for MiChip Hybridization

The mastermix solution for labelling reaction was prepared as follows;

<i>MiChip Labelling mix</i>	<i>Volume (<math>\mu</math>l)</i>
RNase free water (Accugene)	3.1
T4 RNA ligase buffer (10x) (Ambion)	3.2
50% Polyethylene glycol (PEG 6000) (Fluka)	10
Cy-dye Linker (100 $\mu$ M) (Biospring)	2
RNase inhibitor (40U/ $\mu$ l) (Ambion)	0.5
ATP (0.2M) (Sigma)	0.2
T4 RNA ligase (5U/ $\mu$ l) (Ambion)	3

**Table 2 -9 MiChip labelling mastermix**

RNA (5 $\mu$ g in a volume of 10 $\mu$ l) was added to 20 $\mu$ l of mastermix, vortexed and centrifuged (80xg) briefly to ensure all the liquid collected at the bottom of the tube. Speeds higher than 80 x g are not recommended as this causes salt precipitation (Castoldi, Schmidt et al. 2008). The mixture was then placed in the dark and incubated overnight (12-16 hours) at 4°C.

#### 2.4.4.3 Sample Precipitation

The labelled RNA was denatured for 5 minutes at 95°C which also inactivates the T4 ligase and the RNase inhibitor. The sample was centrifuged briefly to collect the liquid at the bottom of the tube and then kept on ice. Precipitation mix was then prepared as follows:

<i>MiChip Precipitation mix</i>	<i>Volume (<math>\mu</math>l)</i>
RNase free water	58.7
Sodium Acetate (Ambion) (3M, pH 5.5)	10.3
Linear Acrylamide (Ambion) (5 $\mu$ g/ $\mu$ l)	1

**Table 2 -10 MiChip precipitation mix**

Precipitation mix (70ul) was added to the each sample followed by 300 $\mu$ l of 100% ethanol. RNA was precipitated at -80°C for 60 minutes followed by centrifugation (20,000x g; 30 minutes; 4°C). The supernatant was removed and the pellet was washed with 1ml of 75% ethanol. The samples were then vortexed and centrifuged (16,000x g; 5 minutes). The supernatant was removed and the pellets were air-dried for 5-10 minutes at room temperature.

#### 2.4.4.4 Hybridisation of Labelled MiRNAs to MiChip

The labelled RNA pellets were dissolved in 150µl of RNase-free water and 300 µl of 1.5x hybridization buffer (37.5% formamide, 7.5x SSC, 0.15% SDS, 150µg ml<sup>-1</sup> Herringperm DNA in RNase free water) was added. The samples were denatured at 95°C for five minutes and then centrifuged at 16,000xg for 5 minutes at room temperature. For hybridization, the samples were pipetted onto the microarray gasket slide (Agilent technologies) and the array (MiRCURY™ LNA miRNA Arrays) placed on top. This was then put into the microarray chamber (Agilent technologies) and loaded into the Agilent oven to hybridize for 16-18 hours at 54°C at a speed of 4 (~15-20rpm).

#### 2.4.4.5 Post-hybridization Washing of MiChip

At the end of the hybridisation the slides were removed from the microarray chambers and stringently washed. The slide washing protocol is as follows:

<i>Wash buffer</i>	<i>Time and temperature</i>
2x SSC (Sodium saline citrate (20x), 0.1% SDS)	10 minutes at room temperature
0.2x SSC	10 minutes at room temperature
0.1x SSC	10 minutes at room temperature
0.1x SSC	10 minutes at room temperature
Double distilled H <sub>2</sub> O	10 minutes at room temperature

**Table 2-11 Post-hybridization washing protocol**

Following the washing procedure the rinsed arrays were centrifuged at 450 x g for 2 minutes at room temperature in 50ml Falcon tubes.

#### **2.4.4.6 Scanning of MiChip Arrays and Image Analysis**

The array slides were scanned using the GenePix 4200AL laser scanner (Auto Loader, Axon Instruments) using the A532 channel and with the pixel saturation tolerance set to 0.2% according to the manufacturers' protocol. The tiff images generated by the scanner were loaded into the Genepix 6 microarray analysis software. The artefact associated spots were removed by software and visual-guided flags. The signal intensity was measured by the local background subtraction method as a function of the median of foreground pixels minus median of background pixels (Castoldi, Schmidt et al. 2008). The signal intensity values were saved in a '.GPR' file format for import into the GeneSpring 7.0 platform (Agilent Technologies) for data analysis.

#### **2.4.4.7 Data Analysis**

Microarray data analysis was performed in conjunction with Dr Enda O' Connell, NUI Galway. The MiChip array files were imported for analysis into GeneSpring GX 7.3. The data were normalized using the default Per-Chip and Per-Gene-Normalizations to compensate for the difference in detection efficiency between spots and inter-slide variability as follows: values below 0.01 were set to 0.01; each measurement was divided by the 50th percentile of all measurements in that sample; each miRNA value was divided by the median of its measurements in all samples; (if the median of the raw values was below 10 then each measurement for that miRNA was divided by 10 if the numerator was above 10, otherwise the measurement was removed from further analysis.) A number of controls were present on the MiChip; these include labelling controls, (which are the complementary sequences of artificial RNA spikes designed by Exiqon for hybridization of their own array), an empty control (i.e position where no probe was spotted on the array hence they should be empty- as these are labelled as 'empty' any signal associated with them will be excluded from the normalization) and a defined concentration of Cy3-labelled capture probe to monitor the binding efficiency of the capture probes in different print runs. These control spots were removed from further analysis before quality control (QC) steps were carried out on the data set. To determine if the data were fit for statistical tests, a box plot was generated to determine how consistent replicate distributions were and to see if the samples were normalized around 1.0. Principal components analysis (PCA) is a tool used to characterize the most abundant themes that reoccur in many genes in the experiment under analysis. Both PCA and hierarchical clustering were also used to investigate how similar the samples are based on gene expression profiles and any outlying samples between replicates removed. A list of miRNAs was created with a standard deviation of <1.0 (SD 1.0) between replicates in both conditions. Next a list of the miRNAs that did not change between undifferentiated MSC and adipogenically differentiated MSCs was generated. The miRNAs that were present in the SD 1.0 group but not in the unchanging group were listed and this list went forward for statistical analysis. ANOVA analysis where the variances were not

assumed equal was carried out on this list. Benjamini and Hochberg Multiple Testing correction was applied with a false discovery rate (FDR) cut off of 0.05. A list of miRNAs from this list with a fold change >1.5 fold was generated.

## **2.5 Protein Analysis Techniques**

### **2.5.1 Protein Lysate Preparation and Western Blot Analysis**

MSCs were detached from the culture surface by trypsinisation as described in section 2.4.1 and lysed in 2% SDS with added protease inhibitors. Protein from a confluent T-25 flask of hela cells was isolated in a similar manner. Mouse heart protein was isolated by finely chopping the heart tissue of a 12 week old C57BL/6 mouse using a sterile blade. The tissue pieces were snap-frozen in liquid nitrogen and pulverised using a Cellcrusher tissue pulveriser (Cellcrusher<sup>TM</sup>). The resulting tissue was then resuspended in 2% SDS with added protease inhibitors.

The protein concentration of the lysate was determined using DC protein assay (Bio-Rad), and comparing to bovine serum albumin (BSA) standards of known concentration. Protein (30µg per lane) was separated by SDS-polyacrylamide gel electrophoresis on 10% acrylamide gels and transferred to polyvinylidene fluoride membrane (Invitrogen). The membranes were blocked for 1 hour in blocking buffer (5% non-fat milk and 0.05% Tween 20 in 1 x TBS (10mM Tris Ph 7.4, 150mM NaCl) and probed with the appropriate primary antibody (Table 2-12) in 5% blocking buffer overnight. Anti-GAPDH antibody was used to ensure the protein loading in each lane was comparable. The membranes were washed for 3 (1 minute) washes in TBS/0.05% Tween-20(TBS-T) followed by 3 (15 minutes) washes in TBS-T. For detection the appropriate horseradish peroxidase-conjugated (HRP)-conjugated secondary antibodies (anti-rabbit IgG, anti-mouse IgG-Pierce) were used at 1:3,000 dilutions for 2 hours at room temperature. The membranes were washed for 3 (1 minute) washes in TBS-T followed by 3 (15 minutes) washes in TBS-T. The reactive bands were visualized using the ECL Plus Western Blot detection system (GE Healthcare) on the FluorChem<sup>TM</sup> Imaging System (Alpha Innotech).

<b>Antibody</b>	<b>Source</b>	<b>Dilution</b>	<b>Conditions</b>	<b>Supplier</b>
<b>P27</b>	<b>Mouse Monoclonal</b>	<b>1:1000</b>	<b>O/N @ 4°C</b>	<b>BD BioSciences</b>
<b>P57</b>	<b>Rabbit Polyclonal</b>	<b>1:1000</b>	<b>O/N @ 4°C</b>	<b>Santa Cruz Biotechnology</b>
<b>TLE3</b>	<b>Rabbit Polyclonal</b>	<b>1:200</b>	<b>O/N @ 4°C</b>	<b>Santa Cruz Biotechnology</b>
<b>PGC1 <math>\alpha</math></b>	<b>Rabbit Polyclonal</b>	<b>1:500</b>	<b>O/N @ 4°C</b>	<b>Abcam</b>
<b>GAPDH</b>	<b>Rabbit Polyclonal</b>	<b>1:3000</b>	<b>O/N @ 4°C</b>	<b>Abcam</b>

**Table 2-12 Primary Antibodies used in Western Blot Analysis**

## **2.6 Statistical Analysis**

All values are presented as the mean  $\pm$  standard deviation of the mean (SD). Datasets were tested for significance using the Student's T-test to compare between groups. A level of  $p \leq 0.05$  was considered statistically significant.

### **3 Identification of MiRNAs Regulated During Mesenchymal Stem Cell Adipogenesis**

## **3.1 Introduction**

### **3.1.1 Experimental Aims and Objectives**

The work described in this thesis aims to determine the role of miRNAs in hMSC differentiation to adipocytes. MiRNAs have previously been implicated in many critical biological processes such as proliferation, morphogenesis, apoptosis and differentiation, including adipogenesis of human and mouse pre-adipocytes. The aim of the experiments discussed in this chapter is to determine which miRNA(s) are regulated during the process of hMSC adipogenesis. It is our hypothesis that miRNAs which play an important role in adipogenesis will be up or downregulated significantly between undifferentiated and adipogenically differentiating MSCs.

At the time these experiments commenced there was only one publication reporting a role for miRNAs in the process of adipogenesis. This work, performed on human pre-adipocytes, reported an important role for miR-143 in adipogenic differentiation (Esau, Kang et al. 2004). Pre-adipocytes, although easily accessible and easy to work with, can give only limited information about the process of differentiation due to their prior commitment to the adipogenic lineage. Thus, although this work was informative regarding the role of miRNAs in the generation of mature adipocytes from pre-adipocytes, it revealed no information regarding miRNA involvement in commitment of an undifferentiated cell to the adipogenic lineage. For this reason, an understanding of miRNAs in an human MSC model was still required. In order to determine which miRNAs have altered expression levels in differentiating MSCs compared to undifferentiated MSCs, a microarray study was performed.

### **3.1.2 MiRNA Analysis Methods**

MiRNAs have proven to be quite difficult to investigate with a high level of sensitivity and specificity due to a number of reasons. The small size of miRNAs, (average length of 22 nucleotides) means that microarrays routinely used for investigating mRNA expression are not suitable for miRNAs. MiRNA expression profiling methods have to be very specific due the high degree of sequence similarity among groups of miRNAs. Members of the let-7 family for instance have very similar sequences sometimes differing by as little as one nucleotide (Johnson, Grosshans et al. 2005). In addition, analysis methods should ideally discriminate between the mature and precursor miRNA forms (the mature miRNA sequence is within the precursor miRNA structure). MiRNAs do not contain a consensus sequence such as the Poly(A) tail, present in message RNAs, to allow their selective purification and amplification (Benes and Castoldi 2010). Another feature of miRNAs that makes them difficult to analyze is the lack of homogeneity in their GC content proportions, which results in a wide range or significant variation of melting temperatures in the population of miRNAs under investigation.

Northern blotting with radiolabelled probes (Valoczi, Hornyik et al. 2004), quantitative PCR (Q-PCR) of precursor or mature miRNAs (Shi and Chiang 2005), oligonucleotide microarray/macroarrays (Krichevsky, King et al. 2003), bead-based profiling methods and DNA microarrays spotted onto glass surfaces (Miska, Alvarez-Saavedra et al. 2004; Baskerville and Bartel 2005) have been used by various groups for miRNA expression analysis. Some of these methods require a large amount of starting material. Others require the amplification and/or labelling of miRNAs which can be labour-intensive and can introduce bias to the results. In addition a number of these methods are not specific enough to overcome the issues described such as discriminating between members of the same family.

### 3.1.2.1 MiChip System for MiRNA Analysis

Microarray profiling adapted for miRNA expression has emerged as the one of the most useful methods for comparing miRNA levels. This is due to the ability of this technique to simultaneously screen a large number of miRNAs and to compare multiple samples at moderate expense. The miRNA analyses performed in the experiments described in this chapter were carried out using the MiChip; a microarray platform specifically adapted for miRNAs based on the technology of Locked Nucleic Acids (LNA) probes.

LNA are 2'-O, 4'-C-methylene-linked ribonucleotide derivative (Koshkin, Singh et al. 1998; Obika, Nanbu et al. 1998; Petersen and Wengel 2003). In LNA the furanose ring of the ribose sugar is chemically locked in this RNA-like conformation due to the introduction of a methylene bridge between the 2' oxygen of ribose and the 4' carbon (Figure 3-1). This locks the conformation and reduces the flexibility and increases the organization of the phosphate backbone.

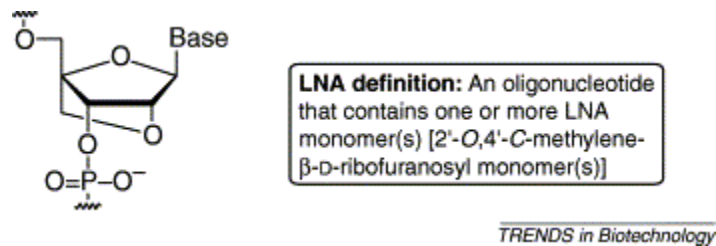


**Figure 3-1 Structure and definition of LNA (Petersen and Wengel 2003)**

The MiChip platform was developed and described by Castoldi *et al* in 2006. They hypothesized that LNA- modified capture probes would facilitate more specific miRNA detection than previous methods (Baskerville and Bartel 2005). They designed LNA probes to capture (and therefore detect) miRNAs with a uniform melting temperature of 72°C (miRNA melting temperatures are normally 45°C to 74°C)(Castoldi, Schmidt et al. 2008). This melting temperature was standardised by adjusting the number of LNA monomers incorporated into each capture probe. This group demonstrated that even a single mismatch can destabilise the heteroduplex thus allowing discrimination between members of the same family of miRNAs which can differ by as little as a single nucleotide (Griffiths-Jones 2004; Castoldi, Schmidt et al. 2006).

## 3.2 Results

### 3.2.1 Isolation and Characterization of hMSCs

Bone marrow aspirates were obtained through the donor program in place between REMEDI and the University College Hospital, Galway. All donors were young (18-30) and healthy (Section 2.1.1). MSCs from donors were isolated under identical conditions in accordance with published protocols (Prockop 1997) as per section 2.1.1. These cells were then verified as *bona fide* MSCs according to the guidelines set out by the International Society for Cellular Therapy (ISCT) which states that MSCs must express CD105, CD73 and CD90 (95% of the population) as measured by flow cytometry. They must lack expression of CD45, CD34, CD14 or CD11b, CD79 $\alpha$  or CD19 and HLA class II (90% positive) (Dominici, Le Blanc et al. 2006). According to this report, the cells must adhere to plastic upon culturing and must differentiate to osteoblasts, adipocytes and chondrocytes upon standard *in vitro* differentiating conditions.

In order to demonstrate that the research described was performed on *bona fide* MSCs, the cell surface marker expression and the ability of the cells to differentiate to adipocytes, chondrocytes and osteocytes was assessed (Figure 3.2 to figure 3-5). These assays are routinely performed on all batches of MSCs used in the Regenerative Medicine Institute (REMEDI).

### 3.2.1.1 Surface Marker Analysis

Flow cytometric analysis of surface markers of MSCs was performed (Caroline Curtin, NUI, Galway) as per section 2.1.2.1. Controls included cells alone (no primary antibody) and cells incubated with a mouse IgG1-PE isotype control which did not demonstrate a significant increase in fluorescence. HMSCs showed positive expression of surface antigens CD90, CD105 and CD73 and were negative for CD45 and CD34 expression. This was characteristic of an MSC population (Figure 3-2) and consistent with the expected properties of an MSC (Dominici, Le Blanc et al. 2006).

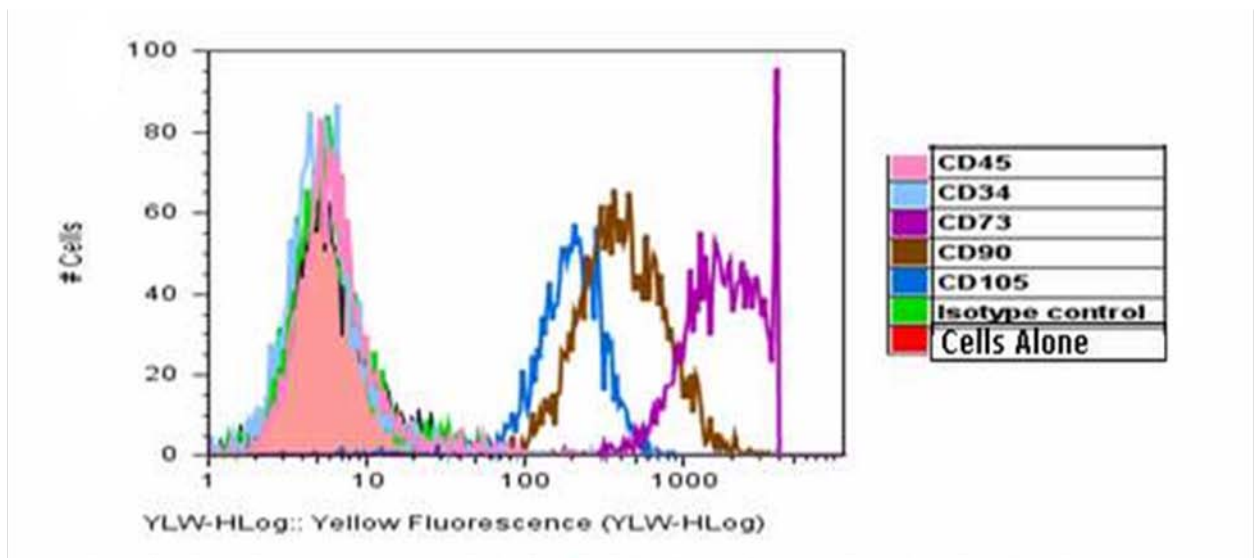


**Figure 3 -2 Characterisation of Cell Surface Proteins of HMSCs**

Cell surface marker characterisation of hMSCs, as measured by the Guava Express program on the Guava Easyocyte machine (Isotype Control=Green, Cells Alone=Red CD45=Pink, CD34=Pale Blue, CD73=Purple, CD90=Brown, CD105=Dark Blue,). HMSCs were positive for CD90, CD105 and CD73 and negative for the hematopoietic markers CD34 and CD45. Isotype control did not show an increase in fluorescence compared to cells alone.

### 3.2.1.2 Osteogenesis

MSCs cultured according to the osteogenic protocol (Section 2.1.2.2.1) successfully differentiated to osteocytes as shown by Von Kossa staining (Section 2.1.2.2.2) where areas of mineralized calcium appear as black deposits (Figure 3-3B) compared to undifferentiated MSCs (Figure 3-3A). Quantitative calcium assays performed as per section 2.1.2.2.3 revealed a statistically significant increase in calcium levels in osteogenically treated MSCs compared to undifferentiated MSCs (Figure 3-3C).

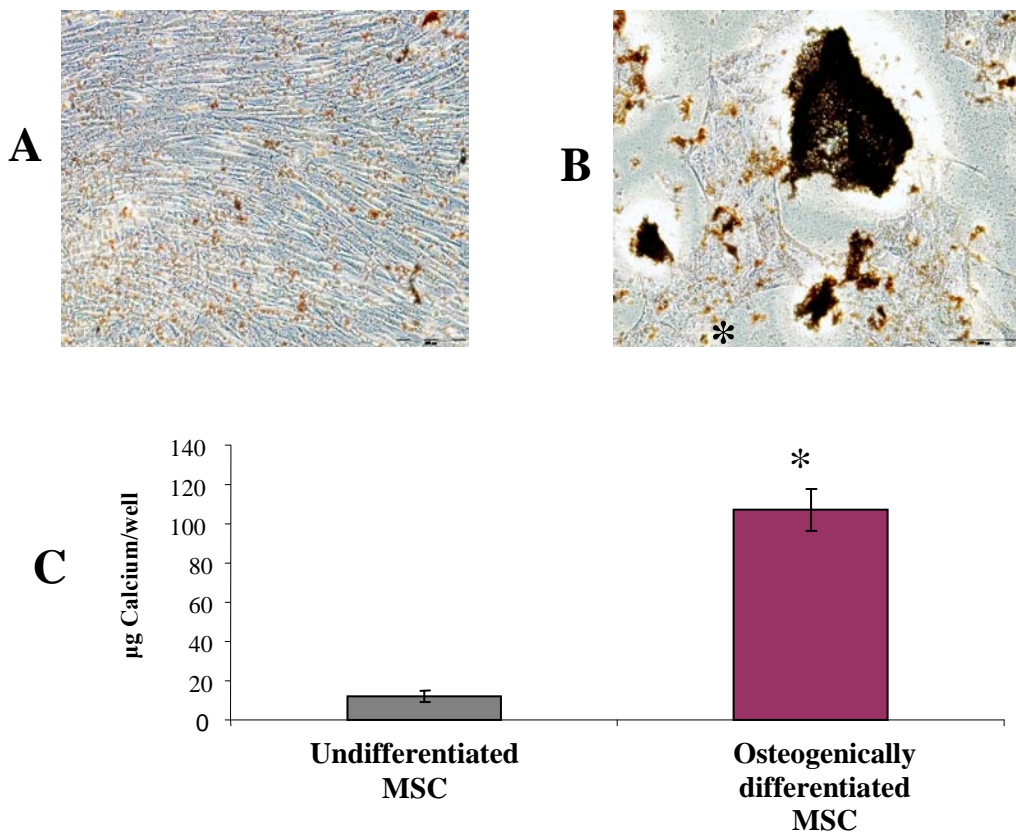


**Figure 3 -3 Osteogenic Differentiation of hMSCs**

Phase contrast micrograph (10x objective) of undifferentiated MSCs (A) and osteogenically differentiated MSCs (B) stained with Von Kossa stain after 14 days of differentiation. (C) Graph of calcium content (µg/well) in undifferentiated and osteogenically treated MSCs. Error bars represent standard deviation of the mean (n=3 donors); \*p≤0.05 compared to undifferentiated hMSCs.

### 3.2.1.3 Chondrogenesis

Chondrogenesis was induced by pelleting the cells and culturing them with Complete Chondrogenic Medium (CCM) as per section 2.1.2.3.1. As a negative (undifferentiated) control, cells were treated with Incomplete Chondrogenic Medium (ICM) lacking the agonist TGF $\beta$ . Pellets cultured in CCM stained positive for proteoglycans using Safranin O stain (Section 2.1.2.3.3) (Figure 3-4B) whereas no proteoglycans could be visualised in pellets cultured in ICM (Figure 3.4A). Chondrogenic differentiation was quantified by measuring the glysoaminoglycan (GAG) per unit DNA content (Figure 3-4C). The GAG/DNA ratio was significantly higher in CCM treated pellets than ICM treated pellets as determined by the DMMB and DNA assays, as described in section 2.1.2.3.4, demonstrating chondrogenic differentiation.

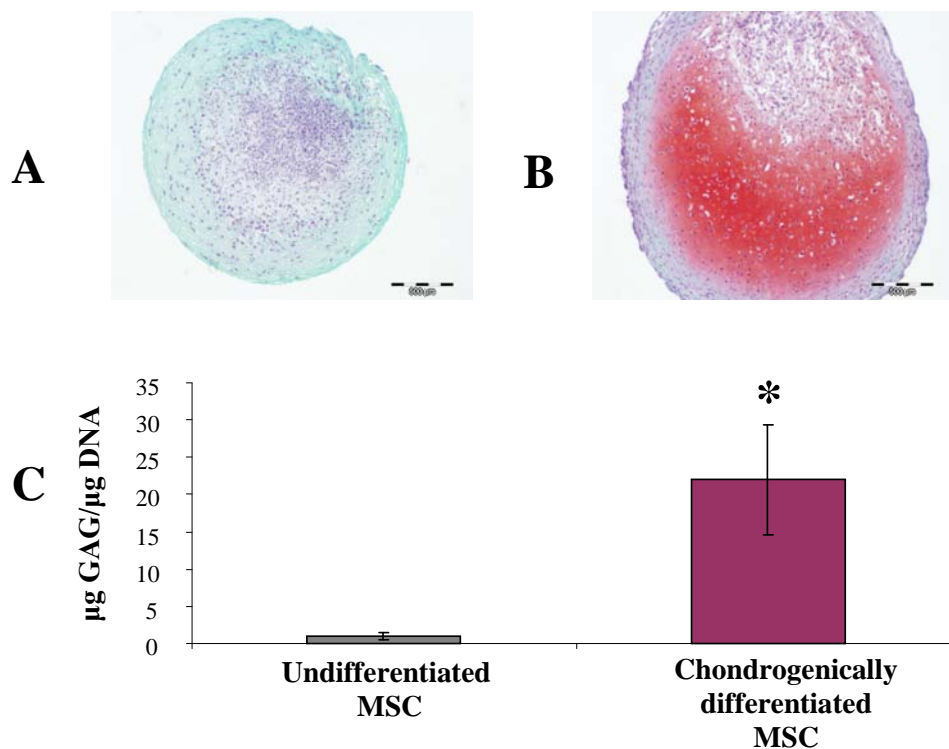


**Figure 3 -4 Chondrogenic Differentiation of hMSCs**

Phase contrast micrograph (4x objective) of undifferentiated (A) and chondrogenically differentiated MSC pellets (B) stained with Safranin O stain 21 days after induction of chondrogenesis. Sulphated proteoglycans appear red/pink. (C) Graph of Glycosaminoglycan (GAG) concentration per  $\mu\text{g}$  DNA in control and chondrogenically treated MSCs. Error bars represent standard deviation of the mean (n=3 donors); \*p $\leq$ 0.05 compared to undifferentiated hMSCs.

### 3.2.2 Adipogenesis

MSCs were cultured for 2 days after confluence was reached, then were induced to undergo adipogenesis using a hMSC adipogenic induction protocol adapted from the literature (Pittenger, Mackay et al. 1999; Janderova, McNeil et al. 2003), as per section 2.1.2.4.1. Primary dermal fibroblasts from 3 donors were cultured under the same conditions to act as control cells for the differentiation assay. Fibroblasts are also from the mesenchymal lineage but do not differentiate to adipocytes (Pittenger, Mackay et al. 1999)

Signs of lipid accumulation occur in the population of MSCs 3-4 days after induction of adipogenesis in accordance with the literature (Janderova, McNeil et al. 2003). These vesicles become more pronounced and visible after the second and third rounds of adipogenic induction. After 14 days, the accumulation of lipid-filled vesicles indicates successful differentiation (Figure 3-5B, C). After 14 days, fibroblasts which were treated with the same adipogenic induction protocol showed no signs of lipid accumulation and thus did not differentiate to adipocytes (Figure 3-5E).

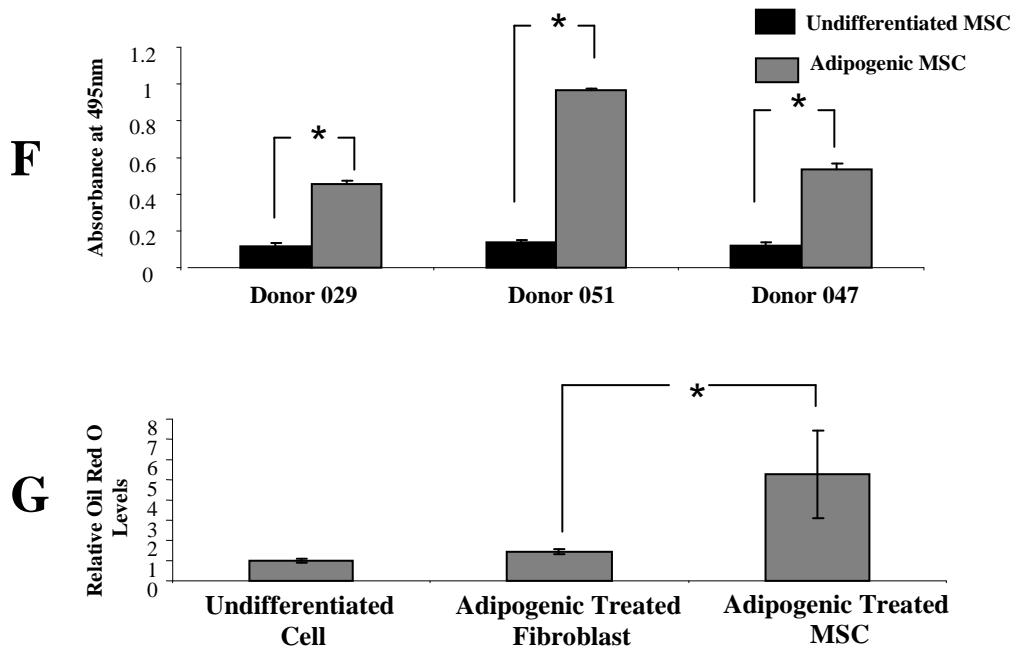
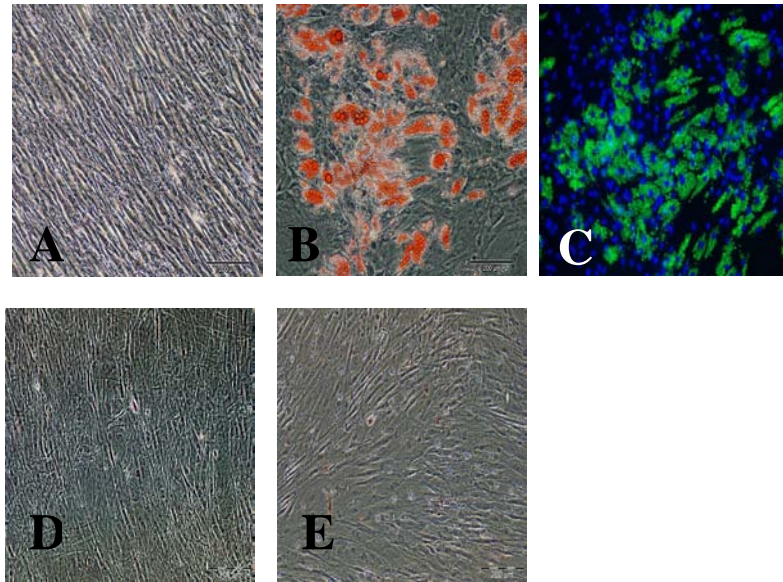
When stained with Oil Red O (as per Section 2.1.2.4.3) undifferentiated MSCs (Figure 3-5A) showed no detectable staining while lipids present in adipogenically differentiated MSCs are stained red (Figure 3-5B). Fibroblasts treated with either MSC growth medium (Figure 3-5D) or adipogenic differentiation medium (Figure 3-5E) also showed no detectable staining. Fluorescent microscopy enabled the visualisation of Nile Red and DAPI (as per section 2.1.2.4.4) stained adipogenically differentiating MSCs, where lipids are stained green and cell nuclei are stained blue (Figure 3-1D).

Figure 3-5F shows the relative level of adipogenic differentiation of MSCs from 3 donors after 14 days as measured by Oil Red O extraction. This shows that lipid accumulation is significantly higher in adipogenically differentiated MSCs than in undifferentiated MSCs in all donors (Figure 3-5F). As evident from this graph, the

level of adipogenic differentiation varies greatly from donor to donor, despite the fact that all donors were isolated, verified and adipogenically differentiated under identical conditions. There are a number of potential reasons which could contribute to the variability in differentiation potential between donors; this is discussed in greater detail in section 3.3.

Figure 3-5G shows that adipogenically treated MSCs have significantly higher levels of lipid accumulation compared to adipogenically treated fibroblasts as measured by Oil Red O extraction. This shows MSCs successfully differentiate to adipocytes while fibroblasts do not.

In conclusion, the population of cells used in the studies described in this thesis are *bone fide* MSCs according to the definition of the International Society for Cellular Therapy (ISCT) i.e. they have the appropriate cell surface markers and are able to undergo adipogenic, osteogenic and chondrogenic differentiation (Dominici, Le Blanc et al. 2006).



**Figure 3 -5 Adipogenic Differentiation of HMSCs**

Phase contrast micrographs (10x objective) of undifferentiated MSCs (A), adipogenically treated MSCs (B), undifferentiated fibroblasts (D), adipogenically treated fibroblasts (E) stained with Oil Red O (Stains lipids red) 14 days after induction of adipogenesis. Fluorescence microscopy (10x objective) of adipogenically differentiated MSCs (C) stained with Nile Red (Stains lipids green) and DAPI (Stains nuclei blue). Oil Red O extraction analysis showed significant lipid accumulation in adipogenically treated MSC compared to undifferentiated MSCs from 3 donors (F) while there was no significant lipid accumulation in adipogenically differentiated fibroblasts compared to undifferentiated fibroblasts (G). This analysis revealed significant adipogenesis in adipogenically differentiated MSCs compared to adipogenically differentiated fibroblasts (G). Error bars represent standard deviation of the mean (n=3 donors), \*p≤ 0.05

### **3.2.3 MiRNA Analysis at Day 5 of Adipogenesis**

#### **3.2.3.1 Differentiation of MSCs for Microarray Analysis**

The aim of these experiments was to determine which miRNAs undergo alterations in expression level during hMSC adipogenesis. By day 5 of adipogenesis, MSCs have taken on the rounded-up morphology of a cell undergoing adipogenesis and the first signs of lipid vesicles are visible, as evident in figure 3-6B. For this reason, day 5 was chosen for microarray-based comparison of miRNA levels in undifferentiated MSCs and adipogenically differentiating MSCs.

MSCs were successfully isolated from 5 young, healthy donors (005,006,007,008 and 009) as described in section 2.1.1 and adipogenesis was induced two days post confluence (Section 2.1.2.4.1) (Pittenger, Mackay et al. 1999). As undifferentiated controls, duplicate cultures were treated with MSC growth medium. Five days after inducing adipogenesis, RNA from undifferentiated and adipogenically differentiated was isolated from all samples as per section 2.4.1.

To confirm that MSCs isolated from each donor were adipogenic, replicate cultures were maintained in culture for 14 days after inducing adipogenesis then stained with the lipid specific dye Oil Red O. MSCs from each donor successfully differentiated into adipocytes, as evident from the accumulation of fat filled vesicles present in the cells (Figure 3-6C). MSCs treated with hMSC growth medium did not show signs of lipid accumulation.

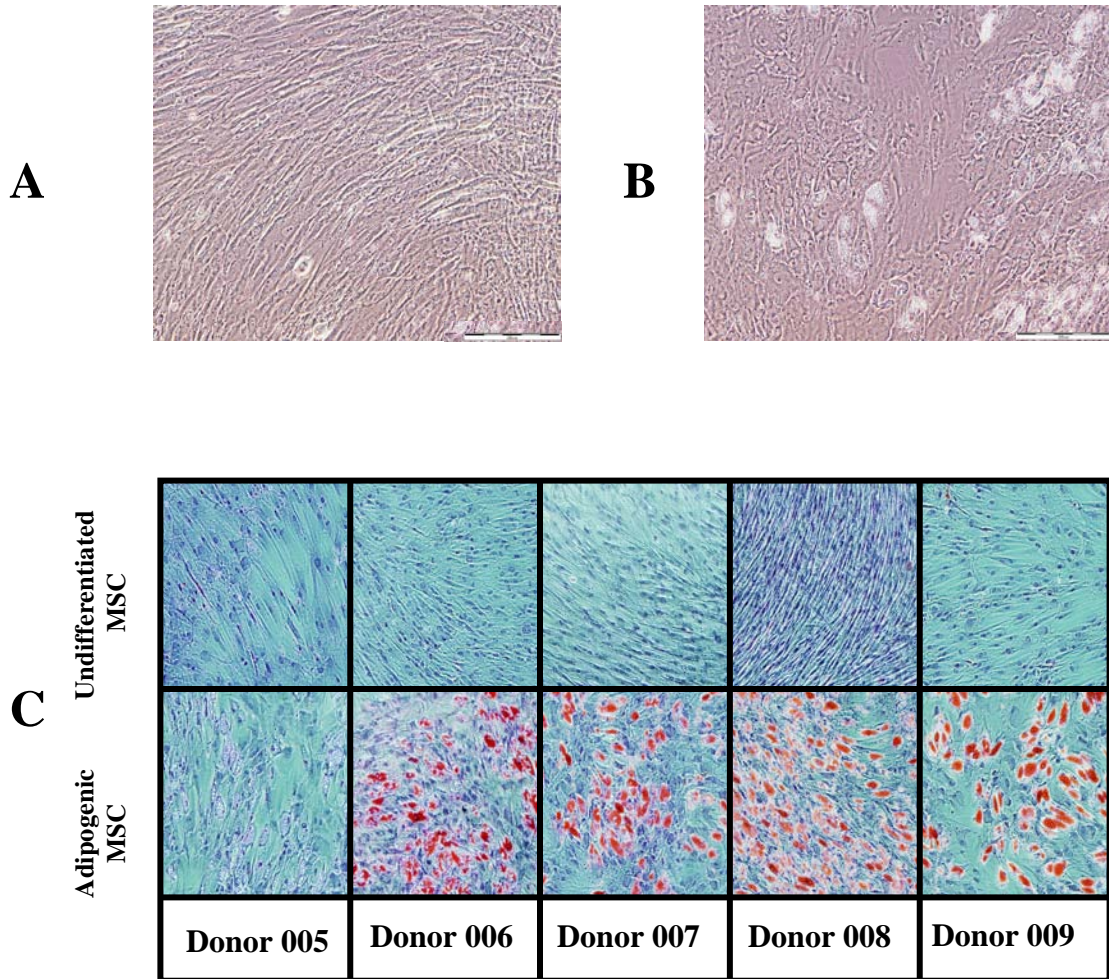


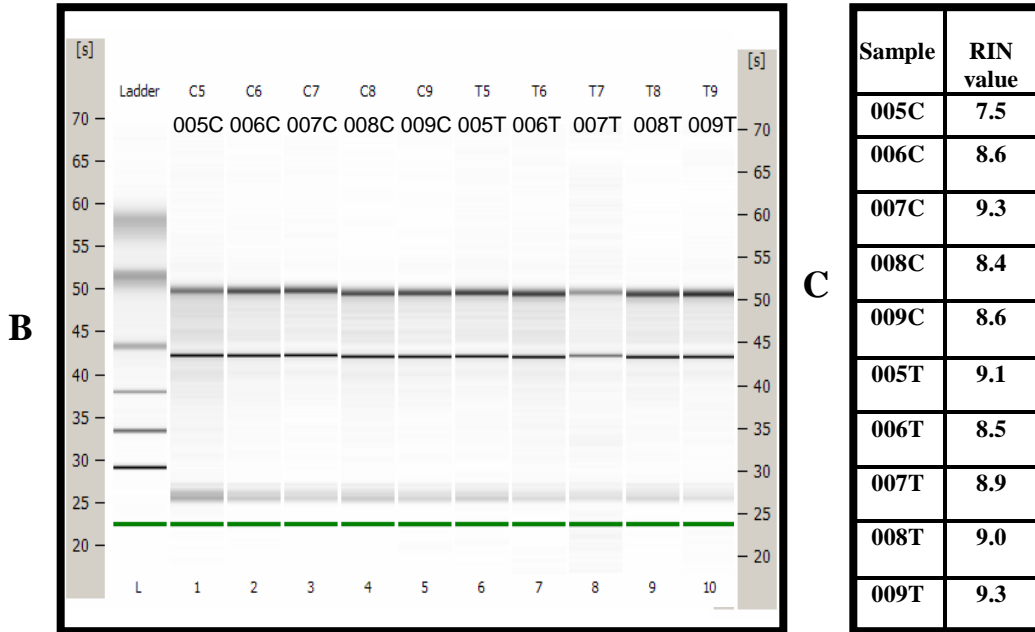
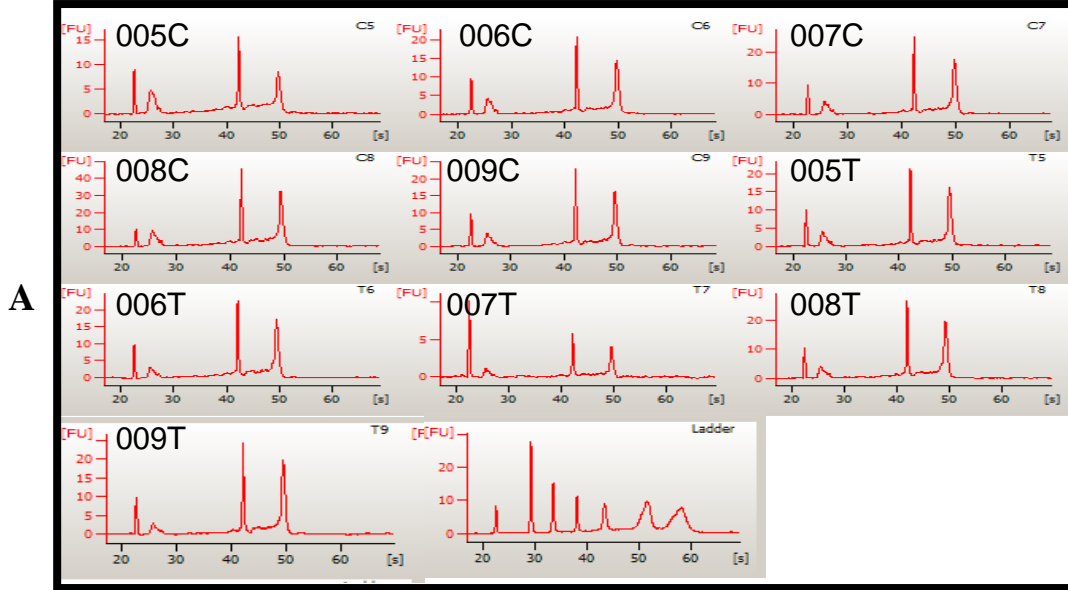
**Figure 3-6 MSCs from 5 donors successfully differentiated to adipocytes**

Phase contrast micrograph (10x objective) of undifferentiated MSC (A) and adipogenically differentiating MSC (B) at day 5 of adipogenesis. Panel of phase contrast micrographs of MSCs from 5 donors stained with Oil Red O at day 14 of adipogenesis (10x objective) (C). The lipid-filled vesicles within cells undergoing adipogenesis are visibly stained red. These are absent in the undifferentiated MSCs. (Donor 005 does not show Oil Red O staining due to a technical error, but the lipid vesicle morphology can clearly be seen indicating positive adipogenesis.)

### **3.2.3.2 Verification of RNA quality for Microarray Analysis**

It has been reported that the quality of results generated from the MiChip microarray is directly related to the quality of the input RNA (Castoldi, Schmidt et al. 2008; Ibberson, Benes et al. 2009). For this reason, it was necessary to ensure that the RNA was of a sufficiently high quality and integrity. RNA from the differentiated and undifferentiated samples from each of the five donors was therefore analysed using the Agilent 2100 Bioanalyzer as per section 2.4.2. This microfluidics-based technique separates the RNA sample based on its size and then detects the separated nucleic acids via laser-induced fluorescence. The result is visualised as an electropherogram, which indicated the relative amount of RNA of a given size (Schroeder, Mueller et al. 2006). The electropherograms in figure 3-7A depict RNA of good quality where 2 distinct ribosomal peaks (18S and 28S) can clearly be seen, which can also be seen in the predicted gel (Figure 3-7B).

The RNA integrity number (RIN) is a software tool used to assign a value to the integrity of the RNA, based on the presence or absence of degradation products in the RNA sample. RIN values range from 1 to 10 , with 1 representing highly degraded RNA and 10 representing RNA of a high integrity (Schroeder, Mueller et al. 2006). RNA with a RIN value greater than 7 is considered necessary to obtain reliable results from a microarray (Ibberson, Benes et al. 2009). As seen in Figure 3-7C each of the samples had a RIN value greater than 7 confirming that the RNA was of sufficient quality to continue to microarray analysis.



Sample	RIN value
005C	7.5
006C	8.6
007C	9.3
008C	8.4
009C	8.6
005T	9.1
006T	8.5
007T	8.9
008T	9.0
009T	9.3

**Figure 3-7 Quality of RNA verified by Bioanalyzer**

Electropherogram (A) and predicted gel (B) of control and treated sample from each donor (005-009) demonstrating the RNA peaks of a successful sample run where C is control (undifferentiated MSC) and T is treated (adipogenically differentiated MSC). Table showing the RNA integrity values (RIN) numbers for each sample which confirms that the RNA was of sufficient quality for microarray analysis (C).

### **3.2.3.3 Genespring Analysis Of Microarray Data**

Using the MiChip platform, the levels of 403 miRNAs were determined in undifferentiating and differentiating MSCs from five donors at day 5 of adipogenesis, as per section 2.4.4. 116 of these miRNAs were expressed in all control hMSCs which represents 29% of all miRNAs on the array.

Following data normalisation (Section 2.4.4.7) miRNA expression levels in control and differentiating groups were compared by 2 methods; Principal Components Analysis (PCA) and hierarchical clustering. PCA is used to determine the most abundant themes present in an experiment and revealed in this instance that there was not a clear difference between the populations of undifferentiated samples (red) and the differentiating samples (yellow) as seen in Figure 3-8A.

Hierarchical clustering determines how similar the samples were based on the miRNA expression profiles. Figure 3-8B shows the hierarchy of clustering of miRNA expression patterns for undifferentiated and differentiating MSCs (five donors). This analysis is consistent with the PCA results in that it did not show a clear clustering of the undifferentiated samples (red) distinct from the differentiating samples (yellow), as would have been expected based on our hypothesis. Statistical analysis was carried out as per section 2.4.4.7 but did not reveal miRNA(s) with a fold change greater than 1.5 in all donors at this stage of adipogenesis.

In conclusion, at day 5 of adipogenic differentiation the miRNA changes between undifferentiated and differentiated cells are less significant than the changes seen in miRNA expression between donors. Based on our analysis, these data indicate that there are no significant changes in miRNA expression level at day 5 of adipogenesis which were reproducible in all 5 donors.

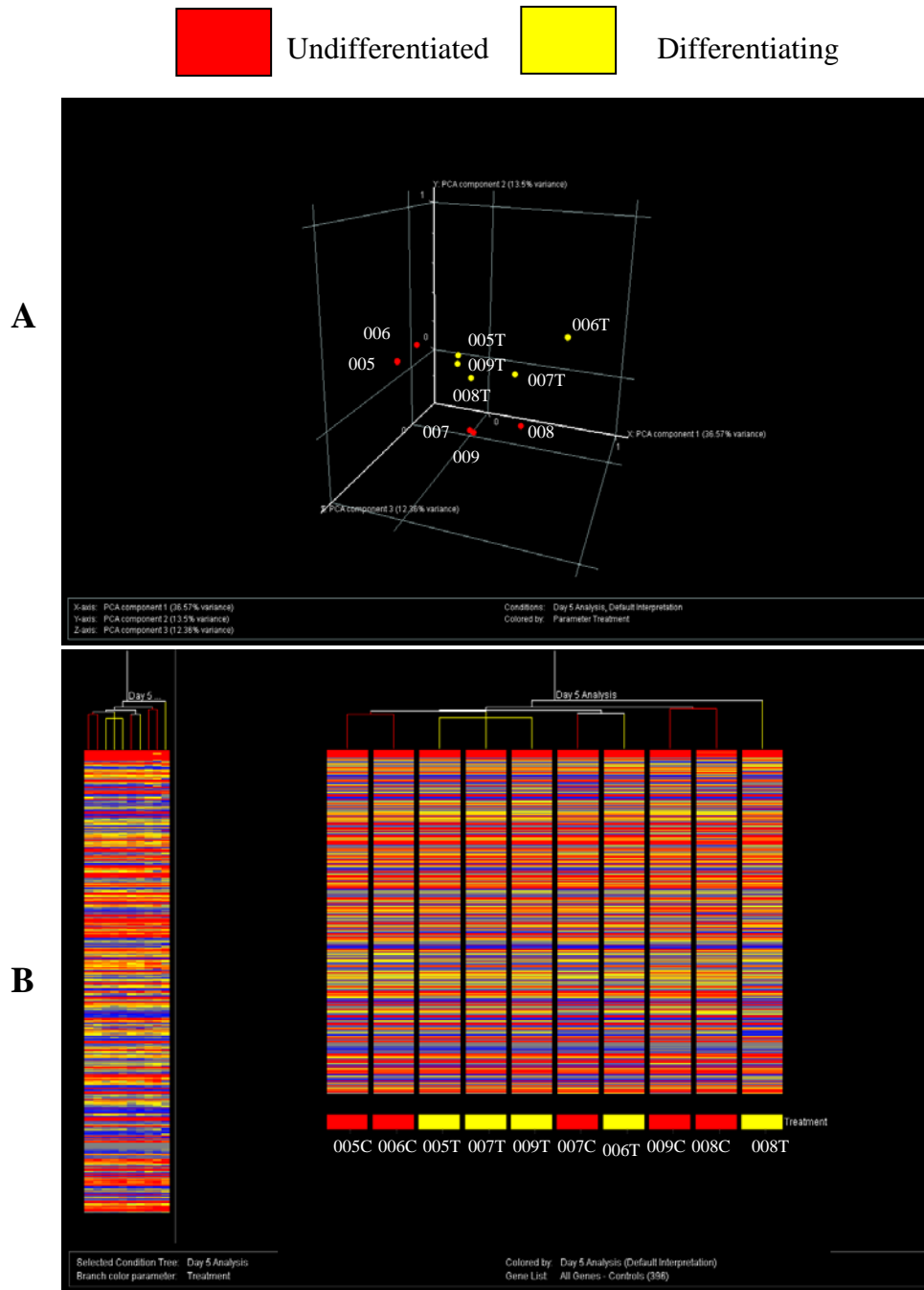


**Figure 3-8 GeneSpring analysis does not reveal significant changes in miRNA expression at day 5 of adipogenesis.**

PCA analysis (A) reveals no clear grouping of the undifferentiating samples (red) and the differentiating samples (yellow). Hierarchical clustering (B) shows no clear grouping of the two conditions confirming no miRNA expression changes of significance between undifferentiated and differentiating MSCs.

#### **3.2.3.4 RT-PCR Confirmation of MiRNA Microarray Data**

It has been reported by a number of groups that microarray-based expression analysis often underestimates the changes occurring between samples (Kothapalli, Yoder et al. 2002; Yao, Rakhade et al. 2004). For this reason, it is best practise to confirm the changes observed by microarray using RT-PCR.

Whilst the array data showed that no miRNAs were changed by more than 1.5 fold in all donors, members of the let-7 family had large changes in MSCs from several but not all of the 5 donors. It was decided to determine the expression levels of these miRNAs in MSCS from all donors using miRNA specific RT-PCR with MSC-derived RNA from all donors. All miRNA-specific PCRs were performed as per section 2.4.3.2 and were normalised to the endogenous control RNU24. However, despite the increased sensitivity of the RT-PCR techniques compared to the array, there were no statistically significant changes in the levels of these miRNAs in MSCS from all donors (Figure 3-9A).

MiRNA-143, previously demonstrated to have a role in adipogenesis, was upregulated 2.6 fold in a human pre-adipocyte cell line (Esau, Kang et al. 2004). However, RT-PCR analysis of the RNA from these MSCs revealed that miR-143 was not significantly regulated at day 5 of adipogenesis in a human MSC model (Figure 3-9B).

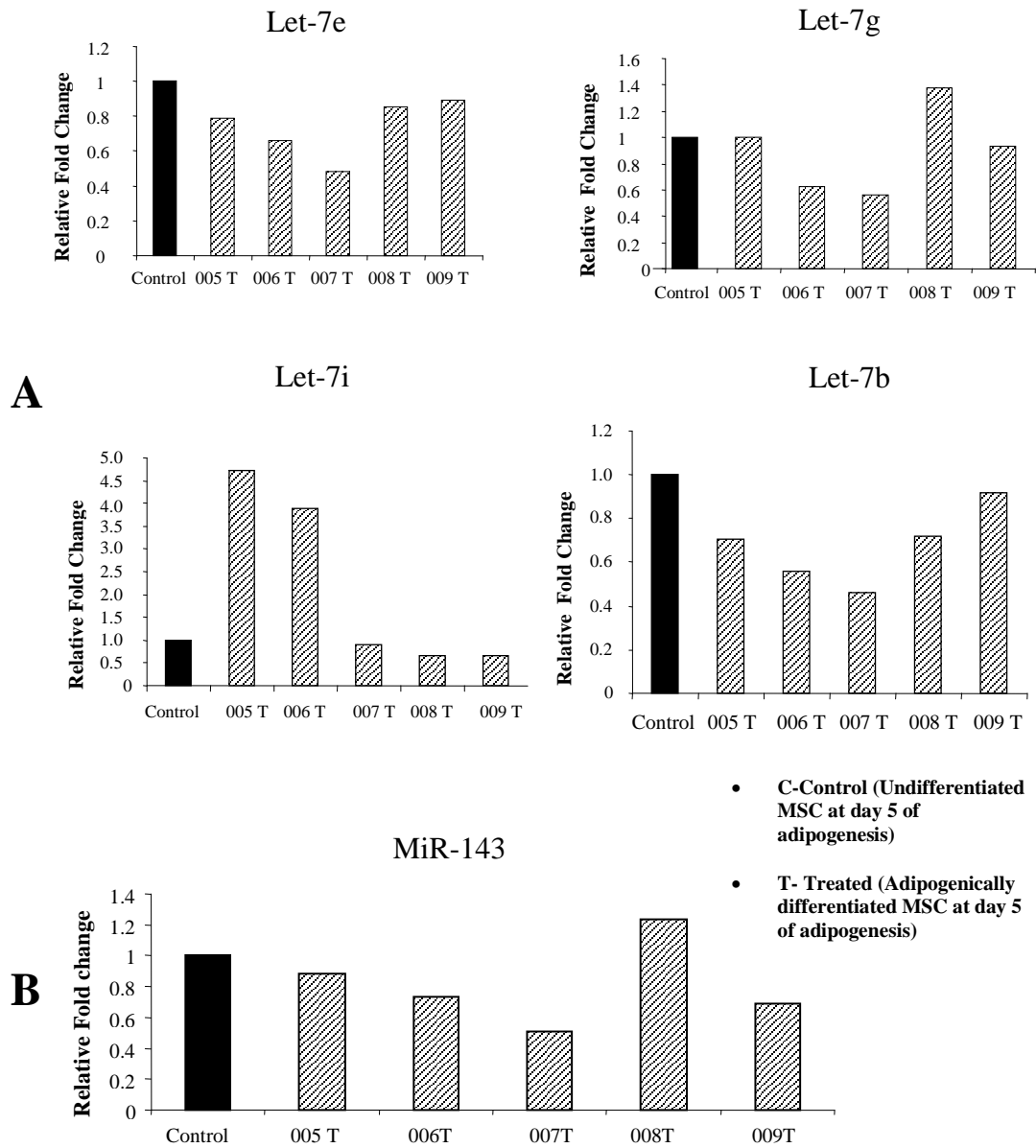


**Figure 3-9 -RT-PCR confirms that there are no significant miRNA changes at day 5 of adipogenesis in MSCs isolated from 5 donors**

MiRNA RT-PCR was used to determine expression levels of (A) members of the let-7 family and (B) miR-143 (an important miRNA in adipogenesis demonstrated in pre-adipocytes) in MSCs 5 days after inducing adipogenesis. All samples were normalised to the endogenous control RNU24 and are presented as a fold change compared to undifferentiated MSCs (n=5 donors).

### **3.2.3.5 Analysis of MiRNA Expression at Day 5 of Adipogenesis**

The results presented above show that at day 5 of adipogenesis, none of the miRNAs detected on the array show significant changes in expression level in MSCs from all 5 donors, despite cells from all 5 donors accumulating significant amounts of lipid (Figure 3-6C). It is possible that miRNAs do not exert an effect on MSC adipogenesis, but this seems unlikely given the many reports published on the roles of miRNAs in various developmental processes. There are two potential explanations why no significant changes in miRNA level were observed at day 5 of MSC adipogenesis by miRNA array analysis.

#### **1. Timing**

It is possible that there are no changes in the levels of specific miRNAs at day 5 of adipogenesis. Perhaps changes in miRNA levels and exertion of their effects (if any) occur at an earlier and/or later stage in the process.

#### **2. Purity of the population**

The second potential reason for failing to detect changes in miRNAs is due to the incomplete differentiation that occurs in an MSC population. We have shown that the differentiation of MSCs to adipocytes is heterogeneous, with variable levels of MSCs forming lipid-filled adipocytes (depending on donor and passage). This is evident from Figure 3-6C where varying degrees of differentiation can be seen in MSCs from each of the 5 donors under investigation.

It is therefore possible, that the changes in miRNA expression level in the differentiating population (which can be from 1.5- 3 fold change in expression (Esau, Kang et al. 2004) may not appear significant due to the ‘masking’ effect of the population of undifferentiated MSCs. A possible solution is to investigate miRNA expression differences between an undifferentiated population of MSCs and a pure population of differentiated adipocytes.

### 3.2.4 Isolating a Pure Population of MSC-Derived Adipocytes

To address both of these variables, we created a pure population of MSC-derived adipocytes using the ‘Ceiling Culture’ method (Zhang, Kumar et al. 2000) as described in section 2.1.2.4.5. This requires significant lipid accumulation by the MSCs and so was performed at day 20 of the adipogenic protocol. Figure 3-10A shows a population of differentiating MSCs at day 20 of adipogenesis, where both undifferentiated and differentiating MSCs can be seen. Following separation by ceiling culture, the MSCs that have differentiated and accumulated enough lipid to be buoyant float to the top as seen in Figure 3-10B (4x) and C (10x). However the undifferentiated MSCs and differentiating MSCs without sufficient lipid to be buoyant fall to the bottom of the flask (Figure 3-10D (4x)). There are no visible undifferentiated cells present in the harvested population (i.e. all cells show the presence of lipid filled vesicles) verifying that a pure population of MSC-derived adipocytes has been isolated.

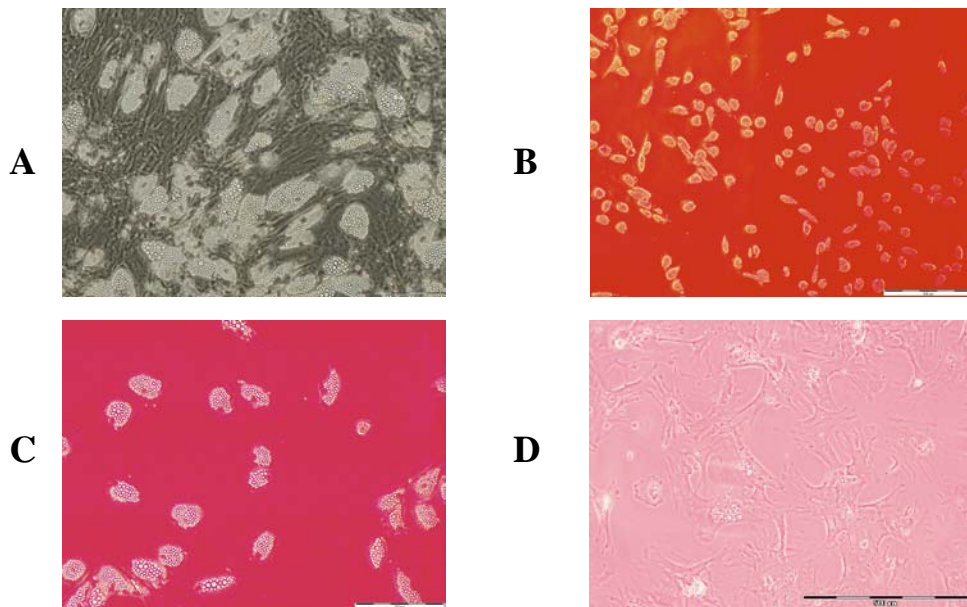


**Figure 3-10 Representative phase contrast micrographs of adipogenically differentiating MSCs before and after using the ‘Ceiling Culture’ method.**

Phase contrast micrographs of differentiating MSC population at day 20 of adipogenesis (A). Following ‘Ceiling Culture’ a pure population of adipogenic MSCs is isolated (B 4x objective, C 10x objective) which does not contain undifferentiated MSCs. Undifferentiated MSCs and differentiating MSCs, which have not formed sufficient lipid droplets, fall to the bottom of the flask (D, 4x objective).

### 3.2.5 Analysis of Changes in MiRNA Expression at Day 20 of Adipogenesis

MiRNA expression levels were compared between undifferentiated MSCs and a pure population of MSC-derived adipocytes using a MiChip microarray (Section 2.4.4) with probes for 526 miRNAs at day 20 of adipogenesis. This comparison was performed in MSCs isolated from four donors (022,023,024,026) (section 2.1.1), selected from the REMEDI primary cell bank. These MSCs were induced to undergo adipogenesis as per section 2.1.2.4.1. At the end point of adipogenesis (20 days after adipogenic induction), a pure population of mature adipocytes was isolated using the ceiling culture method, as described in section 2.1.2.4.5. Figure 3-11A shows the mixed population of differentiating and undifferentiating MSCs at day 20 of the assay. Figure 3-11B shows the population of cells present after applying ceiling culture, this contains only those cells with enough lipid to allow them to float to the top of the flask. The MSCs that have not differentiated or have not accumulated enough lipid to be sufficiently buoyant to float, remain at the bottom of the flask.

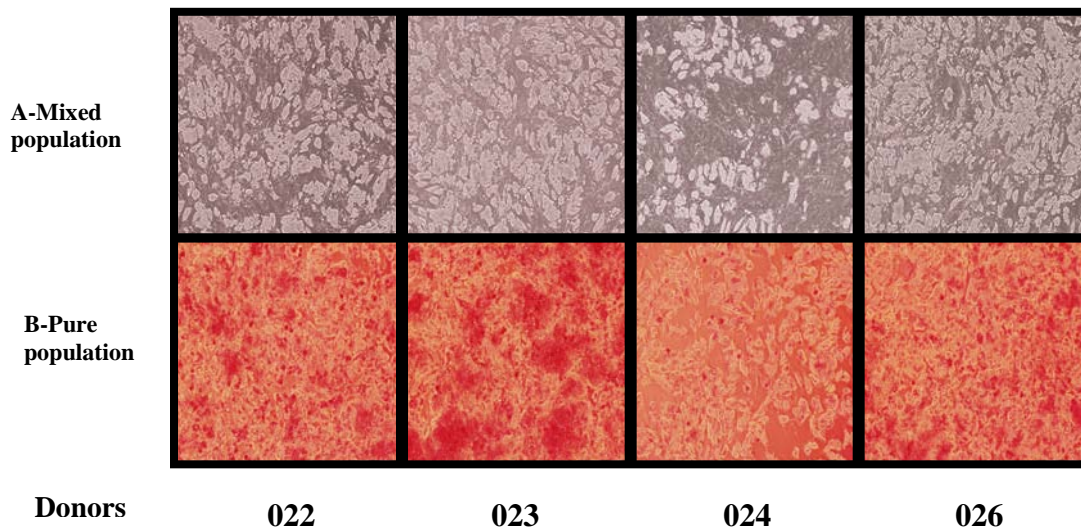
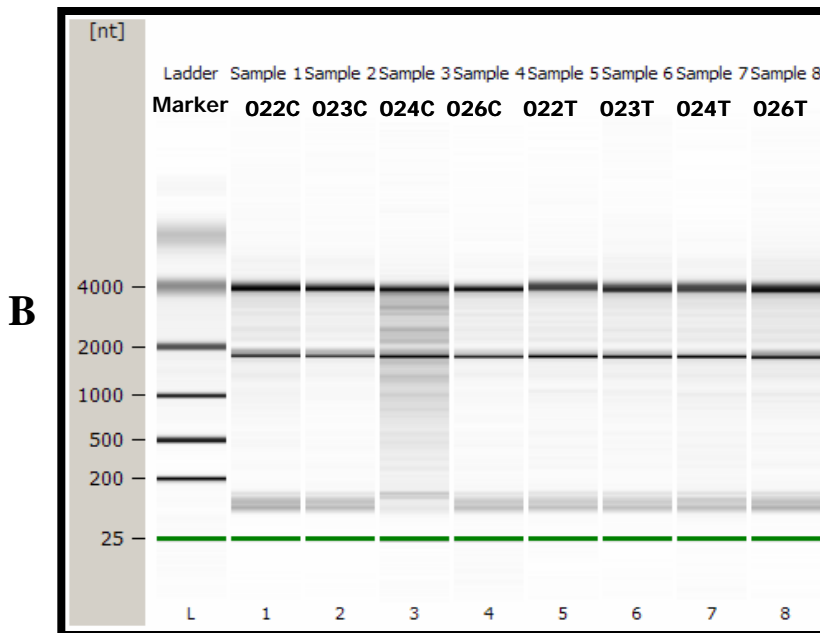
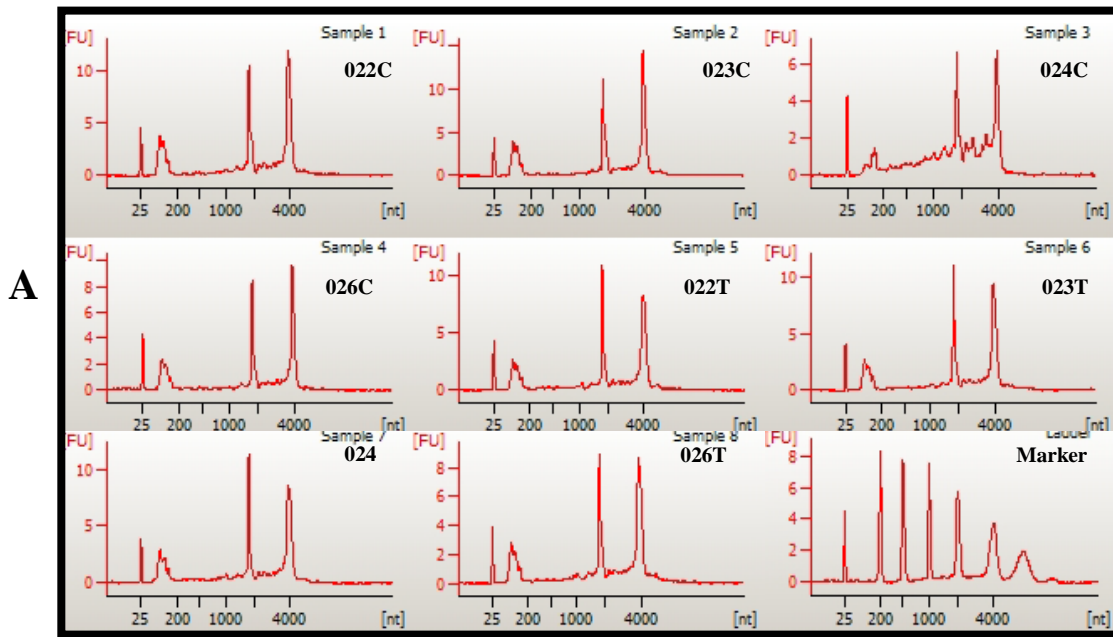


**Figure 3-11 MSCs (4 donors) 20 days after adipogenic induction before and after Ceiling Culture.**

Panel of phase contrast micrographs of MSCs isolated from four donors at day 20 of adipogenesis (A). This panel shows a mixed population of cells with both differentiating and undifferentiating MSCs (10x objective). Panel of phase contrast micrographs showing the pure population of adipocytes following 'Ceiling Culture' (10x objective) (B). There are no signs of undifferentiating MSCs present in this population.

After 24 hours, adipogenic MSCs containing lipid had floated to the top of the flask and attached. The 'Ceiling Culture' protocol was not performed on the undifferentiating (control) MSCs. Since the protocol is based on the buoyant property of adipocyte, the undifferentiated MSCs would not have floated when trypsinised and inverted. It is appreciated that this process could introduce a bias in the array results as the adipogenic samples would have been subject to the additional trypsinisation process.

Total RNA was isolated from all undifferentiated and adipogenically differentiated samples as per section 2.4.1. The quality and integrity of the RNA for each sample was investigated using the Bioanalyzer prior to microarray analysis, as per section 2.4.2. RNA from all samples except 024C was of high quality, as evident from the electropherogram, the predicted gel and a high RIN value as seen in figure 3-12. At the time of microarray analysis, 024C RNA was too dilute and thus had to be concentrated using vacuum centrifugation to obtain an appropriate concentration. This could have affected the integrity of the RNA as both the electropherogram and the predicted gel for 024C show signs of RNA degradation as seen in figure 3-12A, B. The RIN value was also lower than the other samples (Figure 3-12C) and at a value of 6.8 could affect the quality of the results from the microarray for this sample.



**C**

Sample	RIN value
022C	8.5
023C	8.9
024C	6.8
026C	9.1
022T	8.8
023T	8.5
024T	8.2
026T	8.6

**Figure 3-12 Quality of RNA verified by Bioanalyzer**

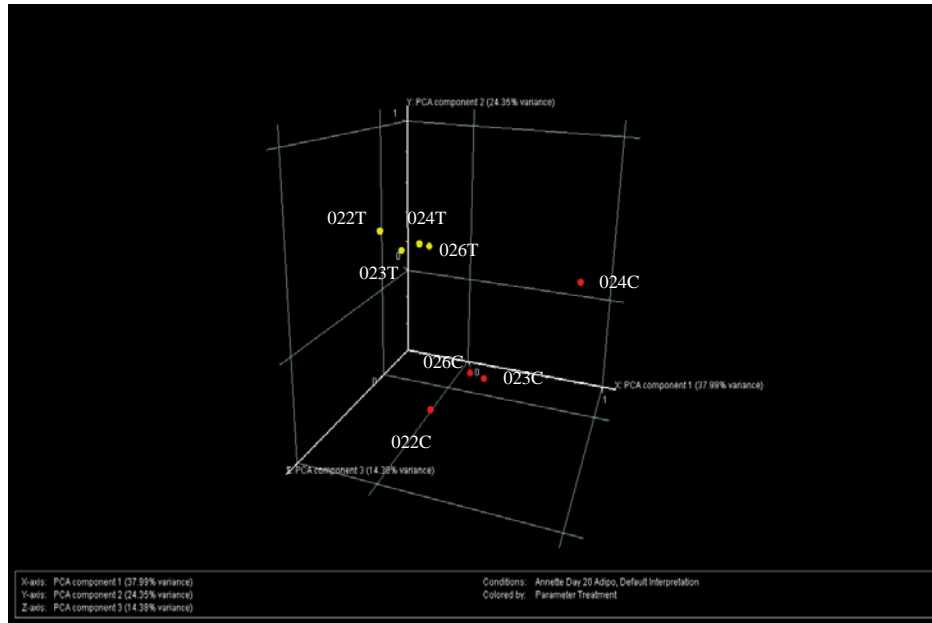
Electropherogram (A) and predicted gel (B) of RNA isolated from control and treated MSCs from each donor demonstrating the RNA peaks of a successful sample run, where C (Control-undifferentiated MSC) and T (Treated- adipogenically differentiated MSC). (C) Table showing the RNA integrity number (RIN) values for each sample.

### **3.2.5.1 GeneSpring Analysis of Day 20 Microarray Data**

The MiChip array data generated was analysed using the GeneSpring data analysis platform. After normalisation of the data, the expression profiles were examined for trends between undifferentiated and differentiated samples (Section 2.4.4.7). This was done using the same two methods used to analyse the day 5 array data; Principal Components Analysis (PCA) and hierarchical clustering. The results of PCA analysis, shown in Figure 3-13A, shows clear clustering between the undifferentiated (red) and the differentiated (yellow) samples implying a difference in miRNA expression between the two conditions. The hierarchical clustering analysis is in agreement with this analysis, showing grouping of the undifferentiated samples (red) and grouping of the differentiated samples (yellow) from each donor (Figure 4-8B). These analyses indicate that the miRNA expression profile of the differentiated samples is distinct from the undifferentiated samples. Statistical analysis performed as per section 2.4.4.7 revealed 20 significant miRNAs with a fold change greater than 1.5 in adipogenically differentiating MSCs compared to control and an adjusted p-value less than 0.05, as seen in figure 3-14. The 20 regulated miRNAs are listed in figure 3-15, 11 of which were significantly downregulated in control MSCs compared to MSC-derived adipocytes at day 20 while 9 were significantly upregulated.

Undifferentiated
  Differentiating

A



B

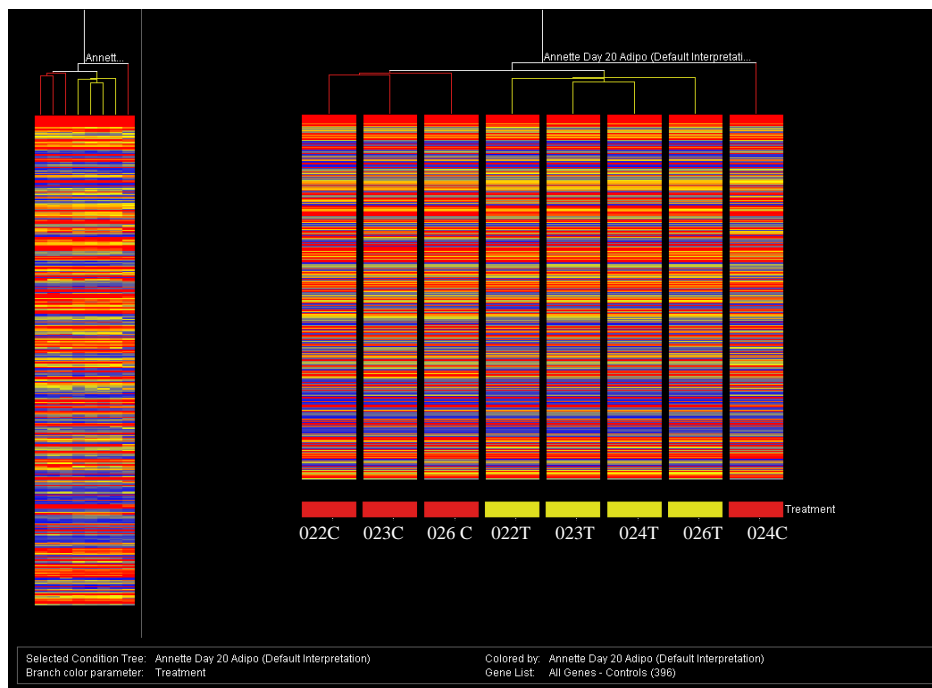


**Figure 3-13 GeneSpring analysis reveals a clear grouping of treated (differentiating) Vs control (undifferentiated) samples at day 20 of adipogenesis across 4 donors.**

PCA analysis (A) reveals clear grouping of the undifferentiated samples (red) Vs the differentiating samples (yellow). Hierarchical clustering (B) shows a grouping of undifferentiated Vs differentiated indicating that there are a number of miRNAs significantly different between the two conditions across all 4 donors.

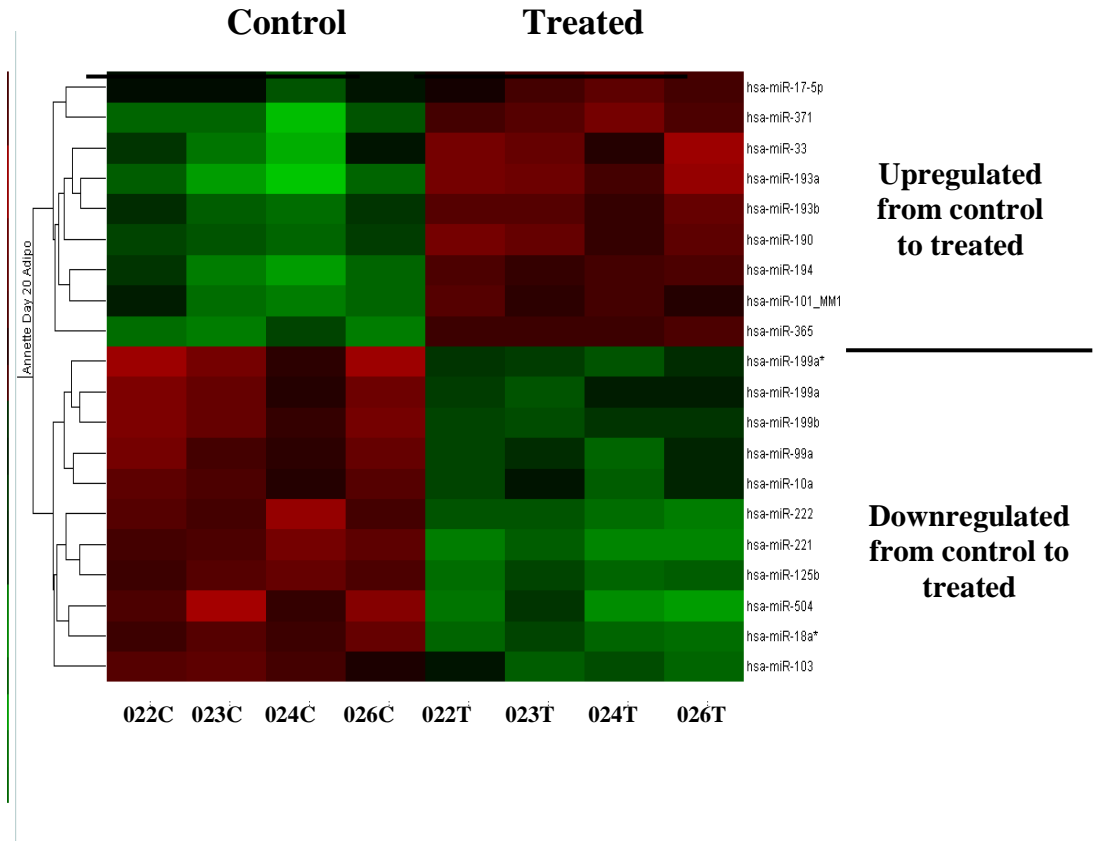


**Figure 3-14 Significantly regulated miRNAs (20) at day 20 of adipogenesis.**

Heatmap generated from GeneSpring analysis. The upper section shows 9 miRNAs whose expression is significantly upregulated from control to treated (Green to red) while the lower section shows 11 miRNAs significantly downregulated from control to treated (Red to green) across all donors

**Downregulated MiRNAs**

<b>MiRNA</b>	<b>Fold Change</b>	<b>P-value</b>
Hsa-miR-504	0.272	0.0208
Hsa-miR-221	0.323	0.00459
Hsa-miR-199a*	0.354	0.0454
Hsa-miR-222	0.359	0.021
Hsa-miR-199b	0.424	0.0262
Hsa-miR-125b	0.425	0.00459
Hsa-miR-18a	0.431	0.00534
Hsa-miR-199a	0.468	0.0316
Hsa-miR-99a	0.486	0.0262
Hsa-miR-103	0.507	0.0179
Hsa-miR-10a	0.547	0.0179

**Upregulated MiRNAs**

<b>MiRNA</b>	<b>Fold Change</b>	<b>P-Value</b>
Hsa-miR-17-5p	1.523	0.0454
Hsa-miR-101_MI	2.055	0.023
Hsa-miR-193b	2.188	0.0107
Hsa-miR-365	2.351	0.0107
Hsa-miR-190	2.368	0.0141
Hsa-miR-194	2.477	0.03
Hsa-miR-33	3.143	0.0352
Hsa-miR-371	3.156	0.03
Hsa-miR-193a	4.634	0.0179

**Figure 3-15 Significantly regulated miRNAs (20) at day 20 of adipogenesis.**

List of 20 significantly regulated miRNAs with fold change  $\geq 1.5$  and and p -value  $\leq 0.05$  from undifferentiated to adipogenically differentiating MSCs in 4 donors at day 20 of adipogenesis.

### **3.2.5.2 RT-PCR Confirmation of Day 20 Microarray Data**

As discussed in section 3.2.3.4, it is necessary to confirm the results of the microarray by RT-PCR. MiRNA specific RT-PCR was performed on RNA used for the day 20 microarray analysis (Section 2.4.3.2). All miRNAs were normalised to the levels of the endogenous control RNU24. Table 3-1 shows the results of the RT-PCR analysis which confirms the microarray analysis for miRNAs-221, 222, 99a, 193a and 17-5p.

MiRNA-221 and miR-222 were confirmed as significantly downregulated between undifferentiated and differentiated MSCs at day 20 of adipogenesis (Figure 3-16) while miR-193a was confirmed as significantly upregulated in all donors (Figure 3-17). The expression of miR-18a was examined by RT-PCR which showed that it is upregulated during adipogenesis, contradicting the results of the microarray which indicated miR-18a was downregulated (Figure 3-18). If the average of the donors is calculated, the expression of miR-17-5p and miR-99a are also confirmed by RT-PCR. However, individual examination of donor expression reveals that in both instances there is one donor that shows a different expression pattern to the others (Figure 3-19).

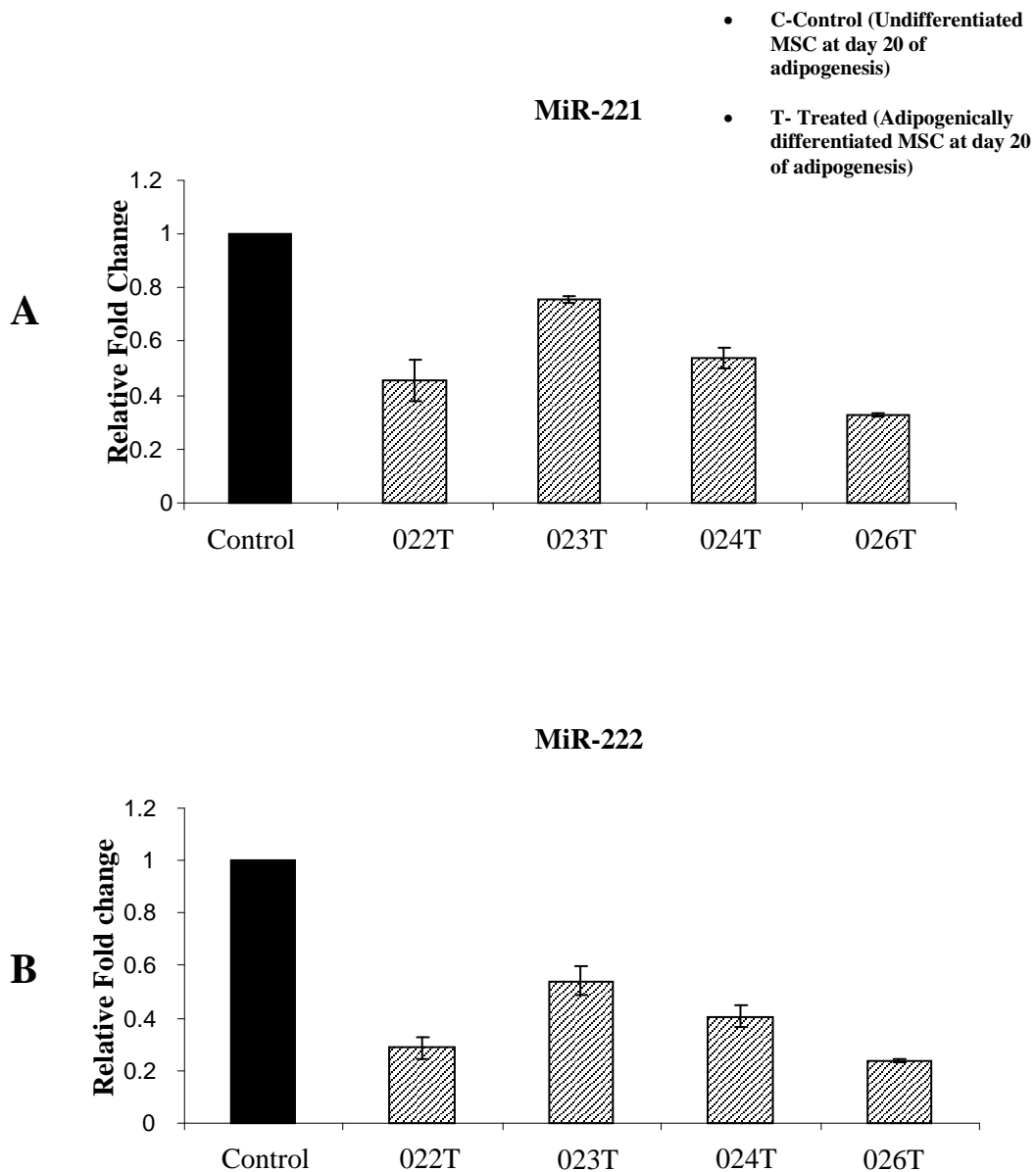


**Figure 3-16 RT- PCR confirms miR-221 and miR-222 are significantly downregulated across all donors at day 20 of adipogenesis**

MiRNA RT-PCR was used to examine the expression of miR-221 and miR-222 in MSCs from 4 donors at day 20 of adipogenesis. All samples were normalised to the endogenous control RNU24 and are presented as a fold change compared to undifferentiated MSCs. Error bars represent technical replicates of each donor, (n=4 donors)

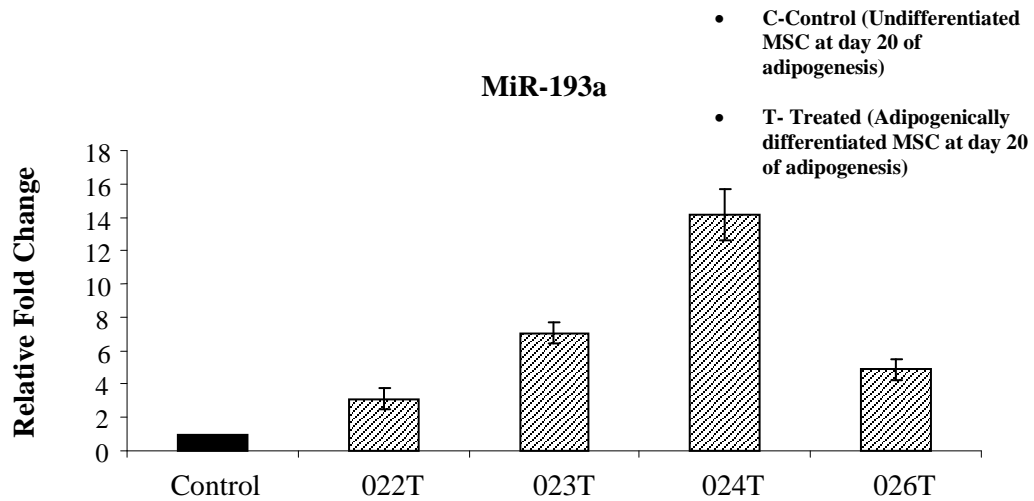


**Figure 3-17 RT- PCR confirms miR-193a is upregulated at day 20 across all donors**

RT-PCR analysis of miR-193a in MSCs from 4 donors at day 20 of adipogenesis. All samples were normalised to the endogenous control RNU24 and presented as a fold change compared to undifferentiated MSCs. Error bars represent technical replicates of each donor, (n=4 donors).

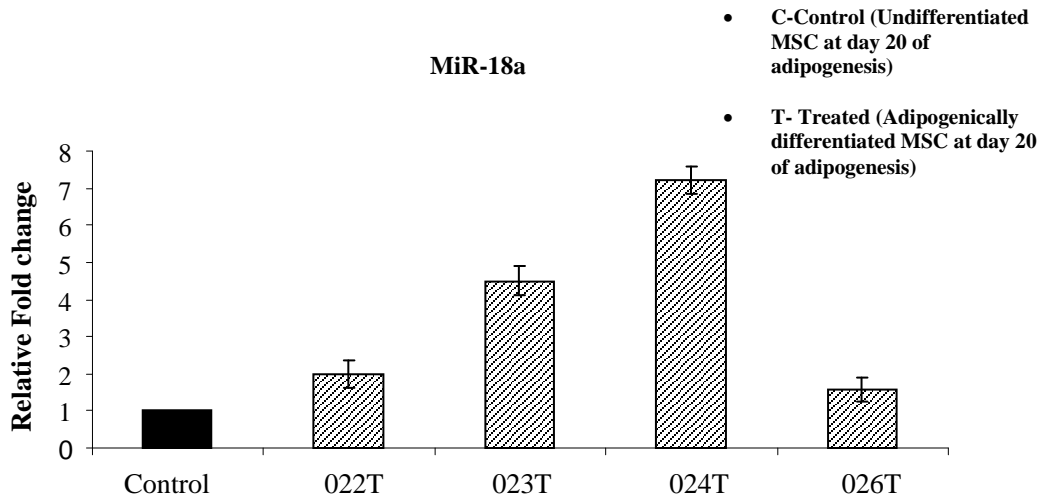


**Figure 3-18- RT-PCR analysis contradicts microarray results and shows miR-18a is upregulated at day 20 of adipogenesis**

RT-PCR analysis of miR-18a in MSCs from 4 donors at day 20 of adipogenesis. All samples were normalised to the endogenous control RNU24 and presented as a fold change compared to undifferentiated MSCs. Error bars represent technical replicates of each donor, (n=4 donors).

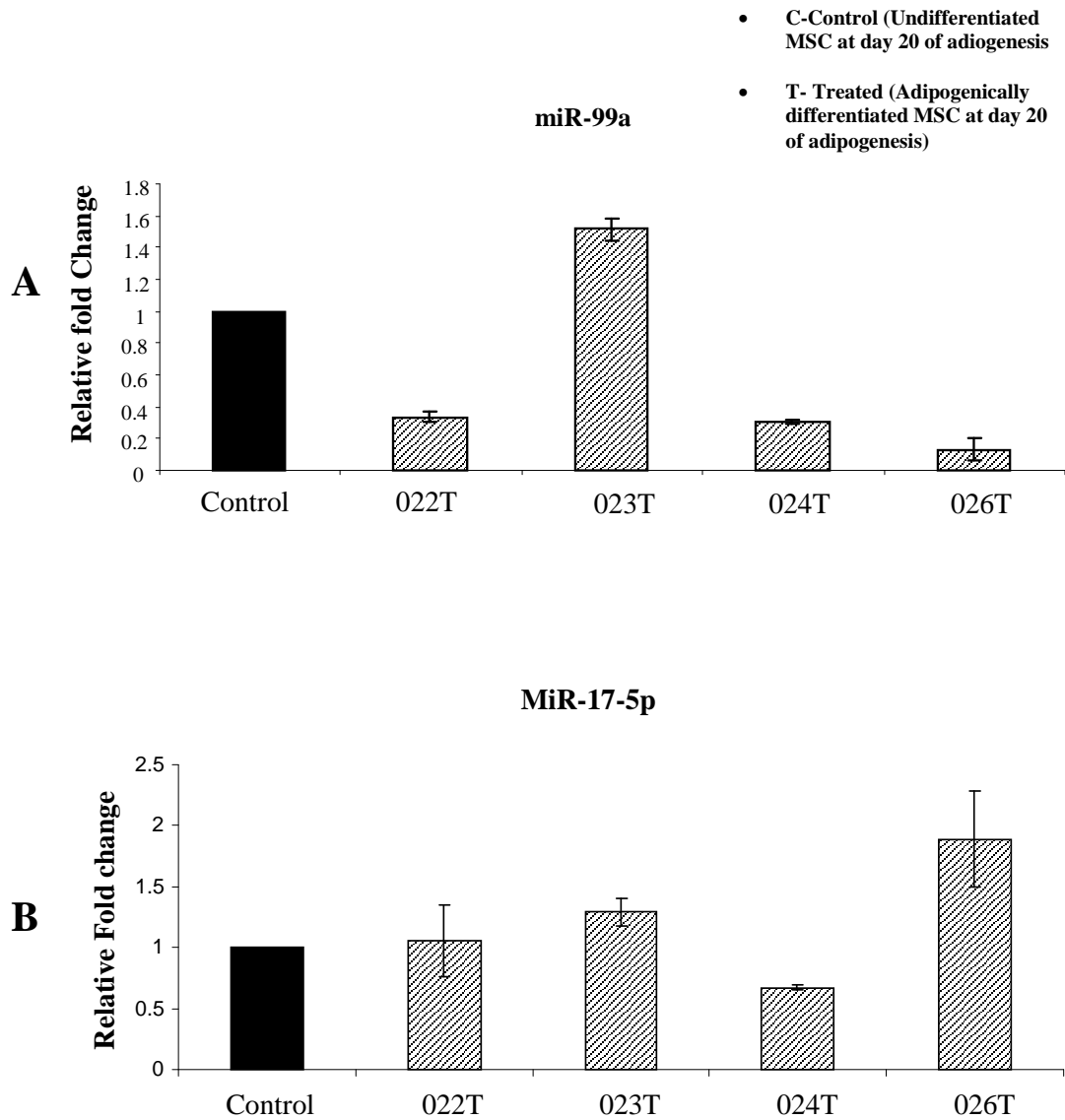


**Figure 3-19 RT- PCR shows donor- donor variability in expression of miR-99a and miR-17-5p at day 20 of adipogenesis**

RT-PCR analysis of miR-99a (A) and miR-17-5p (B) expression across 4 donors. All samples were normalised to the endogenous control RNU24 and presented as a fold change compared to undifferentiated MSCs. Error bars represent technical replicates of each donor, (n=4 donors).

	<b>MiR-221</b>	<b>MiR-222</b>	<b>MiR-99a</b>	<b>MiR-193a</b>	<b>MiR-17-5p</b>	<b>MiR-18a</b>
<b>Microarray</b>	<b>3.09</b> (Downregulated)	<b>2.832</b> (Downregulated)	<b>2.05</b> (Downregulated)	<b>4.64</b> (Upregulated)	<b>1.5</b> (Upregulated)	<b>0.431</b> (Downregulated)
<b>RT-PCR</b>	<b>1.92</b> (Downregulated)	<b>2.719</b> (Downregulated)	<b>1.75</b> (Downregulated)	<b>7.3</b> (Upregulated)	<b>1.2</b> (Upregulated)	<b>3.75</b> (Upregulated)

**Table 3-1 Comparison of miRNA expression changes analysed by microarray and RT-PCR.**

Table showing mean fold change of miR-221,222, 99a, 193a and miR-17-5p measured using RNA isolated from undifferentiated MSC and adipogenic MSC (n=4 donors).

### **3.3 Discussion**

#### **3.3.1 Mesenchymal Stem Cells**

As discussed in section 1.2.1, MSCs are a very attractive cell for use in regenerative medicine due to their ease of isolation, differentiation potential and limited immunogenicity. There is, however much debate as to the definition of the 'true' MSC. This is an issue that has caused much debate in the field of MSC research and it is the focus of many MSC researchers to find one true 'marker' of an MSC, which at present does not exist. As a result, MSCs are characterised based on functionality (i.e. differentiation to adipogenic, osteogenic and chondrogenic lineages) and the expression or absence of a combination of surface markers. The International Society for Cellular Therapy state that 'MSCs must express CD105, CD73 and CD90 ( $\geq 95\%$  of the population) as measured by flow cytometry. They must lack expression of CD45, CD34, CD14 or CD11b, CD79 $\alpha$  or CD19 and HLA class II ( $\leq 2\%$  positive)'.

#### **3.3.2 Differentiation of hMSCs to adipocytes**

MSCs were isolated from a number of donors and validated based on these criteria. *Bona fide* MSCs then were induced to undergo adipogenesis. The level of adipogenic differentiation achieved, ranging from 25%- 60% differentiation in a population of MSCs was consistent with the levels achieved by others (Pittenger, Mackay et al. 1999; Janderova, McNeil et al. 2003). This variability in adipogenic differentiation between donors has been shown by others (Lakshmipathy and Hart 2008) and could potentially be explained by a number of reasons.

Firstly, it is appreciated that the population of cells isolated from human bone marrow could be heterogenous and that the conditions defined by the International Society for Cellular Therapy (ISCT) are not stringent enough to definitively identify a 'true' MSC (Dominici, Le Blanc et al. 2006). For this reason, the cells used in each experiment could actually contain a mixture of undifferentiated stem cells, progenitor cells and tissue specific somatic cells as these could also meet some of the criteria for surface marker expression.

Secondly, each ‘true’ MSC isolated can then go on to vary in differentiation and self-renewal potential. This is evident from numerous clonal studies performed on bone marrow derived MSCs (Pittenger, Mackay et al. 1999; Muraglia, Cancedda et al. 2000; Schieker, Pautke et al. 2007) where 100% differentiation of a clonal population is still not observed. These studies have shown that MSC clones derived from a single cell can be functionally heterogeneous, with clones showing variable levels of differentiation ability. In a study of 185 clones, Quarto *et al* showed that only one third of clones differentiated into all three lineages while most of the clones could differentiate into osteo and chondro but not adipo (Muraglia, Cancedda et al. 2000). Finally, this somewhat crude method of identifying and isolating the MSC could vary in technical accuracy each time and thus incur variability in the proportion of MSCs isolated from preparation to preparation. As well as variability in the number isolated in each preparation, the potential of each ‘true’ MSC may change between donors, as highlighted from the clonal studies.

The fact that a pure population of ‘true’ MSCs cannot be isolated, in combination with the varying levels of differentiation of each cell could also be used to explain the low level of adipogenic differentiation (25%) sometimes observed. These reasons are a more likely cause for the low level of differentiation than the protocol used to induce adipogenic differentiation. The protocol used for preparing adipogenic induction medium (AIM) has been adapted from two key papers in the field of MSC adipogenesis (Pittenger, Mackay et al. 1999; Janderova, McNeil et al. 2003). This is the established protocol used routinely in-house for all MSC adipogenesis experiments and specifically induces the adipogenic differentiation of MSCs. Treatment of human fibroblasts using the identical adipogenic induction protocol does not cause cells to take on an adipocyte-like morphology or to display any signs of lipid accumulation. Janderova *et al* report that the treatment of a population of MSCs with this standard differentiation medium results in 20% of the population efficiently differentiating to adipocytes (Janderova, McNeil et al. 2003). This correlates with the level of differentiation we observed in MSCs treated with adipogenic induction medium and the images presented in this thesis are

representative of this. These images are consistent with other such images presented by others in the literature (Pittenger, Mackay et al. 1999; Janderova, McNeil et al. 2003).

### **3.3.3 Identification of Significantly Regulated MiRNAs at Day 5 of Adipogenesis**

It was assumed that miRNAs which play regulatory roles during adipogenesis would undergo changes in expression level during differentiation. To identify changes in global miRNA expression level, a microarray analysis was performed.

An initial miRNA analysis, performed 5 days after inducing adipogenesis, identified no reproducible changes greater than 1.5 fold when differentiating and undifferentiated MSCs were compared. This was a surprising result, given the many reports published on the roles of miRNAs in various developmental processes. It was thought perhaps, that this was due to the timing of the analysis and that miRNAs were not playing a role at an early stage in adipogenesis. However, recently other groups have shown expression changes and roles for miRNAs at early stages in adipogenesis, albeit in MSCs from different sources. Karbiener *et al* showed that miR-27b is significantly decreased at day 3 of adipogenesis in MSCs derived from human adipose tissue (Karbiener, Fischer et al. 2009). Jung *et al* showed that in MSCs derived from adipose tissue the expression of miR-21 peaked 3 days into adipogenesis and that overexpression of this miRNA had a positive effect on adipogenesis through modulating the TGF- $\beta$  pathway (Kim, Hwang et al. 2009).

Another possible reason for not identifying significant changes in miRNA level at this stage of adipogenesis is the heterogeneity of the differentiating population i.e. that potentially a lack of change in the undifferentiated proportion may mask a subtle change in the expression level in the minority cells which are differentiating.

### 3.3.4 Identification of Significantly Regulated MiRNAs at Day 20 of Adipogenesis

In order to address this issue we isolated a pure population of differentiating MSCs using the ‘Ceiling Culture’ method at day 20 of adipogenesis and repeated the miRNA array analysis using RNA from MSCs isolated from 4 donors. To our knowledge, this is the first miRNA expression analysis performed on a pure population of differentiating MSC-derived adipocytes. The ‘Ceiling Culture’ protocol is a method of separating fat-filled adipocytes from a population of non-mature adipocytes, in this case a mixed population of differentiating and undifferentiating MSCs. This is an effective method of creating a pure population of differentiated adipocytes. It was decided not to perform the ‘Ceiling Culture’ protocol on the undifferentiating (control) MSCs. Since the protocol is based on the buoyant property of adipocytes i.e. containing enough lipid to be bouyant, the undifferentiated MSCs would not have floated when trypsinised and inverted. It is appreciated that this difference could introduce a bias in the array results as the adipogenic samples would have been subject to the trypsinisation process whereas the undifferentiated MSCs were not. The microarray results were confirmed using the same populations of MSCs upon which the microarray had been performed. In addition, the results of our microarray have been confirmed by Skarn *et al* (Skarn, Namlos et al. 2011) who also show the expression of miR-221 and miR-222 is significantly downregulated and by Bork *et al* (Bork, Horn et al. 2010) who also show downregulation of miR-99a, mir-199a and miR-199b expression in adipogenic differentiation. We can therefore, be reasonably confident that not performing the ‘ceiling culture’ on the controls did not introduce a bias into the microarray results with respect to these miRNAs.

This analysis identified 20 miRNAs which had expression changes of greater than 1.5 fold in MSCs from all 4 donors at day 20 of adipogenesis, 11 miRNAs were downregulated and 9 were upregulated more than 1.5 fold (Figure 3-15). A 2008 study identified 20 miRNAs that were significantly upregulated during adipogenesis and one that was downregulated in 3 donors (Oskowitz, Lu et al. 2008). Only 3

miRNAs (miR-125b, miR-199a and miR-103) were identified in their analyses which are identified in ours. However, Oskowitz *et al* describe miR-125b, miR-199a and miR-103 as being upregulated across all time points examined (Day 0, 1, 3, 7 and 14) in adipogenesis while we show downregulation of these miRNAs at day 20 of adipogenesis.

As mentioned previously, Bork *et al* also performed a miRNA expression analysis on MSCs at day 14 of adipogenic differentiation. In agreement with our data, they saw the downregulation of miR-199a, miR-199b, miR-99a, and miR-221. Interestingly, this group identify miR-371 as a key positive regulator of hMSC adipogenesis though they do not identify it as being differentially expressed by miRNA array analysis. In contrast, we identified a significant 3-fold upregulation of miR-371 by microarray analysis at day 20 of adipogenesis. There was in fact, no overlap in miRNAs identified in adipogenic differentiation of hMSCs by the Oskowitz or the Bork groups. MiR-143, a key miRNA in adipogenesis as described by Esau *et al* (Esau, Kang et al. 2004) was verified by Oskowitz *et al* but was not identified as being significantly regulated in the work described in this thesis or by Bork *et al*.

There is therefore, very little overlap between the results of all three studies, despite having the same aim, i.e to identify significantly regulated miRNAs in hMSCs undergoing adipogenic differentiation.

The differences observed could be potentially explained by several differences in the set up of the studies;

1. The different methods used to analyse miRNA expression in hMSCs undergoing adipogenesis.

We and Bork *et al* used an LNA-based microarray approach in our analysis whereas Oskowitz *et al* used a bead-based flowcytometric method. In all cases, however the expression levels are compared between undifferentiated and adipogenically differentiated cells and thus seems like an unlikely reason for observing such different patterns of expression. As previously mentioned, there are numerous

methods of investigating miRNA expression patterns. Perhaps the discrepancy in miRNA expression patterns between these studies highlights the need for a study to determine consistency in results between methods.

2. The method used to induce adipogenesis in the MSCs.

A recent publication by Scott *et al* highlighted the lack of standardisation of techniques for adipogenic induction of MSCs (Scott, Nguyen et al. 2011). They noted that there is variability between published protocols for the adipogenic induction of human bone marrow derived MSCs, thus making it difficult to compare between publications. Figure 3-20, below illustrates the variability in concentration of the three major components of adipogenic induction media used for human bone marrow derived MSCs (Insulin, Dexamethasone, IBMX) between publications.

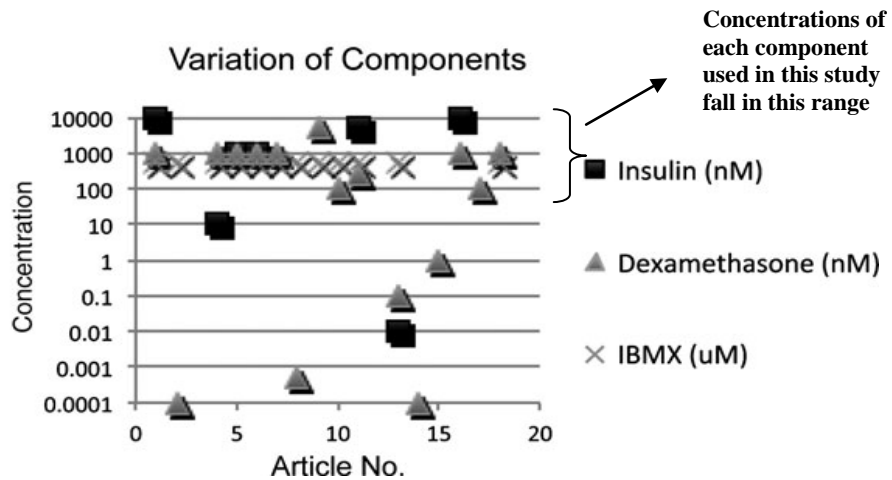


**Figure 3-20 taken from ‘Current Methods of Adipogenic Differentiation of Mesenchymal Stem Cells’ (Scott, Nguyen et al. 2011)**

There is a notable difference in the level of confluence at which induction of adipogenesis occurs between the three groups. We induced adipogenesis when the cells were two days post confluence to ensure contact inhibition as recommended (Janderova, McNeil et al. 2003). Oskowitz *at al* began induction when the cells were 90% confluent, while Bork *et al* induce adipogenesis at normal seeding density (i.e. 5000 MSCs/cm<sup>2</sup>). This difference in confluency could have an effect on

miRNA expression. As discussed by Scott *et al*, different groups use different concentrations of components in their adipogenic induction medium (Scott, Nguyen *et al*. 2011). In this case, Oskowitz *et al* do not add insulin to this medium and use lower concentrations of dexamethasone and indomethacin than that used in the adipogenic induction medium used here and used by Bork *et al*. Potentially the differences in the concentrations of adipogenic induction reagents could have an effect on the expression levels of miRNAs expressed in MSCs.

### 3. The passage number of the MSCs under analysis.

The MSCs used in these experiments here were one passage higher than the MSCs used by Oskowitz *et al*. Bork *et al* do not state what passage number of the MSCs used for the experiments described but state that they were culture expanded for 2-3 months. This suggests that the MSCs used in their experiments would be of a much higher passage than used in either our work or that by Oskowitz *et al*. It would be more accurate and relevant to compare population doublings than passages but this data is not available from any of the studies described.

### 4. The level of purity of the populations under analysis.

We sorted the fully differentiated adipocytes from the undifferentiated population to establish the miRNAs that change in the differentiation process. These studies show the results of miRNA expression in a population of differentiating MSCs; our miRNA expression analysis was performed on a pure population of adipocytes compared to undifferentiated MSCs. The Oskowitz group or the Bork group did not create a pure population. It is possible that these miRNAs have different expression patterns depending on the level of maturity of the adipocyte. As this study was performed on primary MSCs isolated from human donors, donor-donor variability of miRNA expression needs to be appreciated. Our study and the study by Bork *et al* was performed on MSCs from 4 donors while the study performed by Oskowitz *et al* was performed three donors.

This variability in results confirms that care needs to be taken when drawing conclusions from a miRNA expression study. Potentially, even minor changes in a study could have large and significant changes in the results. This is demonstrated by the different expression patterns of miRNAs in these three seemingly identical studies and thus indicates the need to confirm microarray studies by other methods e.g. PCR, Northern blotting and assays to determine the functional consequences of overexpression and knockdown.

### 3.3.5 MiRNAs Regulated during Adipogenesis

In preparing to study whether any of these miRNA(s) could be a candidate for regulating MSC behaviour, it was important to consider the previously known roles of these miRNAs. Of the 20 miRNAs identified, 6 have been reported as being important in adipogenesis and other MSC related processes as seen in Table 3-2.

MiRNA	Fold change MSC to Adipo	Pathway	Predicted Target	Experimentally Validated?	Reference
<b>miR-199a</b>	2.1 fold Downregulated	Adipogenesis Osteogenesis Chondrogenesis	Leukemia Inhibitory Factor (LIF) Smad1	Yes	(Oskowitz, Lu et al. 2008) (Lin, Kong et al. 2009)
<b>miR-125b</b>	2.3 fold Downregulated	Osteogenesis	No predicted target	-----	(Mizuno, Yagi et al. 2008)
<b>miR-17-92</b>	1.5 fold Upregulated	Adipogenesis	Retinoblastoma-related gene2 (RB2/p130)	Yes	(Wang, Li et al. 2008)
<b>miR-371</b>	3.2 fold Upregulated	Adipogenesis Senescence in MSCs	DNA methyltransferase 3A (DNMT3A)	No	(Wagner, Horn et al. 2008)
<b>miR-103</b>	1.97 fold Downregulated	Adipogenesis	Pantothenate Kinase1 (PANK1)	No	(Wilfred, Wang et al. 2007; Xie, Lim et al. 2009)
<b>miR-99a</b>	2.05 fold Downregulated	Differential expression in MSCs from different sources	No predicted target	-----	(Wang, Kao et al. 2010)
<b>miR-221</b>	3.67 Downregulated	Adipogenesis Chondrogenesis	P27 Mdm2	Yes Yes	(Skarn, Namlos et al. 2011) (Kim, Song et al. 2010)
<b>miR-222</b>	2.68 Downregulated	Adipogenesis	P27	Yes	(Skarn, Namlos et al. 2011)

**Table 3-2 Published roles for identified miRNAs from microarray associated with MSC functions**

### **3.3.5.1 MiR-199 Cluster**

Hsa-miR-199a, hsa-miR-199a\* and hsa-miR-199b were downregulated between 2 and 3 fold from undifferentiated MSCs to adipogenic MSCs. This miRNA family was discovered by a number of groups independently in two different species (Lagos-Quintana, Rauhut et al. 2003) (Lim, Glasner et al. 2003). Oskowitz *et al* found that hsa-miR-199a was upregulated in hMSC adipogenesis (Oskowitz, Lu et al. 2008) and targets the cytokine LIF. As previously described, MSCs have the ability to differentiate into chondrocytes making them a very useful model for studying and possibly treating conditions such as osteoarthritis. Hsa-miR-199\* has been shown to be important in the process of chondrogenesis (Lin, Kong et al. 2009) through targeting Smad1 which is a well characterized component of BMP-2 signalling.

### **3.3.5.2 MiR-125b**

Although no role had been described for this miRNA in adipogenesis at the time, it had been reported that miR-125b was involved in osteogenesis from mouse MSCs (ST2 cells) (Mizuno, Yagi et al. 2008). The expression of miR-125b increases as osteogenesis progresses and it was shown that transfection of murine MSCs with exogenous miR-125b blocks osteogenesis through the inhibition of cell proliferation. In contrast to the downregulation of miR-125b seen in these experiments Oskowitz *et al* report a upregulation of this miRNA in hMSCs undergoing adipogenesis (Oskowitz, Lu et al. 2008).

### **3.3.5.3 MiR-17-92 Cluster**

MiR-17-5p, miR-17-3p, miR-18a, miR-19a, miR-20a, miR-19b and miR-92a make up the miR-17-92 cluster of miRNAs located on chromosome 13. Two members of this cluster; miR-17-5p and miR-18a were found to be significantly regulated between undifferentiated MSCs and adipogenic MSCs (Figure 3-15). MiR-17-5p was upregulated 1.5 fold while miR-18a was downregulated 2.3 fold from undifferentiated to differentiated MSCs. Li *et al* have reported a role for mir-17-5p in adipogenesis in a mouse pre-adipocyte cell line. This group reports that five members of the miR-17-92 cluster were upregulated at 4 hours and 24 hours after

initiating adipogenesis. They correlate this upregulation to 2 key stages during murine adipogenesis, at 4 hours with G phase and at 24 hours with the end of clonal expansion (Differentiation of murine pre-adipocytes and how it differs to human adipogenesis has been discussed in section 1.4). The authors conclude that the miR-17-92 cluster accelerates adipocyte differentiation through the downregulation of the tumor suppressor Rb2/p130 (Wang, Li et al. 2008).

#### **3.3.5.4 MiR-371**

Microarray analysis identified miR-371 as significantly upregulated (3.1 fold) from control to adipogenically differentiated MSC. In 2008, research was performed on the identification of mRNAs and miRNAs associated with senescence in MSCs (Wagner, Horn et al. 2008). MSCs, after proliferating in culture for long periods of time (7-12 passages) start to demonstrate signs of senescence. These include differences in morphology including enlargement, altered expression of cell surface markers and eventually the cells cease to proliferate. Analysis of mRNA expression revealed that the changes in expression occur continuously as the cells are cultured and are not restricted to the later passages. MiRNA expression analysis revealed that miR-371 was one miRNA identified as being upregulated with increasing passages and thus its expression has been linked with the process of senescence in MSCs. Although not experimentally verified, DNA methyl transferase 3A (DNMT3A) is a predicted target of miR-371, which correlates with previous studies which suggests epigenetic modifications play a role in senescence. As a result, the authors suggest that the senescence associated upregulation of miR-371 amongst other miRNAs causes a change in the methylation pattern potentially resulting in the senescence associated changes seen in MSCs. Recently, this group also identified a role for miR-371 as a regulator of hMSC adipogenesis. They show that transiently transfecting MSCs with miR-371 and inducing the cells to undergo adipogenesis caused a significant increase in lipid accumulation. Additionally, the transfection of miR-371 stimulated expression of the adipogenic transcripts ADIPOQ and FABP4 even under non-differentiation conditions (Bork, Horn et al. 2010). They show that transfection of MSCs with miR-371 up-regulated expression of the predicted target

DNMT3A. They, thus suggest that miR-371 could play a role in maintaining the balance between self-renewal and differentiation through modulation of its predicted target DNMT3A.

#### **3.3.5.5 MiR-221 and MiR-222**

With a mean downregulation 3.67 and 2.78 fold respectively, miR-221 and miR-222 are two of the miRNAs with the largest change between undifferentiated and adipogenic MSCs in all 4 donors. MiR-221 and miR-222 were not identified as significantly regulated in adipogenesis by Osokwitz *et al* (Osokowitz, Lu et al. 2008). MiR-221 and miR-222 are part of the same miRNA family located in a cluster in an intergenic region on the X chromosome separated by 727 bases (Griffiths-Jones 2004; Lewis, Burge et al. 2005). This level of downregulation combined with evidence of these miRNAs in other developmental processes (Felli, Fontana et al. 2005; Kuehbacher, Urbich et al. 2008; Cardinali, Castellani et al. 2009) encouraged us to investigate whether a functional role exists for miR-221 and miR-222 in hMSC adipogenesis.

Since these experiments have commenced, a publication detailing a role for miR-221 and miR-222 in hMSC adipogenesis has been released. Skarn *et al* reported that these miRNAs act as negative regulators of adipogenic differentiation of both immortalized and primary hMSCs (Skarn, Namlos et al. 2011). This will be discussed in greater detail in the next chapter.

## **4 The Effects of Manipulation of Expression of MiR-221 and MiR-222 on hMSC Adipogenesis**

## **4.1 Introduction**

### **4.1.1 Experimental Aims and Objectives**

The work described in chapter 3 described studies which showed a significant regulation of miRNAs in the process of hMSC adipogenesis. This microarray analysis study identified 20 miRNAs that change significantly between undifferentiated MSCs and adipogenic MSCs. It is possible that the observed miRNA changes are merely a consequence of adipogenesis or they may actively participate in the differentiation process.

The aim of the experiments described in this chapter was to establish if one or more of these regulated miRNAs plays a functional role in adipogenic differentiation. If a functional effect is found for a miRNA(s), the next step would be to establish the target mRNA(s) through which it mediates its effect and the pathway through which it is working. If successfully achieved, this work will expand the currently limited understanding of hMSC adipogenesis.

#### 4.1.2 MiRNA and MSC

In the previous chapter, it was established that there were 20 miRNAs which demonstrate significantly regulated expression levels in MSC-derived adipocytes compared to undifferentiated MSCs (Figure 3-15). Analysis revealed 11 of these miRNAs were downregulated at day 20 of adipogenesis and 9 were upregulated. With a 3.67 and 2.78 fold downregulation respectively, miR-221 and miR-222 represent two of the miRNAs with the highest degree of change between undifferentiated and adipogenic MSCs in all 4 donors.

#### 4.1.3 MiR-221 and MiR-222

MiR-221 and miR-222 are part of the same miRNA family and are located in a cluster in an intergenic region on the X chromosome separated by just 727 bases as seen in figure 4-1 (Griffiths-Jones 2004; Lewis, Burge et al. 2005).

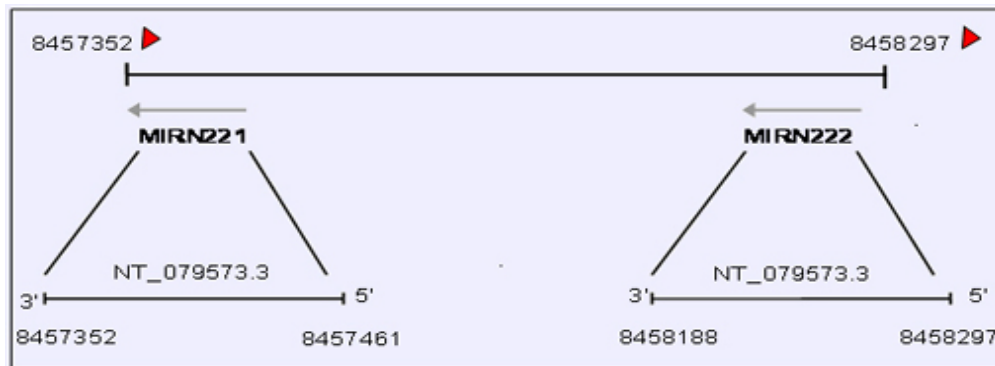


**Figure 4-1- Genomic localization of miR-221 and miR-222 on chromosome X**

Both miRNAs have an identical seed sequence and have been shown to be expressed from the same pri-miRNA precursor in c-kit positive HUVEC cells (Poliseno, Tuccoli et al. 2006). This provides an explanation for similar patterns of expression and function of these two miRNAs and suggests co-ordinated transcriptional regulation (Baskerville and Bartel 2005). Of the 20 miRNAs identified in the microarray, miR-221 and miR-222 are among the best characterized although research to-date has focused on their roles in the progression of cancer. Regulation by miR-221 and 222 have been confirmed in chronic lymphocytic leukemia (Frenquelli, Muzio et al. 2010) , in glioblastoma (Zhang, Kang et al. 2009; Zhang,

Wang et al. 2009), in breast cancer (Miller, Ghoshal et al. 2008; Zhao, Lin et al. 2008) and in papillary thyroid carcinoma (Visone, Russo et al. 2007) amongst others. Both miRNAs have also been attributed roles in other process such as the differentiation of muscle cells (Cardinali, Castellani et al. 2009; Liu, Cheng et al. 2009), the process of angiogenesis (Kuehbacher, Urbich et al. 2008) and in erythropoiesis (Felli, Fontana et al. 2005).

Based on (1) the change in expression of both miRNAs as MSCs undergo adipogenesis and (2) the ability of both miRNAs to modulate the differentiation and maturation of another cell type; the skeletal muscle cell, we hypothesized that miR-221 and miR-222 could also be involved in hMSC adipogenic differentiation. The aim of the experiments described in this chapter was to focus on miR-221 and miR-222 to determine: (1) how soon they are downregulated after initiating adipogenesis and (2) if the overexpression and knockdown of miR-221 and/or miR-222 had a significant functional effect on the ability of hMSCs to differentiate to adipocytes.

## 4.2 Results

### 4.2.1 MiR-221 and miR-222 are downregulated throughout hMSC adipogenesis

Microarray analysis identified miR-221 and miR-222 as being downregulated at day 20 of hMSC adipogenesis. To determine the stage at which the downregulation begins, RNA was isolated as per section 2.4.1 from MSCs from three donors 1-14 days after inducing adipogenic differentiation. The levels of mature miR-221 and miR-222 were determined using miRNA specific RT-PCR (Figure 4-2) with all samples normalized to levels of the endogenous control RNU24 as per section 2.4.3.2.

In contrast to the microarray analysis which was performed on a pure population of hMSC adipocytes, the RT-PCR timecourse analysis of miR-221 and miR-222 was performed on RNA from a 'mixed population' containing differentiating and undifferentiating MSCs. It was not possible to isolate the differentiating MSCs from the undifferentiating MSCs at earlier stages based on the 'ceiling culture' method as MSCs at these stages would not contain sufficient lipid to separate and float to the top of the flask. Both miRNA 221 and 222 were downregulated within 48 hours of inducing adipogenesis and remained downregulated (compared to undifferentiated cells) throughout the duration of the differentiation assay (Figure 4-2). As described in section 2.1.2.4.1 inducing adipogenesis in MSCs involves three rounds of induction with 'rest' stages where the cells are cultured in maintenance medium between each induction round. Figure 4-2B highlights the expression of miR-221 and miR-222 in the first 72 hours of expression and shows that there is significant downregulation in expression of miR-221 24 hours after induction of adipogenesis while miR-222 shows significant downregulation after 48 hours of differentiation. This shows that both miRNAs are significantly downregulated 72 hours after induction of adipogenesis. This significant early downregulation in expression of both miRNAs is consistent with a role for miR-221 and miR-222 in the adipogenic differentiation of hMSCs rather than being a consequence of it.

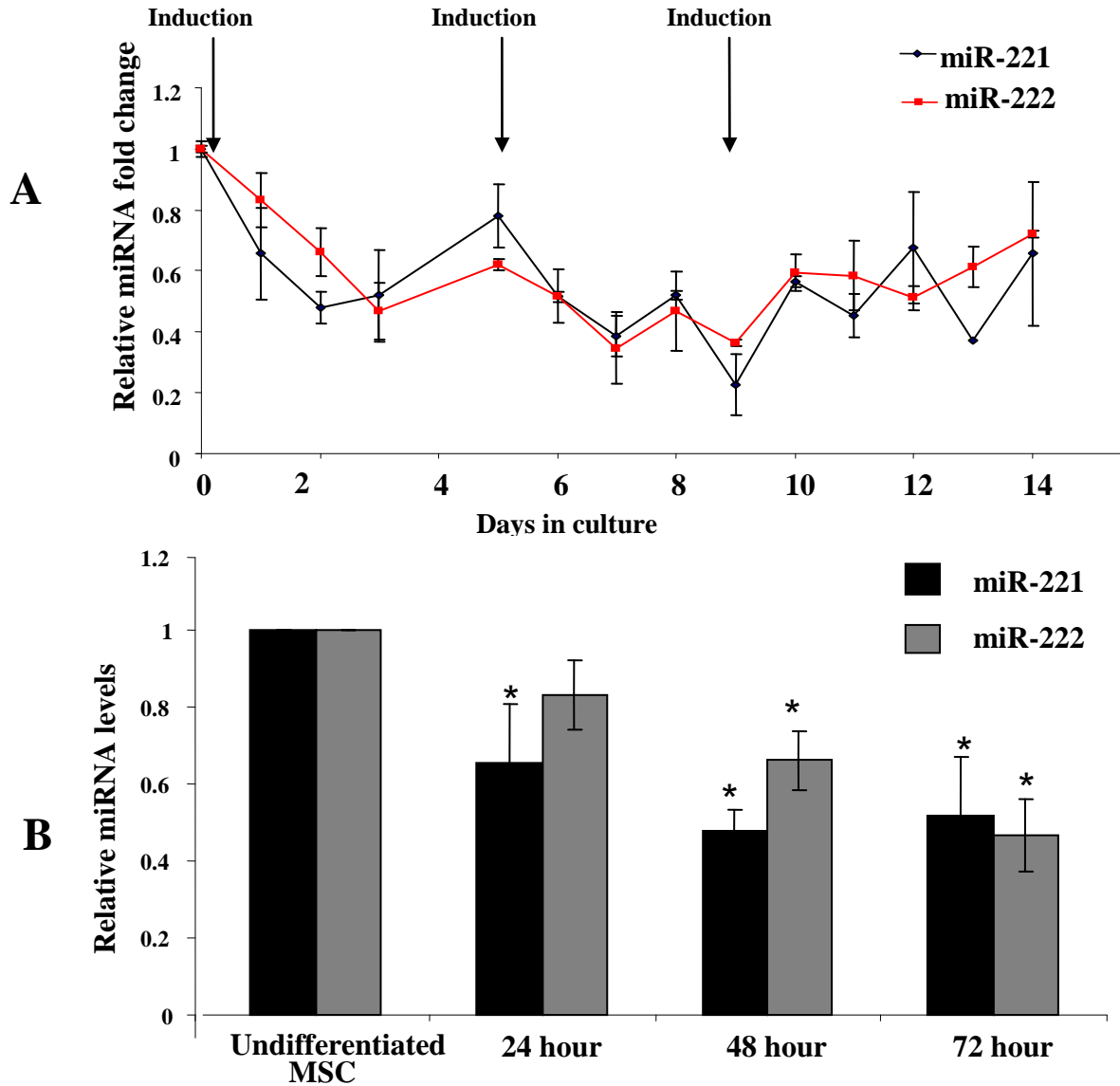


**Figure 4-2 RT-PCR shows that miR-221 and miR-222 are downregulated during adipogenesis**

MiRNA-specific RT-PCR was used to examine the expression of miR-221 and miR-222 between 1 and 14 days after initiating adipogenesis (A). MiRNA expression for the first 72 hours (B) are shown in more detail, highlighting that miR-221 and miR-222 were significantly downregulated in the first 72 hours of adipogenesis compared to undifferentiated MSCs. All samples were normalized to the endogenous control RNU24. Error bars represent standard deviation of the mean (n=3 donors), \*p≤ 0.05.

#### **4.2.2 MiR-221 and miR-222 are downregulated in hMSC Osteogenesis and Chondrogenesis**

As well as their adipogenic potential, MSCs have the ability to differentiate into other cell types including osteocytes and chondrocytes (Pittenger, Mackay et al. 1999). A question therefore arises: Is the downregulation of miR-221 and miR-222 specific to the adipogenic differentiation or a necessary event for the differentiation of MSCs to any lineage? To determine the answer, expression analysis of miR-221 and miR-222 was performed as MSCs differentiate to osteocytes and chondrocytes.

RNA was isolated from hMSCs undergoing differentiation to osteocytes and chondrocytes from days 1-14. MiR-221 and miR-222 expression levels were analysed using miRNA specific RT-PCR. While miR-221 and miR-222 are downregulated in all three lineages, significant downregulation of expression is seen for both miRNAs only at a mid timepoint (day 7) in chondrogenesis and a late (day 14) timepoint in chondrogenesis. So while the early downregulation of expression seen in adipogenesis points to a role for these miRNAs in the process of differentiation it is possible that in the other two lineages, it is as a consequence of differentiation rather than a contributing factor. Taken together, these results suggest that the downregulation of miR-221 and miR-222 could be an important event for hMSC differentiation to occur in all three lineages.

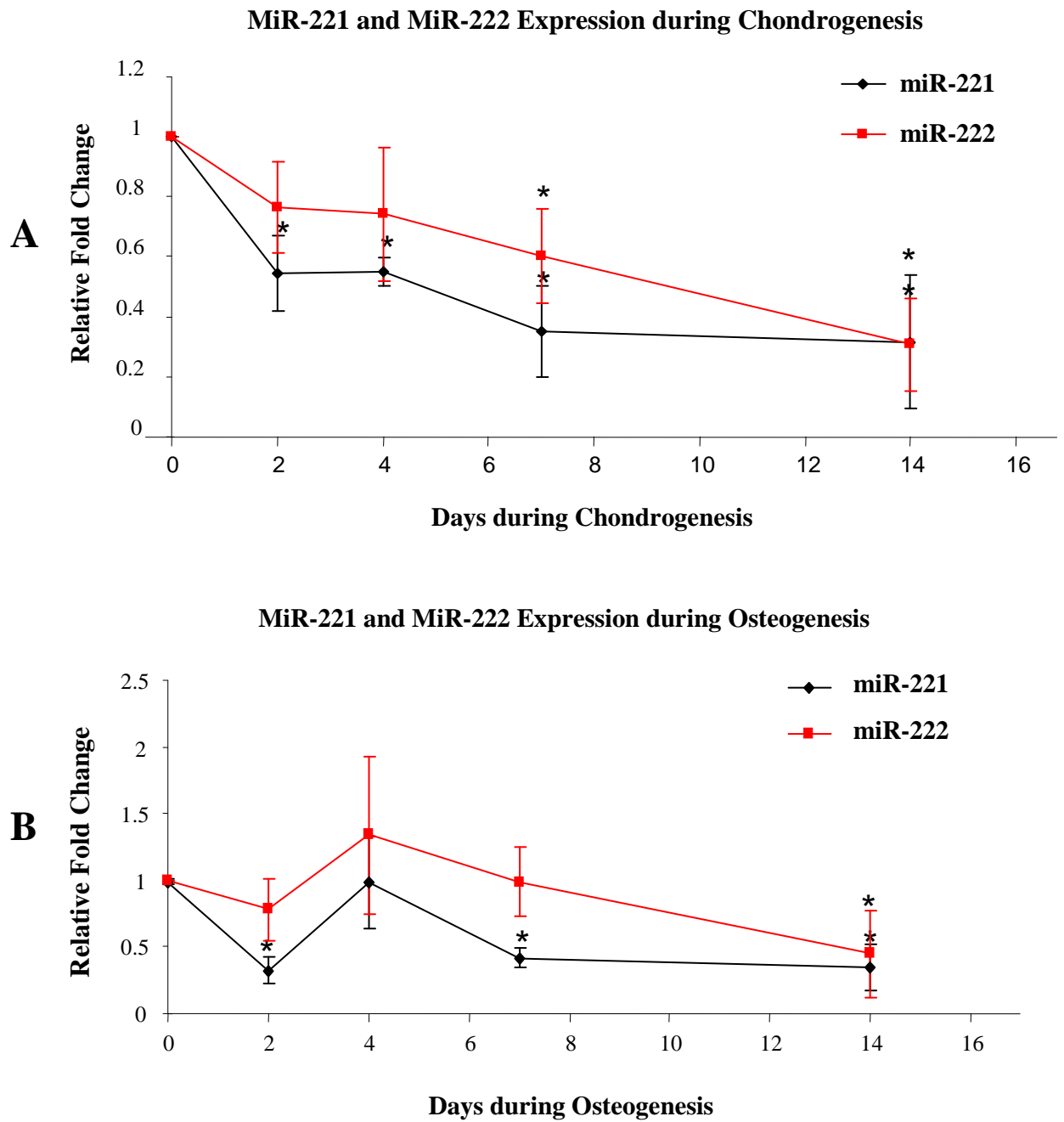


**Figure 4-3-RT-PCR shows that miR-221 and miR-222 are downregulated during osteogenesis and chondrogenesis**

MiRNA-specific RT-PCR was used to examine the expression of miR-221 and miR-222 at the indicated timepoints after inducing osteogenesis (A) or chondrogenesis (B). All samples were normalized to the endogenous control RNU24. Error bars represent standard deviation of the mean (n=3 donors), \*p $\leq$  0.05.

### **4.2.3 Overexpression of miRNAs 221 and 222 in MSCs**

Is the downregulation of miR-221 and/or miR-222 a necessary event for adipogenesis to occur? If the downregulation of these miRNAs is an important event, it would be predicted that preventing the downregulation would affect adipogenesis. To address this question, we aimed to determine if the overexpression of miR-221 and/or miR-222 affects the ability of an MSC to undergo adipogenic differentiation.

#### **4.2.3.1 Construction of a miR-221 and miR-222 overexpression vector**

The region of genomic DNA encoding both miR-221 and miR-222 was amplified by PCR and cloned into the mammalian expression vector pcDNA<sup>TM</sup> 3.3-Topo® TA cloning vector (Invitrogen) as per section 2.2.1. This vector allows constitutive expression from a Cytomegalovirus (CMV) promoter present in its backbone, which has the ability to induce the strong expression of target genes in a wide variety of cells and cell lines (Boshart, Weber et al. 1985). The pcDNA 3.3 vector expressing miR-221 and miR-222 was successfully generated and verified by restriction enzyme analysis and sequencing.

#### **4.2.3.2 Nucleofection of MSCs with miR-221/222 overexpression plasmid**

A paper published in 2005 by Lemoli *et al* described 'Nucleofection as an efficient non-viral transduction technique for human bone marrow-derived mesenchymal stem cells' without causing toxicity to the cells. Nucleofection combines electrical parameters and cell-type specific solutions to drive plasmid DNA, oligonucleotides as well as siRNA to the cell nucleus (Aluigi, Fogli et al. 2006). The manufacturer (Lonza Technologies) recommends two nucleofector programs to achieve optimal transfection efficiency of hMSCs, high transfection (HT (C-17) and high viability (HV (U-23))).

Using the Nucleofector High Transfection program, MSCs were transfected with either 221/222 vector or an 'empty' (i.e. no insert) pcDNA3.3 vector as described in section 2.3.2. As an additional control, MSCs were nucleofected without the addition of plasmid DNA using the High transfection (HT) and the High viability (HV) programs.

RNA was isolated from all cultures 24, 48 and 72 hours after nucleofection and the relative levels of miR-221 and miR-222 were assessed using RT-PCR. All samples were normalized to levels of RNU24. Compared to MSCs nucleofected with 'empty' vector, there is no significant difference in the levels of miR-221 and miR-222 upon nucleofection with the miR-221/222 overexpression vector at 24, 48 or 72 hours (Figure 4-4C).

MSCs nucleofected without plasmid DNA showed a large change in miR-221 and miR-222 expression when used with the High Viability (HV) and High Transfection (HT) programs. An increase in miR-222 expression was observed in all instances while miR-221 expression was decreased 24 hours post nucleofection using the HV program (Figure 4-4D) compared to untransfected MSCs.

In conclusion, whilst nucleofection achieved efficient plasmid delivery, this method failed to deliver the required miRNA overexpression. The nucleofected MSCs displayed an abnormal phenotype (Figure 4-4A, B) and a reduced ability to proliferate once plated for the adipogenesis assay. Furthermore, as nucleofection provides transient transfection it is anticipated that any miRNA overexpression would last for only 3-5 days at best and would not therefore be optimal for use in an adipogenesis assay, which takes 14 days.

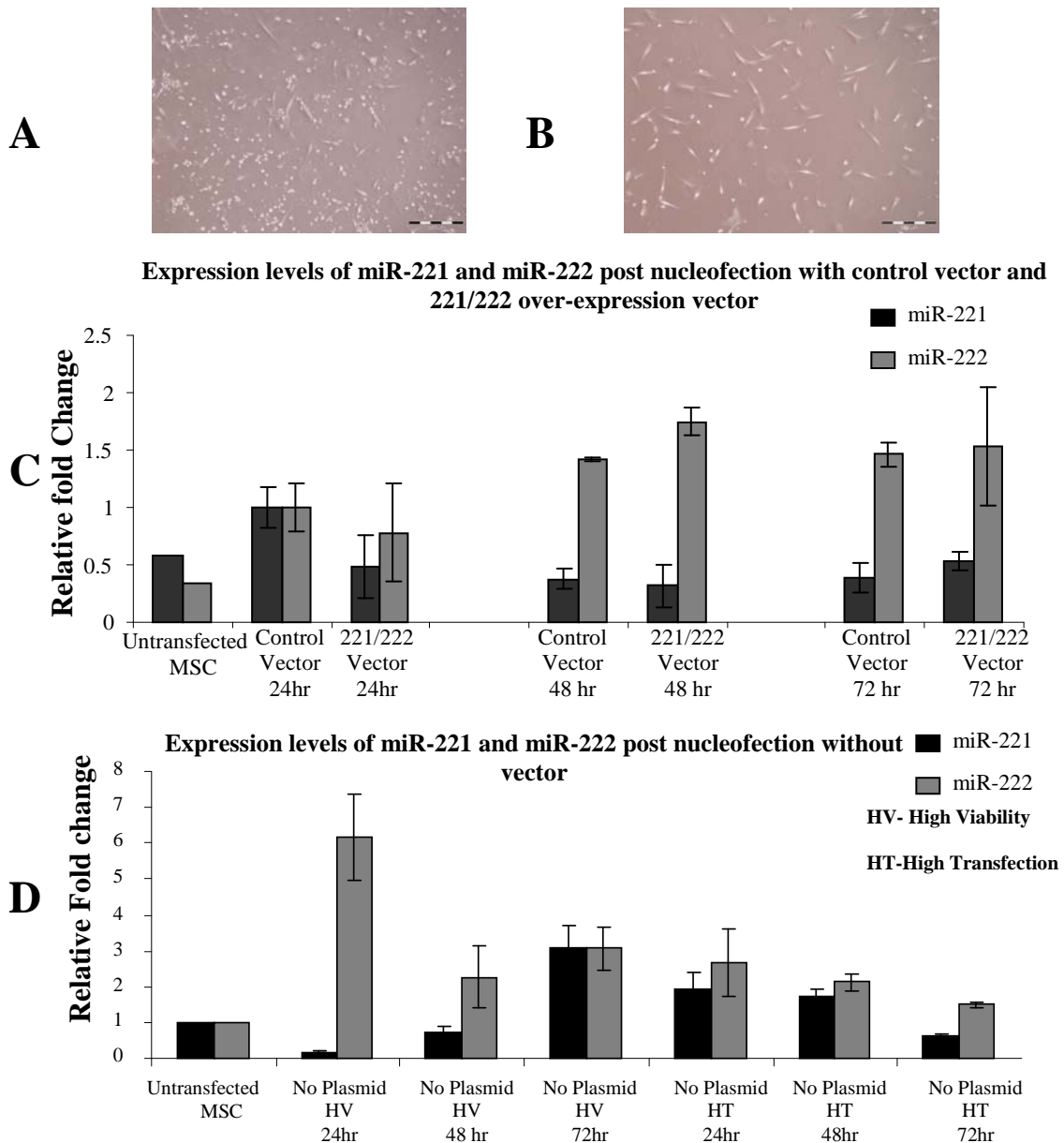


**Figure 4-4 Nucleofection of hMSCs with miR-221/222 overexpression vector**

Phase contrast micrographs of MSCs post nucleofection 48 hours (A) and 5 days post delivery (B). MiRNA specific RT-PCR was used to determine the expression of miR-221 and miR-222 in untransfected MSCs and MSCs nucleofected with empty vector or miR-221/222 overexpression vector 24hrs, 48hrs and 72hrs after nucleofection (C). All expression levels were normalized to the endogenous control RNU24 and are presented relative to the level observed in MSCs nucleofected with control vector. MiR-221 and miR-222 expression levels, normalized to RNU24 and presented relative to untransfected MSCs, were determined in MSCs transfected without plasmid DNA using the high viability (HV) and high transfection (HT) programs on the nucleofector (D). Error bars represent standard deviation of the mean (n=3 donors).

#### **4.2.3.3 Lentiviral Delivery Of miR-221 And miR-222 To hMSCs**

To determine the effects of miR-221 and miR-222 overexpression on hMSC adipogenesis, long term overexpression is desirable to cover the duration of the differentiation assay (2-3 weeks). Viral transduction is a very efficient strategy and depending on the vector selected, can be a long term method of delivering genes to difficult to transfect cells such as MSCs. Viral vectors available include retroviruses, adenoviruses, adeno-associated viruses, herpes simplex virus and flaviviruses (Hermens and Verhaagen 1998; Klimatcheva, Rosenblatt et al. 1999).

The desired long-term ( $\geq 4$  weeks) expression of a viral transgene is best achieved using a vector which integrates into the host genome. Adenoviruses and herpes simplex virus-based vectors both lack the ability to stably integrate into the host genome. Adeno-associated virus can integrate into the genome but requires the aid of an additional virus e.g adenovirus or herpes simplex virus. Therefore, a lentiviral or retroviral vector would be the most suitable viral vector due to its ability to stably integrate into the genome. Others have shown that lentiviral transduction does not adversely affect the morphology or differentiation ability of MSCs (McMahon, Conroy et al. 2006; Bocker, Rossmann et al. 2007).

MiR-221 and miR-222 precursor clones (System Biosciences) were successfully packaged into lentiviral vectors as described in section 2.3.1. A precursor clone for miR-126 (System Biosciences) (a miRNA which does not change in level during hMSC adipogenesis as seen in Figure 4-5) was also packaged into a lentiviral vector and served as a control for any non-specific effects of miRNA overexpression. A GFP lentiviral vector (pWPT-GFP) served to control for lentiviral-mediated effects. The functional titers of all lentiviral preparations were calculated using qRT-PCR for the viral gag sequence to measure integrated DNA as per section 2.3.1.1.2.

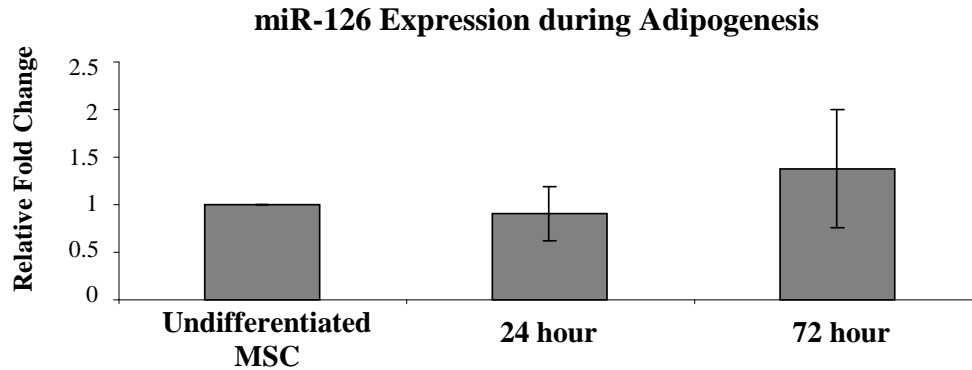


**Figure 4-5 RT-PCR shows that the expression of miR-126 does not change during adipogenesis**

MiRNA-specific RT-PCR was used to examine the expression of miR-126 in the first 72 hours of hMSC adipogenesis. Expression was normalized to the endogenous control RNU24. Error bars represent standard deviation of the mean (n=3 donors).

MSCs isolated from 3 donors were transduced with miR-221, mir-222, miR-126 or GFP viral vectors at a Multiplicity of Infection (MOI) 50 (Lee, Kohn et al. 2004; McMahon, Conroy et al. 2006) (Section 2.3.1.2.1). Lisa McGinley (REMEDI, Galway) showed that lentiviral transduction of MSCs at a MOI 50 results in 70-85% transduction of the MSC population with no detrimental effects on proliferation or differentiation (Personal communication). The GFP coding sequence on the miRNA expression constructs allowed monitoring of transduction efficiency.

Transducing MSCs with miR-221, miR-222, miR-126 or GFP at an MOI 50 delivered the vector to 70-80% of the population as monitored by GFP expression (Figure 4-6A and B). RNA was isolated from all MSCs 3 days post transduction (Section 2.4.1) and the expression levels of miR-221 and miR-222 measured using miRNA specific RT-PCR (Section 2.4.3.2). Expression in all samples was normalized to the endogenous control RNU24. MSCs overexpressing miR-126 showed a significant 50-fold increase compared to untransduced MSCs (Figure 4-6C). Transducing MSCs at an MOI 50 with miR-221 and miR-222 resulted in a significant 4-fold overexpression of miR-221 and a significant 5.5-fold overexpression of miR-222 when compared to MSCs overexpressing miR-126 as seen in figure 4-6D.

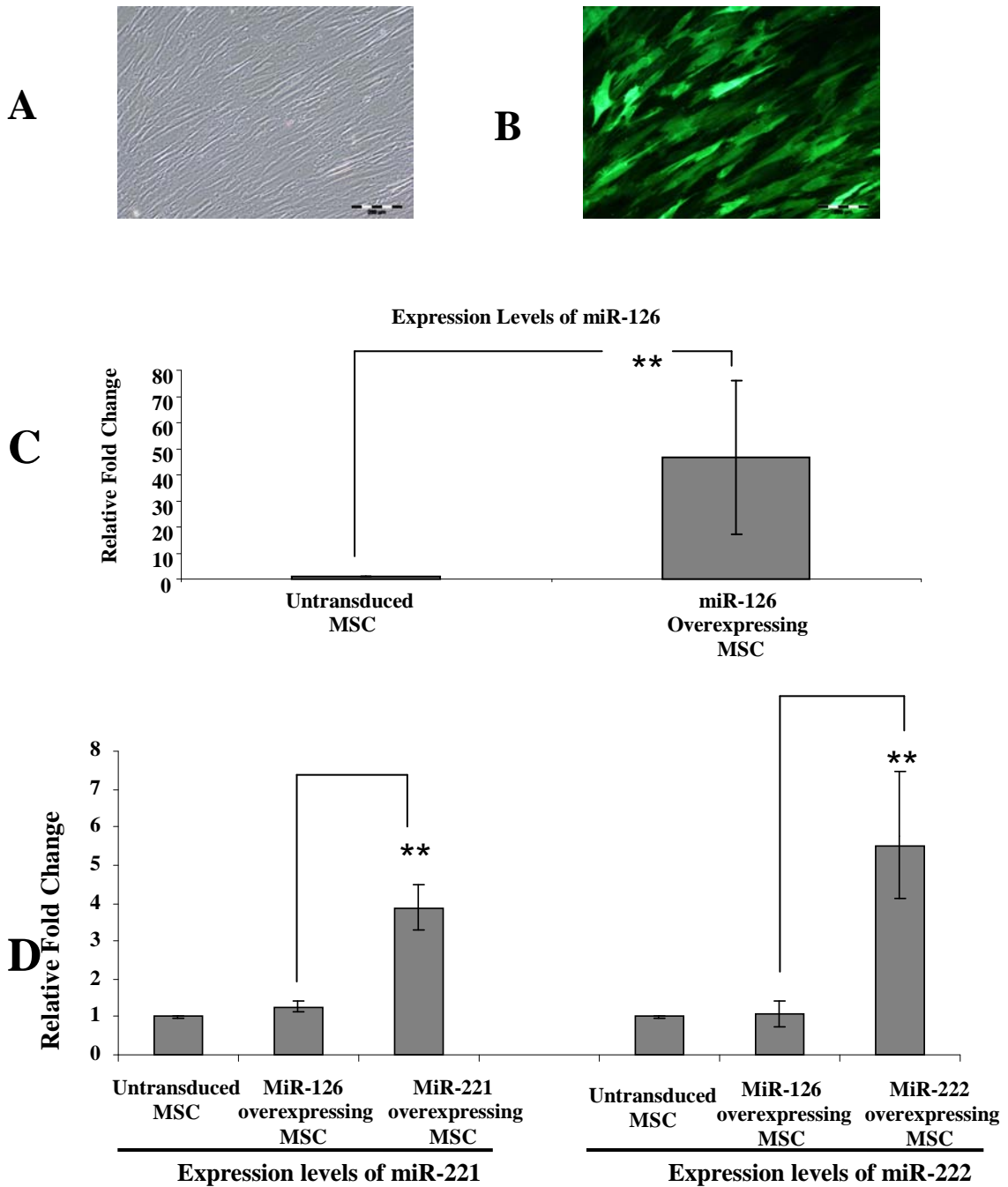


**Figure 4-6 Lentiviral mediated overexpression of miR-221 and miR-222 72 hours post transduction**

Phase contrast micrograph (10x) (A) and fluorescent micrograph (B) of MSCs transduced with lentivirally delivered miRNA expression constructs. A GFP coding sequence on the miRNA expression construct allows monitoring of transduction efficiency. MiRNA RT-PCR for miR-126 shows a 50-fold overexpression compared to untransduced MSCs (C). MiR-221 and miR-222 shows a 4-fold overexpression of miR-221 and a 5.5-fold overexpression of miR-222 compared to miR-126 transduced MSCs 72 hours post transduction (D). All samples were normalized to the endogenous control RNU24. Error bars represent standard deviation of the mean (n=3 donors), \*\*p≤ 0.01.

#### **4.2.4 Overexpression of miRNAs 221 and 222 in hMSCs reduces adipogenesis**

To determine if overexpression of miR-221 and/or 222 affects MSC adipogenesis, GFP transduced MSCs and MSCs overexpressing miR-126, miR-221, miR-222 or miR-221 and miR-222 from 3 different donors were induced to undergo adipogenesis as per section 2.1.2.4.1.

Figure 4-7 shows the effects of overexpressing miR-221 and/or miR-222 on hMSC adipogenesis compared to GFP transduced MSCs or MSCs overexpressing miR-126. One of the first signs of an adipogenically-differentiating MSC is the change in morphology; the MSC changes from its characteristic fibroblast-like shape to a more rounded phenotype. At day 3 of adipogenesis (Figure 4-7A), when the first visible signs of adipogenesis occur, there appears to be less cells 'rounding up' in the miR-221 and miR-222 overexpressing MSC populations than in the control populations. By day 8 of adipogenesis (Figure 4-7B), the effect is more evident, with the control MSC (untransduced, miR-126 overexpressing MSCs, GFP transduced MSCs) populations exhibiting the typical morphology of a population undergoing adipogenesis. In contrast, the miR-221 and 222 transduced populations exhibit a broader, flatter morphology (Figure 4-7B).

At day 14, all MSC populations were stained with Oil Red O as described in section 2.1.2.4.2. As evident in figure 4-8C, the lipid-filled vesicles of differentiated MSCs were stained red, these were not present in any of the undifferentiated MSCs (i.e. maintained in hMSC growth medium; data not shown). The Oil Red O was extracted and measured to quantify the relative levels of accumulated lipids. The overexpression of miR-126 and lentiviral transduction with a control GFP vector did not affect accumulation of lipids compared to untransduced MSCs, as measured by Oil Red O extraction (Figure 4-8).

The overexpression of either miR-221 or miR-222 in hMSCs appeared to reduce adipogenesis as measured by lipid accumulation, Figure 4-7C. However analysis showed that this reduction was not statistically significant compared to MSCs overexpressing miR-126. Extraction and quantitation of the Oil Red O confirmed that co-expression of miR-221 and miR-222 in hMSCs significantly reduced

adipogenesis compared to MSCs overexpressing miR-126 as measured by lipid accumulation (Figure 4-8).

Conditions in which miR-221 and miR-222 are expressed at a similar level and function additively have been reported (Galardi, Mercatelli et al. 2007; Medina, Zaidi et al. 2008; Cardinali, Castellani et al. 2009). MiR-221 and miR-222 are often co-expressed in tumor derived cell lines (He, Jazdzewski et al. 2005; Pallante, Visone et al. 2006). Both miRNAs are clustered on chromosome X and are within 727 bases of each other. They are derived from the same transcript and can therefore be generated from the same precursor RNA (Medina, Zaidi et al. 2008). MiR-221 and miR-222 have similar sequences and there is evidence that they target many of the same mRNAs (le Sage, Nagel et al. 2007; Fornari, Gramantieri et al. 2008). This could explain why a significant reduction in lipid accumulation was only observed upon overexpression of both miR-221 and miR-222.

Therefore, the overexpression of miR-221 and miR-222 reduced lipid accumulation in hMSCs undergoing adipogenesis compared to MSCs overexpressing miR-126. This is consistent with the hypothesis that the downregulation of expression of these miRNAs is an important event in the process of hMSC adipogenic differentiation.

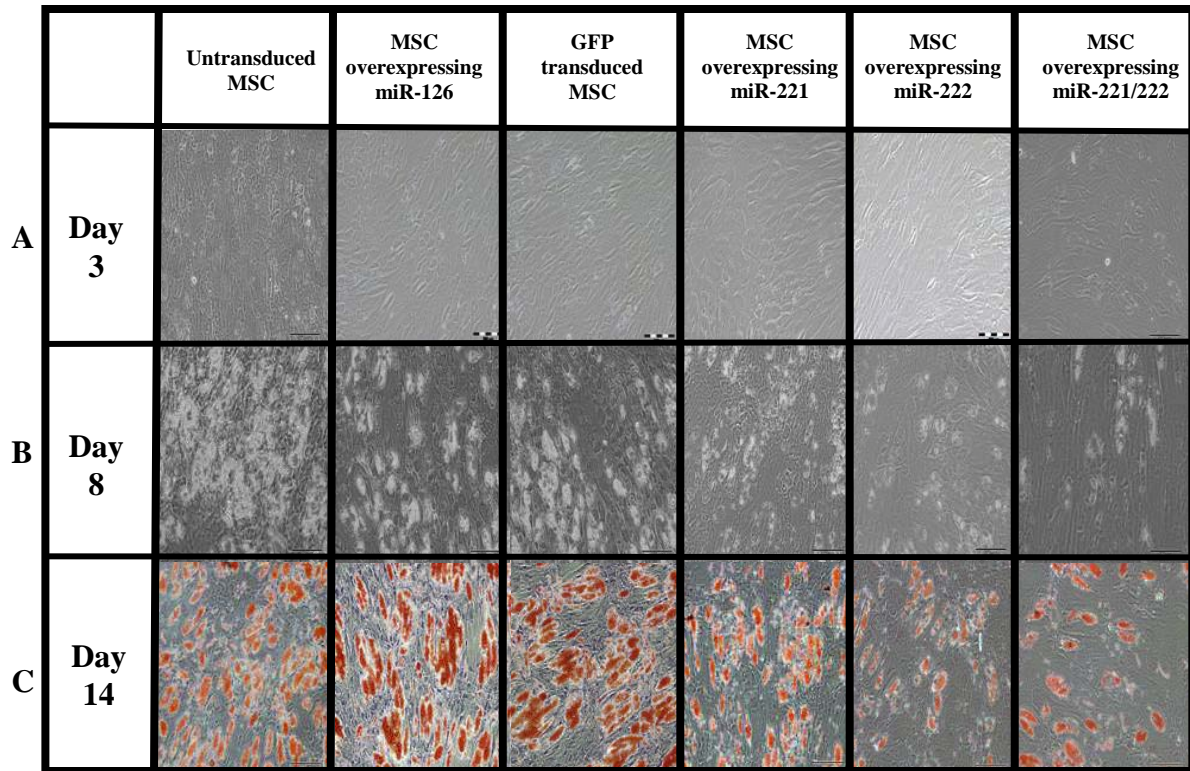


**Figure 4-7 Overexpression of miR-221 or miR-222 reduces adipogenesis in hMSCs**

Phase-contrast micrographs (10x) showing the effects of overexpressing miR-221, miR-222 or both miR-221 and 222 compared to MSCs overexpressing miR-126 or GFP at day 3 (A), and day 8 (B) of hMSC adipogenesis. At day 14, all populations were treated with Oil Red O which stains lipid vesicles red (C). This shows that overexpressing miR-221 and miR-222 reduces hMSC appears to reduce adipogenesis compared to the control populations. (Images representative of 3 donors)

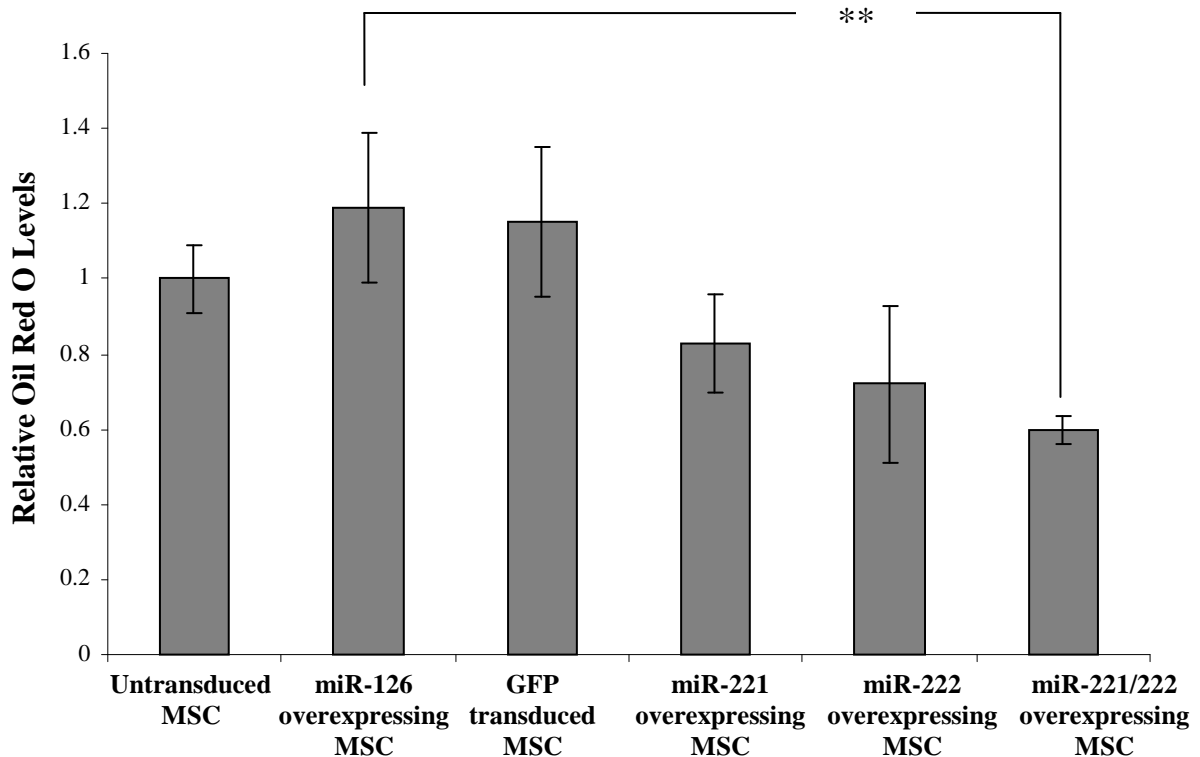


**Figure 4-8 Coexpression of miR-221 and miR-222 significantly reduces hMSC adipogenesis as measured by lipid accumulation.**

Untransduced MSCs, MSCs overexpressing miR-221, miR-222 and both miR-221 and miR-222 were stained with Oil Red O stain 14 days after inducing adipogenesis with MSCs overexpressing miR-126 and GFP transduced MSCs acting as controls. This stain was extracted and quantified at 495nm. MSCs overexpressing miR-221/222 showed significantly lower levels of Oil Red O compared to MSCs overexpressing miR-126. Error bars represent standard deviation of the mean (n=3 donors), \*\*p≤ 0.01.

#### **4.2.5 Overexpression of miRNAs 221 and 222 in hMSCs does not affect hMSC osteogenesis**

MiR-221 and miR-222 are downregulated in osteogenesis as well as adipogenesis (Figure 4-3A). In order to determine whether downregulation is required for osteogenesis, untransduced MSCs, GFP transduced MSCs, MSCs overexpressing miR-126 and MSCs overexpressing miR-221 and miR-222 were induced to undergo osteogenesis as per section 2.1.2.2. Quantitative calcium assays performed 14 days after inducing osteogenesis showed that each population of differentiated MSCs showed a significant increase in calcium accumulation compared to their undifferentiated equivalent. However, analysis revealed no significant difference between GFP transduced MSCs, miR-126 overexpressing MSCs, untransduced MSCs and MSCs overexpressing miR-221 and miR-222 (Figure 4-9). Therefore, although the overexpression of miR-221 and miR-222 reduces the ability of an MSC to differentiate to adipocytes, the ability to undergo osteogenic differentiation remains largely unaffected.

Unlike adipogenesis, a significant downregulation of expression of both miR-221 and miR-222 was only observed at day 14 of osteogenic differentiation. Potentially, the downregulation of miR-221 and 222 is a necessary event for adipogenic differentiation to occur while in osteogenesis the downregulation in expression of these miRNAs is as a consequence of differentiation. This could explain why a functional difference is not observed upon the overexpression of miR-221 and miR-222 in osteogenesis compared to adipogenesis.

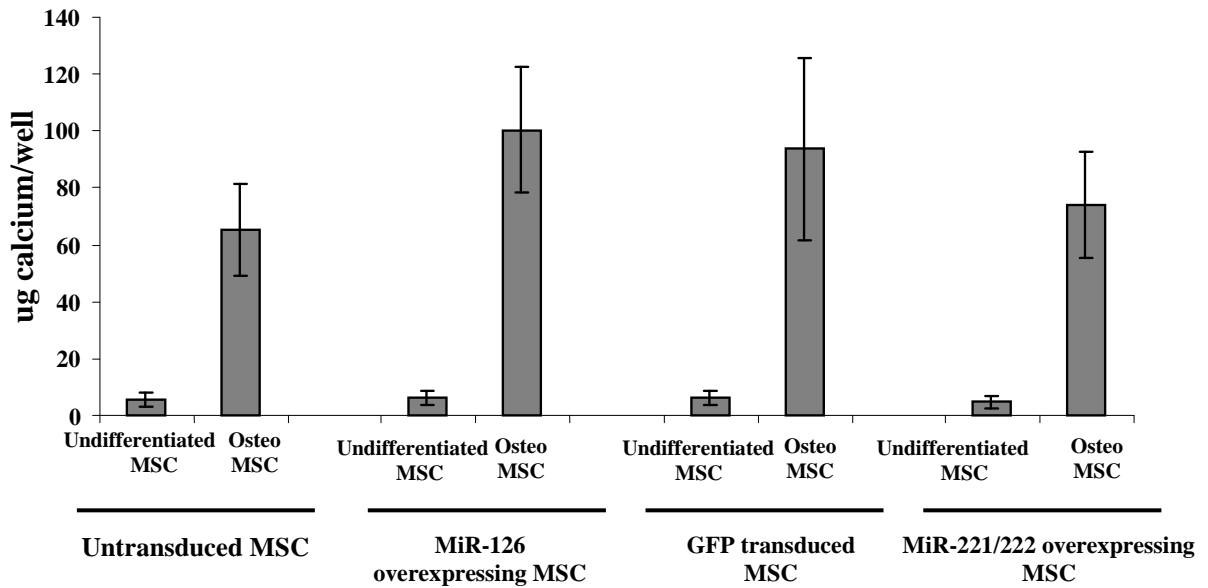


**Figure 4-9 Overexpression of miR-221 and miR-222 has no significant effect on hMSCs undergoing osteogenesis.**

Analysis of calcium deposition was performed at day 14, no significant change in calcium level is seen between untransduced MSCs, MSCs overexpressing miR-221 and 222, MSCs overexpressing miR-126 and GFP transduced MSCs. Error bars represent standard deviation of the mean (n=3 donors).

#### **4.2.6 Overexpressing miR-221 and miR-222 reduces the upregulation of key transcripts during adipogenesis**

In an effort to determine the mechanism via which miRNAs 221 and 222 reduce adipogenesis, an attempt was made to determine whether early events of adipogenesis were influenced. To do so, the changes in expression levels of transcription factors important in the early stages of adipogenesis were analyzed. The transcription factors were the (1) CCAAT-enhancer-binding-protein  $\alpha$  (C/EBP  $\alpha$ ) and (2) perioxosome proliferative activated receptor  $\gamma$  (PPAR $\gamma$ ). These two transcription factors have been shown to play key roles in the induction and maintenance of the adipogenic phenotype. The expression of a key adipogenic factor, fatty acid binding protein 4 (FABP4) was also analyzed. These factors all undergo an increase in transcript level early in adipogenesis as described in section 1.4.3.

Untransduced MSCs, MSCs overexpressing miR-221 and miR-222, and MSCs overexpressing miR-126 were induced to undergo adipogenesis. Duplicate undifferentiated cultures were also set up. RNA was isolated from all cultures 72 hours after inducing adipogenesis and RT-PCR analysis performed as per section 2.4.3.1. Expression levels were normalized to levels of RNA polymerase II (RNA pol II) transcript. No significant difference in expression level was seen between untransduced MSCs and miR-126 overexpressing MSCs for FABP4, C/EBP $\alpha$  or PPAR $\gamma$ . MSCs overexpressing miR-221 and miR-222 showed a reduced level of upregulation of PPAR $\gamma$  (10-fold upregulation) compared to MSCs overexpressing miR-126 (30-fold upregulation) (Figure 4-10A). C/EBP $\alpha$  is upregulated 30-fold 72 hours into adipogenesis in miR-126 overexpressing MSCs, compared to a 10-fold upregulation in the miR-221 and miR-222 overexpressing population, as seen in figure 4-10B. Upregulation of the Fatty Acid Binding Protein 4 (FABP4) transcript were reduced from a 6,000-fold upregulation in miR-126 overexpressing MSCs to a 2,500-fold upregulation in miR-221/222 overexpressing MSCs (Figure 4-10C). These results show that the overexpression of miR-221/222 not only affects late aspects of adipogenic differentiation i.e. lipid accumulation but also affects transcriptional events that occur within the first 3 days of adipogenic differentiation. With upregulation of these key adipogenic factors reduced by approximately 2-fold it follows that the total level of lipid accumulation would be significantly reduced. Thus two possible scenarios arise; (1) Co-expressing miR-221 and miR-222 in a population of MSCs reduces the ability of the cell to undergo adipogenic differentiation through the reduced upregulation of key transcripts involved in the process or (2) less MSCs are responding to differentiation and there is less upregulation of the transcripts as a result.

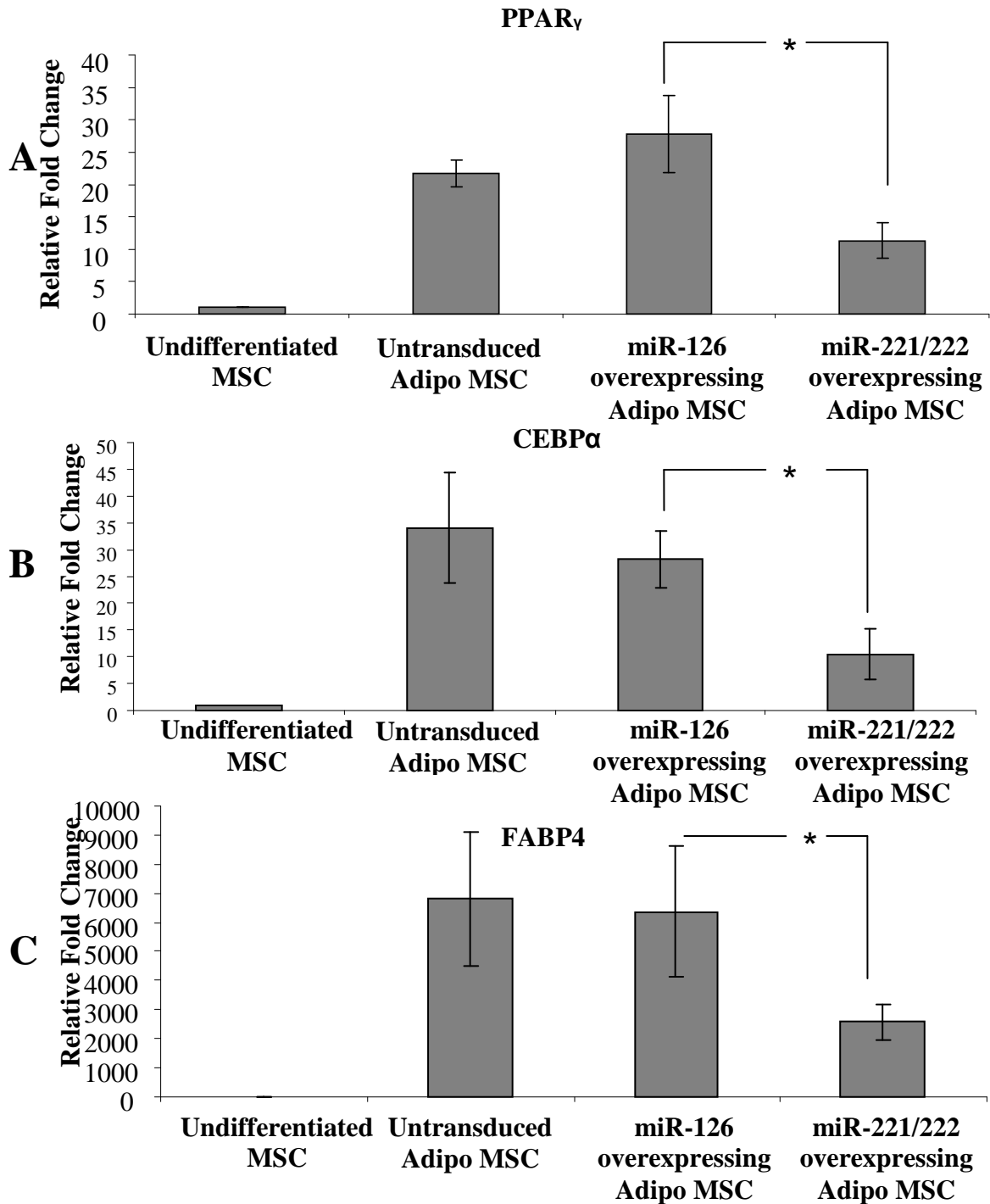


**Figure 4-10 Co-expression miR-221 and miR-222 in hMSCs reduces the upregulation of key transcripts during adipogenesis.**

Expression of the adipogenesis related transcripts (A) PPAR $\gamma$ , (B) C/EBP $\alpha$  and (C) FABP4 in untransduced MSCs and MSCs overexpressing miR-221 and miR-222 compared to MSCs overexpressing miR-126 (values are presented relative to undifferentiated-matched hMSCs). RT-PCR was performed using RNA isolated 72 hours after the induction of adipogenesis. Expression levels were normalized to the levels of RNA pol II transcript. Error bars represent standard deviation of the mean (n=3 donors), \*p $\leq$  0.05.

#### **4.2.7 Inhibition of activity of miRNAs 221 and 222 in MSCs**

The expression of miR-221 and miR-222 significantly decreases as adipogenesis proceeds, with the overexpression of both miRNAs significantly reducing hMSC adipogenesis. This suggests that miR-221 and miR-222 could be regulating a key protein or proteins necessary for the progression of adipogenic differentiation. If this targeted protein acts as a rate-limiting step in adipogenesis it is possible that reducing miR-221 and miR-222 expression or their activity and thus increasing the expression of the target protein may have an observable effect on adipogenesis. This possibility was examined by analysing the effects of inhibition of miR-221 and miR-222 activity on hMSC adipogenesis.

MiRZip anti-sense miRNAs are stably expressed RNAi hairpins that have anti-miRNA activity. MiRZip shRNAs against miR-221 and miR-222 (System BioSciences) were delivered using lentiviral vectors as described in section 2.3.1.2.1 and will further be referred to as sh-221 and sh-222, respectively. A miRZip containing a scramble shRNA (System BioSciences) was used as a control and will further be referred to as scramble shRNA. The lentiviral vector delivery will permit long term inhibition of activity of miR-221 and miR-222.

These miRZip shRNAs produce short single stranded anti miRNAs that competitively bind their endogenous miRNA target and inhibit its function. As a result, the manufacturers suggest that there may not be a difference in the level of miR-221 or miR-222 upon transduction with either shRNA. To confirm this, the expression of miR-221 or miR-222 was determined in MSCs with reduced miR-221 and miR-222 activity, 72 hours post transduction by miRNA specific RT-PCR analysis as per section 2.4.3.2. Figure 4-11 shows that indeed, expression of miR-221 or miR-222 is significantly reduced in MSCs transduced with sh-221 or sh-222, respectively compared to MSCs transduced with a shRNA containing a scramble sequence.

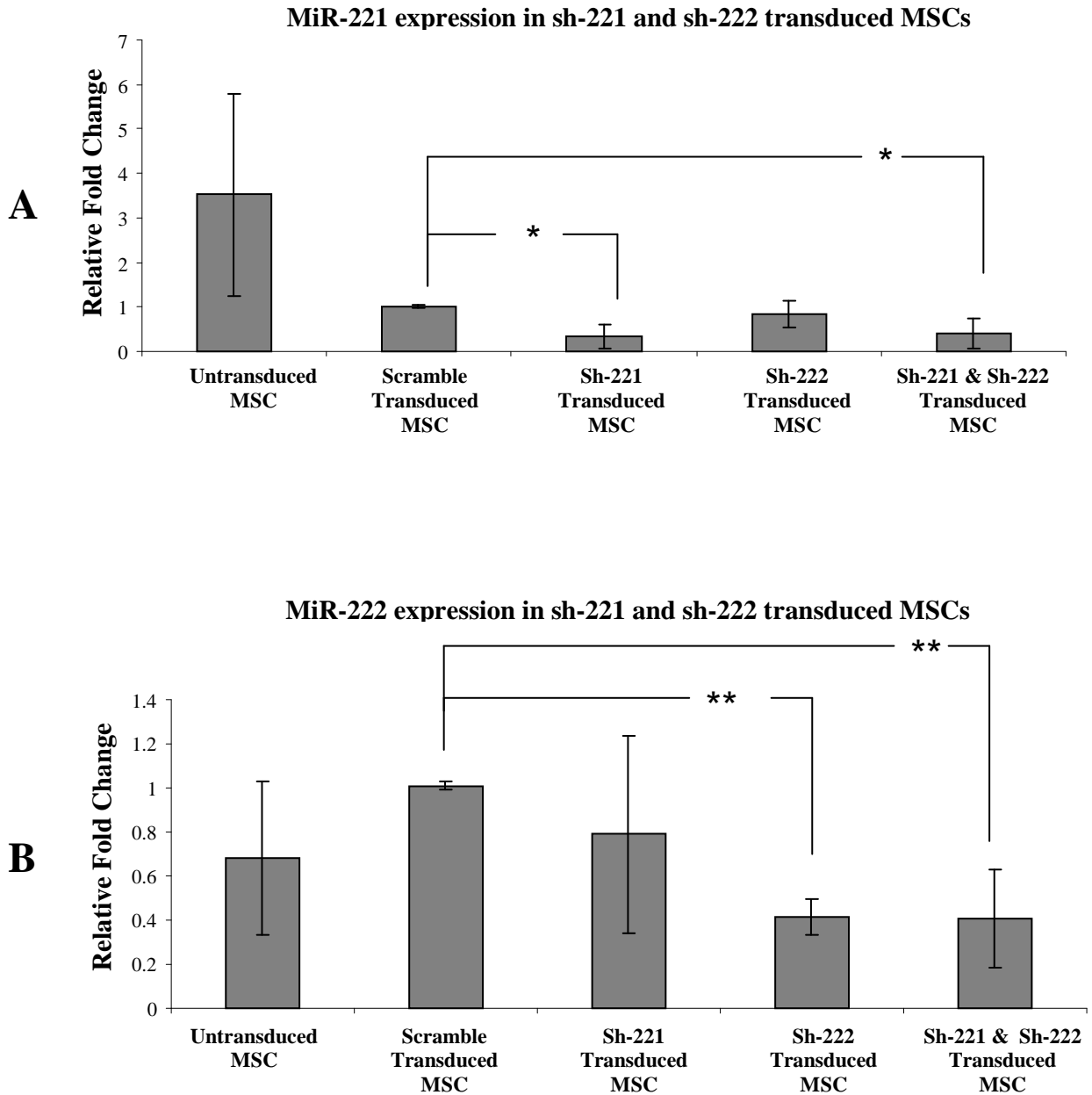


**Figure 4-11 Transduction of MSCs with sh-221 and/or sh-222 significantly reduces expression of miR-221 and/or miR-222**

Expression of the miR-221 (A) and miR-222 (B) in untransduced MSCs and MSCs transduced with a scramble shRNA, sh-221, sh-222 or both sh-221 and sh-222 (values are presented relative to scramble transduced hMSCs). RT-PCR was performed using RNA isolated 72 hours after transduction with shRNAs. Expression levels were normalized to the levels of RNU24. Error bars represent standard deviation of the mean (n=3 donors), \*p≤ 0.05, \*\*p≤ 0.01

To investigate the effects of the inhibition of miR-221 and miR-222 activity, MSCs isolated from 3 donors were transduced with sh-221, sh-222 and a scramble shRNA at a MOI 50. The shRNA expression constructs include a GFP coding sequence which allows monitoring of transduction efficiency. Transduction at a MOI 50 resulted in an 70-85% transduction efficiency of the MSC population.

MSCs transduced with sh-221, sh-222 and both sh-221 and sh-222 displayed an unhealthy and stressed morphology as early as 24 hours post transduction compared to MSCs transduced with a scramble shRNA transduced at the same MOI. As the cells were maintained in culture, many MSCs transduced with sh-221 and/or sh-222 detached from the culture surface (Figure 4-12). At 96 hours post transduction, 50-60,000 MSCs remained in the sh-221/222 transduced populations compared 140,000 MSCs present in the scramble shRNA transduced population (Figure 4-13). The sh-221 and sh-222 populations contained less cells than originally plated (100,000) suggesting that the reduction in cell number was presumably due to cell death and not due to a prevention in proliferation alone.

The overall aim of this experiment was to examine the effects of inhibition of miR-221 and 222 activity on hMSC adipogenesis. As described in section 2.1.2.4.1, to induce adipogenic differentiation in a population of hMSCs, the cells should be 2 days post confluence. As hMSCs transduced with sh-221 or sh-222 detached from the plate and presumably died upon delivery of the sh-221 or sh-222, a confluent layer of cells was not achievable. For this reason, MSCs with inhibited miR-221 and miR-222 activity could not be induced to undergo adipogenic differentiation.

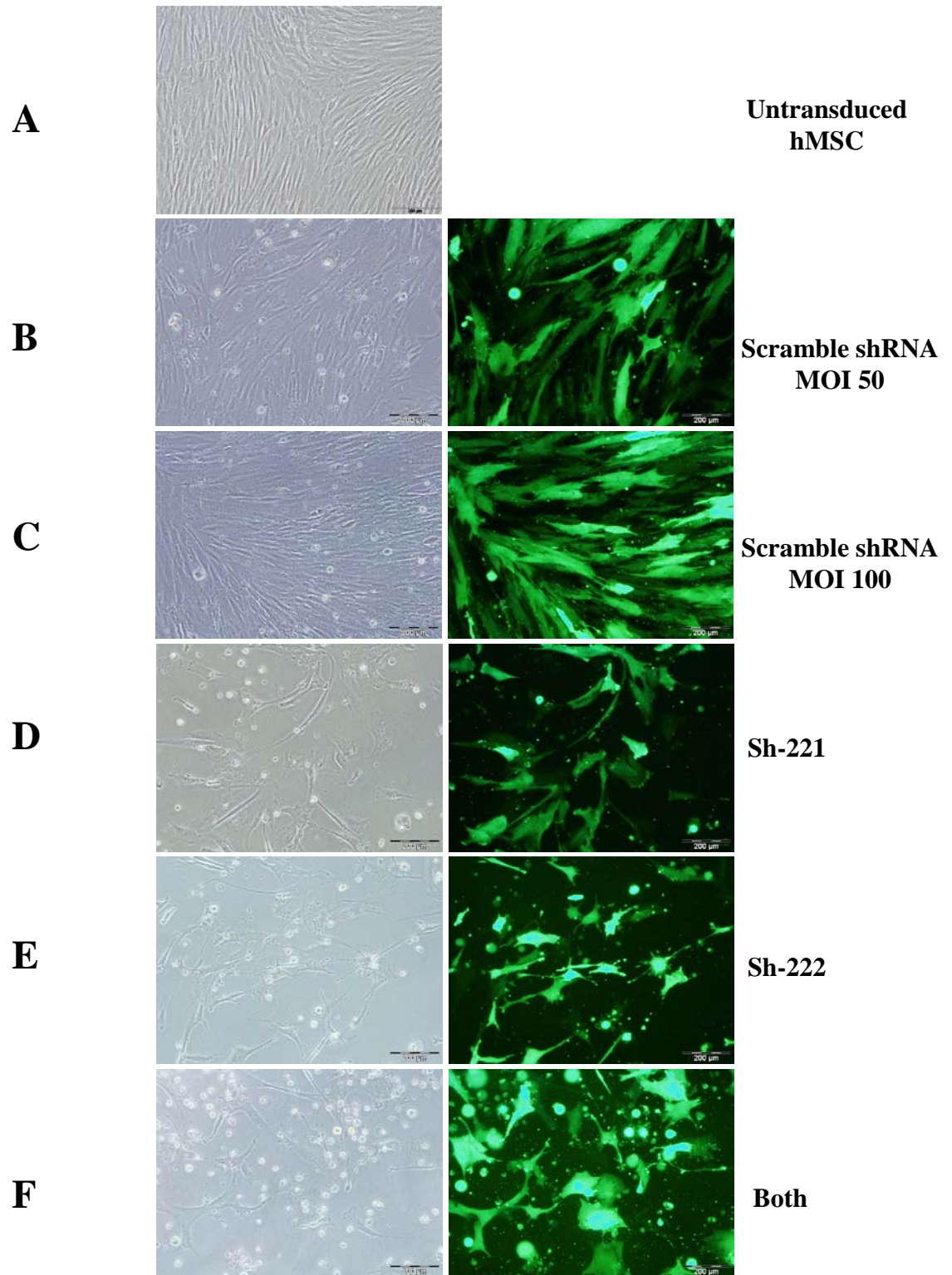


**Figure 4-12 The inhibition of miR-221 or miR-222 activity results in loss of hMSCs 96 hours post transduction**

Panel of phase contrast micrographs and corresponding fluorescence micrographs (10x) of untransduced hMSCs (A) and hMSCs 96 hours post transduction with scramble shRNA (MOI 50) (B), scramble shRNA (MOI 100) (C), sh-221 (MOI 50) (D), sh-222 (MOI 50) (E) and sh-221 and 222 (MOI 50 each) (F).

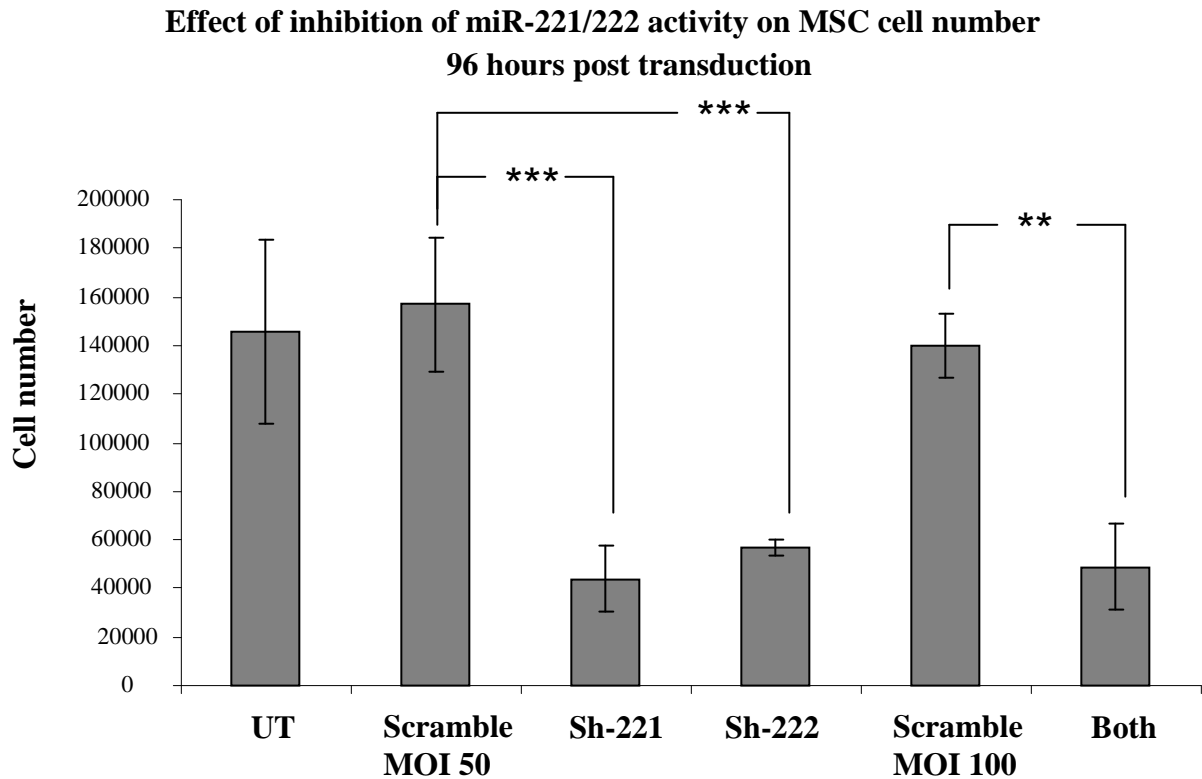


**Figure 4-13 The inhibition of miR-221 or miR-222 activity causes significant loss of hMSCs 96 hours post transduction**

The number of MSCs 96 hours post transduction with sh-221, sh-222 or both sh-221 and sh-222 were counted and compared to the number MSCs post transduction with a scramble shRNA or untransduced MSCs. The inhibition of miR-221 or miR-222 activity causes significant loss of cells in a population of hMSCs compared to MSCs transduced with a scramble shRNA. Error bars represent standard deviation of the mean (n=3 donors), \*\*p≤ 0.01, \*\*\*P≤0.001.

#### 4.2.8 Potential targets of miR-221 and miR-222 in hMSC adipogenesis

As demonstrated, the overexpression of miR-221 and 222 reduces adipogenesis which suggests these miRNAs are targeting a protein or proteins involved in adipogenesis. The next step is to identify this protein, which presumably is upregulated during differentiation, given that miR-221 and 222 are significantly downregulated during adipogenesis. Correct identification of a miRNA target can however, for a number of reasons, be a challenging task. In mammalian systems, miRNAs can exert their effects through the inhibition of translation, promotion of mRNA decay or a combination of both (Bartel 2009; Hendrickson, Hogan et al. 2009; Thomas, Lieberman et al. 2010). MiRNAs bind to their target mRNA by partial complementarity over a short 'seed' sequence that comprises nucleotides 2-7 (Lewis, Shih et al. 2003; Thomson, Bracken et al. 2011). A single miRNA can regulate potentially hundreds of genes but often the level of suppression of a target gene can be quite small (Thomas, Lieberman et al. 2010). In addition, despite much research the rules of miRNA targeting are still not completely understood. Bioinformatic algorithms, although limited in their accuracy are the most commonly used approach for generating a list of potential miRNA targets, these were discussed in more detail in section 1.5.6.

In order to create a short list of potential targets for miR-221 and 222 the target prediction algorithms; MiRanda (John, Enright et al. 2004), Pictar (Krek, Grun et al. 2005) and TargetScan (Lewis, Shih et al. 2003; Lewis, Burge et al. 2005) were employed. A search for targets of miR-221 and miR-222 in MiRanda returned 5,670 targets for miR-221 and 5,434 targets for miR-222. PicTar generated a list of 279 potential targets for miR-221 and 240 potential targets for miR-222 while TargetScan predicted 423 potential targets for both miR-221 and miR-222. Published studies have shown that although these algorithms are a good starting point for the identification of potential targets a large percentage of the predicted genes are not *bona fide* targets. For this reason, we combined the list generated with results in the literature to identify a potential target(s) for miR-221 and miR-222 in hMSC adipogenesis.

The cyclin-dependent kinase inhibitors (CKIs) P27 (Kip1) and P57 (Kip2) were both identified as potential targets of miR-221 and 222 using the miRanda, Pictar and TargetScan algorithms. In addition, p27 and p57 have been verified as targets of miR-221 and 222 in the cancer models; chronic lymphocytic leukemia (Frenquelli, Muzio et al.) and glioblastomas (le Sage, Nagel et al. 2007; Zhang, Kang et al. 2009). More relevant for development as opposed to a disease system, a recent paper by Cardinali *et al* showed a role for miR-221 and 222 in the process of myogenic differentiation by directly targeting p27 (Cardinali, Castellani et al. 2009). Given that a role for miR-221 and miR-222 has been established in a developmental setting through targeting p27, it seemed logical to determine whether this and/or p57 are potential targets in the context of adipogenesis. Hence, studies to determine whether p27 or p57 could be targeted by miR-221 and/or miR-222 during adipogenesis were performed and will now be described.

#### **4.2.8.1 Are miR-221 and miR-222 acting through p27 and/or p57 in adipogenesis?**

To determine whether p27 and/or p57 are possible targets of miR-221/222 in adipogenesis it was first necessary to determine whether they are regulated during hMSC adipogenesis. As miRNAs act post-transcriptionally, it was necessary to monitor both the RNA and the protein levels. Because miR-221 and miR-222 showed the highest level of downregulation in the first 72 hours of adipogenesis-RNA and protein were isolated at 24 hours, 48 hours and 72 hours after induction of adipogenesis. MSCs from three different donors were used as per section 2.4.1 (RNA) and section 2.5.1(protein). Undifferentiated MSCs (MSCs at the same seeding density as adipogenically treated MSCs) treated with hMSC growth medium were used as a control.

#### **4.2.8.2 P57 (Kip2, CDKN1C)**

P57 is a cyclin-dependent kinase inhibitor and an experimentally validated target of miR-221 and miR-222 in a cancer model (Fornari, Gramantieri et al. 2008). No role has been described for p57 in hMSC adipogenesis. P57 is expressed in confluent MSCs and drops significantly in expression 24 hours after adipogenesis has been induced. P57 mRNA expression rises 48 hours after induction and shows a level of expression significantly higher than pre-differentiation MSCs 72 hours after adipogenesis was induced (Figure 4-14A).

Western blot analysis (section 2.5.1) showed that P57 protein expression appears to increase compared to undifferentiated MSCs 24 hours after adipogenesis has been induced, however statistical analysis revealed this was not significant. P57 protein expression does not significantly change between the levels present in confluent MSCs and the levels present 48 hours and 72 hours after adipogenesis was induced (Figure 4-14B). P57 protein levels were normalized to glyceraldehyde 3-phosphate dehydrogenase (GAPDH) levels to control for variations in protein loading.

In general, miRNA expression will have an inverse relationship with its target i.e. it is expected if miRNA expression decreases, the expression of its target protein will increase. P57 protein expression is not consistent with that expected for a target of miR-221 and miR-222, as there is no significant change in target expression. P57 was therefore not further pursued as a potential target of miR-221 and 222 during hMSC adipogenesis.

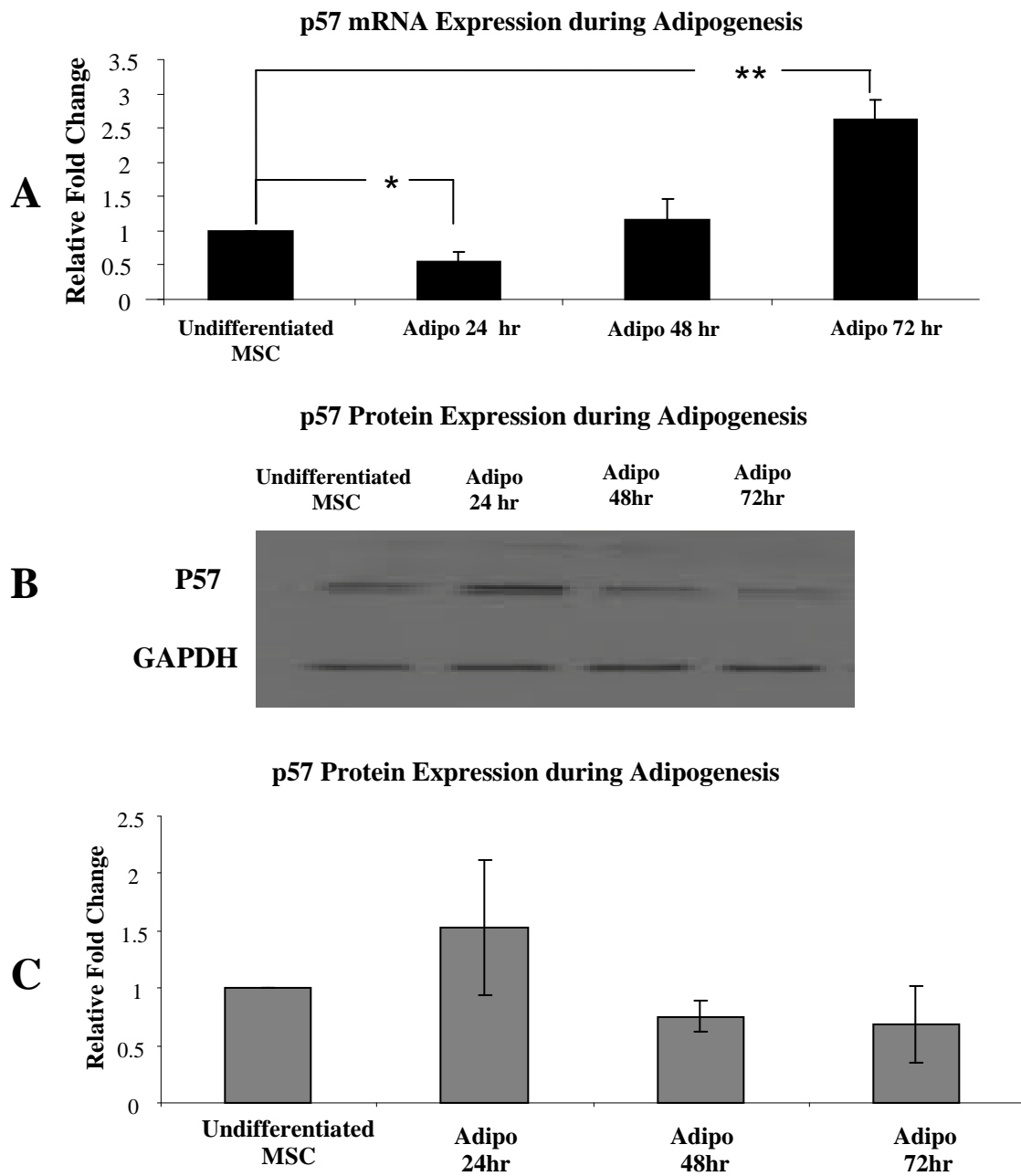


**Figure 4-14 P57 mRNA and protein expression levels 24hours, 48hours and 72 hours after induction of adipogenesis.**

RT-PCR analysis of P57 mRNA expression 24hrs, 48hrs and 72hrs after adipogenesis has been induced (A). All samples were normalized to expression levels of RNA pol II transcript and are reported relative to expression in undifferentiated MSCs. Western blot analysis of p57 and GAPDH protein expression 24hrs, 48hrs and 72hrs after adipogenesis has been induced (B). Densitometric analysis of p57 protein bands (C). All samples were normalized to expression of GAPDH protein and are reported relative to expression in undifferentiated MSCs. Error bars represent standard deviation of the mean (n=3 donors), \* $p \leq 0.05$ , \*\* $p \leq 0.01$

#### **4.2.8.3 P27 (Kip1,CDKN1B)**

RT-PCR analysis shows that similar to p57, p27 mRNA expression is decreased compared to undifferentiated MSCs 24 hours after induction of adipogenesis. The expression of p27 transcript increases 48 hours after adipogenesis has been induced and returns to pre-differentiation levels by 72 hours (Figure 4-15A).

Western blot analysis shows that p27 protein expression is high in confluent undifferentiated MSCs but drops in expression 24 hours after adipogenesis was induced. The expression of p27 protein then increases as adipogenesis progresses, showing a significantly higher level of expression than undifferentiated MSCs 72 hours after induction of adipogenesis (Figure 4-15B).

These data are consistent with p27 being a target during adipogenesis for two reasons; Firstly, expression of its transcript does not decrease as adipogenesis progresses (figure 4-15A). Secondly, p27 protein expression increases 72 hours after the induction of adipogenesis correlating with the decreased expression of miR-221 and miR-222 (Figure 4-15C).

To determine whether p27 expression correlates with that expected for a target of miR-221 and miR-222, its mRNA and protein levels were determined in populations of MSCs overexpressing both miRNAs compared to the level of expression in miR-126 overexpressing MSCs during adipogenesis.

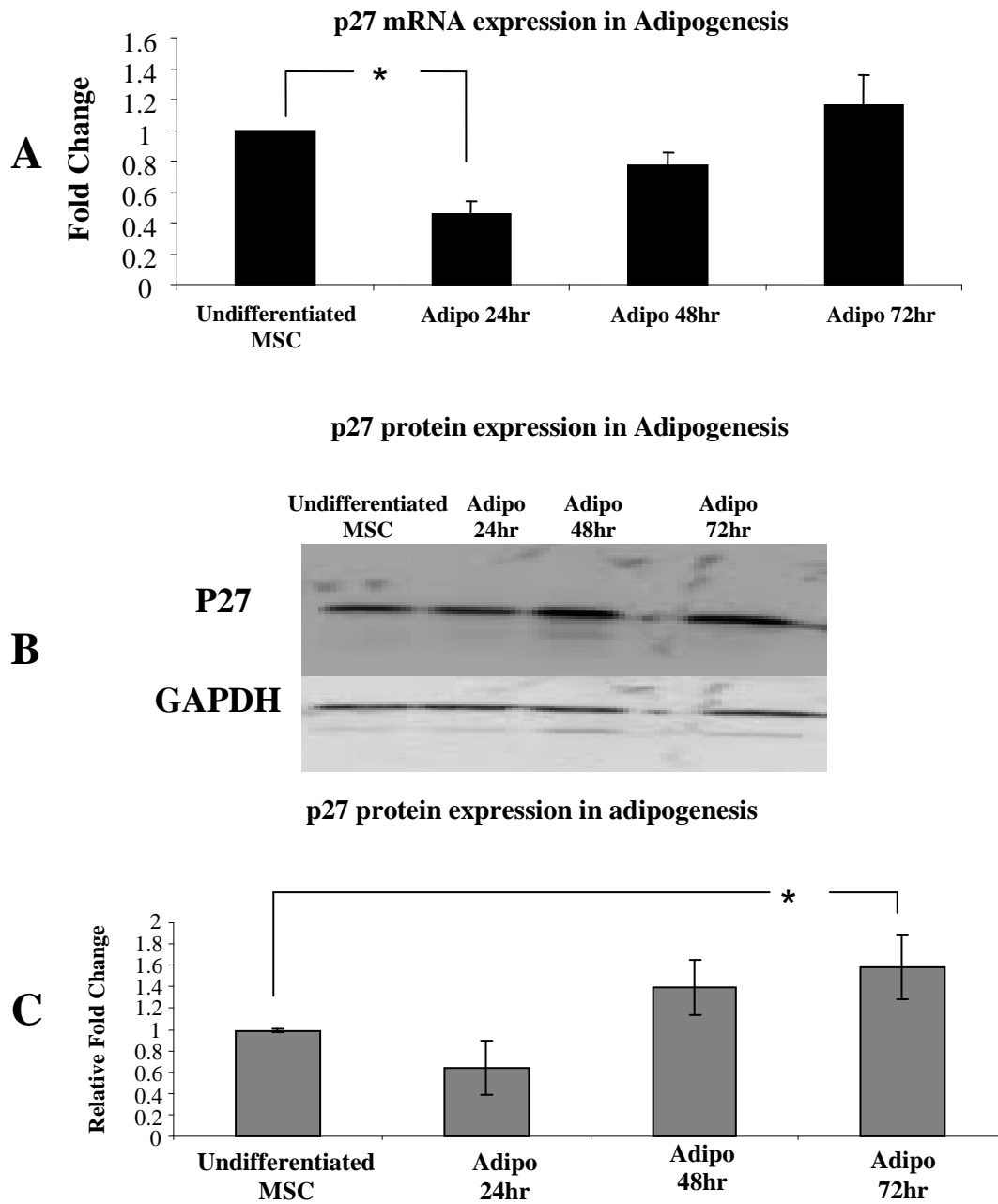


**Figure 4-15 P27 mRNA and protein expression 24hr, 48hr and 72 hour after induction of adipogenesis.**

RT-PCR analysis of p27 mRNA expression 24hrs, 48hrs and 72hrs after adipogenesis has been induced (A). All samples were normalized to expression levels of RNA pol II transcript and are reported relative to expression in undifferentiated MSCs. Western blot analysis of p27 and GAPDH protein expression 24hrs, 48hrs and 72hrs after adipogenesis has been induced (B). Densitometric analysis of p27 protein bands (C). All samples were normalized to expression of GAPDH protein and are reported relative to expression in undifferentiated MSCs. Error bars represent standard deviation of the mean (n=3 donors), \*p $\leq$  0.05

#### 4.2.9 Co-expressing miR-221 and miR-222 causes a reduction in p27 protein but does not significantly reduce p27 transcript.

A comparison of p27 mRNA and protein expression in MSCs overexpressing miR-221 and miR-222 with MSCs overexpressing miR-126 during adipogenesis could provide evidence that p27 has a direct relationship with these miR-221 and miR-222. If p27 is a target of these miRNAs in hMSC adipogenesis, overexpression of these miRNAs should decrease p27 protein levels. RT-PCR analysis shows that a 4-fold and 5.5-fold overexpression of miR-221 and miR-222 respectively, does not significantly reduce p27 transcript compared to MSCs overexpressing miR-126 (figure 4-16). Western blot analysis showed that p27 protein is significantly reduced in miR-221 and 222 overexpressing MSCs compared to MSCs overexpressing miR-126 72 hours after the induction of adipogenesis (Figure 4-17). This correlates with work by Skarn *et al* who also report significant reduction of p27 protein 72 hours after the induction of adipogenesis in MSCs overexpressing miR-221 and 222 but report no change in p27 transcript at the same timepoint compared to control cells (Skarn, Namlos et al. 2011). During the process of adipogenesis, there are many changes in gene expression. It cannot be determined from the expression analysis presented here whether p27 levels are altered as a consequence of the miRNA changes or whether they are altered through some other miR-221 and miR-222 independent mechanism.

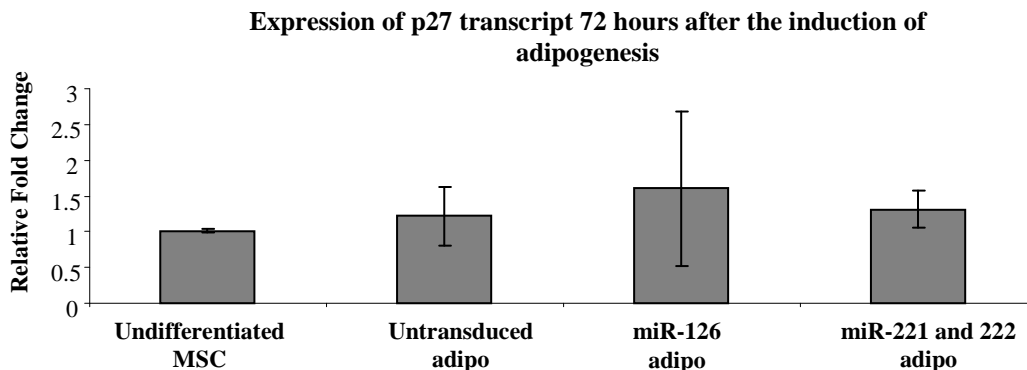


**Figure 4-16 Co-expressing miR-221 and miR-222 does not reduce p27 transcript during adipogenesis**

RT-PCR analysis showing p27 mRNA expression is not significantly reduced in miR-221 and 222 overexpressing MSCs compared to MSCs overexpressing miR-126, 72 hours after adipogenesis was induced. All samples are normalized to RNA polymerase. Error bars represent standard deviation of the mean (n=3 donors).

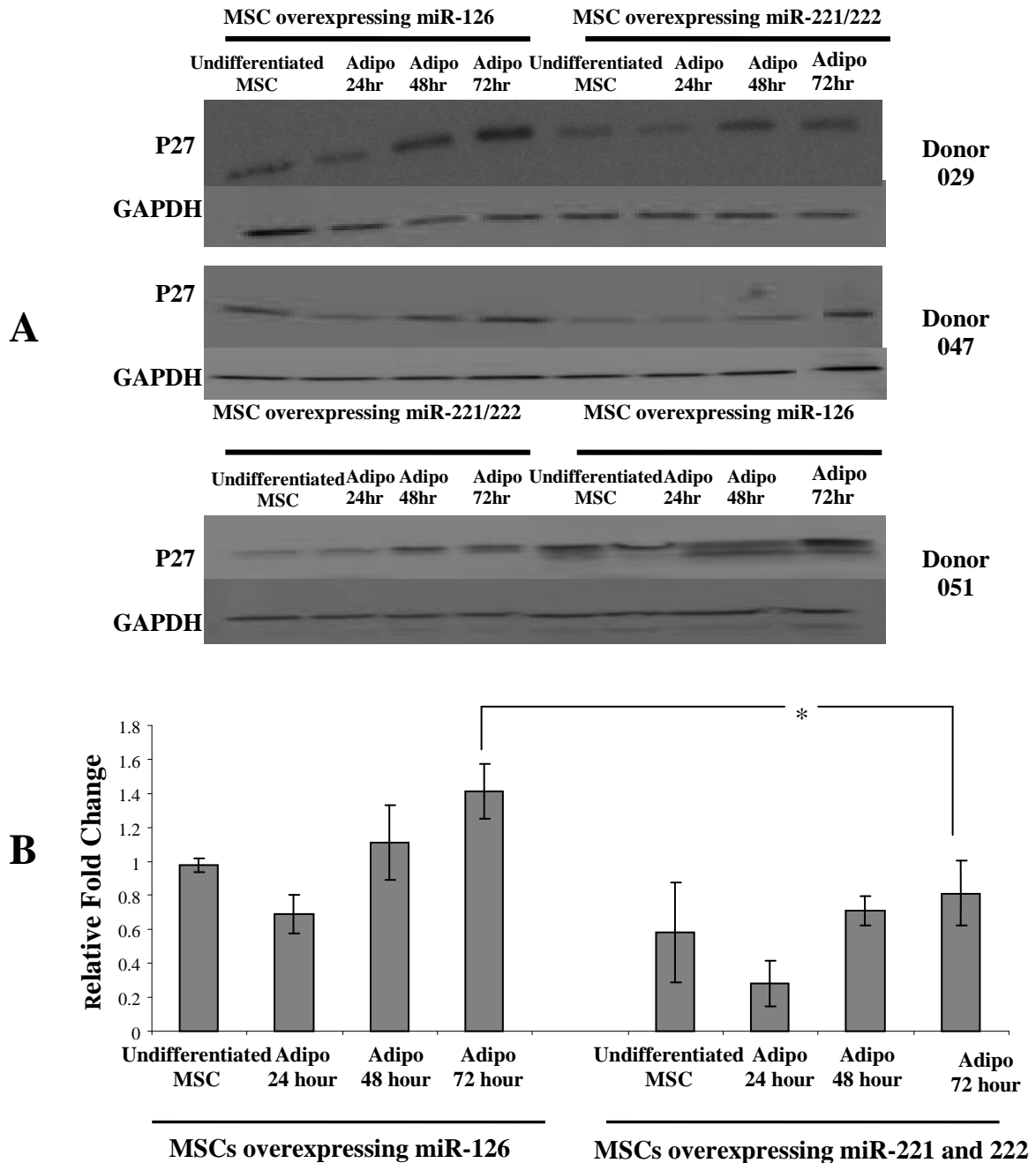


**Figure 4-17 Co-expressing miR-221 and miR-222 significantly reduces p27 protein 72 hours after the induction of adipogenesis**

Western blot analysis shows p27 protein expression is reduced in miR-221, miR-222 overexpressing MSCs compared to MSCs overexpressing miR-126 in the first 3 days of adipogenesis in 3 donors (A). Densitometric analysis of p27 protein bands during first 72 hours of adipogenesis in MSCs overexpressing miR-126 compared to miR-221 and 222 overexpressing MSCs (B). All samples are normalized to GAPDH expression. Error bars represent standard deviation of the mean (n=3 donors), \*p $\leq$  0.05.

#### **4.2.10 Luciferase Reporter Assay Confirms p27 as a direct target of miR-221 and miR-222 in HEK293T Cells**

The expression of p27 protein significantly increases as adipogenesis progresses while the expression levels of miR-221 and miR-222 decrease. Upon overexpression of miR-221 and miR-222, the levels of p27 protein significantly decrease after 72 hours in adipogenesis. This is consistent with p27 protein expression being modulated by miR-221 and miR-222. To determine if this is the case, evidence of a direct interaction between miR-221/222 and p27 is required.

Several methods have been developed to confirm an interaction between a miRNA and its predicted target as described in section 1.5.7. One of the most commonly used methods involves delivering a luciferase-based reporter vector to the cells of interest so the luciferase activity can be measured upon addition of the miRNA under investigation. This study used the pMIR-Report (Applied Biosystems); a miRNA expression reporter vector system that contains a firefly luciferase reporter gene under the control of a CMV promoter (Figure 4-18A). The predicted miRNA target sequence, i.e. all or part of the 3'UTR can be cloned downstream of the luciferase coding sequence. The luciferase transcript will then be subject to the same regulation as the miRNA target. A pMIR- Report luciferase vector containing the 3'UTR of p27 (Luc-p27) was a kind gift from Gary Stein, University of Massachusetts. A pMIR-Report luciferase vector (Luc-Empty) which does not contain a 3' UTR with the predicted miRNA binding site was used as a control.

It is recommended to perform this experiment in cells with low endogenous levels of the miRNA(s) of interest. The interaction between p27 and miR-221/222 was therefore determined in the readily- transfectable HEK293T cell line (293T) as per section 2.3.3.1. 293T cells were transfected with Luc-p27 or with Luc-Empty. Both 293T cell populations were then transfected with either miR-221 or miR-222 or both miR-221 and 222. As a miRNA control, both populations were transfected with miR-126. All populations were transfected with a renilla luciferase vector (pRL-CMV) (Figure 4-18B) a gift from Dr. Daniel O' Toole, Department of Anaesthesia NUIG to act as an internal transfection control.

All samples were analyzed for luciferase activity 48 hours after transfection with the miRNA vectors as per section 2.3.3.1.1. All firefly luciferase signals were normalized to the renilla luciferase activity in the same sample. All populations were successfully transfected as evident from the high levels of luciferase activity detected. Figure 4-19 shows that there is no significant difference in luciferase activity between Luc-Empty and Luc-p27 transfected 293T cells when both were transfected with miR-126. Luc-p27 transfected 293T cells showed a significant decrease in luciferase activity compared to luc-empty 293T cells when both were transfected with miR-221, miR-222 or miR-221 and 222. This is consistent with the findings of other groups who have also demonstrated this (Gillies and Lorimer 2007; le Sage, Nagel et al. 2007; Fornari, Gramantieri et al. 2008). These results suggest that the 3' UTR of p27 is a direct target of the miRNAs 221 and 222 but it is not a direct target of the miRNA-126.

It is appreciated that identifying a direct interaction between miR-221, miR-222 and p27 3'UTR using this reporter vector does not confirm conclusively that these miRNAs are regulating adipogenesis through regulation of p27. In order to definitively say this, experiments that directly modulate p27 expression need to be performed in addition to the luciferase reporter experiments.

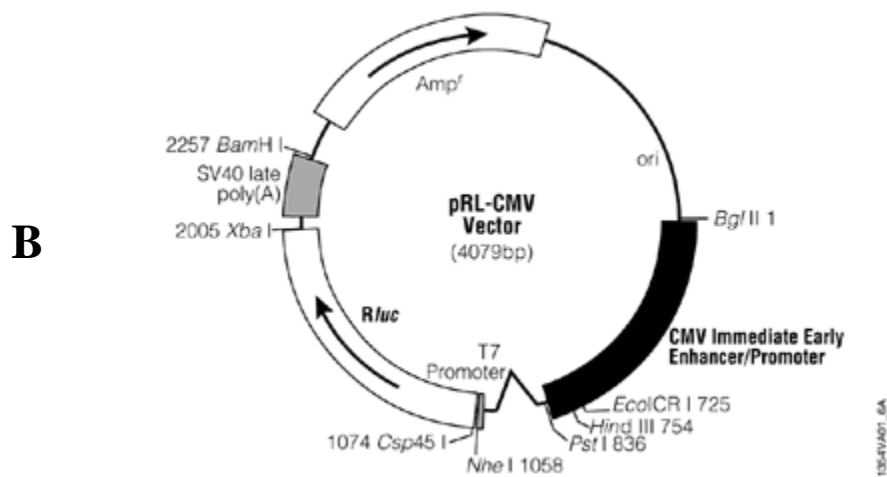
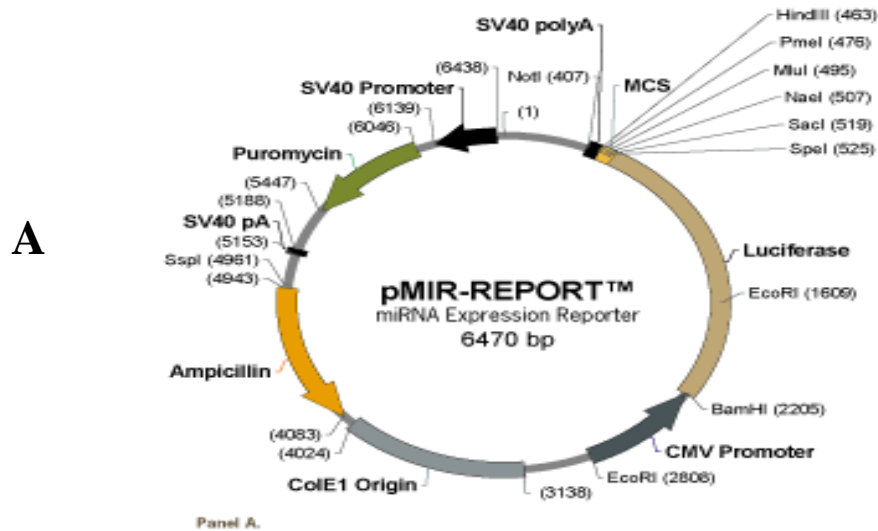


**Figure 4-18 Luciferase Reporter construct and Renilla vector construct used to identify relationship between miR-221/222 and P-27**

(A) The 3' UTR of p27 was cloned into PMIR-REPORT luciferase vector (Luc-p27). PMIR-Report which does not contain a 3' UTR with a predicted miRNA binding site was used as a control (Luc-Empty). (B) Renilla luciferase vector construct (pRL-CMV) which was used as an internal transfection control.

### P27 luciferase reporter activity in the presence of miR-221 and/or miR-222

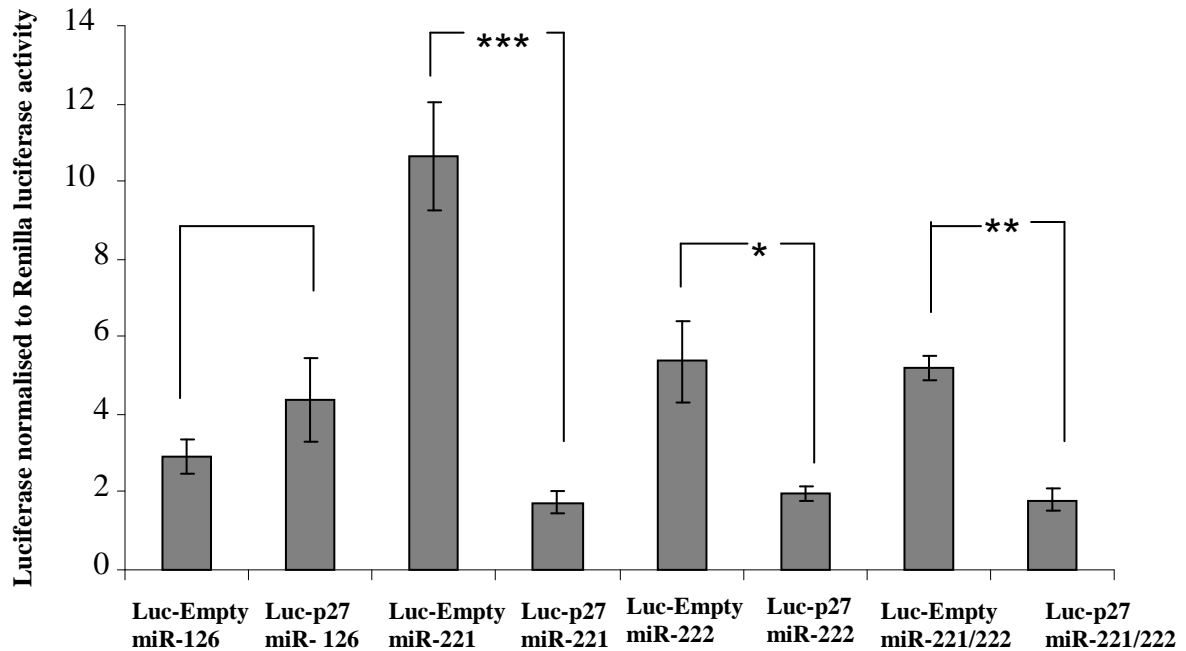


**Figure 4-19 Luciferase Reporter assay identifies a direct relationship between miR-221, miR-222 and p27**

Luciferase activity of Luc-p27 and Luc-Empty transfected 293T cells was measured after transfection with miR-221, miR-222 or miR-221 and 222. To act as a miRNA control, Luc-Empty and Luc-p27 transfected 293T cells were also transfected with miR-126. All luciferase signals were normalized to renilla luciferase activity in the same sample. Error bars represent standard deviation of the mean (n=3 biological replicates). \*p $\leq$  0.05, \*\*P $\leq$  0.01, \*\*\*P $\leq$  0.001

#### **4.2.11 Inhibition of miR-221 and miR-222 activity causes an increase in p27 luciferase activity**

The overexpression of miR-221 and/or miR-222 significantly decreased luciferase activity from 293T cells transfected with a luciferase reporter construct containing the 3' UTR of p27 (Luc-p27). To further investigate p27 as a potential target of miR-221 and 222, the luciferase activity of 293T cells transfected with Luc-p27 was determined after inhibiting miR-221 and/or miR-222. Based on the decrease in luciferase activity observed following overexpression of miR-221 and/or miR-222 (Figure 4-19), it would be expected that the inhibition of miR-221 and/or miR-222 activity would cause an increase in Luc-p27 luciferase activity.

As described in section 2.3.3.1, 293T cells were transfected with Luc-p27 or with Luc-Empty. Both 293T cell populations were then transfected with either sh-221 or sh-222 or both sh-221 and 222. As a control, both populations were transfected with a scramble shRNA. All populations were transfected with a renilla luciferase vector to act as an internal transfection control.

All samples were analyzed for luciferase activity 48 hours after transfection with the vectors as per section 2.3.3.1.1. Firefly luciferase levels were normalized to renilla luciferase activity. There was no significant difference in luciferase activity between Luc-Empty and Luc-p27 transfected 293T cells when both populations were transfected with scramble shRNA. Luc-p27 transfected 293T cells showed a significant increase in luciferase activity compared to luc-empty 293T cells when both were transfected with sh-221, sh-222 or sh-221 and 222 (Figure 4-20).

The inhibition of miR-221 and miR-222 causes an increase in luciferase activity in cells transfected with a reporter containing the 3'UTR of p27. This provides further evidence for regulation of p27 by miR-221 and miR-222.

**P27 luciferase reporter activity upon inhibition of miR-221 and/or miR-222 activity**

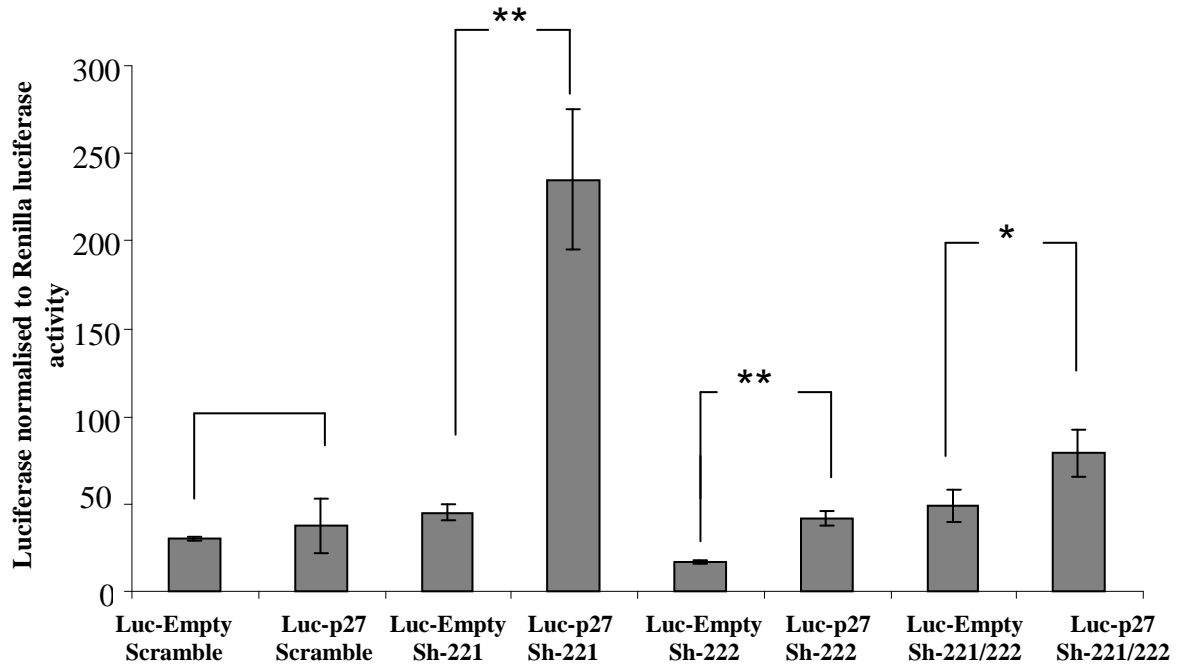


**Figure 4-20 Luciferase activity of p27 luciferase reporter construct is significantly increased upon inhibition of miR-221 and/or miR-222**

Luciferase activity of Luc-p27 and Luc-Empty transfected 293T cells was measured after transfection with sh-221, sh-222 or sh-221 and 222. To act as a control, both populations were also transfected with a shRNA containing a scramble sequence. All luciferase signals were normalized to renilla luciferase activity in the same sample. Error bars represent standard deviation of the mean (n=3 biological replicates), \*p≤ 0.05, \*\*P≤0.01.

#### 4.2.12 Inhibition of miR-221 and miR-222 activity causes an increase in p27 transcript expression

The previous data are consistent with p27 as a target for miR-221 and miR-222. As a further confirmation of a relationship between miR-221 and miR-222 and p27, the expression of p27 transcript was measured in MSCs with reduced miR-221 and miR-222 activity. 72 hours post transduction RT-PCR analysis revealed a significant increase in p27 transcript level in MSCs transduced with sh-221, sh-222 or both sh-221 and 222 compared to MSCs transduced with a scramble shRNA at a corresponding MOI (Figure 4-21). However, it was not possible to determine p27 protein expression in MSCs with reduced miR-221 and 222 activity. As described in section 4.2.7 and figure 4-13, very few MSCs remained 72 hours post transduction with sh-221 and/or sh-222 and so sufficient protein could not be obtained for western blot analysis.

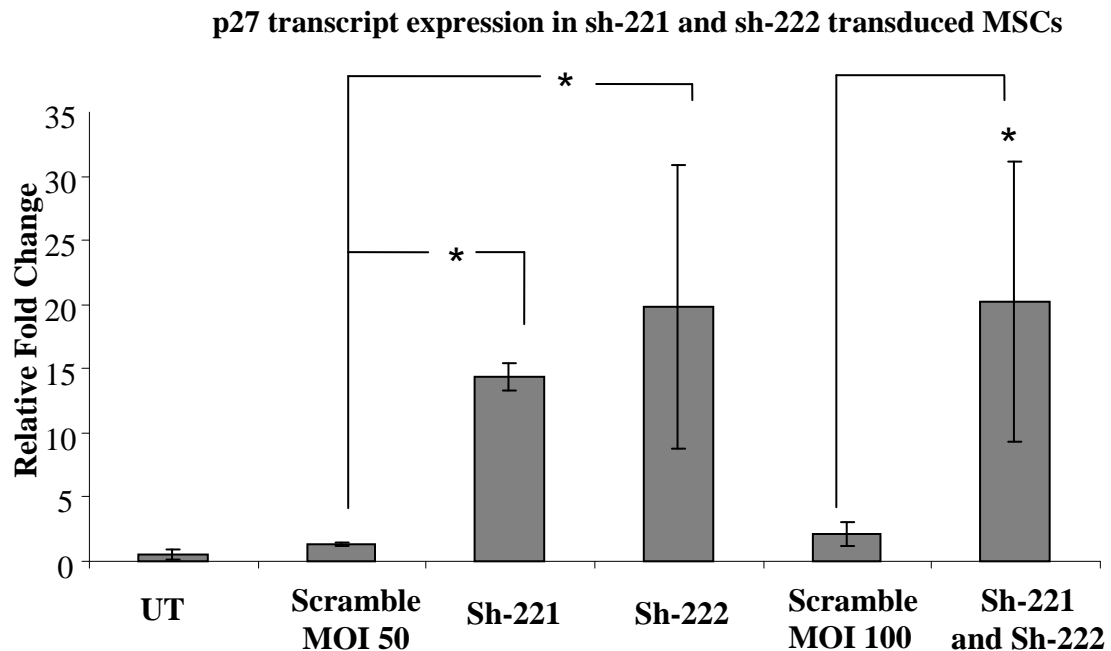


**Figure 4-21 The inhibition of miR-221 or miR-222 activity causes a significant increase in the expression of p27 transcript in hMSCs.**

P27 transcript expression as measured by RT-PCR in MSCs lentivirally transduced with sh-221, sh-222, both sh-221 and sh-222 and a scramble shRNA 72 hours post transduction. Expression was normalized to the expression of RNA pol II transcript. Error bars represent standard deviation of the mean (n=3 donors), \*p $\leq$  0.05.

#### **4.2.13 Add back of p27 does not rescue miR-221 and miR-222 inhibition of adipogenesis**

##### **4.2.13.1 Construction of a p27 overexpression vector**

In brief, the overexpression of the miRNAs 221 and 222 causes a reduction in hMSC adipogenesis as measured by lipid accumulation and the reduced upregulation of key transcripts. P27 is a predicted target of miR-221 and miR-222 which has been confirmed in various cancer models. These experiments show that the overexpression of miR-221 and miR-222 causes a reduction in the level of p27 protein as adipogenesis proceeds while no significant effect is seen on the level of p27 transcript. A direct interaction has also been identified between miR-221/222 and p27 using a luciferase reporter vector containing the 3'UTR of p27. Inhibition of miR-221 and miR-222 activity leads to an increase in p27 transcript in MSCs. The overexpression of miR-221 and 222 prevents the upregulation of p27 during hMSC adipogenesis. In addition, others have shown that the siRNA knockdown of p27 significantly reduces hMSC adipogenesis (Kang, Choi et al. 2008). Taken together, could the mechanism of miR-221 and miR-222 inhibition of adipogenesis be mediated through the regulation of p27 expression? One way to investigate this possibility is to determine whether the overexpression of p27 (without a UTR) can rescue the reduced adipogenesis in miR-221 and miR-222 overexpressing MSCs? A p27 overexpression vector was constructed as per section 2.2.2, to determine the effects of adding back p27 to MSCs overexpressing the inhibitory miRNAs. Briefly, the protein coding sequence of p27 (with no UTR sequence) was amplified by RT-PCR and cloned into the pCR8 Gateway Cloning vector (Invitrogen) by TOPO cloning. The p27 coding sequence was then transferred to a lentiviral vector backbone, pWPT which had been modified to incorporate a Gateway cloning cassette (a kind gift from Dr Andrew Hillmann, REMEDI, NUI Galway) using recombinase (Invitrogen). This vector will now be referred to as the pWPT-p27 vector.

As p27 is a cyclin dependent kinase inhibitor it is expected that its overexpression would result in a halting of the cell cycle and thus a reduction in cell division.

Before this plasmid was used for production of lentiviral vectors, the functionality of the p27 produced was tested. To do so, 293Ts cells were transfected with the pWPT-p27 plasmid as per section 2.3.3.2 with a control GFP plasmid (pWPT-GFP) as a transfection control. Untransfected 293T cells and both populations of transfected 293T cells were trypsinised and counted 72 hours post transfection. There was a significant decrease in cell number in the population transfected with the pWPT-p27 vector compared to the GFP transfected population (Figure 4-22). This is the expected outcome of p27 overexpression construct due to the role of p27 in cell cycle control.

The pWPT-p27 plasmid was used to derive a lentiviral vector as per section 2.3.1. The functionality of the p27 produced from the lentiviral vector was tested in MSCs by transducing populations of MSCs with pWPT-p27 or with a lentiviral pWPT-GFP vector as per section 2.3.1.2.2.1. Untransduced MSCs and both populations of transduced MSCs were counted 72 hours post transduction. As with the previous experiment, there was a significant decrease in cell number in MSCs transduced with pWPT-p27 compared to pWPT-GFP transduced MSCs (Figure 4-23). This thus validated the functionality of the p27 overexpression vector.

### 293T cell number post pWPT-p27 transfection

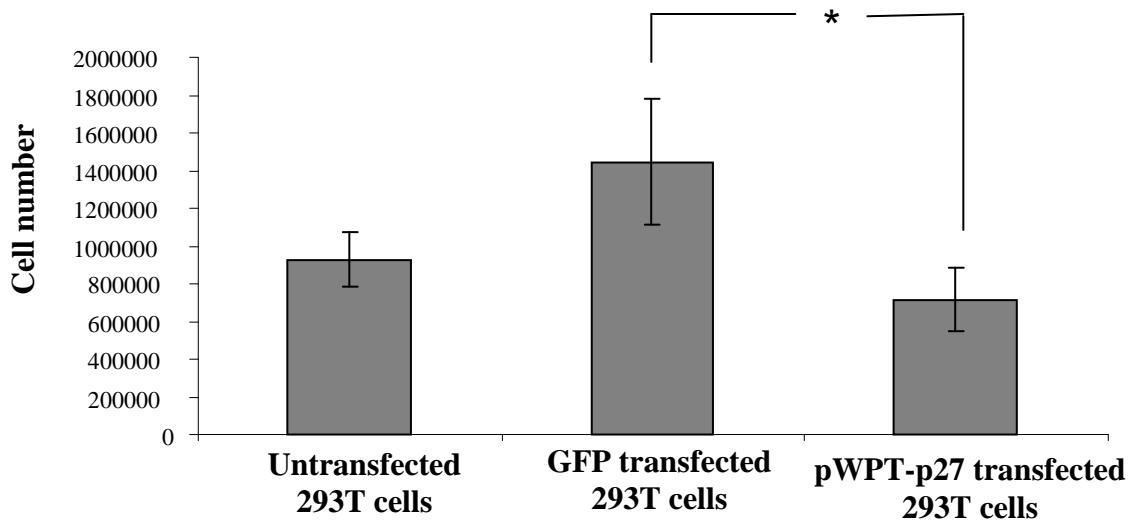


**Figure 4-22 293T number post transfection with pWPT-p27 vector**

293T cells transfected with pWPT-p27 plasmid showed a significant reduction in cell number 48 hours post transfection compared with 293T cells transfected with a control pWPT-GFP plasmid. Error bars represent standard deviation of the mean (n=3 biological replicates), \*p $\leq$  0.05.

### MSC number post lentiviral pWPT-p27 transduction

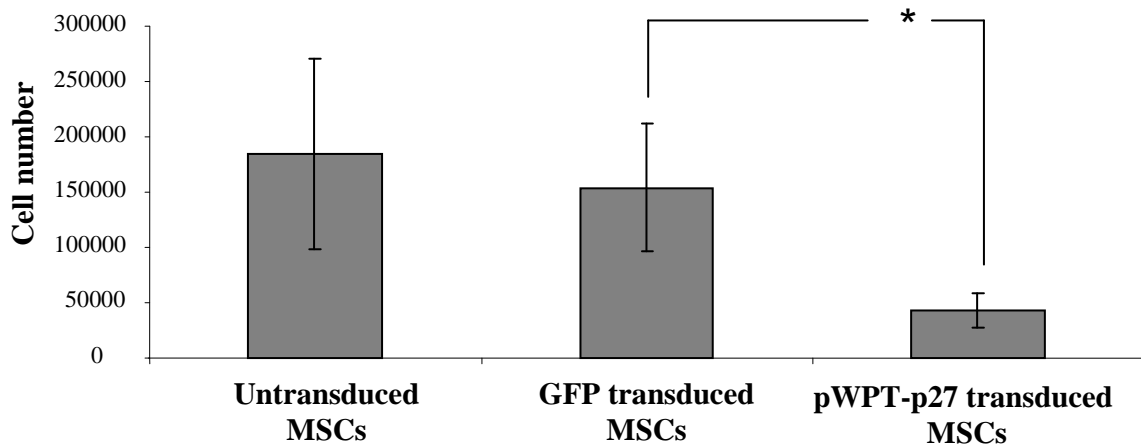


**Figure 4-23 MSC number post transduction pWPT-p27 vector**

MSCs lentivirally transduced with pWPT-p27 plasmid at a MOI 50 showed a significant reduction in cell number 72 hours post transduction compared to MSCs lentivirally transduced with a control GFP plasmid. Error bars represent standard deviation of the mean (n=3 donors), \*p $\leq$  0.05.

#### 4.2.13.2 Overexpression of p27 in MSCs overexpressing miR-221 and 222

MSCs isolated from three donors were transduced with miR-221 and 222 or miR-126. These populations of MSCs along with an untransduced MSC population were then split into three groups. One group was not transduced with any vector, one was transduced with pWPT-p27 lentiviral vector at an MOI 50 and the final was transduced with pWPT-GFP lentiviral vector at the same MOI. A schematic of this experiment is shown in figure 4-24.

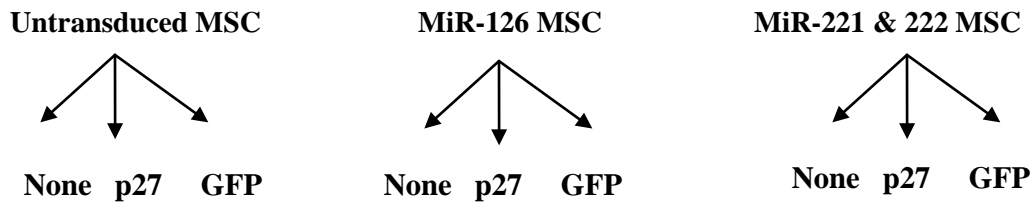
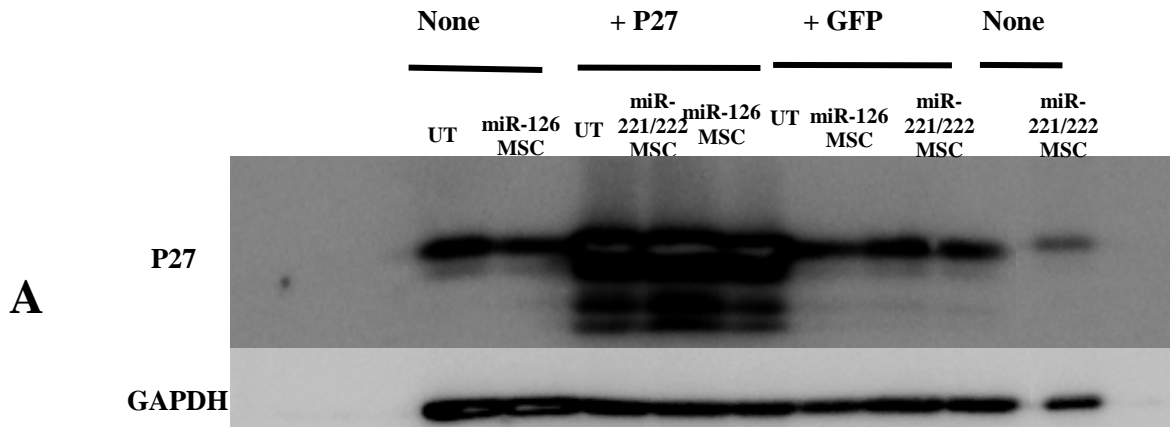


**Figure 4-24 Outline of p27 ‘add-back’ to MSCs overexpressing miR-221 and 222 with appropriate controls**

As described in section 2.1.2.4.1, to induce adipogenesis in a population of MSCs, the cells must be 2 days post confluence. It was a concern, that if the MSCs were transduced at subconfluence, they would not grow to reach a state of confluence necessary to induce adipogenesis, based on the results of section 4.2.14.1 (Figure 4-23). For this reason, all populations were lentivirally transduced with pWPT-p27 or pWPT-GFP once they had reached confluence. Protein was isolated from all populations 72 hours post transduction and p27 protein expression levels were determined by western blot analysis as per section 2.5.1.

Figure 4-25 shows a significant overexpression of p27 protein expression following transduction with the lentiviral pWPT-p27 vector compared to the populations transduced with lentiviral pWPT-GFP. This is seen in the MSC population overexpressing miR-221 and miR-222 as well as the untransduced MSC population and the population overexpressing miR-126. This demonstration of p27 overexpression in MSCs combined with the observed effect on MSC and 293T cell number confirms the functionality of the p27 produced from the vector and thus we can use it with confidence for future experiments to examine the effects of p27 overexpression.



**Expression of p27 protein after transduction with pWPT-p27 or pWPT-GFP**

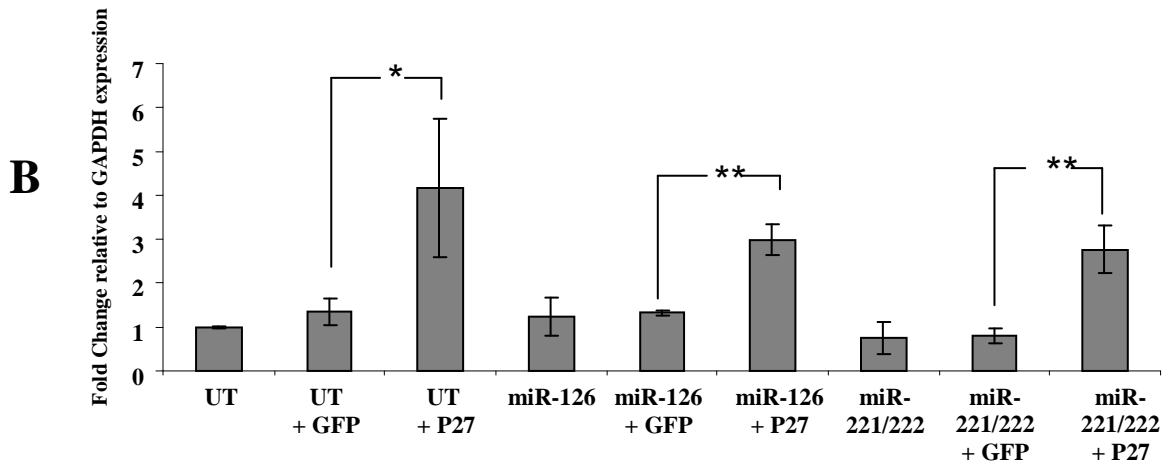


**Figure 4-25 Transduction of hMSCs with PWPT-p27 vector causes an increase in p27 protein expression**

(A) Western blot analysis of p27 and GAPDH protein showing that lentiviral transduction of hMSCs with PWPT-p27 vector causes a significant increase in p27 protein expression compared to hMSCs transduced with GFP lentivirus 72 hours post transduction. (B) Densitometric analysis of p27 protein bands 72 hours after transduction with pWPT-p27 or pWPT-GFP. All samples are normalized to GAPDH protein expression. Error bars represent standard deviation of the mean (n=3 donors), \*p≤ 0.05, \*\*p≤0.01.

#### **4.2.13.3 Overexpression of p27 has no significant effect on hMSC adipogenesis**

MSCs from three donors were transduced with miR-221 and miR-222 at an MOI 50. Untransduced MSCs and MSCs transduced with miR-126 at an MOI 50 were used as controls. Cultures of each population were then further transduced with either pWPT-p27 vector or lentiviral pWPT-GFP as per figure 4-24 and induced to undergo adipogenesis.

Figure 4-26 shows that the overexpression of p27 does not significantly increase or decrease adipogenesis in untransduced or miR-126 overexpressing MSCs compared to MSCs transduced with lentiviral pWPT-GFP. The MSC population overexpressing miR-221 and 222 showed a reduction in adipogenesis throughout the assay, as previously demonstrated (Figure 4-8). This was evident by the significant difference in lipid accumulation compared to the MSC population overexpressing miR-126. The MSC populations overexpressing miR-221 and 222 and then transduced with the pWPT-p27 vector showed no difference in Oil Red O binding compared to the same populations transduced with lentiviral pWPT-GFP.

Therefore, although the overexpression of miR-221 and miR-222 causes a reduction in p27 protein and lipid accumulation, the add-back of p27 does not rescue the reduction in lipid accumulation although it rescues the reduction in p27 protein (Figure 4-26). This suggests that although the overexpression of miR-221 and miR-222 reduces p27 protein at the early stages of adipogenesis, this alone does not contribute to the reduction observed in lipid accumulation. Potentially, the level of overexpression achieved with pWPT-p27 was too high and examining the effect of p27 overexpression closer to physiological level would be of more benefit.

It is probable that the overexpression of miR-221 and miR-222 causes a change in expression in many proteins involved in the adipogenic differentiation of MSCs. Indeed, the mechanism of action of miRNAs is to target multiple genes at one time and although a reduction in p27 protein is observed upon overexpression of miR-221/222, it is likely that the expression of many other proteins is also reduced as a result.

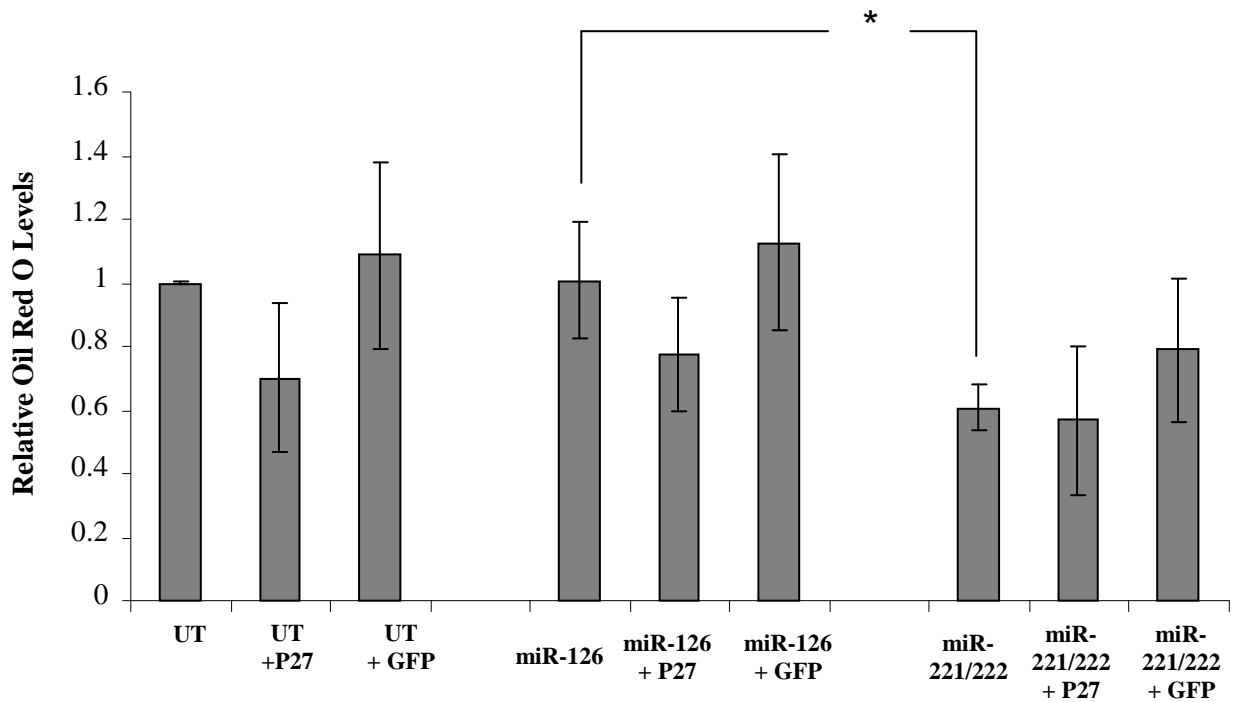


**Figure 4-26 Transduction of miR-221/222 overexpressing hMSCs with pWPT-p27 vector does not recover adipogenesis**

Untransduced MSCs, MSCs overexpressing miR-126 and MSCs overexpressing miR-221 and 222 were lentivirally transduced with either pWPT-p27 or pWPT-GFP at an MOI 50 or were untransduced. Cells were induced to undergo adipogenesis. After 14 days, all populations were stained with Oil Red O which was then extracted and quantified at 495nm. Transduction with pWPT-p27 did not significantly change bound Oil Red O levels compared to pWPT-GFP lentiviral transduction in untransduced MSCs or MSCs overexpressing miR-126. MSCs overexpressing miR-221/222 showed significantly lower levels of Oil Red O compared to MSCs overexpressing miR-126. This reduced level of adipogenesis was not significantly increased (i.e. restored) by transduction with pWPT-p27 or pWPT-GFP. Error bars represent standard deviation of the mean (n=3 donors), \*p≤ 0.05.

#### **4.2.14 Identification of other targets for miR-221 and miR-222 in adipogenesis**

Two validated candidates of miR-221/222 are p57 and p27. P57 protein does not change significantly as adipogenesis proceeds suggesting it is not the target through which miR-221 and 222 are acting in hMSC adipogenesis. P27 protein expression is significantly downregulated upon overexpression of miR-221 and 222 72 hours after the induction of adipogenesis; p27 transcript is upregulated in MSCs with inhibited miR-221 and miR-222 however rescuing p27 protein expression did not result in a rescue of lipid accumulation.

As discussed in sections 1.5.6 and 4.2.8 the identification of miRNA targets is one of the most challenging aspects of current miRNA research. A search using the target prediction algorithm MiRanda returned more than 5000 potential targets of miR-221 and 222. Therefore, in an attempt to create a shortlist of miR-221 and miR-222 targets which are expressed in hMSCs, a miRNA target prediction program called Sylamer (van Dongen, Abreu-Goodger et al. 2008) was employed. Sylamer is a miRNA identification program developed by the Enright group (van Dongen, Abreu-Goodger et al. 2008). The input for the program is a genelist from mRNA microarray data organised in order of expression change, but also including transcripts which do not undergo significant changes in expression level. In this case, array data from a comparison of undifferentiated MSCs to adipogenically differentiated hMSCs. The mRNA microarray was performed at day 20 of adipogenesis on the same RNA samples as the miRNA microarray (L.Howard, data not shown). The Sylamer algorithm reveals significant enrichment or depletion of miRNA seed sequences in 3' UTRs. In this case, no significant enrichment or depletion of seed sequences was observed, however the software did provide a list of miR-221 and miR-222 targets that are expressed in hMSCs.

This was used as a starting point to identify potential targets of miR-221 and miR-222 which are expressed during adipogenesis. However, it should be noted that miR-221 and miR-222 are downregulated and have roles early in the process of adipogenesis and so a microarray performed at an earlier timepoint, (ideally day 3 of adipogenesis) would have been more beneficial. Using this program, a list of 7 mRNAs that contained putative binding sites for miR-221 and miR-222 and that

were either upregulated or demonstrated no change in transcript level was compiled (Table 4-1). In addition, three other candidate targets were selected for further experimentation based on evidence in the literature; PGC1 $\alpha$ : a cofactor of PPAR $\gamma$  and an important factor in the decision between white and brown fat determination (Puigserver and Spiegelman 2003) (Tiraby, Tavernier et al. 2003) (Spiegelman, Puigserver et al. 2000; Liang and Ward 2006). Mdm2: a target of miR-221 which has been shown to have a role in the regulation of chondrogenic differentiation in chick limb mesenchymal stem cells (Kim, Song et al. 2010). TLE3: a dual function transcriptional coregulator of adipogenesis (Villanueva, Waki et al. 2011). Table 4-1 summarises these potential targets, their potential roles in adipogenesis and the region of their 3' UTR which contains a putative miR-221/222 binding site (taken from [www.miRanda.org](http://www.miRanda.org)). All potential targets contain putative binding sites for both miR-221 and miR-222, apart from Mdm2 which only contains a predicted binding site for miR-221.

RNA isolated from MSCs overexpressing miR-221 and miR-222, MSCs overexpressing miR-126 and untransduced MSCs were used to examine the expression of these potential targets by RT-PCR in the first 72 hours of adipogenesis. As the expression of miR-221 and miR-222 decreases during differentiation, a potential target of these miRNAs is expected to have an expression pattern that is either unchanging or increasing during adipogenesis. The expression patterns of these potential targets, as determined by RT-PCR is shown in figure 4-27 to figure 4-30 and summarised in Table 4-2 below.

Gene	Function/Role in adipogenesis	Sequence alignment
<b>Glycerol-3-phosphate dehydrogenase 2 (GPD2)</b>	Enzyme catalysing lipid metabolism and lipid marker	3' cuuugggucGUCUGUUACAUCGa 5' hsa-miR-221            2717:5' ugucuguuuCAAUAUGUAGCu 3' GPD2 3' ugggucaucggUCUACAUCGa 5' hsa-miR-222         2719:5' ucuguuucaaaAUAUGUAGCu 3' GPD2
<b>Mitogen-activated protein kinase (MAP3K10)</b>	Negative regulator of TGF- $\beta$	3' cuuuGGGUCGUCUG--UUACAUCGa 5' hsa-miR-221   :              18:5' ccgcCUGGGCAGCCAUGAAUGUAGCg 3' MAP3K10 3' ugggUCAUCGGU-C-UACAUCGa 5' hsa-miR-222 :                21:5' ccugGGCAGCCAUGAAUGUAGCg 3' MAP3K10
<b>Oxysterol binding protein-like 3 (OSBPL3)</b>	Implicated in lipid synthesis and metabolism	3' cuuugggucgucuguUACAUCGa 5' hsa-miR-221          3589:5' uugcuuaucucccucAUGUAGCu 3' OSBPL3 3' ugggucaucGGUCUACAUCGa 5' hsa-miR-222          3591:5' gcuuaucuccCUCAUGUAGCu 3' OSBPL3
<b>Regulatory factor X (RFX7)</b>	Transcription factor for ALMS1 transcription, whose expression modulated adipogenesis	3' cuuugggucGUCUGUUACAUCGa 5' hsa-miR-221 :           1:5' auuguguuuUAUAACAUGUAGCa 3' RFX7 3' ugggucaucggUCUACAUCGa 5' hsa-miR-222         3:5' uguguuuuauACAUGUAGCa 3' RFX7
<b>Fatty acid binding protein 2 (FABP2)</b>	Key factor for lipogenesis	3' cuuugggucgucuguUACAUCGa 5' hsa-miR-221          253:5' uccauguugcuuuauAUGUAGCc 3' FABP2 3' ugGGU-CAUCG--GUCUACAUCGa 5' hsa-miR-222           :         252:5' guCCAUGUUGCUUUAUUAUGUAGCc 3' FABP2
<b>Kruppel-like factor 3 (KLF3)</b>	Zinc finger transcription repressor	3' cuUUGGGUCGUCUGU---UACAUCGa 5' hsa-miR-221 :   :              1302:5' caGAUCAGGGAUUAUAUAUGUAGCu 3' KLF3 3' ugggucaucgGUCUACAUCGa 5' hsa-miR-222 :         1307:5' cagggauucaUAUAUGUAGCu 3' KLF3
<b>Murine double Minute 2 (MDM2)</b>	Published role in chondrogenic differentiation (Kim, Song et al. 2010)	3' cuUUGGG-UCGUCUGUUACAUCGa 5' hsa-miR-221    : :   :            170:5' auAAUUUGACUUGAAUAUGUAGCu 3' MDM2
<b>Transducin-like enhancer protein 3 (TLE3)</b>	Transcriptional coregulator of adipogenesis (Villanueva, Waki et al. 2011)	3' cuUUGGGUCGUCUGUUACAUCGa 5' hsa-miR-221 : :     : :       1512:5' caGGCUCUCCAUG-GAUGUAGCa 3' TLE3 3' uggGUC--AUCGGU--CUACAUCGa 5' hsa-miR-222                   1509:5' uggCAGGCUCUCCAUGGAUGUAGCa 3' TLE3
<b>PPAR<math>\gamma</math> coactivator-1<math>\alpha</math> (PGC1<math>\alpha</math>)</b>	Promotes brown fat differentiation in MSCs (Huang, Chen et al. 2011)	3' cuuuGGGUCGUCUGUUACAUCGa 5' hsa-miR-221 : : :        :       3208:5' cuuuUUUAAAAGA-GAUGUAGCa 3' PPARGC1A 3' ugggucaucggUCUACAUCGa 5' hsa-miR-222          3209:5' uuuuuuuuuagAGAUGUAGCa 3' PPARGC1A

**Table 4-1 Potential miR-221 and miR-222 targets, their possible role in adipogenesis and the region of 3' UTR containing putative miR-221/222 binding sites**

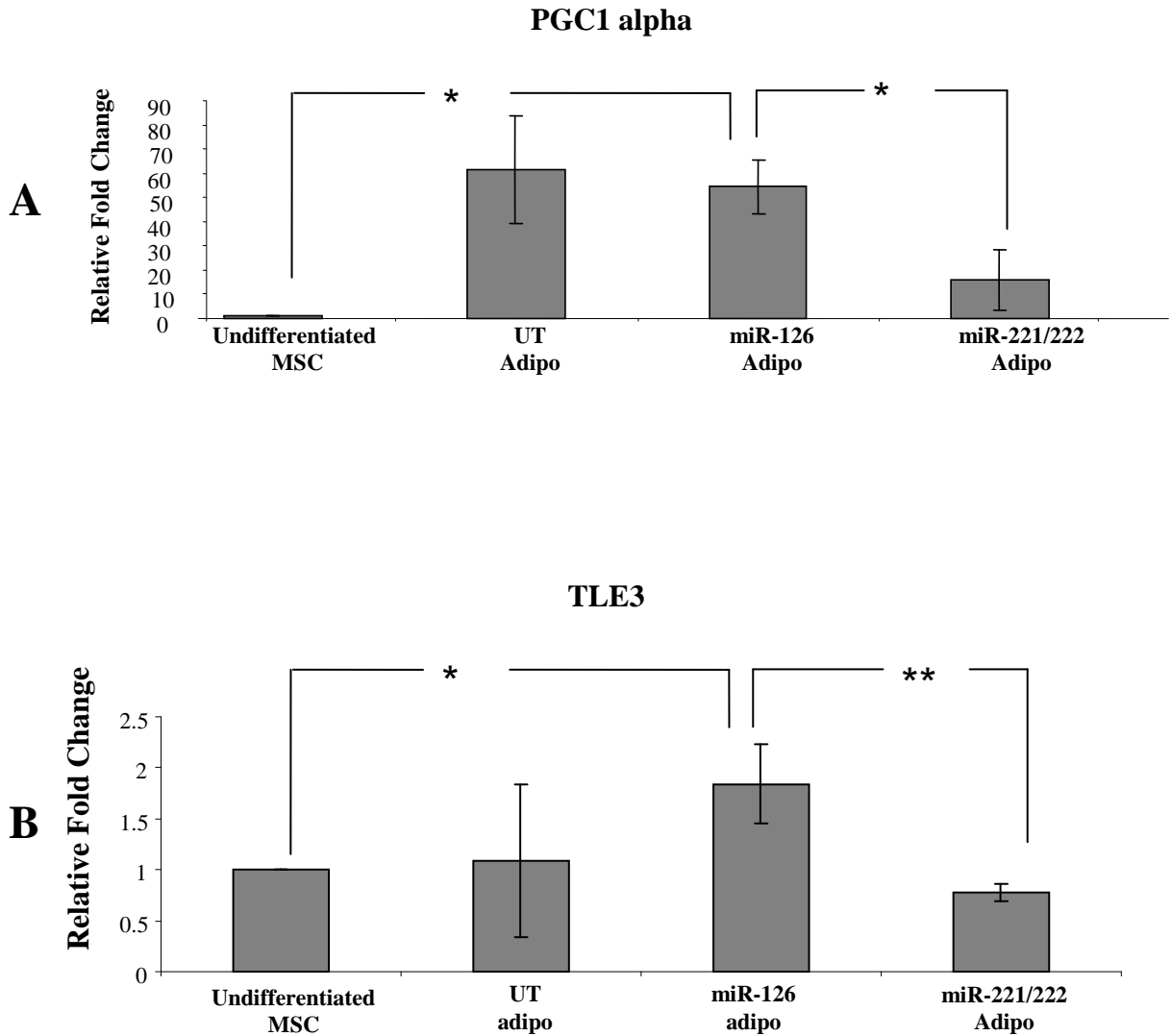


**Figure 4-27 Potential miR-221 and miR-222 targets: PGC1 $\alpha$  and TLE3 show increased expression 72 hours post induction of adipogenesis**

Expression of the potential miR-221 and miR-222 targets (A) PGC1 $\alpha$  and (B) TLE3 in untransduced MSCs and MSCs overexpressing miR-221 and miR-222 compared to MSCs overexpressing miR-126 (values are presented relative to undifferentiated-matched hMSCs for each population). RT-PCR was performed using RNA isolated 72 hours after the induction of adipogenesis. Expression levels were normalized to the levels of RNA pol II transcript. Error bars represent standard deviation of the mean (n=3 donors), \*p $\leq$  0.05, \*\*P $\leq$  0.01.

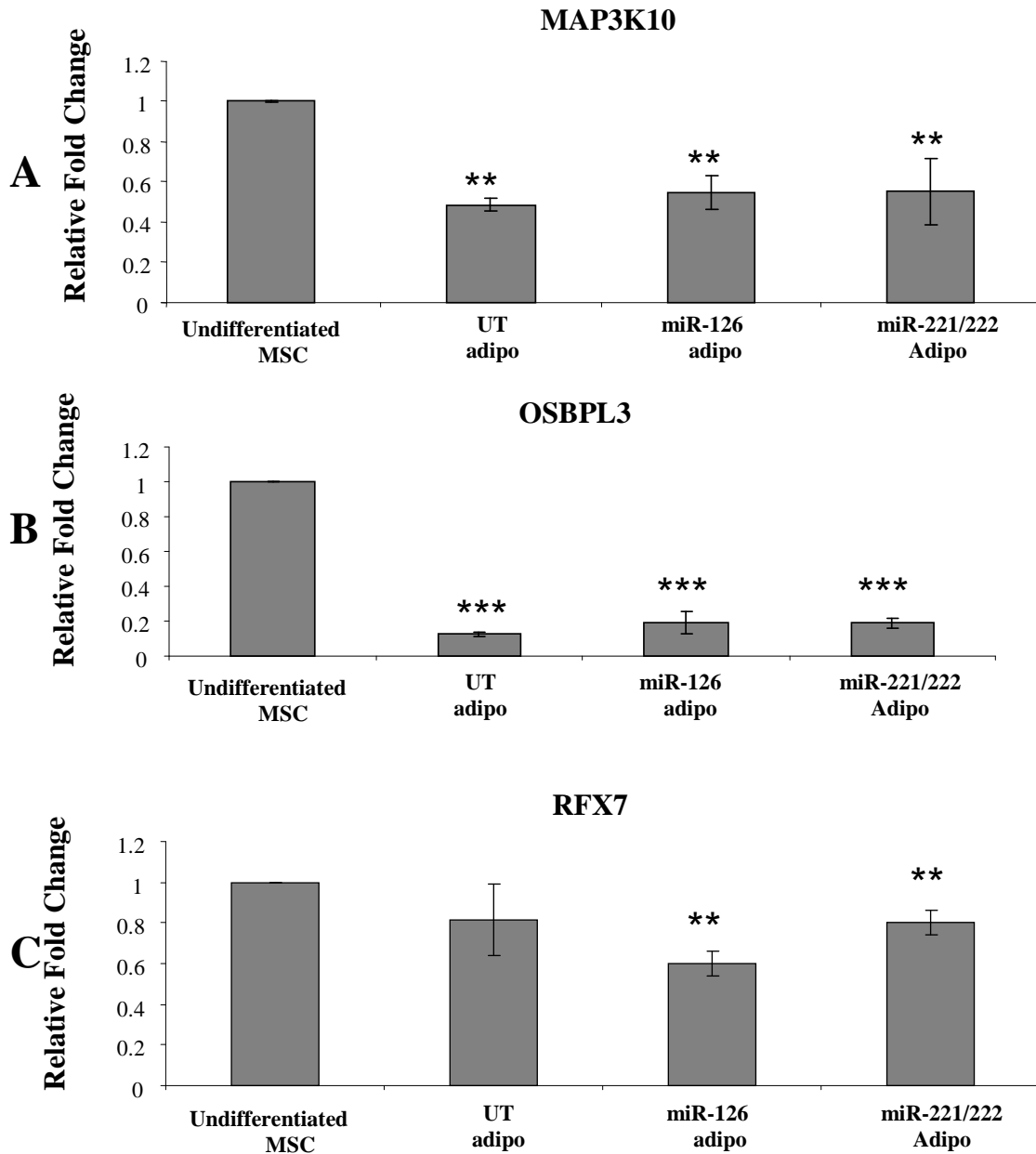


**Figure 4-28 Potential miR-221 and miR-222 targets, MAP3K2, OSBPL3 and RFX7 show decreased expression 72 hours post induction of adipogenesis**

Expression of the potential miR-221 and miR-222 targets (A) MAP3K10, (B) OSBPL3 and (C) RFX7 in untransduced MSCs and MSCs overexpressing miR-221 and miR-222 compared to MSCs overexpressing miR-126 (values are presented relative to undifferentiated-matched hMSCs for each population). RT-PCR was performed using RNA isolated 72 hours after the induction of adipogenesis. Expression levels were normalized to the levels of RNA pol II transcript. Error bars represent standard deviation of the mean (n=3 donors), \*\*P≤ 0.01, \*\*\*P≤ 0.001

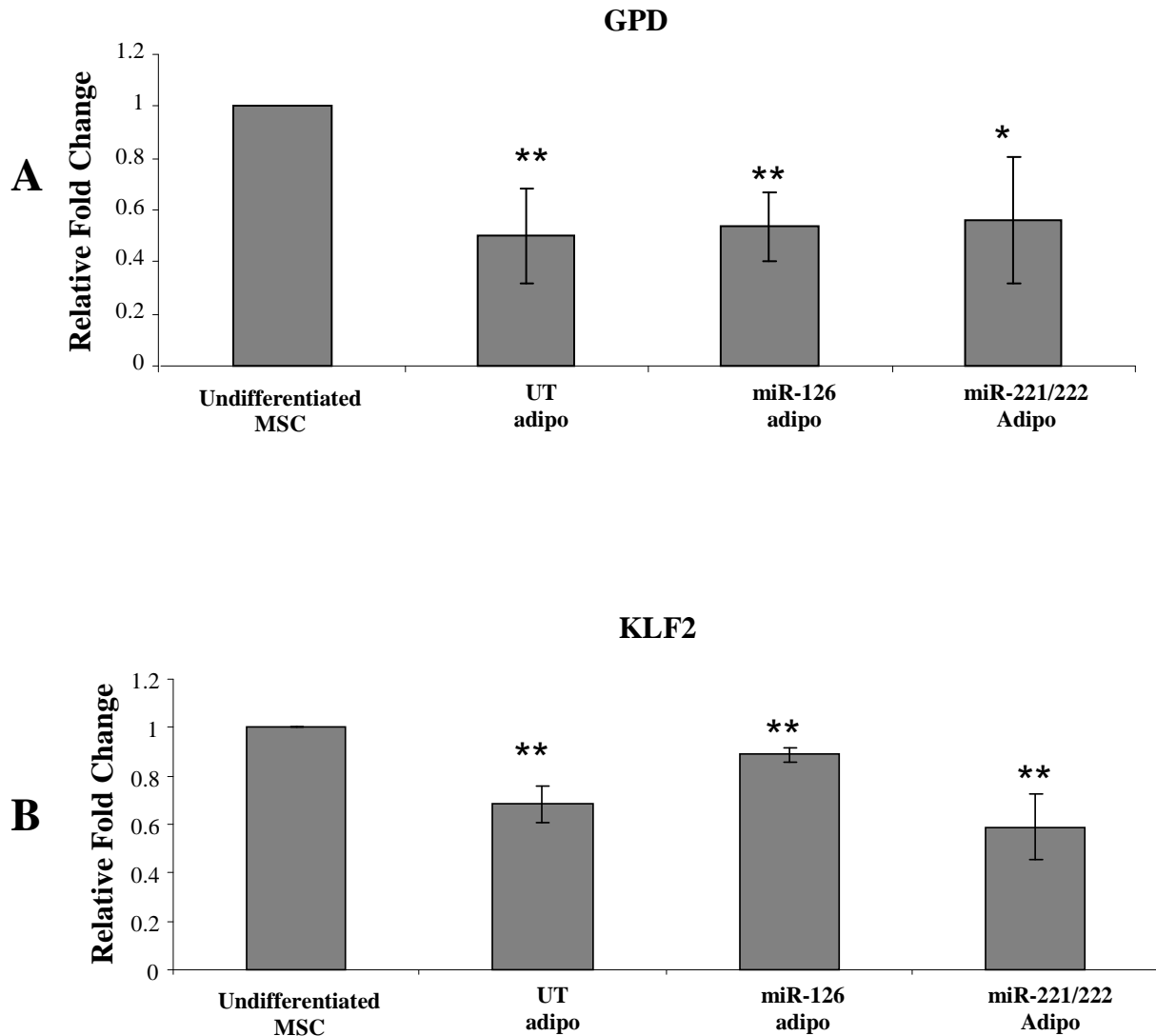


**Figure 4-29 Potential miR-221 and miR-222 targets, GPD and KLF2 show decreased expression 72 hours post induction of adipogenesis**

Expression of the potential miR-221 and miR-222 targets (A) GPD and (B) KLF2 in untransduced MSCs and MSCs overexpressing miR-221 and miR-222 compared to MSCs overexpressing miR-126 (values are presented relative to undifferentiated-matched hMSCs for each population). RT-PCR was performed using RNA isolated 72 hours after the induction of adipogenesis. Expression levels were normalized to the levels of RNA pol II transcript. Error bars represent standard deviation of the mean (n=3 donors), \*p $\leq$  0.05, \*\*P $\leq$  0.01.

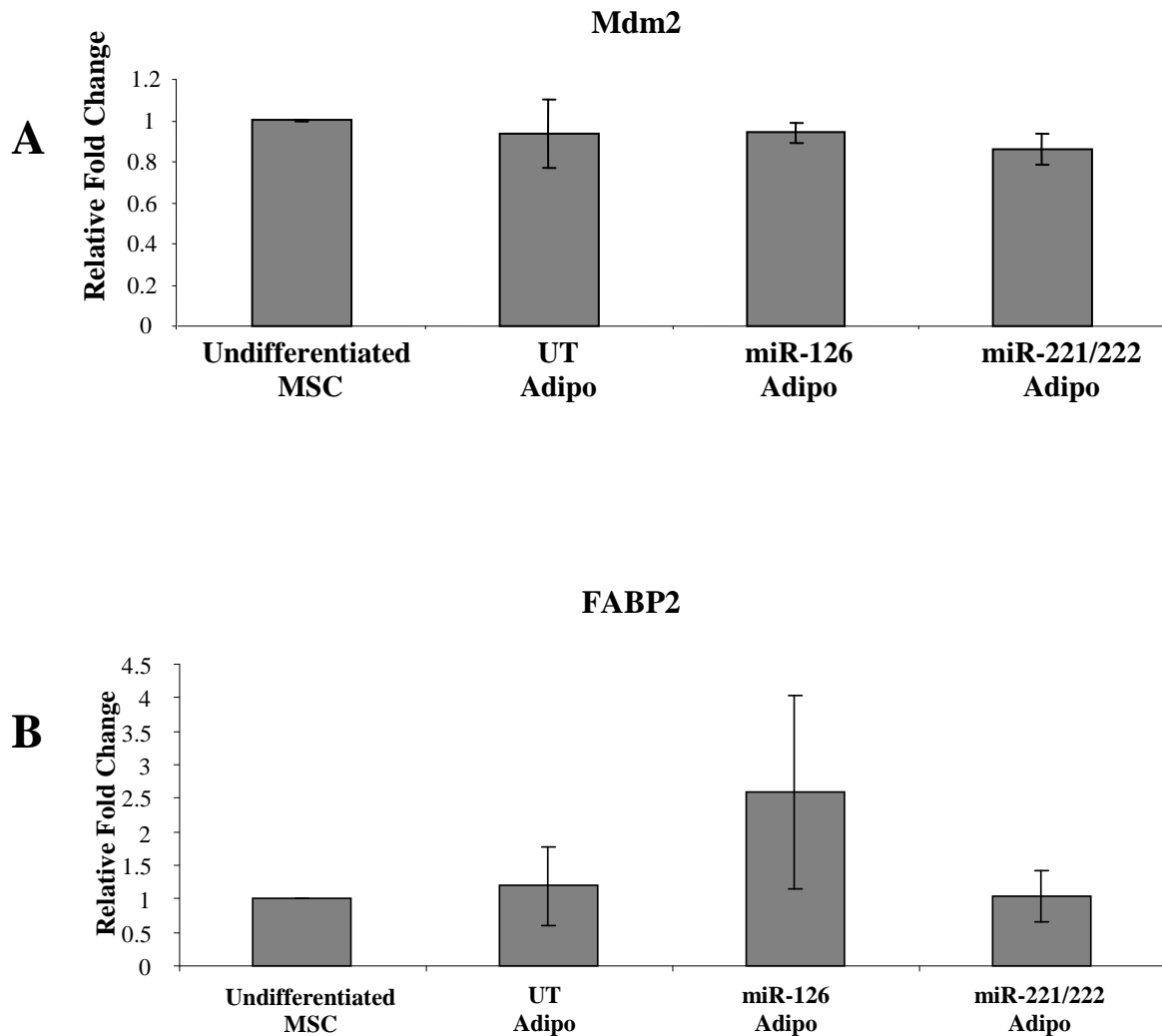


**Figure 4-30 Potential miR-221 and miR-222 targets, Mdm2 and FABP2 do not change in expression 72 hours post induction of adipogenesis**

Expression of the potential miR-221 and miR-222 targets Mdm2 and FABP2 in untransduced MSCs and MSCs overexpressing miR-221 and miR-222 compared to MSCs overexpressing miR-126 (values are presented relative to undifferentiated-matched hMSCs for each population). RT-PCR was performed using RNA isolated 72 hours after the induction of adipogenesis. Expression levels were normalized to the levels of RNA pol II transcript. Error bars represent standard deviation of the mean (n=3 donors).

Potential miR-221/222 target	Transcript Expression MSC to Adipo	Transcript expression miR-126 adipo MSCs	Transcript expression miR-221/222 adipo MSCs
<b>PGC1<math>\alpha</math></b>	Upregulated	54.49 $\pm$ 11.07	15.98 $\pm$ 12.43
<b>TLE3</b>	Upregulated	1.84 $\pm$ 0.389	0.776 $\pm$ 0.091
<b>MAP3K10</b>	Downregulated	0.54 $\pm$ 0.0844	0.55 $\pm$ 0.163
<b>OSBPL3</b>	Downregulated	0.194 $\pm$ 0.065	0.189 $\pm$ 0.026
<b>RFX7</b>	Downregulated	0.598 $\pm$ 0.059	0.803 $\pm$ 0.06
<b>GPD2</b>	Downregulated	0.536 $\pm$ 0.130	0.563 $\pm$ 0.243
<b>KLF2</b>	Downregulated	0.888 $\pm$ 0.029	0.587 $\pm$ 0.134
<b>MDM2</b>	Unchanging	0.94 $\pm$ 0.04819	0.86 $\pm$ 0.07629
<b>FABP2</b>	Unchanging	2.587 $\pm$ 1.43	1.04 $\pm$ 0.38

**Table 4-2 Expression of potential miR-221 and miR-222 targets 72 hours post induction of adipogenesis**

As previously discussed, miR-221 and miR-222 decrease in expression during adipogenesis. A potential target of these miRNAs would be expected, therefore to have an mRNA expression pattern that is either increasing or unchanging during differentiation. The mRNA expression of MAP3K10, OSBPL3, RFX7, GPD2 and KLF2 decreased 72 hours after the induction of adipogenesis. This is not a pattern consistent with a target of miR-221 and miR-222 in adipogenesis and so these candidates were ruled out from any further analysis. The mRNA expression of Mdm2 and FABP2 did not change significantly during adipogenesis. This suggests that they could be potential candidates of miR-221 and miR-222 and protein analysis would be necessary to investigate this further. The expression of TLE3 and PGC1 $\alpha$  significantly increased 72 hours after the induction of adipogenesis consistent with an expected mRNA expression pattern of miR-221 and miR-222. These candidates were therefore chosen for further examination.

#### 4.2.14.1 PGC1 $\alpha$ as a potential target of miR-221 and miR-222 in hMSC adipogenesis

PGC1 $\alpha$  was chosen for further analysis as it showed a high level of upregulation (55 fold in MSCs overexpressing miR-126) 72 hours after the induction of adipogenesis (Figure 4-27A, Table 4-2). MSCs overexpressing miR-221/222 showed a significantly reduced level of upregulation of PGC1 $\alpha$  (16-fold) (Figure 4-27A, Table 4-2). PGC1 $\alpha$  is highly expressed in brown adipose tissue and is thought to be involved in the expression of genes related to thermogenesis. The overexpression of PGC1 $\alpha$  has been shown to induce brown adipogenic differentiation of MSCs, suggesting that this factor may determine the fate of an MSC during adipose development (Huang, Chen et al. 2011). However, despite the increase in PGC1 $\alpha$  mRNA in adipogenesis compared to undifferentiated MSCs the level is still too low to be detected by western blot analysis (Figure 4-31). Mouse heart protein (a source of PGC1 $\alpha$ ) was used as positive control to check that the antibody was functional; this antibody recognises its epitope in human, mouse and zebrafish species. This confirms that PGC1 $\alpha$  is undetectable because the protein is present at low levels rather than because there are problems with the antibody or blotting condition. For this reason, PGC1 $\alpha$  as a target of miR-221 and 222 in hMSC adipogenesis was ruled out from further analysis.

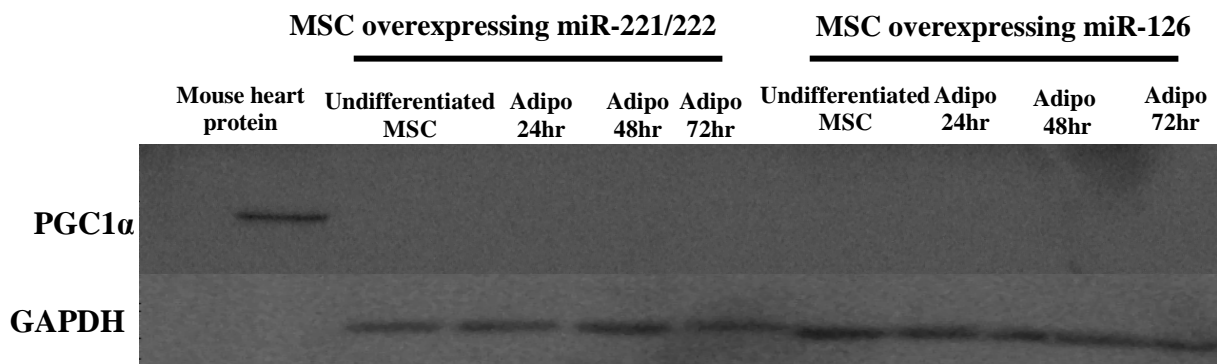


**Figure 4-31 Expression of the potential miR-221/222 target PGC1 $\alpha$  protein cannot be detected in hMSCs undergoing adipogenesis.**

Western blot analysis of PGC1 $\alpha$  in miR-222 and 222 overexpressing MSCs (30 $\mu$ g) compared to MSCs overexpressing miR-126 (30 $\mu$ g) in the first 3 days of adipogenesis. Mouse heart protein (30 $\mu$ g) was used as a positive control. GAPDH was used as a loading control.

#### **4.2.14.2 TLE3 as a potential target of miR-221 and miR-222 in hMSC adipogenesis**

As with PGC1 $\alpha$ , the mRNA expression of TLE3 is significantly upregulated in adipogenically differentiating MSCs compared to undifferentiating MSCs (1.84 fold upregulated) (Figure 4-27B). MSCs overexpressing miR-221/222 show reduced level of expression of TLE3 compared to miR-126 overexpressing MSCs 72 hours after the induction of adipogenesis (Figure 4-27B). TLE3 (Transducin-like enhancer protein 3) is a member of the groucho family of transcription factors, recently identified as been important in adipocyte biology (Villanueva, Waki et al. 2011). TLE3 acts as a coregulator of two opposing aspects of adipogenesis. It acts as a coactivator of PPAR $\gamma$ , a key regulator and activator of adipogenesis. At the same time, TLE3 acts as a corepressor for TCF, a member of the Wnt signalling pathway which acts as an inhibitor of adipogenesis.

As mentioned, an expected target of miR-221/222 would have an mRNA that is either increasing or unchanging in the first 72 hours of adipogenesis. As miR-221 and miR-222 decrease during adipogenesis, the protein expression of a predicted target would therefore be expected to increase as adipogenesis proceeds. Figure 4-32 shows that in MSCs overexpressing miR-126, TLE3 protein expression increases transiently 24 hours after the induction of adipogenesis. This upregulation is not observed in MSCs overexpressing miR-221 and 222. However, TLE3 expression rapidly decreases below pre-differentiation level at 48 and 72 hours into adipogenesis which is not consistent with TLE3 as a target of miR-221 and 222 in adipogenesis.

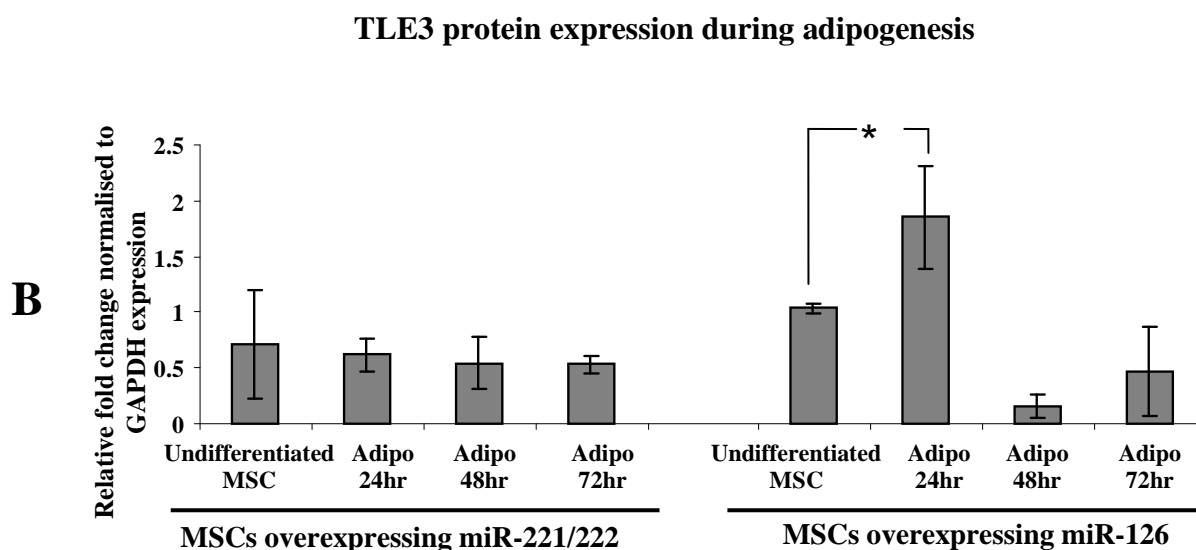
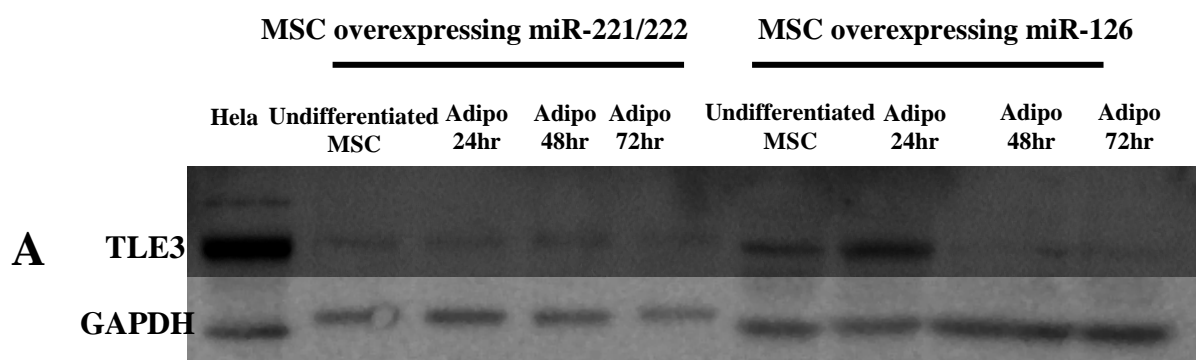


**Figure 4-32 Expression of the potential miR-221/222 target TLE3 protein in the first 72 hours of hMSC adipogenesis**

Western blot analysis of TLE3 in miR-222 and 222 overexpressing MSCs compared to MSCs overexpressing miR-126 in the first 3 days of adipogenesis (A). All samples are normalized to GAPDH expression. All samples were normalized to expression of GAPDH protein and are reported relative to expression in undifferentiated MSCs overexpressing miR-126. Densitometric analysis of TLE3 protein bands (B). Error bars represent standard deviation of the mean (n=3 donors), \*p< 0.05.

## 4.3 Discussion

### 4.3.1 Downregulation of miR-221 and miR-222 during hMSC differentiation

The results of the previous chapter showed that 20 miRNAs were regulated in MSC-derived adipocytes compared to undifferentiated MSCs. We have demonstrated that miR-221 and miR-222 were two of the most downregulated miRNAs. Both were downregulated early and for the duration of the adipogenic process, with a 50% drop in expression level of both occurring within 72 hours of inducing adipogenesis. This significant downregulation of both miRNAs at an early stage of differentiation is consistent with miR-221 and 222 playing a role in the regulation of adipogenesis rather than being a consequence of the differentiation process. The expression of miR-221 and miR-222 was also decreased during both osteogenic and chondrogenic differentiation, however a significant decrease in both miRNAs was only observed at mid (chondrogenesis) and late (osteogenesis) timepoints of the assay. The expression of miR-221 and miR-222 is also downregulated during the myogenic differentiation of primary and established myogenic cells (Cardinali, Castellani et al. 2009). Collectively, this information suggests that the loss of miR-221/222 may be important for achieving a fully differentiated phenotype in mesenchymal lineages.

It is possible that these miRNAs are part of a network keeping the cells in an undifferentiated state. As miRNAs work by repressing the translation of their target mRNAs, this downregulation on differentiation may contribute to the differentiated phenotype by enhancing the expression of differentiation specific factors to increase. It is therefore possible that through the fine-tuning of the levels of multiple proteins, miRNAs confer tighter regulation than transcription factors alone in acting as the switch regulating the decision between stemness and commitment (Stark, Brennecke et al. 2005).

Our hypothesis was that the downregulation of these miRNAs is an important step in hMSC adipogenesis; if this is true then preventing this downregulation would affect hMSC adipogenic differentiation ability.

#### **4.3.2 Overexpressing miR-221 and 222 significantly reduces hMSC adipogenesis**

The aim of these experiments was to determine the effect of overexpression of miR-221 and 222 on hMSC adipogenesis. The hMSC adipogenic program takes at least 14 days therefore a long lasting and stable form of gene delivery was required. For this reason, overexpression of miR-221 and 222 was achieved using a viral vector. Lentiviral vectors delivered a 4-fold overexpression of miR-221 and a 5.5-fold overexpression of miR-222. Of note, miRNA expression changes associated with overexpression are relatively low compared to mRNA expression changes. The level of overexpression observed in MSCs combined with the fact that miR-221 and 222 fall approximately 3 fold during differentiation correlates to an overall 12-15 fold overexpression of the miRNAs in the first 72 hours of adipogenesis. MSCs overexpressing miR-126 (a miRNA that does not change during adipogenic differentiation) were used to control for any miRNA overexpression effects. Lentiviral transduction of MSCs with miR-126 resulted in a 50-fold overexpression, ~10 times higher than the level of miR-221 and miR-222 overexpression even though both populations were transduced at a MOI 50.

MSCs overexpressing miR-221 or miR-222 had compromised adipocyte differentiation in terms of the amount of lipid accumulated compared to MSCs overexpressing miR-126. However, this result was not statistically significant when a student T-test was performed. MiR-221 and miR-222 expression are often co-regulated and they are thought to act in a coordinated and synergistic fashion (Galardi, Mercatelli et al. 2007; le Sage, Nagel et al. 2007). Due to this, we hypothesized that the combined overexpression of miR-221 and miR-222 would have a more pronounced effect on hMSC adipogenesis than overexpression of either miRNA alone. MSCs transduced with both miR-221 and miR-222 significantly differentiated to a lesser extent than MSCs overexpressing miR-126 as measured by lipid accumulation.

In 2011, Skarn *et al* reported that the expression of miR-221 and miR-222 decreases during adipogenesis of both immortalized and primary hMSCs. In agreement with the data shown here, primary hMSCs showed a significant decrease in triglyceride

accumulation when transiently transfected with a synthetic miR-222 precursor (which represents miR-221 and miR-222). Immortalized hMSC-Tert20 cells also showed a significant decrease in triglyceride accumulation when overexpression of miR-221 and 222 was achieved using an adenoviral vector (Skarn, Namlos et al. 2011).

In order to determine the stage at which miR-221 and miR-222 were acting in adipogenesis we looked at the expression of early adipogenic transcription factors, C/EBP $\alpha$  and PPAR $\gamma$ . Within 72 hours of inducing adipogenesis (chosen due to the large downregulation seen in the expression of both miRNAs at this stage), miR-221/222 overexpressing MSCs had significantly lower levels of upregulation of the adipogenic transcripts C/EBP $\alpha$ , PPAR $\gamma$  and FABP4 than miR-126 overexpressing MSCs. Note that this transcript analysis was performed on a population of cells and thus the reduced upregulation observed could potentially be due to an effect of fewer cells undergoing adipogenesis and/or less upregulation in each cell. To definitively verify this was the case, expression could be determined using single cell assays, such as single-cell PCR or immunofluorescence. This observation is again confirmed by Skarn *et al* who also show that the expression of PPAR $\gamma$  and C/EBP $\alpha$  mRNA is significantly downregulated 72hours after adipogenesis has been induced. In addition, they show that the protein levels of PPAR $\gamma$  and C/EBP $\alpha$  are significantly downregulated in miR-221/222 overexpressing MSCs at the same timepoint (Skarn, Namlos et al. 2011).

These results suggest that miR-221 and miR-222 have an effect at an early stage in adipogenic differentiation and that the downregulation of these miRNAs in the first 72 hours is a key event in the progression of hMSC adipogenesis. For example, if changes were seen in lipid accumulation but not in upregulation of transcription factors, it could be assumed that the miRNAs were directly suppressing lipid synthesis rather than modulating the differentiation process.

### 4.3.3 MiR-221 and miR-222 as safeguards of 'stemness' in hMSCs

The expression of miR-221 and 222 is significantly downregulated in osteogenesis and chondrogenesis, as well as adipogenesis. The downregulation of these miRNAs across all three lineages of MSC differentiation suggests a potential role for miR-221 and 222 in maintaining the 'stemness' of the MSC. This is supported by the observed effect on lipid accumulation upon overexpression of the miRNAs. In a similar manner, Cardinali *et al* demonstrate that overexpressing these miRNAs resulted in a delay in withdrawal from the cell cycle and inhibition of sarcomeric protein accumulation (Cardinali, Castellani et al. 2009). A role for miR-221 has been demonstrated in the chondrogenic differentiation of chick limb mesenchymal stem cells through the negative regulation of its target *mdm2* (Kim, Song et al. 2010).

These results are paralleled by the described role for miR-221 and miR-222 in skeletal muscle differentiation (Karbiener, Fischer et al. 2009). Both miRNAs are downregulated during myogenic cell differentiation and the forced co-expression of miR-221 and 222 in myoblasts reduced the expression of muscle specific proteins and showed defects in sarcomere assembly. Similar to the downregulation observed during adipogenesis, both miRNAs are also downregulated during differentiation of myogenic cells suggesting that the downregulation of these miRNAs may be an important event for differentiation to progress.

However, in contrast to adipogenesis the overexpression of miR-221 and 222 had no demonstrable effect on osteogenic differentiation. Significant downregulation of miR-221 and 222 occurs relatively late during osteogenic differentiation. Where both miRNAs are significantly downregulated 72 hours after induction of adipogenesis, a significant downregulation of both is not observed in osteogenesis until day 14 of the assay. This could suggest that these miRNAs do not play a functional role in the acquisition of the osteogenic phenotype but that the change is more likely a consequence of the differentiation. This result, in contrast to the others is not in keeping with a role for miR-221 and 222 in maintaining the 'stemness' of the MSC.

#### **4.3.4 Cell number is significantly reduced in hMSCs with reduced activity of miR-221 and miR-222**

The overexpression of miR-221 and miR-222 resulted in a significant decrease in hMSC adipogenesis. This is presumably due to a decrease in a target protein(s) of miR-221 and 222. Conversely, it could be postulated that knocking down the expression of these miRNAs would cause an increase in this/these key protein(s). If the level of this protein is limiting adipogenesis, then increasing the level of the protein could potentially cause an increase in the level of adipogenesis. One strategy to investigate the effects of reduced miR-221 and miR-222 on the progression of hMSC adipogenesis is to deliver a shRNA that specifically binds to either miRNA and thus reduces their activity. As with the overexpression study, it was necessary to deliver this vector for the duration of the hMSC adipogenic program, which takes at least 14 days. Therefore, attempts to achieve inhibition of miR-221 or miR-222 were performed using lentiviral mediated delivery of short hairpin RNAs (shRNAs) against miR-221 and miR-222.

The manufacturers suggest that lentiviral transduction of the shRNAs against miR-221 and miR-222 would not necessarily result in a significant difference in miRNAs level. However, expression analysis revealed that the level of these two miRNAs is in fact significantly reduced in MSCs transduced with sh-221 and/or sh-222 compared to transduction with a shRNA containing a scramble sequence.

Transduction of a population of MSCs with either sh-221, sh-222 or both sh-221 and sh-222 resulted in significant (70%) reduction in cell number 96 hours post transduction compared with MSCs transduced with a vector containing a scramble shRNA, and 40% less cells than were originally plated. It is well established that these miRNAs regulate the cell cycle through the negative regulation of the cell cycle inhibitors p27 and p57 in cancer models (Fornari, Gramantieri et al. 2008; Medina, Zaidi et al. 2008; Frenquelli, Muzio et al. 2010). Transduction with a shRNAs against miR-221 or miR-222 resulted in a significant increase in p27 transcript and presumably p27 protein expression (which could not be measured here as there were too few cells remaining for western blot analysis). As p27 plays an important role in the regulation of the cell cycle, it is possible that the effect observed is at least, in part due to an increase in the expression of p27 protein,

causing the cells to exit the cell cycle. However, it seems unlikely that the loss of cells is solely due to an increase in p27 mRNA or protein expression. The knockdown of miR-221/222 in human glioma cells significantly increased cell apoptosis by directly upregulating the pro-apoptotic protein PUMA (P53 upregulated modulator of adipogenesis) compared to cells treated with a scramble oligonucleotide. The pro-apoptotic factors bax and caspase 3/7 were also upregulated upon knockdown of the miRNAs in these cells (Zhang, Zhang et al. 2010).

These studies provide a possible explanation for the effect of inhibition of miR-221 and 222 activity on hMSC behaviour. It is appreciated that these studies have been performed in cancer models and so caution must be observed when interpreting our results performed on primary hMSCs. Potentially, however the reduction in cell number observed could be due to cell death, which could be triggered in hMSCs with reduced miR-221 and 222 activity. Based on previous studies, this could be due to upregulation of p27 in combination with upregulation of components of the apoptotic pathway.

#### **4.3.5 What is the target(s) of miR-221 and miR-222 in hMSC adipogenesis?**

The overexpression of miR-221 and 222 significantly reduces adipogenesis compared to control populations. We have shown that the adipogenesis related transcripts C/EBP $\alpha$ , PPAR $\gamma$  and FABP4 are reduced in adipogenesis upon overexpression of the miRNAs. The 3' UTRs of these transcripts do not contain predicted binding sites for miR-221 or miR-222 and so it is suspected that the target regulated by these miRNAs is acting upstream of these factors. To identify the pathway through which this effect is being mediated, it is necessary to identify the key target (s) of miR-221/222 in adipogenesis.

Many studies have demonstrated that the cyclin-dependent kinase inhibitors, p27 and p57 are direct targets of miR-221 and miR-222 (Galardi, Mercatelli et al. 2007; Fornari, Gramantieri et al. 2008; Medina, Zaidi et al. 2008). Therefore p27 and p57 protein and transcript levels were analyzed to determine whether their expression was consistent with that expected for targets of miR-221 or miR-222 during the first 3 days of adipogenesis. As both miRNAs decrease during this time, it would be

expected that a predicted target would either show an increase in mRNA expression or remain unchanging. Both p27 and p57 show a drop in mRNA expression 24 hours after induction but rise as adipogenesis progresses consistent with regulation by miR-221 and miR-222.

However, western blot analysis showed that the expression of p57 protein does not change significantly as adipogenesis progresses. It would be expected that the protein expression of a miR-221 and miR-222 target would increase during differentiation. These results suggested that p57 is not the relevant target for miR-221/222 during adipogenesis despite being a proven target in other systems. P57 mRNA expression significantly increases as adipogenesis proceeds while expression of p57 protein does not change significantly which suggests a potential miRNA mediated regulation by an upregulated miRNA or other post transcriptional regulation during adipogenesis. As a consequence, p57 was not pursued as a potential target.

#### **4.3.6 P27 as a potential target for miR-221 and miR-222 in Adipogenesis**

There is evidence to support a role for p27 in hMSC adipogenesis. Previous work has shown that p27 protein levels increase as adipogenesis proceeds in hMSCs and that the siRNA knockdown of p27 in hMSCs resulted in reduced lipid accumulation, as measured by Oil Red O extraction (Kang, Choi et al. 2008). Much of what is known of the mechanism of adipogenesis is derived from studies using a murine 3T3L1 cell line. These cells undergo a round of clonal expansion upon induction of adipogenesis, an event which is not seen in human MSC adipogenesis (Janderova, McNeil et al. 2003; Qian, Li et al. 2010). 3T3L1 studies have shown p27 decreases at the initiation of mitotic clonal expansion but accumulates at the termination of the expansion step. In contrast to the hMSC study, the overexpression of p27 in 3T3L1s reduces adipogenesis (Okada, Sakai et al. 2009). A recently published report showed that p27 knockout mice developed obesity due to adipocyte hyperplasia. It is possible this was as a result of increased proliferation of preadipocytes and their subsequent differentiation to mature adipocytes (Naaz, Holsberger et al. 2004). These reports suggest a key, albeit different role for the cyclin dependent kinase inhibitor p27 in both murine and human adipogenesis.

The increased level of p27 protein measured during hMSC adipogenesis could be consistent with it being a target of miR-221 and/or miR-222. We hypothesised that the overexpression of miR-221 and miR-222 reduced adipogenesis by decreasing the expression of p27. PCR analysis revealed that the overexpression of miR-221 and miR-222 did not cause a reduction in the upregulation of p27 transcript, a result that was also seen in the study by Skarn *et al* (Skarn, Namlos et al. 2011). In a pattern typical of miRNA-mediated regulation, the overexpression of miR-221 and 222 significantly reduced the upregulation of p27 protein 72 hours after the induction of adipogenesis, which was again seen by the Skarn group (Skarn, Namlos et al. 2011).

#### **4.3.7 Luciferase reporter assays as a method of verifying an interaction between a miRNA and its target**

One of the major challenges facing miRNA research is identifying with confidence the target of a specific miRNA. While monitoring the mRNA and protein level of a predicted target is a good starting point, it is difficult to determine whether alterations in target levels occur because of a direct interaction with miRNA or via a secondary i.e. an indirect effect. This is evident here where significant decreases in mRNA levels are observed for PPAR $\gamma$ , C/EBP $\alpha$  and FABP4 upon overexpression of miR-221 and 222, even though these transcripts do not contain putative binding sites for either miRNA in their 3' UTRs. This is also evident at the protein level where a reduction in expression of PPAR $\gamma$  and C/EBP $\alpha$  occurs as a result of overexpression of miR-221 and 222 (Skarn, Namlos et al. 2011).

The standard method currently used to determine an interaction between a miRNA and its target are luciferase reporter assays delivered to a suitable cell. Such a cell would be one that is easy to transfect and has relatively low levels of the miRNA of interest. A luciferase reporter can be constructed by cloning the 3' UTR of the target gene downstream of a luciferase reporter. This reporter can then be delivered to the cell, then the luciferase activity can be measured and analysed in the presence and absence of the miRNA(s) of interest. Constructs with a mutated miRNA target site can also be used to demonstrate a direct miRNA effect where loss of regulation is observed. These assays can be used as a starting point to identify a direct

miRNA:target interaction but it is appreciated that these constructs do not demonstrate binding of the endogenous miRNA to the target. Experiments to directly modulate the target should also be performed to verify a direct miRNA:target interaction. This will be discussed further in section 4.3.8.

In order to determine whether there is a direct interaction between the miR-221 and/or miR-222 and their target, a luciferase reporter containing the 3' UTR of p27 cloned after the luciferase stop codon was used (Luc-p27). This reporter construct had previously been used to demonstrate a direct interaction between miR-221, miR-222 and the p27 3' UTR in human T98G glioblastoma cells (Medina, Zaidi et al. 2008). 293T cells that were transfected with Luc-p27 showed a significant drop in luciferase activity upon transfection with miR-221 and/or miR-222 compared to the Luc-Empty luciferase activity. 293T cells transfected with Luc-p27 show no reduction in luciferase activity upon transfection with miR-126, verifying that this was a direct interaction between miR-221, miR-222 and p27.

A luciferase construct containing the 3' UTR was also used in combination with a shRNA lentiviral vector against miR-221 or miR-222 (sh-221 or sh-222). If p27 is a target of miR-221 or 222, it would be expected that there would be an increase in luciferase activity upon transfection with Luc-p27 and sh-221 or sh-222. In keeping with this expectation, a significant increase in luciferase activity was observed in 293T cells with reduced activity of miR-221 and/or 222. In addition, p27 mRNA expression was significantly increased in MSCs transduced with sh-221 and/or sh-222 compared to MSCs transduced with a shRNA containing a scramble sequence.

These results, in combination with evidence in the literature (Gillies and Lorimer 2007; le Sage, Nagel et al. 2007; Fornari, Gramantieri et al. 2008) suggest that p27 is a direct target of miR-221 and miR-222.

#### **4.3.8 Overexpression of p27 has no significant effect on levels of hMSC adipogenesis**

The evidence provided thus far, suggests that the miRNAs 221 and 222 have an important role in the normal functioning of a hMSC. This is suggested by a number

of key observations. Firstly, the expression of these two miRNAs drops significantly as hMSCs lose their 'stemness' and commit to either the adipogenic, osteogenic or chondrogenic lineages. The inhibition of miR-221 and miR-222 leads to a loss in cell number due to halt in proliferation and/or cell death. The overexpression of both miRNAs causes a reduction in lipid accumulation during adipogenesis and causes a decrease in upregulation in the expression of a number of key adipogenic transcripts within 72 hours. This suggests that both miRNAs could play a role in adipogenesis.

It would be desirable to identify the target mRNA for miR-221 and 222 which mediates this effect on adipogenesis. However, it is probable that these miRNAs target many mRNAs and that the observed effects may not be due to a single miRNA target. As an example, the Sylamer algorithm identified 500 genes enriched in miR-155 binding sites in T-helper cells isolated from a mouse knockout model of miR-155 (van Dongen, Abreu-Goodger et al. 2008).

Currently, the best characterised target of miR-221 and 222 is p27. There are reported roles for p27 in human adipogenic differentiation. P27 protein undergoes changes in level consistent with it being a target of miR-221 and 222 in adipogenesis i.e. its expression increases as miR-221 and 222 decrease. Independently of adipogenesis we have also shown that p27 transcript levels increase in undifferentiating MSCs when miR-221 and 222 activity is inhibited using shRNAs. As the overexpression of miR-221 and 222 caused a significant reduction in p27 protein expression in adipogenesis, potentially minimising or preventing this reduction in protein could rescue the reduction in lipid accumulation if p27 is the mediator of the miRNA effect.

To overexpress p27, a lentiviral vector was constructed and delivered to MSCs. Transduction with this vector resulted in a significant increase in p27 protein compared to cells transduced with a control GFP vector. P27 plays an important role in the cell cycle and its overexpression results in a halting of the cell cycle. As expected, delivery of the p27 vector resulted in a reduction in cell number in both 293T cells and hMSCs. This result is in keeping with previous results showing that

overexpression of p27 causes cell cycle arrest in fibroblasts (Rivard, L'Allemain et al. 1996)

It was the aim of this experiment to investigate the possibility that the reduction in lipid accumulation observed in miR-221 and 222 overexpressing MSCs was due to a reduction in p27 protein. From our data, it is apparent that if the p27 construct was delivered to proliferating MSCs, they would exit the cell cycle and thus stop proliferating. It would be expected that the cells would not reach the required level of confluence necessary to induce adipogenic differentiation. Therefore, the p27 overexpression vector was delivered to cells once they had reached confluence and were ready for the induction of adipogenesis.

The 3-fold overexpression of p27 achieved using this vector did not significantly affect the level of lipid accumulation in untransduced MSCs or miR-126 overexpressing MSCs compared to the same MSC populations transduced with a control GFP lentivirus. The 'add-back' of p27 protein did not rescue the reduction in lipid accumulation observed in MSCs overexpressing miR-221 and 222. This could suggest that p27 is not a key factor/sole factor altered by miR-221 and miR-222 in the progression of hMSC adipogenesis, as expected.

The result observed could be due to the technical details of the experiment. A 1.75-fold drop in p27 protein expression was observed in MSCs overexpressing miR-221 and 222 compared to MSCs overexpressing miR-126. It is possible, that the levels of p27 overexpression (3 fold increase compared to GFP transduced miR-221/222 overexpressing MSCs) were not sufficiently high enough to observe a functional effect on the progression of adipogenesis. A significant reduction in cell number was observed when the p27 overexpression vector was delivered to proliferating cells indicating that the overexpressed protein was functional. The level of overexpression makes it seem unlikely that the lack of a significant rescue effect was due an inadequate level of overexpression. Alternatively, it is possible that the level of overexpression of p27 was too high and future experiments could be performed to

vary the level of overexpression achieved e.g transducing MSCs at varying MOIs (this runs the risk of reducing overall expression in the population by virtue of not transducing all of the cells) or creating a new vector using a different promoter which delivers a lower level of expression of the transgene.

The timing of delivery of the p27 overexpression vector could also account in part for the lack of rescue observed. P27 was overexpressed using a lentiviral vector capable of transducing dividing and non-dividing cells. It was decided to transduce the MSCs at confluence as an earlier transduction could halt the cell cycle which would prevent proper induction of adipogenesis. The cells were left for 3 days before adipogenesis was induced. It is possible that transduction at an earlier or later timepoint may have a more functional effect.

This result also suggests that although p27 is a target for miR-221 and miR-222, it is not the sole target through which these miRNAs are modulating adipogenesis, despite the evidence suggesting this as a possibility. How miRNAs modulate their targets is still largely unknown. The available evidence, however suggests that it is an intrinsic and complicated web where one miRNA can have several thousand potential targets and in addition each mRNA can in return be modulated by a number of miRNAs. For this reason, it is unsurprising that the modulation of one potential target, in this case p27 did not rescue the effect of modulation of miR-221 and 222. Possibly, to rescue the effect observed, a number of other miR-221/222 targets would also have to be modulated. Indeed, few studies have shown rescue by reintroducing a target of the miRNAs under investigation. Some (Medina, Zaidi et al. 2008; Cardinali, Castellani et al. 2009; Skarn, Namlos et al. 2011) report miRNA:mRNA interactions based on a correlation between a miRNA and its target mRNA/protein expression without further manipulation of the target.

#### **4.3.9 Prediction of other miR-221 and miR-222 targets in adipogenesis**

One of the biggest hurdles in the field of miRNA research is the identification of the mRNA(s) targeted by the miRNA under investigation. Numerous miRNA

prediction algorithms have been developed such as PicTar (Krek, Grun et al. 2005), MiRanda (Enright, John et al. 2003) and TargetScan (Lewis, Shih et al. 2003). Most of these algorithms are centered on the same principle; i.e. a sequence present in the 3' UTR in a target that is complementary to the 'seed sequence' of the miRNA. Other factors incorporated into these algorithms include the level of conservation across species and the extent of base pairing between the miRNA and the mRNA, with each algorithm having different criteria of importance and relevance. As a result, lists containing thousands of potential targets can be generated for each miRNA. In this case, a search of MiRanda returned 5,670 targets for miR-221 and 5,434 targets for miR-222 leading to difficulties in choosing potential targets for further investigation. Having ruled out confirmed targets of miR-221/222 based on evidence in the literature, a new shortlist of targets was generated using the Sylamer algorithm (van Dongen, Abreu-Goodger et al. 2008). Sylamer uses a gene list generated from microarray data to detect significant enrichment or depletion of miRNA seed sequences. In this case, the program was applied to the list generated by comparing undifferentiated and adipogenically differentiated MSCs at day 20 of adipogenesis. This did not report any significant enrichment or depletion of miRNA seed sequences in this comparison, but it was used to identify targets expressed by either population of cells which contained putative miR-221 and miR-222 binding sites. Transcripts which were upregulated or did not change were selected for further evaluation. The list of selected transcripts consisted of FABP2, MAP3K2, OSBPL3, RFX7, GPD and KLF2. A search of the literature revealed three additional candidates, PGC1 $\alpha$ , MDM2 and TLE3 which chosen for further examination based on their potential roles in hMSC behaviour.

As previously stated, an expected target of miR-221/222 would show an increase in protein expression as adipogenesis progresses. The candidate transcript level would be unchanging or would increase. Candidates that decrease in expression would be considered unlikely targets of miR-221 and miR-222 during adipogenic differentiation.

Analysis of mRNA expression of potential candidates eliminated OSBPL3, RFX7, GPD, and KLF2 from further experimentation as their expression decreased during adipogenesis. PGC1 $\alpha$ , TLE3 and FABP2 remained as potential targets as they increased in expression as adipogenesis progressed. The expression of Mdm2 did not change significantly during adipogenesis and so depending on the expression of Mdm2 protein it could be a potential of miR-221/222. Based on evidence in the literature and the significant increase in expression of their mRNA, PGC1 $\alpha$  and TLE3 were selected for further examination.

#### **4.3.10 PGC1 $\alpha$ as a potential target for miR-221/222 in hMSC adipogenesis**

As discussed in section 1.3.3, the adipose tissue organ consists of two types of adipose tissue, white adipose tissue (WAT) and brown adipose tissue (BAT). This section discusses the potential therapeutic benefits of converting WAT to BAT to treat obesity. There is evidence to suggest that PGC1 $\alpha$  could be a potential therapeutic agent in the conversion of MSCs to a brown adipocyte phenotype. Indeed, experiments have shown that the overexpression of PGC1 $\alpha$  in MSCs significantly increased markers of brown adipogenesis and mitochondrial activity (Huang, Chen et al. 2011). Interestingly, the overexpression of PGC1 $\alpha$  inhibited the ability of MSCs to differentiate to white adipocytes. This group suggest therefore that PGC1 $\alpha$  may play a key role in determining the fate of an MSC during adipose development. Given that PGC1 $\alpha$  is a predicted target of miR-221 and 222, it could be postulated that both miRNAs also play a role in this determination step.

The significant increase in mRNA expression (55 fold upregulation) of PGC1 $\alpha$  in the first 72 hours of adipogenesis concomitant with the decrease in miR-221 and 222 suggested that its expression could be modulated by these miRNAs. In addition, MSCs overexpressing miR-221 and 222 showed a significant reduction in the upregulation of PGC1 $\alpha$  mRNA compared to MSCs overexpressing a control miRNA at this timepoint. Unfortunately, efforts to examine the expression of PGC1 $\alpha$  protein were unsuccessful as it was too low to be detected in undifferentiated MSCs and MSCs in the first 72 hours of adipogenesis. This is in keeping with others in the

literature who also state that it cannot be detected in WAT (Puigserver, Wu et al. 1998; Liang and Ward 2006)

#### **4.3.11 TLE3 as a potential target for miR-221/222 in hMSC adipogenesis**

TLE3 is a newly identified factor with a role in adipogenesis, suggested to act as both a coactivator of PPAR $\gamma$  and a corepressor of TCF (a member of the Wnt signalling pathway)(Villanueva, Waki et al. 2011). So far, the only report for TLE3 in adipogenesis demonstrated a role for this protein in the murine pre-adipocyte 3T3L-1 cell line. In this model, both the TLE3 mRNA and protein expression increase as adipogenesis progresses. As previously discussed, the pathways of adipogenic differentiation vary in results from studies performed on the human and murine models, discussed in section 1.4.2. The bioinformatic prediction algorithm miRanda identified TLE3 as a target of miR-221 and miR-222 and analysis of its mRNA expression and protein expression pattern in the first 72 hours of hMSC adipogenesis was performed.

The significant upregulation of TLE3 mRNA in hMSCs 72 hours after the induction of adipogenesis was consistent with a potential target of miR-221 and miR-222. This was also consistent with the upregulation of TLE3 mRNA expression in the adipogenic differentiation of 3T3L-1 cells. In combination with this, the level of upregulation of TLE3 mRNA was significantly reduced in MSCs overexpressing miR-221 and 222 compared to the control population, again suggesting its expression could be modulated by these miRNAs. TLE3 protein expression increased significantly 24 hours after the induction of adipogenesis but then rapidly dropped to levels below pre-differentiation after 48 hours of adipogenesis. The overexpression of miR-221 and 222 prevents the increase in TLE3 protein expression 24 hours after the induction of adipogenesis which potentially is a key factor in the differentiation process. Unfortunately, the rapid decrease of TLE3 protein after 48 hours is not a protein expression pattern consistent with modulation by miR-221 and miR-222 in adipogenesis.

In conclusion, it seems unlikely that TLE3 is the sole target through which miR-221 and 222 are modulating adipogenesis. Although there is an increase in expression of TLE3 protein 24 hours after the induction of adipogenesis (in keeping with the drop in miR-221 and miR-222 expression), the quick and significant drop at 48 hours would suggest that its expression is not being modulated by these miRNAs. TLE3 mRNA expression is significantly upregulated 72 hours after the induction of adipogenesis while its protein expression is significantly downregulated suggesting that TLE3 may be under the control of a different miRNA or a different form of post-transcriptional regulation.

#### **4.3.12 Concluding remarks**

We have provided evidence to suggest that the downregulation of miR-221 and miR-222 is an important event in hMSC adipogenesis. MSCs overexpressing both miRNAs displayed reduced adipogenesis as evident by reduced lipid accumulation and reduced upregulation of key adipogenic transcripts. Bioinformatic algorithms predict that the CKI p27 is a target of miR-221 and miR-222. We have shown there is an increase in p27 protein 72 hours after the induction of adipogenesis. Overexpression of miR-221 and miR-222 reduced p27 protein expression at this timepoint in MSCs undergoing adipogenic differentiation. Many results described in this thesis pointed to the cyclin dependent kinase inhibitor, p27 as a target through which these miRNAs are acting. However, the 'add-back' of p27 did not rescue the reduction in lipid accumulation observed upon overexpression of miR-221 and 222.

Additional attempts to predict the target through which miR-221 and 222 are acting did not result in the identification of one key factor responsible for the observed effect on hMSC adipogenesis. Indeed, based on the large number of predicted targets for both miRNAs, it is probable that miR-221 and miR-222 modulate a number of targets during adipogenic differentiation. Future experiments involving other methods of miRNA target identification, which are discussed in section 1.5.7 i.e. immunoprecipitation of components of the RISC complex or use of biotinylated synthetic miRNAs could be used to generate a new list of candidate targets of these miRNAs. Large scale functional assays involving the modulation of a number of targets of miR-221 and miR-222 could then be performed to attempt to rescue the observed reduction in lipid accumulation. From here, it may be possible to identify with confidence the target (s) through which miR-221 and miR-222 are modulating hMSC adipogenesis.

## **5 Discussion**

## **5.1 MiRNAs In The Regulation Of hMSC Adipogenesis**

A better understanding of the molecular mechanism of adipogenesis is necessary to aid in the struggle against obesity. MSCs have been identified as an appropriate model system in which to study the factors involved in the differentiation of an uncommitted adult stem cell to an adipocyte. A better understanding of the roles miRNAs play in this commitment step could provide information on the regulation of adipogenesis.

The aim of the work described here was to determine whether miRNAs play a role in the adipogenic differentiation of hMSCs. The initial experimental approach was to identify miRNAs which had significant changes in expression level between undifferentiated MSCs and MSCs at an early stage of adipogenic differentiation.

## **5.2 Identifying miRNAs regulated during hMSC Adipogenesis**

### **5.2.1 MiRNA expression at day 5 of adipogenesis**

As MSCs can be used to investigate the point at which commitment to the adipogenic lineage occurs, efforts were first placed to identify significantly regulated miRNAs at the early stages of adipogenic differentiation. Day 5 of adipogenesis was therefore chosen as the timepoint for microarray analysis in an attempt to capture the miRNAs important in the commitment step of differentiation. By this stage of adipogenesis, MSCs have taken on the characteristic 'rounded-up' morphology of a cell becoming an adipocyte with the first signs of lipid accumulation appearing in the cell. Therefore, the initial analysis of miRNA expression was performed by comparing undifferentiated MSCs with MSCs after 5 days of adipogenic differentiation.

Given the reports on the roles of miRNAs in differentiation, it was most unexpected when no miRNAs underwent reproducible alterations in expression levels 5 days after adipogenesis had been induced. This could be explained by a number of potential reasons. (1) It is possible that there is no significant regulation of miRNAs at this stage of adipogenesis. (2) It is also probable that the miRNA changes occurring during differentiation may be of relatively low magnitude (e.g.

from 3-10-fold change) compared to changes in mRNA (such as FABP4 which shows a ~6000-fold increase 72 hours after adipogenesis has been induced). As a consequence, subtle miRNA changes during adipogenesis may be masked by the undifferentiating cells in the population.

A further complicating factor is the variation from donor to donor in the proportions of cells which differentiate. In an attempt to maximise the accuracy of the results achieved, microarray identification of a significantly regulated miRNA in adipogenesis was performed on MSCs isolated from 5 donors. Our data presented here (Figure 3-5 and 3-6) has shown that the level of adipogenesis which occurs in a population of MSCs can vary significantly from donor to donor. Potentially the differences in adipogenic differentiation ability between donors contribute to the inability to identify a significant miRNA(s).

It is now widely accepted in the field that the population of cells derived from the bone marrow is not a 'pure' population of MSCs. In fact, there is much debate over the identity of the 'true' MSC (if it exists?) (Bianco, Riminucci et al. 2001; Bianco, Robey et al. 2008; Jones and McGonagle 2008). MSCs are currently identified based on their functionality (their ability to differentiate to adipocytes, osteocytes and chondrocytes) and a combination of positive and negative expression of cell surface markers. Therefore, the population of cells referred to as 'MSCs' could potentially include cells such as undifferentiated stem cells, progenitor cells and tissue specific cells. This suggests that the criteria currently set for the identification of MSCs may not be stringent enough and highlights the need for the identification for a more specific MSC marker. In addition, there is evidence to suggest that such a marker will never be identified, due to the fact that the 'phenotypic fingerprint' of an MSC appears to change depending on its microenvironment making the identification of one marker even more difficult (Bianco, Riminucci et al. 2001).

Secondly, numerous studies performed on clonal MSC populations have revealed that the MSC can be functionally heterogenous in terms of differentiation and self-renewal potential (Pittenger, Mackay et al. 1999; Muraglia, Cancedda et al. 2000). In studies performed on clones derived from single cells, 100% of the population

still did not differentiate. Given that the number of MSCs isolated from each preparation is likely to vary from donor to donor combined with the varying heterogeneity of each cell, it is unsurprising that such variation in levels of differentiation is observed.

### **5.2.2 MiRNA expression at Day 20 of Adipogenesis**

Microarray analysis was repeated at a later stage in the assay using a pure population of differentiated adipocytes isolated using the 'Ceiling Culture' method. This sorting step eliminated the issue of heterogeneity of adipogenic differentiation encountered in the day 5 miRNA analysis. Of the 454 miRNAs analysed, 20 miRNAs were found to be significantly regulated (>1.5 fold between undifferentiated and adipogenically differentiated) at day 20 of adipogenesis.

Since these experiments have commenced, other studies have identified miRNAs of significance in adipogenic differentiation of 3T3L1s, human pre-adipocytes, human adipose derived stem cells (hMADS) and immortalized bone marrow derived hMSCs (Esau, Kang et al. 2004; Wang, Li et al. 2008; Karbiener, Fischer et al. 2009; Skarn, Namlos et al. 2011). In addition, similar studies have been performed to identify significantly changing miRNAs in MSCs undergoing adipogenic differentiation (Oskowitz, Lu et al. 2008; Bork, Horn et al. 2010). Given that these studies were all based on the adipogenic differentiation of hMSCs, there is surprisingly little overlap between the miRNAs identified from all three studies. In fact, there was no overlap in miRNAs identified between the Bork study and the Oskowitz study. Only three miRNAs (miR-125b, miR-199a and miR-103) appear on the list generated by our analysis and the list generated by the Oskowitz group. Five of the miRNAs identified by the Bork group overlap with those regulated in our study (hsa-miR-199a, hsa-miR-199b, hsa-miR-99a, hsa-miR-221 and hsa-miR-222). The discrepancies in results across these three arrays highlight the variability in results obtained from microarray studies. This indicates that the results from microarray studies needs to be verified by additional methods such as RT-PCR and that care needs to be taken when drawing conclusions from studies such as these.

### **5.3 MiR-221 and miR-222**

Having identified miRNAs which undergo significant changes in level during adipogenic differentiation, the next step was to determine whether any of these miRNA(s) exerted an effect on the progression of adipogenesis.

Microarray analysis identified that miR-221 and miR-222 are significantly downregulated (3 fold) in adipogenically differentiated MSCs compared to undifferentiated MSCs. Previous to this, roles for these miRNAs were described in muscle differentiation (Cardinali, Castellani et al. 2009), neuronal differentiation (Terasawa, Ichimura et al. 2009), cell cycle progression (Medina, Zaidi et al. 2008) as well as a recently described role for miR-221 in the regulation of high glucose induced endothelial dysfunction (Li, Song et al. 2009). MiR-221 and miR-222 are upregulated in glioblastoma (Gillies and Lorimer 2007), thyroid papillary carcinomas (Visone, Russo et al. 2007) and chronic lymphocytic leukemia (Frenquelli, Muzio et al. 2010). Conversely, miR-221 and miR-222 are downregulated in primary prostate cancer (Ambs, Prueitt et al. 2008; Tong, Fulgham et al. 2009) and acute myeloid leukemia (Felli, Fontana et al. 2005). In 2011, a role was described for miR-221 and miR-222 in the adipogenic differentiation of human bone marrow derived MSCs (Skarn, Namlos et al. 2011).

#### **5.3.1 MiRNA-221 and miRNA-222 in hMSC Differentiation**

We have shown that miR-221 and miR-222 are downregulated as MSCs undergo differentiation to adipocytes. This downregulation occurs in the first three days of adipogenic differentiation. These miRNAs are also downregulated during MSC differentiation to osteocytes and chondrocytes. These data suggest that the downregulation of both miRNAs could be an important event for MSC differentiation and hints possibly that miR-221 and miR-222 could play a role in maintaining the 'stemness' of the MSC. The finding that miR-221 and miR-222 are downregulated during myogenic differentiation of primary and myogenic cell lines is also consistent with this possibility (Cardinali, Castellani et al. 2009).

To establish if a functional role exists for miR-221 and miR-222 in adipogenesis, lentiviral vectors were used to create populations of MSCs overexpressing miR-126, miR-221 or miR-222. While overexpression of either miR-221 or miR-222 appeared to reduce adipogenesis compared to MSCs overexpressing the control miRNA (miR-126), statistical analysis showed that this was not a significant reduction when performed on MSCs from 3 donors. However, MSCs overexpressing both miR-221 and miR-222 showed significantly reduced lipid accumulation when compared to control MSC populations. Additionally, the overexpression of miR-221 and miR-222 significantly reduced the upregulation of key transcripts associated with adipogenesis. In conclusion, the overexpression of miR-221 and miR-222 significantly reduces hMSC adipogenesis as measured by lipid accumulation and reduced upregulation of key adipogenic transcripts. This correlates with studies by others who report similar findings in both primary and immortalized hMSCs undergoing adipogenesis (Skarn, Namlos et al. 2011).

Decreased myogenic differentiation was observed in a myogenic setting upon overexpression of both miR-221 and miR-222 (Cardinali, Castellani et al. 2009) suggesting that the co-operative action of the change in miRNA expression may be necessary to bring about a change in mRNA function. Analysis of predicted targets of miR-221 and miR-222 reveals much overlap between the two miRNAs. This suggests that the overexpression of both miRNAs could be causing the greater downregulation of a key adipogenic transcript(s) compared to the expression of each miRNA singly. Thus relatively small changes in miRNA expression level for a number of cooperating miRNAs can in some cases be insufficient to cause a significant change in target expression. We suspect that this is the reason for a more pronounced decrease in adipogenesis in MSCs overexpressing both miR-221 and miR-222.

### **5.3.2 Inhibiting the activity of miR-221 and 222 causes a reduction in hMSC number**

It could be postulated that if the overexpression of miR-221 and 222 causes a reduction in adipogenesis then the inhibition of their activity could cause an increased level of lipid accumulation (assuming that the miRNA target is a factor limiting adipogenesis). In an attempt to investigate this, shRNAs were delivered to hMSCs which significantly reduced miR-221 and miR-222 expression. The knockdown of miR-221 and 222 activity compromised hMSC survival and caused a significant reduction in cell number compared to cells transduced with a control shRNA. As a result, it was not possible to monitor the effect of miR-221 and miR-222 inhibition on adipogenesis. While the knockdown of miR-221 and miR-222 has been shown to reduce proliferation of vascular smooth muscle cells (Liu, Cheng et al. 2009), we see a reduction in cell number below the number of cells plated. This suggests that reduced proliferation alone does not account for the reduction in hMSCs observed. The knockdown of miR-221 and miR-222 in glioblastoma cell lines, human epithelial cancer cells and a human gastric cancer cell line induced apoptosis (Chun-Zhi, Lei et al. 2010; Zhang, Zhang et al. 2010; Zhang, Zhang et al. 2010). This suggests that the observed reduction in MSC number with reduced levels of miR-221 and miR-222 could be due to cell death caused by induction of adipogenesis. To our knowledge, this is the first time such an effect has been observed in a hMSC model.

### **5.3.3 MiR-221 and miR-222 target prediction**

MiR-221 and miR-222 are known to target the cell cycle inhibitors; p27<sup>kip1</sup> and p57<sup>kip2</sup> (Galardi, Mercatelli et al. 2007; le Sage, Nagel et al. 2007; Fornari, Gramantieri et al. 2008; Medina, Zaidi et al. 2008; Cardinali, Castellani et al. 2009). Because miR-221 and miR-222 are downregulated during adipogenesis it is predicted that their target will be upregulated. However, we have shown that p57 protein expression does not change as adipogenesis progresses, suggesting it is not a target in the context of hMSC adipogenesis. In addition, a role for p57 in

adipogenesis is not evident in the literature and thus we exclude p57 as a potential target of miR-221 and miR-222 during adipogenesis from further analysis.

#### **5.3.4 P27 as a target of miR-221 and miR-222 in hMSC Adipogenesis**

P27 has been implicated to play a role in the progression of adipogenesis, both in a murine and a human model (Morrison and Farmer 1999; Kang, Choi et al. 2008). In 3T3L1 cells p27 protein expression is at its highest pre-differentiation when the preadipocytes are density-arrested. It decreases transiently during the first 48 hours after induction which corresponds to the mitotic clonal expansion stage (MCE) of 3T3L1 adipogenesis. There is evidence to suggest that MCE is not a necessary event for hMSC adipogenesis (Janderova, McNeil et al. 2003; Qian, Li et al. 2010). P27 protein expression returns to predifferentiation levels by 72hours and is maintained at this level throughout adipogenesis (Morrison and Farmer 1999).

In our studies the level of p27 protein rises higher than that observed in confluent MSCs 72 hours after the induction of adipogenesis, while others have shown that this it continues to increase throughout adipogenic differentiation (Kang, Choi et al. 2008). This increase is not observed in murine adipogenesis where p27 levels remain at the predifferentiation level. In addition, p27 transcript expression drops in 3T3L1s after 24 hours of adipogenic induction and remains low while Kang *et al* have shown that p27 mRNA expression increases throughout hMSC adipogenesis (Kang, Choi et al. 2008). The increase in both p27 transcript (Kang, Choi et al. 2008) and protein as adipogenesis proceeds suggest that p27 may play an important (although as of yet unclear) role in hMSC adipogenesis, in addition to its role in the cell cycle.

This finding is in line with a report by Kang *et al* who report that p27 is necessary for hMSC adipogenesis to progress (Kang, Choi et al. 2008). The increased expression of p27 protein concomitant with a decrease in miR-221 and miR-222 expression during adipogenesis suggests that this could be the target through which miR-221 and miR-222 are affecting adipogenesis. Studies by the Kang group

support this (Kang, Choi et al. 2008). They showed that siRNA-mediated reduction of P27 protein resulted in reduced adipogenesis. In keeping with this, we have shown that the overexpression of miR-221/222 reduces adipogenesis, as well as significantly reducing p27 protein.

To verify a direct interaction between miR-221,222 and p27, the 3' UTR of p27 was cloned into a luciferase vector (Luc-p27) and delivered to cells in combination with miR-221 and miR-222. This resulted in decreased luciferase activity compared to the control populations in correlation with previous studies (Galardi, Mercatelli et al. 2007; Medina, Zaidi et al. 2008). We have described additional evidence consistent with p27 being a target for miR-221 and miR-222 in hMSCs as p27 mRNA expression is significantly increased in MSCs with reduced levels of both miRNAs. These results, in combination with evidence from the literature suggest that p27 is a direct target of miR-221 and miR-222 and could be the target through which these miRNAs modulate adipogenesis in hMSCs.

Studies have shown opposing effects of manipulating p27 expression in 3T3L1 cells compared to hMSCs suggesting that p27 plays different roles in murine compared to human adipogenesis. This is in keeping with reports that show the process of murine adipogenic differentiation differs to that of human adipogenic differentiation (Qian, Li et al. 2010). Overexpression of p27 in 3T3L1s resulted in a reduced differentiation as a consequence of preventing MCE (Patel and Lane 1999; Naaz, Holsberger et al. 2004) while others have shown that reducing p27 expression in MSCs reduces adipogenic differentiation capacity (Kang, Choi et al. 2008). In addition, mouse embryonic fibroblasts (MEFs) isolated from p27<sup>-/-</sup> at e13.5 display an increased ability to differentiate compared to wild type (Okada, Sakai et al. 2009). The different patterns of expression and different roles of p27 in human adipogenesis compared to a murine model are shown in Table 5-1.

		<b>Murine Model 3T3L1 cells</b>	<b>Human MSC</b>
<b>Differentiation</b>	<b>p27 Protein</b>	<b>0hr</b> -High-Corresponding to exit from cell cycle <b>24hr</b> -Low-Corresponding to MCE <b>48hr</b> -Increasing- Still below predifferentiation level <b>72hr</b> → <b>End of assay</b> Has returned to predifferentiation levels- Does not increase above this for the course of differentiation	<b>0hr</b> -High-Corresponding to exit from cell cycle <b>24hr</b> -Low <b>48hr</b> -Increasing- Rises above predifferentiation level <b>72hr</b> → <b>End of assay</b> Increasing-Rises significantly higher than predifferentiation levels at 72hr and continues to rise throughout differentiation
	<b>P27 mRNA</b>	<b>0hr</b> -High <b>24hr</b> -Low <b>48hr</b> -Low <b>72hr</b> → <b>End of assay</b> - Low	<b>0hr</b> -High <b>24hr</b> -Low <b>48hr</b> -Increasing-Still below predifferentiaion level <b>72hr</b> → <b>End of assay</b> - Not significantly higher than predifferentiation at 72hr but rises throughout differentiation
<b>Knockdown study</b>		<b>MEFs from p27<sup>-/-</sup> mice</b> - Show <u>increased</u> ability to differentiate compared to wild type mice	<b>hMSCs</b> - siRNA-mediated knockdown of p27- hMSCs show <u>reduced</u> ability to differentiate
<b>Overexpression study</b>		<b>3T3L1 cells</b> - Adipogenesis inhibited	<b>hMSCs</b> - No significant change in lipid accumulation observed in overexpression study
<b><i>In vivo</i> study</b>		P27 knockdown-Increased adipocyte number, increased body weight and obesity	-----

**Table 5-1- P27 research in adipogenesis of 3T3L1 cells and hMSCs**

### 5.3.5 Overexpression of p27 in hMSC Adipogenesis

The results described here and that presented by others in the literature suggest that p27 could be the target through which miR-221 and 222 modulate adipogenesis. The overexpression of miR-221 and miR-222 causes a reduction in p27 protein 72 hours after the induction of adipogenesis. In an attempt to determine if the reduction in adipogenesis was solely attributable to this protein decrease, a vector overexpressing p27 was delivered to hMSCs overexpressing miR-221 and miR-222 and MSCs overexpressing a control miRNA.

The overexpression of p27 had no demonstrable effect on the level of adipogenesis in hMSCs or hMSCs transduced with a control miRNA. This is in contrast to a similar experiment performed in 3T3L1 cells where overexpression of p27 caused a reduction in adipogenesis presumably through the inhibition of clonal cell expansion. As previously discussed, there is evidence to suggest that clonal expansion is not a necessary or key part in hMSC adipogenesis in direct contrast to the murine model. If the reason that p27 overexpression causes a reduction in adipogenesis in a murine model is due to preventing MCE, this could explain why a similar result is not observed in adipogenic differentiation of hMSCs. Additionally, the experiments performed here involved transduction of MSCs with p27 overexpression vector when the cells had reached confluence. Possibly, by the time we transduced with the vector, the cells had already exited the cell cycle and any effect of additional p27 would be redundant.

The aim of this experiment was to determine if the reduction in lipid accumulation observed in miR-221/222 overexpressing MSCs was mediated by a reduction in p27. If so, it could be expected that preventing this reduction through the overexpression of p27 could rescue this reduction in lipid accumulation. However, the overexpression of p27 did not significantly alter the level of lipid accumulation and thus did not restore the levels to that of MSCs overexpressing a control miRNA. This could suggest that p27 is not the sole target through which miR-221 and 222 are modulating adipogenesis. Given the complex mechanism of action of miRNAs, it is likely that the overexpression of miR-221 and 222 causes a reduction in a number of factors involved in hMSC adipogenesis. As a result, the add-back of one

of these factors (in this case p27), is not sufficient to rescue the observed phenotype. More likely, the modulation of a number of key factors would be necessary to rescue the effect.

As discussed, roles for miR-221 and 222 have been identified in a number of models, including glioblastoma, skeletal muscle differentiation and now also in adipogenic differentiation of hMSCs (Medina, Zaidi et al. 2008; Cardinali, Castellani et al. 2009; Skarn, Namlos et al. 2011). P27 has been predicted and verified as a target for miR-221 and 222 in each of these model systems. In each case, the authors state a correlation between the expression of miR-221, 222 and p27. P27 has been experimentally verified as a direct target of both miRNAs using a luciferase reporter vector and so the authors suggest or predict that p27 is the target through which these miRNAs are acting. However, these studies do not include experiments that modulate the expression of p27 concomitant with the modulation of miR-221 and 222. Overall, this highlights a gap that exists in results generated by the overexpression or knockdown of miRNAs. Assumptions made based on correlations of expression between a miRNA and its predicted target are not enough, even when there is evidence of a direct interaction. While luciferase reporter assays and other miRNA target identification strategies are a good starting point for predicting a relationship, further experiments which modulate the predicted target need to be performed to definitively define a miRNA: target interaction.

An example of this is a publication by Kim *et al* who identify miR-221 as regulating chondrogenic differentiation through proteosomal degradation of Slug by targeting Mdm2 (Kim, Song et al. 2010). They first identified miR-221 as being upregulated in chondrogenesis-inhibitory conditions created by inhibition of JNK. They showed that the knockdown of miR-221 reversed the JNK-inhibitor mediated decreases in chondroblast migration and cell proliferation. They searched for targets of miR-221 in chondrogenic differentiation using the common bioinformatic prediction algorithms and identified Mdm2 as a potential target. They confirmed a direct miR-221:Mdm2 interaction using luciferase reporter analysis and went on to show that the overexpression of Mdm2 led up to an upregulation of Slug protein. Consistent with their hypothesis, the overexpression of Slug was associated with a decrease in

cell number. The work described in this thesis, combined with evidence in the literature shows a miRNA: target interaction cannot be definitively identified unless there is modulation of the predicted target in combination with modulation of the miRNA under investigation.

At this stage, therefore the search continues for the target (s) through which miR-221 and 222 are modulating adipogenesis. Target prediction and identification is a limiting step encountered by many researchers trying to identify the mechanism of action of their miRNA of interest. Most algorithms are based on searching for miRNA binding sites in 3' UTRs of potential targets, yet there is evidence to suggest that there are potential binding sites located in the 5' UTRs and in the open reading frame. In addition, most of the algorithms commonly used are based on the structure and evolutionary conservation and do not address the factors involved in miRNA: mRNA targeting in the true *in vivo* setting, as such they could provide inaccurate and misleading results. So while, these algorithms may be retrieving hundreds of potential targets, some targets may be missed due to the criteria of the algorithm approach.

A search for predicted targets of miR-221 and miR-222 generated greater than 1000 potential mRNAs using current bioinformatic algorithms. The next challenge in the field of miRNA research is to develop strategies with which to experimentally verify (as opposed to computationally predict) with confidence the target(s) of the miRNA under investigation. This combined with the development of more advanced and accurate target identification programs will go a long way to achieving a definitive method of identifying a miRNA: target relationship.

### 5.3.6 Final Remarks

The current obesity epidemic has caused an increase in interest in the study of adipose tissue and its developmental origins. We hope that the information provided here will further the understanding of the adipogenic differentiation of hMSCs. In turn, it is hoped an increased understanding of adipogenesis and thus adipose tissue development will aid in the development of new therapies for the treatment of obesity.

We believe that the work presented in this thesis contributes to the existing knowledge on the roles of miRNAs in hMSC adipogenesis. At the time these experiments were performed a role for miRNAs in the adipogenic differentiation of hMSCs had not been reported. The microarray analysis described in this thesis identified 20 miRNAs as being significantly regulated in a pure population of adipogenically differentiating MSCs compared to undifferentiated MSCs at day 20 of adipogenesis. To our knowledge, this is the only microRNA profiling experiment performed on a pure population of hMSC-derived adipocytes.

We demonstrated that the overexpression of miR-221 and miR-222 significantly reduced hMSC adipogenesis as measured by lipid accumulation and reduced upregulation of key adipogenesis related transcripts. The overexpression of miR-221 and miR-222 significantly reduced p27 protein 72 hours after the induction of adipogenesis while p27 mRNA remained unaffected. The studies described in this thesis and from other researchers in the field imply that p27 is the probable target for miR-221 and miR-222 in hMSC adipogenesis. This study is the first to analyse the effects of ‘adding back’ p27 in an attempt to rescue adipogenesis in hMSCs overexpressing miR-221 and miR-222. We demonstrate that the overexpression of p27 does not rescue the reduced lipid accumulation mediated by miR-221 and miR-222 overexpression. This suggests that p27 is not the sole target through which miR-221 and miR-222 are modulating adipogenesis. To our knowledge, this is the first evidence showing that the overexpression of p27 did not significantly alter adipogenesis in untransduced MSCs or MSCs transduced with a control miRNA.

This is the first study reporting changes for miRNAs in all three major lineages of hMSC differentiation. We have shown that miR-221 and miR-222 expression significantly decreases during adipogenesis, osteogenesis and chondrogenesis. This could point to a role for these miRNAs in maintaining the 'stemness' of hMSCs, although we have shown that the overexpression of miR-221 and miR-222 had no significant effect on hMSC osteogenesis.

We have also provided evidence for a link between miR-221, miR-222 and hMSC survival. We have shown that the inhibition of miR-221 and/or miR-222 causes a reduction in cell number below the number of MSCs originally plated. The reduction in cell number is potentially due to cell death, based on evidence in the literature which states the knockdown of miR-221 and miR-222 induces members of the apoptotic pathway.

In conclusion, we have identified clear roles for miRNAs in the process of hMSC adipogenesis. We have increased the information available on the roles of miR-221 and miR-222 in hMSC behaviour, including survival and differentiation and have helped to clarify the role of p27 in hMSC adipogenesis.

## 6 Bibliography

- Abella, A., P. Dubus, et al. (2005). "Cdk4 promotes adipogenesis through PPARgamma activation." Cell Metab **2**(4): 239-49.
- Abrahante, J. E., A. L. Daul, et al. (2003). "The Caenorhabditis elegans hunchback-like gene lin-57/hbl-1 controls developmental time and is regulated by microRNAs." Dev Cell **4**(5): 625-37.
- Ahluwalia, J. K., S. Z. Khan, et al. (2008). "Human cellular microRNA hsa-miR-29a interferes with viral nef protein expression and HIV-1 replication." Retrovirology **5**: 117.
- Akinc, A., M. Thomas, et al. (2005). "Exploring polyethylenimine-mediated DNA transfection and the proton sponge hypothesis." J Gene Med **7**(5): 657-63.
- Aluigi, M., M. Fogli, et al. (2006). "Nucleofection is an efficient nonviral transfection technique for human bone marrow-derived mesenchymal stem cells." Stem Cells **24**(2): 454-61.
- Ambros, V. (2003). "MicroRNA pathways in flies and worms: growth, death, fat, stress, and timing." Cell **113**(6): 673-6.
- Ambros, V. and H. R. Horvitz (1984). "Heterochronic mutants of the nematode Caenorhabditis elegans." Science **226**(4673): 409-16.
- Ambs, S., R. L. Prueitt, et al. (2008). "Genomic profiling of microRNA and messenger RNA reveals deregulated microRNA expression in prostate cancer." Cancer Res **68**(15): 6162-70.
- Anderson, C., H. Catoe, et al. (2006). "MIR-206 regulates connexin43 expression during skeletal muscle development." Nucleic Acids Res **34**(20): 5863-71.
- Arner, P. (2003). "The adipocyte in insulin resistance: key molecules and the impact of the thiazolidinediones." Trends Endocrinol Metab **14**(3): 137-45.
- Barak, Y., M. C. Nelson, et al. (1999). "PPAR gamma is required for placental, cardiac, and adipose tissue development." Mol Cell **4**(4): 585-95.
- Bartel, D. P. (2004). "MicroRNAs: genomics, biogenesis, mechanism, and function." Cell **116**(2): 281-97.
- Bartel, D. P. (2009). "MicroRNAs: target recognition and regulatory functions." Cell **136**(2): 215-33.
- Baskerville, S. and D. P. Bartel (2005). "Microarray profiling of microRNAs reveals frequent coexpression with neighboring miRNAs and host genes." RNA **11**(3): 241-7.
- Benes, V. and M. Castoldi (2010). "Expression profiling of microRNA using real-time quantitative PCR, how to use it and what is available." Methods.
- Berezikov, E., W. J. Chung, et al. (2007). "Mammalian mirtron genes." Mol Cell **28**(2): 328-36.
- Bernstein, E., S. Y. Kim, et al. (2003). "Dicer is essential for mouse development." Nat Genet **35**(3): 215-7.
- Besson, A., S. F. Dowdy, et al. (2008). "CDK inhibitors: cell cycle regulators and beyond." Dev Cell **14**(2): 159-69.
- Bianco, P., M. Riminucci, et al. (2001). "Bone marrow stromal stem cells: nature, biology, and potential applications." Stem Cells **19**(3): 180-92.
- Bianco, P., P. G. Robey, et al. (2008). "Mesenchymal stem cells: revisiting history, concepts, and assays." Cell Stem Cell **2**(4): 313-9.

- Bieback, K., S. Kern, et al. (2004). "Critical parameters for the isolation of mesenchymal stem cells from umbilical cord blood." Stem Cells **22**(4): 625-34.
- Billon, N. and C. Dani (2011). "Developmental Origins of the Adipocyte Lineage: New Insights from Genetics and Genomics Studies." Stem Cell Rev.
- Billon, N., M. C. Monteiro, et al. (2008). "Developmental origin of adipocytes: new insights into a pending question." Biol Cell **100**(10): 563-75.
- Bocker, W., O. Rossmann, et al. (2007). "Quantitative polymerase chain reaction as a reliable method to determine functional lentiviral titer after ex vivo gene transfer in human mesenchymal stem cells." J Gene Med **9**(7): 585-95.
- Bohnsack, M. T., K. Czaplinski, et al. (2004). "Exportin 5 is a RanGTP-dependent dsRNA-binding protein that mediates nuclear export of pre-miRNAs." RNA **10**(2): 185-91.
- Bork, S., P. Horn, et al. (2010). "Adipogenic differentiation of human mesenchymal stromal cells is down-regulated by microRNA-369-5p and up-regulated by microRNA-371." J Cell Physiol **226**(9): 2226-34.
- Bosnakovski, D., M. Mizuno, et al. (2005). "Isolation and multilineage differentiation of bovine bone marrow mesenchymal stem cells." Cell Tissue Res **319**(2): 243-53.
- Boussif, O., F. Lezoualc'h, et al. (1995). "A versatile vector for gene and oligonucleotide transfer into cells in culture and in vivo: polyethylenimine." Proc Natl Acad Sci U S A **92**(16): 7297-301.
- Bracken, C. P., P. A. Gregory, et al. (2008). "A double-negative feedback loop between ZEB1-SIP1 and the microRNA-200 family regulates epithelial-mesenchymal transition." Cancer Res **68**(19): 7846-54.
- Brennecke, J., A. Stark, et al. (2005). "Principles of microRNA-target recognition." PLoS Biol **3**(3): e85.
- Bujan, J., G. Pascual, et al. (2006). "Muscle-derived stem cells used to treat skin defects prevent wound contraction and expedite reepithelialization." Wound Repair Regen **14**(2): 216-23.
- Cai, X., C. H. Hagedorn, et al. (2004). "Human microRNAs are processed from capped, polyadenylated transcripts that can also function as mRNAs." RNA **10**(12): 1957-66.
- Calabrese, J. M., A. C. Seila, et al. (2007). "RNA sequence analysis defines Dicer's role in mouse embryonic stem cells." Proc Natl Acad Sci U S A **104**(46): 18097-102.
- Cardinali, B., L. Castellani, et al. (2009). "MicroRNA-221 and microRNA-222 modulate differentiation and maturation of skeletal muscle cells." PLoS One **4**(10): e7607.
- Carmell, M. A., Z. Xuan, et al. (2002). "The Argonaute family: tentacles that reach into RNAi, developmental control, stem cell maintenance, and tumorigenesis." Genes Dev **16**(21): 2733-42.
- Castoldi, M., S. Schmidt, et al. (2008). "miChip: an array-based method for microRNA expression profiling using locked nucleic acid capture probes." Nat Protoc **3**(2): 321-9.

- Castoldi, M., S. Schmidt, et al. (2006). "A sensitive array for microRNA expression profiling (miChip) based on locked nucleic acids (LNA)." *RNA* **12**(5): 913-20.
- Castrechini, N. M., P. Murthi, et al. (2010). "Mesenchymal stem cells in human placental chorionic villi reside in a vascular Niche." *Placenta* **31**(3): 203-12.
- Chen, C. Z., L. Li, et al. (2004). "MicroRNAs modulate hematopoietic lineage differentiation." *Science* **303**(5654): 83-6.
- Chen, J. F., E. M. Mandel, et al. (2006). "The role of microRNA-1 and microRNA-133 in skeletal muscle proliferation and differentiation." *Nat Genet* **38**(2): 228-33.
- Chen, R., A. B. Alvero, et al. (2008). "Regulation of IKKbeta by miR-199a affects NF-kappaB activity in ovarian cancer cells." *Oncogene* **27**(34): 4712-23.
- Chen, Y. and D. H. Gorski (2008). "Regulation of angiogenesis through a microRNA (miR-130a) that down-regulates antiangiogenic homeobox genes GAX and HOXA5." *Blood* **111**(3): 1217-26.
- Chendrimada, T. P., R. I. Gregory, et al. (2005). "TRBP recruits the Dicer complex to Ago2 for microRNA processing and gene silencing." *Nature* **436**(7051): 740-4.
- Chi, S. W., J. B. Zang, et al. (2009). "Argonaute HITS-CLIP decodes microRNA-mRNA interaction maps." *Nature* **460**(7254): 479-86.
- Chun-Zhi, Z., H. Lei, et al. (2010). "MicroRNA-221 and microRNA-222 regulate gastric carcinoma cell proliferation and radioresistance by targeting PTEN." *BMC Cancer* **10**: 367.
- Cimmino, A., G. A. Calin, et al. (2005). "miR-15 and miR-16 induce apoptosis by targeting BCL2." *Proc Natl Acad Sci U S A* **102**(39): 13944-9.
- Conget, P. A. and J. J. Minguell (1999). "Phenotypical and functional properties of human bone marrow mesenchymal progenitor cells." *J Cell Physiol* **181**(1): 67-73.
- Cordes, K. R. and D. Srivastava (2009). "MicroRNA regulation of cardiovascular development." *Circ Res* **104**(6): 724-32.
- Coulouarn, C., V. M. Factor, et al. (2009). "Loss of miR-122 expression in liver cancer correlates with suppression of the hepatic phenotype and gain of metastatic properties." *Oncogene* **28**(40): 3526-36.
- Cristancho, A. G. and M. A. Lazar (2011). "Forming functional fat: a growing understanding of adipocyte differentiation." *Nat Rev Mol Cell Biol* **12**(11): 722-34.
- Cypess, A. M., S. Lehman, et al. (2009). "Identification and importance of brown adipose tissue in adult humans." *N Engl J Med* **360**(15): 1509-17.
- Dai, Y. and S. Grant (2003). "Cyclin-dependent kinase inhibitors." *Curr Opin Pharmacol* **3**(4): 362-70.
- Darlington, G. J., S. E. Ross, et al. (1998). "The role of C/EBP genes in adipocyte differentiation." *J Biol Chem* **273**(46): 30057-60.
- Dazzi, F., R. Ramasamy, et al. (2006). "The role of mesenchymal stem cells in haemopoiesis." *Blood Rev* **20**(3): 161-71.

- Deschaseaux, F., F. Gindraux, et al. (2003). "Direct selection of human bone marrow mesenchymal stem cells using an anti-CD49a antibody reveals their CD45<sup>med,low</sup> phenotype." *Br J Haematol* **122**(3): 506-17.
- Ding, X. C. and H. Grosshans (2009). "Repression of *C. elegans* microRNA targets at the initiation level of translation requires GW182 proteins." *EMBO J* **28**(3): 213-22.
- Dominici, M., K. Le Blanc, et al. (2006). "Minimal criteria for defining multipotent mesenchymal stromal cells. The International Society for Cellular Therapy position statement." *Cytotherapy* **8**(4): 315-7.
- Elabd, C., C. Chiellini, et al. (2009). "Human multipotent adipose-derived stem cells differentiate into functional brown adipocytes." *Stem Cells* **27**(11): 2753-60.
- Elmen, J., M. Lindow, et al. (2008). "LNA-mediated microRNA silencing in non-human primates." *Nature* **452**(7189): 896-9.
- Enright, A. J., B. John, et al. (2003). "MicroRNA targets in *Drosophila*." *Genome Biol* **5**(1): R1.
- Entenmann, G. and H. Hauner (1996). "Relationship between replication and differentiation in cultured human adipocyte precursor cells." *Am J Physiol* **270**(4 Pt 1): C1011-6.
- Esau, C., X. Kang, et al. (2004). "MicroRNA-143 regulates adipocyte differentiation." *J Biol Chem* **279**(50): 52361-5.
- Fajas, L., K. Schoonjans, et al. (1999). "Regulation of peroxisome proliferator-activated receptor gamma expression by adipocyte differentiation and determination factor 1/sterol regulatory element binding protein 1: implications for adipocyte differentiation and metabolism." *Mol Cell Biol* **19**(8): 5495-503.
- Felli, N., L. Fontana, et al. (2005). "MicroRNAs 221 and 222 inhibit normal erythropoiesis and erythroleukemic cell growth via kit receptor down-modulation." *Proc Natl Acad Sci U S A* **102**(50): 18081-6.
- Fernyhough, M. E., J. L. Vierck, et al. (2004). "Primary adipocyte culture: Adipocyte purification methods may lead to a new understanding of adipose tissue growth and development." *Cytotechnology* **46**(2-3): 163-172.
- Fontana, L., E. Pelosi, et al. (2007). "MicroRNAs 17-5p-20a-106a control monocytopoiesis through AML1 targeting and M-CSF receptor upregulation." *Nat Cell Biol* **9**(7): 775-87.
- Forman, J. J., A. Legesse-Miller, et al. (2008). "A search for conserved sequences in coding regions reveals that the let-7 microRNA targets Dicer within its coding sequence." *Proc Natl Acad Sci U S A* **105**(39): 14879-84.
- Fornari, F., L. Gramantieri, et al. (2008). "MiR-221 controls CDKN1C/p57 and CDKN1B/p27 expression in human hepatocellular carcinoma." *Oncogene* **27**(43): 5651-61.
- Forstemann, K., Y. Tomari, et al. (2005). "Normal microRNA maturation and germline stem cell maintenance requires Loquacious, a double-stranded RNA-binding domain protein." *PLoS Biol* **3**(7): e236.
- Frenquelli, M., M. Muzio, et al. "MicroRNA and proliferation control in chronic lymphocytic leukemia: functional relationship between miR-221/222 cluster and p27." *Blood*.

- Frenquelli, M., M. Muzio, et al. (2010). "MicroRNA and proliferation control in chronic lymphocytic leukemia: functional relationship between miR-221/222 cluster and p27." Blood.
- Frenquelli, M., M. Muzio, et al. (2010). "MicroRNA and proliferation control in chronic lymphocytic leukemia: functional relationship between miR-221/222 cluster and p27." Blood **115**(19): 3949-59.
- Friedenstein, A. J., S. Piatetzky, II, et al. (1966). "Osteogenesis in transplants of bone marrow cells." J Embryol Exp Morphol **16**(3): 381-90.
- Friedman, R. C., K. K. Farh, et al. (2009). "Most mammalian mRNAs are conserved targets of microRNAs." Genome Res **19**(1): 92-105.
- Fruhbeck, G., J. Gomez-Ambrosi, et al. (2001). "The adipocyte: a model for integration of endocrine and metabolic signaling in energy metabolism regulation." Am J Physiol Endocrinol Metab **280**(6): E827-47.
- Fu, M., M. Rao, et al. (2005). "Cyclin D1 inhibits peroxisome proliferator-activated receptor gamma-mediated adipogenesis through histone deacetylase recruitment." J Biol Chem **280**(17): 16934-41.
- Galardi, S., N. Mercatelli, et al. (2007). "miR-221 and miR-222 expression affects the proliferation potential of human prostate carcinoma cell lines by targeting p27Kip1." J Biol Chem **282**(32): 23716-24.
- Gangaraju, V. K. and H. Lin (2009). "MicroRNAs: key regulators of stem cells." Nat Rev Mol Cell Biol **10**(2): 116-25.
- Georgantas, R. W., 3rd, R. Hildreth, et al. (2007). "CD34+ hematopoietic stem-progenitor cell microRNA expression and function: a circuit diagram of differentiation control." Proc Natl Acad Sci U S A **104**(8): 2750-5.
- Gesta, S., Y. H. Tseng, et al. (2007). "Developmental origin of fat: tracking obesity to its source." Cell **131**(2): 242-56.
- Ghorbani, M., T. H. Claus, et al. (1997). "Hypertrophy of brown adipocytes in brown and white adipose tissues and reversal of diet-induced obesity in rats treated with a beta3-adrenoceptor agonist." Biochem Pharmacol **54**(1): 121-31.
- Giarratana, M. C., L. Kobari, et al. (2005). "Ex vivo generation of fully mature human red blood cells from hematopoietic stem cells." Nat Biotechnol **23**(1): 69-74.
- Gillies, J. K. and I. A. Lorimer (2007). "Regulation of p27Kip1 by miRNA 221/222 in glioblastoma." Cell Cycle **6**(16): 2005-9.
- Glazov, E. A., P. A. Cottee, et al. (2008). "A microRNA catalog of the developing chicken embryo identified by a deep sequencing approach." Genome Res **18**(6): 957-64.
- Grady, W. M., R. K. Parkin, et al. (2008). "Epigenetic silencing of the intronic microRNA hsa-miR-342 and its host gene EVL in colorectal cancer." Oncogene **27**(27): 3880-8.
- Green, H. and M. Meuth (1974). "An established pre-adipose cell line and its differentiation in culture." Cell **3**(2): 127-33.
- Greenspan, P., E. P. Mayer, et al. (1985). "Nile red: a selective fluorescent stain for intracellular lipid droplets." J Cell Biol **100**(3): 965-73.

- Gregory, R. I., K. P. Yan, et al. (2004). "The Microprocessor complex mediates the genesis of microRNAs." Nature **432**(7014): 235-40.
- Griffiths-Jones, S. (2004). "The microRNA Registry." Nucleic Acids Res **32**(Database issue): D109-11.
- Griffiths-Jones, S. (2006). "miRBase: the microRNA sequence database." Methods Mol Biol **342**: 129-38.
- Griffiths-Jones, S., R. J. Grocock, et al. (2006). "miRBase: microRNA sequences, targets and gene nomenclature." Nucleic Acids Res **34**(Database issue): D140-4.
- Griffiths-Jones, S., H. K. Saini, et al. (2008). "miRBase: tools for microRNA genomics." Nucleic Acids Res **36**(Database issue): D154-8.
- Guo, H., N. T. Ingolia, et al. (2010). "Mammalian microRNAs predominantly act to decrease target mRNA levels." Nature **466**(7308): 835-40.
- Guttilla, I. K. and B. A. White (2009). "Coordinate regulation of FOXO1 by miR-27a, miR-96, and miR-182 in breast cancer cells." J Biol Chem **284**(35): 23204-16.
- Hammond, S. M. (2005). "Dicing and slicing: the core machinery of the RNA interference pathway." FEBS Lett **579**(26): 5822-9.
- Hanna, J. H., K. Saha, et al. (2010). "Pluripotency and cellular reprogramming: facts, hypotheses, unresolved issues." Cell **143**(4): 508-25.
- Hatfield, S. D., H. R. Shcherbata, et al. (2005). "Stem cell division is regulated by the microRNA pathway." Nature **435**(7044): 974-8.
- Hauer, H. and G. Entenmann (1991). "Regional variation of adipose differentiation in cultured stromal-vascular cells from the abdominal and femoral adipose tissue of obese women." Int J Obes **15**(2): 121-6.
- He, H., K. Jazdzewski, et al. (2005). "The role of microRNA genes in papillary thyroid carcinoma." Proc Natl Acad Sci U S A **102**(52): 19075-80.
- Hendrickson, D. G., D. J. Hogan, et al. (2008). "Systematic identification of mRNAs recruited to argonaute 2 by specific microRNAs and corresponding changes in transcript abundance." PLoS One **3**(5): e2126.
- Hendrickson, D. G., D. J. Hogan, et al. (2009). "Concordant regulation of translation and mRNA abundance for hundreds of targets of a human microRNA." PLoS Biol **7**(11): e1000238.
- Hermens, W. T. J. M. C. and J. Verhaagen (1998). "Viral vectors, tools for gene transfer in the nervous system." Progress in Neurobiology **55**(4): 399-432.
- Hossain, A., M. T. Kuo, et al. (2006). "Mir-17-5p regulates breast cancer cell proliferation by inhibiting translation of AIB1 mRNA." Mol Cell Biol **26**(21): 8191-201.
- Houbaviy, H. B., L. Dennis, et al. (2005). "Characterization of a highly variable eutherian microRNA gene." RNA **11**(8): 1245-57.
- Houbaviy, H. B., M. F. Murray, et al. (2003). "Embryonic stem cell-specific MicroRNAs." Dev Cell **5**(2): 351-8.
- Hu, E., P. Tontonoz, et al. (1995). "Transdifferentiation of myoblasts by the adipogenic transcription factors PPAR gamma and C/EBP alpha." Proc Natl Acad Sci U S A **92**(21): 9856-60.

- Huang, P. I., Y. C. Chen, et al. (2011). "PGC-1alpha mediates differentiation of mesenchymal stem cells to brown adipose cells." J Atheroscler Thromb **18**(11): 966-80.
- Huang, T. H., B. Fan, et al. (2007). "MiRFinder: an improved approach and software implementation for genome-wide fast microRNA precursor scans." BMC Bioinformatics **8**: 341.
- Ibberson, D., V. Benes, et al. (2009). "RNA degradation compromises the reliability of microRNA expression profiling." BMC Biotechnol **9**: 102.
- Inoue, N., N. Yahagi, et al. (2008). "Cyclin-dependent kinase inhibitor, p21WAF1/CIP1, is involved in adipocyte differentiation and hypertrophy, linking to obesity, and insulin resistance." J Biol Chem **283**(30): 21220-9.
- Ivey, K. N., A. Muth, et al. (2008). "MicroRNA regulation of cell lineages in mouse and human embryonic stem cells." Cell Stem Cell **2**(3): 219-29.
- Jackson, L., D. R. Jones, et al. (2007). "Adult mesenchymal stem cells: differentiation potential and therapeutic applications." J Postgrad Med **53**(2): 121-7.
- Jaiswal, N., S. E. Haynesworth, et al. (1997). "Osteogenic differentiation of purified, culture-expanded human mesenchymal stem cells in vitro." J Cell Biochem **64**(2): 295-312.
- Janderova, L., M. McNeil, et al. (2003). "Human mesenchymal stem cells as an in vitro model for human adipogenesis." Obes Res **11**(1): 65-74.
- Jiang, J., Z. Lv, et al. (2010). "Adult rat mesenchymal stem cells differentiate into neuronal-like phenotype and express a variety of neuro-regulatory molecules in vitro." Neurosci Res **66**(1): 46-52.
- Jiang, Q., M. G. Feng, et al. (2009). "Systematic validation of predicted microRNAs for cyclin D1." BMC Cancer **9**: 194.
- John, B., A. J. Enright, et al. (2004). "Human MicroRNA targets." PLoS Biol **2**(11): e363.
- Johnson, S. M., H. Grosshans, et al. (2005). "RAS Is Regulated by the let-7 MicroRNA Family." Cell **120**(5): 635-647.
- Jones, E. and D. McGonagle (2008). "Human bone marrow mesenchymal stem cells in vivo." Rheumatology (Oxford) **47**(2): 126-31.
- Kadri, S., V. Hinman, et al. (2009). "HHMMiR: efficient de novo prediction of microRNAs using hierarchical hidden Markov models." BMC Bioinformatics **10 Suppl 1**: S35.
- Kajimoto, K., H. Naraba, et al. (2006). "MicroRNA and 3T3-L1 pre-adipocyte differentiation." RNA **12**(9): 1626-32.
- Kaneda, R. and K. Fukuda (2009). "MicroRNA is a new diagnostic and therapeutic target for cardiovascular disease and regenerative medicine." Circ J **73**(8): 1397-8.
- Kanellopoulou, C., S. A. Muljo, et al. (2005). "Dicer-deficient mouse embryonic stem cells are defective in differentiation and centromeric silencing." Genes Dev **19**(4): 489-501.
- Kang, J. W., Y. Choi, et al. (2008). "The effects of cyclin-dependent kinase inhibitors on adipogenic differentiation of human mesenchymal stem cells." Biochem Biophys Res Commun **366**(3): 624-30.

- Karbiener, M., C. Fischer, et al. (2009). "microRNA miR-27b impairs human adipocyte differentiation and targets PPARgamma." Biochem Biophys Res Commun **390**(2): 247-51.
- Karginov, F. V., C. Conaco, et al. (2007). "A biochemical approach to identifying microRNA targets." Proc Natl Acad Sci U S A **104**(49): 19291-6.
- Kershaw, E. E. and J. S. Flier (2004). "Adipose tissue as an endocrine organ." J Clin Endocrinol Metab **89**(6): 2548-56.
- Kim, D., J. Song, et al. (2010). "MicroRNA-221 regulates chondrogenic differentiation through promoting proteosomal degradation of slug by targeting mdm2." J Biol Chem.
- Kim, J. B., H. M. Wright, et al. (1998). "ADD1/SREBP1 activates PPARgamma through the production of endogenous ligand." Proc Natl Acad Sci U S A **95**(8): 4333-7.
- Kim, V. N., J. Han, et al. (2009). "Biogenesis of small RNAs in animals." Nat Rev Mol Cell Biol **10**(2): 126-39.
- Kim, Y. J., S. J. Hwang, et al. (2009). "MiR-21 regulates adipogenic differentiation through the modulation of TGF-beta signaling in mesenchymal stem cells derived from human adipose tissue." Stem Cells **27**(12): 3093-102.
- Klimatcheva, E., J. D. Rosenblatt, et al. (1999). "Lentiviral vectors and gene therapy." Front Biosci **4**: D481-96.
- Kloting, N., S. Berthold, et al. (2009). "MicroRNA expression in human omental and subcutaneous adipose tissue." PLoS One **4**(3): e4699.
- Koshkin, A. A., S. K. Singh, et al. (1998). "LNA (Locked Nucleic Acids): Synthesis of the adenine, cytosine, guanine, 5-methylcytosine, thymine and uracil bicyclonucleoside monomers, oligomerisation, and unprecedented nucleic acid recognition." Tetrahedron **54**(14): 3607-3630.
- Kothapalli, R., S. J. Yoder, et al. (2002). "Microarray results: how accurate are they?" BMC Bioinformatics **3**: 22.
- Kozak, E. R. a. L. P. (2009). "Have we entered the brown adipose tissue renaissance?" obesity reviews: 265-268.
- Krek, A., D. Grun, et al. (2005). "Combinatorial microRNA target predictions." Nat Genet **37**(5): 495-500.
- Krichevsky, A. M., K. S. King, et al. (2003). "A microRNA array reveals extensive regulation of microRNAs during brain development." RNA **9**(10): 1274-81.
- Kuehbacher, A., C. Urbich, et al. (2008). "Targeting microRNA expression to regulate angiogenesis." Trends Pharmacol Sci **29**(1): 12-5.
- Kuhn, D. E., M. M. Martin, et al. (2008). "Experimental validation of miRNA targets." Methods **44**(1): 47-54.
- Kutner, R. H., X. Y. Zhang, et al. (2009). "Production, concentration and titration of pseudotyped HIV-1-based lentiviral vectors." Nat Protoc **4**(4): 495-505.
- Lagos-Quintana, M., R. Rauhut, et al. (2003). "New microRNAs from mouse and human." RNA **9**(2): 175-9.
- Lakshmiathy, U. and R. P. Hart (2008). "Concise review: MicroRNA expression in multipotent mesenchymal stromal cells." Stem Cells **26**(2): 356-63.

- le Sage, C., R. Nagel, et al. (2007). "Regulation of the p27(Kip1) tumor suppressor by miR-221 and miR-222 promotes cancer cell proliferation." EMBO J **26**(15): 3699-708.
- Lee, C. I., D. B. Kohn, et al. (2004). "Morphological Analysis and Lentiviral Transduction of Fetal Monkey Bone Marrow-Derived Mesenchymal Stem Cells." Mol Ther **9**(1): 112-123.
- Lee, R. C., R. L. Feinbaum, et al. (1993). "The *C. elegans* heterochronic gene *lin-4* encodes small RNAs with antisense complementarity to *lin-14*." Cell **75**(5): 843-54.
- Lee, Y., K. Jeon, et al. (2002). "MicroRNA maturation: stepwise processing and subcellular localization." EMBO J **21**(17): 4663-70.
- Lee, Y., M. Kim, et al. (2004). "MicroRNA genes are transcribed by RNA polymerase II." EMBO J **23**(20): 4051-60.
- Lees, E. (1995). "Cyclin dependent kinase regulation." Curr Opin Cell Biol **7**(6): 773-80.
- Lewis, B. P., C. B. Burge, et al. (2005). "Conserved seed pairing, often flanked by adenosines, indicates that thousands of human genes are microRNA targets." Cell **120**(1): 15-20.
- Lewis, B. P., I. H. Shih, et al. (2003). "Prediction of mammalian microRNA targets." Cell **115**(7): 787-98.
- Li, S., H. Fu, et al. (2009). "MicroRNA-101 regulates expression of the v-fos FBJ murine osteosarcoma viral oncogene homolog (FOS) oncogene in human hepatocellular carcinoma." Hepatology **49**(4): 1194-202.
- Li, Y., Y. H. Song, et al. (2009). "MicroRNA-221 regulates high glucose-induced endothelial dysfunction." Biochem Biophys Res Commun **381**(1): 81-3.
- Liang, H. and W. F. Ward (2006). "PGC-1alpha: a key regulator of energy metabolism." Adv Physiol Educ **30**(4): 145-51.
- Lim, L. P., M. E. Glasner, et al. (2003). "Vertebrate microRNA genes." Science **299**(5612): 1540.
- Lin, E. A., L. Kong, et al. (2009). "miR-199a, a bone morphogenic protein 2-responsive MicroRNA, regulates chondrogenesis via direct targeting to Smad1." J Biol Chem **284**(17): 11326-35.
- Liu, J., M. A. Carmell, et al. (2004). "Argonaute2 is the catalytic engine of mammalian RNAi." Science **305**(5689): 1437-41.
- Liu, J., F. V. Rivas, et al. (2005). "A role for the P-body component GW182 in microRNA function." Nat Cell Biol **7**(12): 1261-6.
- Liu, J., M. A. Valencia-Sanchez, et al. (2005). "MicroRNA-dependent localization of targeted mRNAs to mammalian P-bodies." Nat Cell Biol **7**(7): 719-23.
- Liu, X., Y. Cheng, et al. (2009). "A necessary role of miR-221 and miR-222 in vascular smooth muscle cell proliferation and neointimal hyperplasia." Circ Res **104**(4): 476-87.
- Livak, K. J. and T. D. Schmittgen (2001). "Analysis of relative gene expression data using real-time quantitative PCR and the 2(-Delta Delta C(T)) Method." Methods **25**(4): 402-8.
- Lovat, F., N. Valeri, et al. (2011). "MicroRNAs in the pathogenesis of cancer." Semin Oncol **38**(6): 724-33.

- Lowell, B. B., S. S. V, et al. (1993). "Development of obesity in transgenic mice after genetic ablation of brown adipose tissue." Nature **366**(6457): 740-2.
- Luria, E. A., A. F. Panasyuk, et al. (1971). "Fibroblast colony formation from monolayer cultures of blood cells." Transfusion **11**(6): 345-9.
- Lytle, J. R., T. A. Yario, et al. (2007). "Target mRNAs are repressed as efficiently by microRNA-binding sites in the 5' UTR as in the 3' UTR." Proc Natl Acad Sci U S A **104**(23): 9667-72.
- Makeyev, E. V., J. Zhang, et al. (2007). "The MicroRNA miR-124 promotes neuronal differentiation by triggering brain-specific alternative pre-mRNA splicing." Mol Cell **27**(3): 435-48.
- Martinelli, R., C. Nardelli, et al. (2010). "miR-519d overexpression is associated with human obesity." Obesity (Silver Spring) **18**(11): 2170-6.
- Mattout, A., A. Biran, et al. (2011). "Global epigenetic changes during somatic cell reprogramming to iPS cells." J Mol Cell Biol **3**(6): 341-50.
- Mayr, C., M. T. Hemann, et al. (2007). "Disrupting the pairing between let-7 and Hmga2 enhances oncogenic transformation." Science **315**(5818): 1576-9.
- Maziere, P. and A. J. Enright (2007). "Prediction of microRNA targets." Drug Discov Today **12**(11-12): 452-8.
- McGregor, R. A. and M. S. Choi (2011). "microRNAs in the regulation of adipogenesis and obesity." Curr Mol Med **11**(4): 304-16.
- McMahon, J. M., S. Conroy, et al. (2006). "Gene transfer into rat mesenchymal stem cells: a comparative study of viral and nonviral vectors." Stem Cells Dev **15**(1): 87-96.
- Medina, R., S. K. Zaidi, et al. (2008). "MicroRNAs 221 and 222 bypass quiescence and compromise cell survival." Cancer Res **68**(8): 2773-80.
- Meister, G., M. Landthaler, et al. (2004). "Human Argonaute2 mediates RNA cleavage targeted by miRNAs and siRNAs." Mol Cell **15**(2): 185-97.
- Meister, G. and T. Tuschl (2004). "Mechanisms of gene silencing by double-stranded RNA." Nature **431**(7006): 343-9.
- Melton, C., R. L. Judson, et al. (2010). "Opposing microRNA families regulate self-renewal in mouse embryonic stem cells." Nature **463**(7281): 621-6.
- Miller, T. E., K. Ghoshal, et al. (2008). "MicroRNA-221/222 confers tamoxifen resistance in breast cancer by targeting p27Kip1." J Biol Chem **283**(44): 29897-903.
- Min, H. and S. Yoon (2010). "Got target? Computational methods for microRNA target prediction and their extension." Exp Mol Med **42**(4): 233-44.
- Miska, E. A., E. Alvarez-Saavedra, et al. (2004). "Microarray analysis of microRNA expression in the developing mammalian brain." Genome Biol **5**(9): R68.
- Mizuno, Y., K. Yagi, et al. (2008). "miR-125b inhibits osteoblastic differentiation by down-regulation of cell proliferation." Biochem Biophys Res Commun **368**(2): 267-72.
- Morrison, R. F. and S. R. Farmer (1999). "Role of PPARgamma in regulating a cascade expression of cyclin-dependent kinase inhibitors, p18(INK4c) and p21(Waf1/Cip1), during adipogenesis." J Biol Chem **274**(24): 17088-97.

- Mourelatos, Z., J. Dostie, et al. (2002). "miRNPs: a novel class of ribonucleoproteins containing numerous microRNAs." Genes Dev **16**(6): 720-8.
- Muraglia, A., R. Cancedda, et al. (2000). "Clonal mesenchymal progenitors from human bone marrow differentiate in vitro according to a hierarchical model." J Cell Sci **113** ( Pt 7): 1161-6.
- Muraglia, A., A. Corsi, et al. (2003). "Formation of a chondro-osseous rudiment in micromass cultures of human bone-marrow stromal cells." J Cell Sci **116**(Pt 14): 2949-55.
- Murchison, E. P., J. F. Partridge, et al. (2005). "Characterization of Dicer-deficient murine embryonic stem cells." Proc Natl Acad Sci U S A **102**(34): 12135-40.
- Naaz, A., D. R. Holsberger, et al. (2004). "Loss of cyclin-dependent kinase inhibitors produces adipocyte hyperplasia and obesity." FASEB J **18**(15): 1925-7.
- Nakayama, K. I. and K. Nakayama (2006). "Ubiquitin ligases: cell-cycle control and cancer." Nat Rev Cancer **6**(5): 369-81.
- Nedergaard, J., T. Bengtsson, et al. (2007). "Unexpected evidence for active brown adipose tissue in adult humans." Am J Physiol Endocrinol Metab **293**(2): E444-52.
- Nishino, K., M. Toyoda, et al. (2011). "DNA methylation dynamics in human induced pluripotent stem cells over time." PLoS Genet **7**(5): e1002085.
- Obika, S., D. Nanbu, et al. (1998). "Stability and structural features of the duplexes containing nucleoside analogues with a fixed N-type conformation, 2'-O,4'-C-methyleneribonucleosides." Tetrahedron Letters **39**(30): 5401-5404.
- Oireachtas.ie, H. o. t. (2011). "Obesity- A growing problem?" Oireachtas Library and Research Service No.6.
- Okada, M., T. Sakai, et al. (2009). "Skp2 promotes adipocyte differentiation via a p27Kip1-independent mechanism in primary mouse embryonic fibroblasts." Biochem Biophys Res Commun **379**(2): 249-54.
- Okamoto, T., T. Aoyama, et al. (2002). "Clonal heterogeneity in differentiation potential of immortalized human mesenchymal stem cells." Biochem Biophys Res Commun **295**(2): 354-61.
- Okamura, K., J. W. Hagen, et al. (2007). "The mirtron pathway generates microRNA-class regulatory RNAs in Drosophila." Cell **130**(1): 89-100.
- Olena, A. F. and J. G. Patton (2009). "Genomic organization of microRNAs." J Cell Physiol **222**(3): 540-5.
- Orom, U. A. and A. H. Lund (2007). "Isolation of microRNA targets using biotinylated synthetic microRNAs." Methods **43**(2): 162-5.
- Ortega, F. J., J. M. Moreno-Navarrete, et al. (2010). "MiRNA expression profile of human subcutaneous adipose and during adipocyte differentiation." PLoS One **5**(2): e9022.
- Oskowitz, A. Z., J. Lu, et al. (2008). "Human multipotent stromal cells from bone marrow and microRNA: regulation of differentiation and leukemia inhibitory factor expression." Proc Natl Acad Sci U S A **105**(47): 18372-7.
- Pallante, P., R. Visone, et al. (2006). "MicroRNA deregulation in human thyroid papillary carcinomas." Endocr Relat Cancer **13**(2): 497-508.

- Patel, Y. M. and M. D. Lane (1999). "Role of calpain in adipocyte differentiation." Proc Natl Acad Sci U S A **96**(4): 1279-84.
- Petersen, C. P., M. E. Bordeleau, et al. (2006). "Short RNAs repress translation after initiation in mammalian cells." Mol Cell **21**(4): 533-42.
- Petersen, M. and J. Wengel (2003). "LNA: a versatile tool for therapeutics and genomics." Trends in Biotechnology **21**(2): 74-81.
- Petersen, M. and J. Wengel (2003). "LNA: a versatile tool for therapeutics and genomics." Trends Biotechnol **21**(2): 74-81.
- Petit, B., K. Masuda, et al. (1996). "Characterization of crosslinked collagens synthesized by mature articular chondrocytes cultured in alginate beads: comparison of two distinct matrix compartments." Exp Cell Res **225**(1): 151-61.
- Pfaffl, M. W. (2001). "A new mathematical model for relative quantification in real-time RT-PCR." Nucleic Acids Res **29**(9): e45.
- Pierdomenico, L., L. Bonsi, et al. (2005). "Multipotent mesenchymal stem cells with immunosuppressive activity can be easily isolated from dental pulp." Transplantation **80**(6): 836-42.
- Pillai, R. S., C. G. Artus, et al. (2004). "Tethering of human Ago proteins to mRNA mimics the miRNA-mediated repression of protein synthesis." RNA **10**(10): 1518-25.
- Pittenger, M. F., A. M. Mackay, et al. (1999). "Multilineage potential of adult human mesenchymal stem cells." Science **284**(5411): 143-7.
- Poliseno, L., A. Tuccoli, et al. (2006). "MicroRNAs modulate the angiogenic properties of HUVECs." Blood **108**(9): 3068-71.
- Prockop, D. J. (1997). "Marrow stromal cells as stem cells for nonhematopoietic tissues." Science **276**(5309): 71-4.
- Puigserver, P. and B. M. Spiegelman (2003). "Peroxisome proliferator-activated receptor-gamma coactivator 1 alpha (PGC-1 alpha): transcriptional coactivator and metabolic regulator." Endocr Rev **24**(1): 78-90.
- Puigserver, P., Z. Wu, et al. (1998). "A cold-inducible coactivator of nuclear receptors linked to adaptive thermogenesis." Cell **92**(6): 829-39.
- Qian, S. W., X. Li, et al. (2010). "Characterization of adipocyte differentiation from human mesenchymal stem cells in bone marrow." BMC Dev Biol **10**: 47.
- Ramirez-Zacarias, J. L., F. Castro-Munozledo, et al. (1992). "Quantitation of adipose conversion and triglycerides by staining intracytoplasmic lipids with Oil red O." Histochemistry **97**(6): 493-7.
- Reichert, M. and D. Eick (1999). "Analysis of cell cycle arrest in adipocyte differentiation." Oncogene **18**(2): 459-66.
- Ricquier, D. and F. Bouillaud (2000). "Mitochondrial uncoupling proteins: from mitochondria to the regulation of energy balance." J Physiol **529 Pt 1**: 3-10.
- Rivard, N., G. L'Allemain, et al. (1996). "Abrogation of p27Kip1 by cDNA antisense suppresses quiescence (G0 state) in fibroblasts." J Biol Chem **271**(31): 18337-41.
- Rodriguez, A., S. Griffiths-Jones, et al. (2004). "Identification of mammalian microRNA host genes and transcription units." Genome Res **14**(10A): 1902-10.

- Rosen, E. D. (2005). "The transcriptional basis of adipocyte development." Prostaglandins Leukot Essent Fatty Acids **73**(1): 31-4.
- Rosen, E. D. and O. A. MacDougald (2006). "Adipocyte differentiation from the inside out." Nat Rev Mol Cell Biol **7**(12): 885-96.
- Rosen, E. D., P. Sarraf, et al. (1999). "PPAR gamma is required for the differentiation of adipose tissue in vivo and in vitro." Mol Cell **4**(4): 611-7.
- Rosen, E. D. and B. M. Spiegelman (2000). "Molecular regulation of adipogenesis." Annu Rev Cell Dev Biol **16**: 145-71.
- Rosen, E. D., C. J. Walkey, et al. (2000). "Transcriptional regulation of adipogenesis." Genes Dev **14**(11): 1293-307.
- Rozemuller, H., H. J. Prins, et al. (2010). "Prospective isolation of mesenchymal stem cells from multiple mammalian species using cross-reacting anti human monoclonal antibodies." Stem Cells Dev.
- Ruby, J. G., C. H. Jan, et al. (2007). "Intronic microRNA precursors that bypass Drosha processing." Nature **448**(7149): 83-6.
- Saito, T., J. E. Dennis, et al. (1995). "Myogenic Expression of Mesenchymal Stem Cells within Myotubes of mdx Mice in Vitro and in Vivo." Tissue Eng **1**(4): 327-43.
- Saito, T. and P. Saetrom (2010). "MicroRNAs - targeting and target prediction." N Biotechnol.
- Sarruf, D. A., I. Iankova, et al. (2005). "Cyclin D3 promotes adipogenesis through activation of peroxisome proliferator-activated receptor gamma." Mol Cell Biol **25**(22): 9985-95.
- Sastry, L., T. Johnson, et al. (2002). "Titering lentiviral vectors: comparison of DNA, RNA and marker expression methods." Gene Ther **9**(17): 1155-62.
- Schieker, M., C. Pautke, et al. (2007). "Human mesenchymal stem cells at the single-cell level: simultaneous seven-colour immunofluorescence." J Anat **210**(5): 592-9.
- Schroeder, A., O. Mueller, et al. (2006). "The RIN: an RNA integrity number for assigning integrity values to RNA measurements." BMC Mol Biol **7**: 3.
- Scott, M. A., V. T. Nguyen, et al. (2011). "Current methods of adipogenic differentiation of mesenchymal stem cells." Stem Cells Dev **20**(10): 1793-804.
- Seale, P., B. Bjork, et al. (2008). "PRDM16 controls a brown fat/skeletal muscle switch." Nature **454**(7207): 961-7.
- Seale, P., S. Kajimura, et al. (2007). "Transcriptional control of brown fat determination by PRDM16." Cell Metab **6**(1): 38-54.
- Seggerson, K., L. Tang, et al. (2002). "Two genetic circuits repress the *Caenorhabditis elegans* heterochronic gene *lin-28* after translation initiation." Dev Biol **243**(2): 215-25.
- Sehm, T., C. Sachse, et al. (2009). "miR-196 is an essential early-stage regulator of tail regeneration, upstream of key spinal cord patterning events." Dev Biol **334**(2): 468-80.
- Sekiya, I., B. L. Larson, et al. (2002). "Expansion of human adult stem cells from bone marrow stroma: conditions that maximize the yields of early progenitors and evaluate their quality." Stem Cells **20**(6): 530-41.

- Seo, G. J., C. J. Chen, et al. (2009). "Merkel cell polyomavirus encodes a microRNA with the ability to autoregulate viral gene expression." *Virology* **383**(2): 183-7.
- Serrero, G. and N. Lepak (1996). "Endocrine and paracrine negative regulators of adipose differentiation." *Int J Obes Relat Metab Disord* **20 Suppl 3**: S58-64.
- Shi, R. and V. L. Chiang (2005). "Facile means for quantifying microRNA expression by real-time PCR." *Biotechniques* **39**(4): 519-25.
- Skarn, M., H. M. Namlos, et al. (2011). "Adipocyte Differentiation of Human Bone Marrow-Derived Stromal Cells Is Modulated by MicroRNA-155, MicroRNA-221, and MicroRNA-222." *Stem Cells Dev.*
- Slaby, O., M. Svoboda, et al. (2007). "Altered expression of miR-21, miR-31, miR-143 and miR-145 is related to clinicopathologic features of colorectal cancer." *Oncology* **72**(5-6): 397-402.
- Sottile, V., C. Halleux, et al. (2002). "Stem cell characteristics of human trabecular bone-derived cells." *Bone* **30**(5): 699-704.
- Spiegelman, B. M. and J. S. Flier (1996). "Adipogenesis and obesity: rounding out the big picture." *Cell* **87**(3): 377-89.
- Spiegelman, B. M., P. Puigserver, et al. (2000). "Regulation of adipogenesis and energy balance by PPARgamma and PGC-1." *Int J Obes Relat Metab Disord* **24 Suppl 4**: S8-10.
- Stark, A., J. Brennecke, et al. (2005). "Animal MicroRNAs confer robustness to gene expression and have a significant impact on 3'UTR evolution." *Cell* **123**(6): 1133-46.
- Sugihara, H., N. Yonemitsu, et al. (1987). "Proliferation of unilocular fat cells in the primary culture." *J Lipid Res* **28**(9): 1038-45.
- Sun, L., H. Xie, et al. (2011). "Mir193b-365 is essential for brown fat differentiation." *Nat Cell Biol* **13**(8): 958-65.
- Takahashi, K. and S. Yamanaka (2006). "Induction of pluripotent stem cells from mouse embryonic and adult fibroblast cultures by defined factors." *Cell* **126**(4): 663-76.
- Takahashi, Y., A. R. Forrest, et al. (2009). "MiR-107 and MiR-185 can induce cell cycle arrest in human non small cell lung cancer cell lines." *PLoS One* **4**(8): e6677.
- Tanaka, T., N. Yoshida, et al. (1997). "Defective adipocyte differentiation in mice lacking the C/EBPbeta and/or C/EBPdelta gene." *EMBO J* **16**(24): 7432-43.
- Tang, F., M. Kaneda, et al. (2007). "Maternal microRNAs are essential for mouse zygotic development." *Genes Dev* **21**(6): 644-8.
- Tang, Q. Q., T. C. Otto, et al. (2003). "Mitotic clonal expansion: a synchronous process required for adipogenesis." *Proc Natl Acad Sci U S A* **100**(1): 44-9.
- Tay, Y., J. Zhang, et al. (2008). "MicroRNAs to Nanog, Oct4 and Sox2 coding regions modulate embryonic stem cell differentiation." *Nature* **455**(7216): 1124-8.
- Terasawa, K., A. Ichimura, et al. (2009). "Sustained activation of ERK1/2 by NGF induces microRNA-221 and 222 in PC12 cells." *FEBS J* **276**(12): 3269-76.
- Thomas, M., J. Lieberman, et al. (2010). "Desperately seeking microRNA targets." *Nat Struct Mol Biol* **17**(10): 1169-74.

- Thomson, D. W., C. P. Bracken, et al. "Experimental strategies for microRNA target identification." Nucleic Acids Res **39**(16): 6845-53.
- Thomson, D. W., C. P. Bracken, et al. (2011). "Experimental strategies for microRNA target identification." Nucleic Acids Res **39**(16): 6845-53.
- Tiraby, C. and D. Langin (2003). "Conversion from white to brown adipocytes: a strategy for the control of fat mass?" Trends Endocrinol Metab **14**(10): 439-41.
- Tiraby, C., G. Tavernier, et al. (2003). "Acquirement of brown fat cell features by human white adipocytes." J Biol Chem **278**(35): 33370-6.
- Tong, A. W., P. Fulgham, et al. (2009). "MicroRNA profile analysis of human prostate cancers." Cancer Gene Ther **16**(3): 206-16.
- Tontonoz, P., E. Hu, et al. (1994). "Stimulation of adipogenesis in fibroblasts by PPAR gamma 2, a lipid-activated transcription factor." Cell **79**(7): 1147-56.
- Uccelli, A., L. Moretta, et al. (2006). "Immunoregulatory function of mesenchymal stem cells." Eur J Immunol **36**(10): 2566-73.
- Valoczi, A., C. Hornyik, et al. (2004). "Sensitive and specific detection of microRNAs by northern blot analysis using LNA-modified oligonucleotide probes." Nucleic Acids Res **32**(22): e175.
- van Dongen, S., C. Abreu-Goodger, et al. (2008). "Detecting microRNA binding and siRNA off-target effects from expression data." Nat Methods **5**(12): 1023-5.
- Villanueva, C. J., H. Waki, et al. (2011). "TLE3 is a dual-function transcriptional coregulator of adipogenesis." Cell Metab **13**(4): 413-27.
- Visone, R., L. Russo, et al. (2007). "MicroRNAs (miR)-221 and miR-222, both overexpressed in human thyroid papillary carcinomas, regulate p27Kip1 protein levels and cell cycle." Endocr Relat Cancer **14**(3): 791-8.
- Wagner, W., P. Horn, et al. (2008). "Replicative senescence of mesenchymal stem cells: a continuous and organized process." PLoS One **3**(5): e2213.
- Wahid, F., A. Shehzad, et al. (2010). "MicroRNAs: synthesis, mechanism, function, and recent clinical trials." Biochim Biophys Acta **1803**(11): 1231-43.
- Wang, K. H., A. P. Kao, et al. (2010). "Comparative expression profiles of mRNAs and microRNAs among human mesenchymal stem cells derived from breast, face, and abdominal adipose tissues." Kaohsiung J Med Sci **26**(3): 113-22.
- Wang, Q., Y. C. Li, et al. (2008). "miR-17-92 cluster accelerates adipocyte differentiation by negatively regulating tumor-suppressor Rb2/p130." Proc Natl Acad Sci U S A **105**(8): 2889-94.
- Wang, Y., S. Baskerville, et al. (2008). "Embryonic stem cell-specific microRNAs regulate the G1-S transition and promote rapid proliferation." Nat Genet **40**(12): 1478-83.
- Wang, Y., R. Medvid, et al. (2007). "DGCR8 is essential for microRNA biogenesis and silencing of embryonic stem cell self-renewal." Nat Genet **39**(3): 380-5.
- Wightman, B., I. Ha, et al. (1993). "Posttranscriptional regulation of the heterochronic gene lin-14 by lin-4 mediates temporal pattern formation in *C. elegans*." Cell **75**(5): 855-62.
- Wilfred, B. R., W. X. Wang, et al. (2007). "Energizing miRNA research: a review of the role of miRNAs in lipid metabolism, with a prediction that miR-103/107 regulates human metabolic pathways." Mol Genet Metab **91**(3): 209-17.

- Wu, Z., N. L. Bucher, et al. (1996). "Induction of peroxisome proliferator-activated receptor gamma during the conversion of 3T3 fibroblasts into adipocytes is mediated by C/EBPbeta, C/EBPdelta, and glucocorticoids." Mol Cell Biol **16**(8): 4128-36.
- Wu, Z., E. D. Rosen, et al. (1999). "Cross-regulation of C/EBP alpha and PPAR gamma controls the transcriptional pathway of adipogenesis and insulin sensitivity." Mol Cell **3**(2): 151-8.
- Wu, Z., Y. Xie, et al. (1995). "Conditional ectopic expression of C/EBP beta in NIH-3T3 cells induces PPAR gamma and stimulates adipogenesis." Genes Dev **9**(19): 2350-63.
- Xie, H., B. Lim, et al. (2009). "MicroRNAs induced during adipogenesis that accelerate fat cell development are downregulated in obesity." Diabetes **58**(5): 1050-7.
- Xu, P., S. Y. Vernooy, et al. (2003). "The Drosophila microRNA Mir-14 suppresses cell death and is required for normal fat metabolism." Curr Biol **13**(9): 790-5.
- Xu, W., X. Zhang, et al. (2004). "Mesenchymal stem cells from adult human bone marrow differentiate into a cardiomyocyte phenotype in vitro." Exp Biol Med (Maywood) **229**(7): 623-31.
- Yamanaka, S. (2009). "A fresh look at iPS cells." Cell **137**(1): 13-7.
- Yao, B., S. N. Rakhade, et al. (2004). "Accuracy of cDNA microarray methods to detect small gene expression changes induced by neuregulin on breast epithelial cells." BMC Bioinformatics **5**: 99.
- Yeh, W. C., Z. Cao, et al. (1995). "Cascade regulation of terminal adipocyte differentiation by three members of the C/EBP family of leucine zipper proteins." Genes Dev **9**(2): 168-81.
- Yigit, E., P. J. Batista, et al. (2006). "Analysis of the C. elegans Argonaute family reveals that distinct Argonautes act sequentially during RNAi." Cell **127**(4): 747-57.
- Young, H. E., M. L. Mancini, et al. (1995). "Mesenchymal stem cells reside within the connective tissues of many organs." Dev Dyn **202**(2): 137-44.
- Yu, J. Y., K. H. Chung, et al. (2008). "MicroRNA miR-124 regulates neurite outgrowth during neuronal differentiation." Exp Cell Res **314**(14): 2618-33.
- Zhang, C., C. Kang, et al. (2009). "Co-suppression of miR-221/222 cluster suppresses human glioma cell growth by targeting p27kip1 in vitro and in vivo." Int J Oncol **34**(6): 1653-60.
- Zhang, C., G. Wang, et al. (2009). "[Up-regulation of p27(kip1) by miR-221/222 antisense oligonucleotides enhances the radiosensitivity of U251 glioblastoma]." Zhonghua Yi Xue Yi Chuan Xue Za Zhi **26**(6): 634-8.
- Zhang, C., J. Zhang, et al. (2010). "PUMA is a novel target of miR-221/222 in human epithelial cancers." Int J Oncol **37**(6): 1621-6.
- Zhang, C. Z., C. S. Kang, et al. (2009). "[Inhibitory effect of knocking down microRNA-221 and microRNA-222 on glioma cell growth in vitro and in vivo]." Zhonghua Zhong Liu Za Zhi **31**(10): 721-6.
- Zhang, C. Z., J. X. Zhang, et al. (2010). "MiR-221 and miR-222 target PUMA to induce cell survival in glioblastoma." Mol Cancer **9**: 229.

- Zhang, H. H., S. Kumar, et al. (2000). "Ceiling culture of mature human adipocytes: use in studies of adipocyte functions." J Endocrinol **164**(2): 119-28.
- Zhang, J., Q. Sun, et al. (2012). "Loss of microRNA-143/145 disturbs cellular growth and apoptosis of human epithelial cancers by impairing the MDM2-p53 feedback loop." Oncogene.
- Zhang, R., Y. Peng, et al. (2007). "Rapid evolution of an X-linked microRNA cluster in primates." Genome Res **17**(5): 612-7.
- Zhang, Y., J. Guo, et al. (2009). "Down-regulation of miR-31 expression in gastric cancer tissues and its clinical significance." Med Oncol.
- Zhao, J. J., J. Lin, et al. (2008). "MicroRNA-221/222 negatively regulates estrogen receptor alpha and is associated with tamoxifen resistance in breast cancer." J Biol Chem **283**(45): 31079-86.
- Zhou, B., S. Wang, et al. (2007). "miR-150, a microRNA expressed in mature B and T cells, blocks early B cell development when expressed prematurely." Proc Natl Acad Sci U S A **104**(17): 7080-5.
- Zhou, X., J. Zhang, et al. (2010). "Reduction of miR-21 induces glioma cell apoptosis via activating caspase 9 and 3." Oncol Rep **24**(1): 195-201.
- Zuk, P. A., M. Zhu, et al. (2001). "Multilineage cells from human adipose tissue: implications for cell-based therapies." Tissue Eng **7**(2): 211-28.

